A Cyclophane-Based Approach to Highly Strained [*n*]Cycloparaphenylenes and Synthesis of Hexa-substituted Pyrenes and Their Application to Polycyclic Aromatic Hydrocarbon Synthesis

by

Mengzhou Wang

A dissertation submitted to the Graduate Faculty of
Auburn University
in partial fulfillment of the
requirements for the Degree of
Doctor of Philosophy

Auburn, Alabama
May 07, 2022

Keywords: cycloparaphenylenes, macrocycle, pyrene functionalization, Scholl reaction, cross-coupling

Approved by

Bradley L. Merner, Chair, Associate Professor of Chemistry and Biochemistry
Stewart Schneller, Professor of Chemistry and Biochemistry
Byron Farnum, Associate Professor of Chemistry and Biochemistry
Rashad Karimov, Assistant Professor of Chemistry and Biochemistry

Abstract

Chapter 1: The synthesis of highly strained carbon nanoring, [4]CPP and its potential precursor has been an ever-increasing level of interest in the past few decades. The biggest challenge in CPP synthesis is macrocyclization and aromatization. Two macrocyclization strategies have been developed for the syntheses of [4]CPP derivative and [5]CPP as well as several intermediates as the potential precursors for [4]CPP derivative and [5]CPP.

Chapter 2: The synthesis of 1,2,4,5,7,8-hexasubstituted pyrene has been achieved by initially functionalization the K-region of pyrene. Bromination, borylation, and oxidation reactions afford high regioselectivity at 1,8-position, which controlled the functionalization of 2,7-position. 1,2,4,5,7,8-hexasubstituted pyrene is a valuable building block for the construction of polycyclic aromatic hydrocarbons, several pi-extension reactions have been conducted on hexasubstituted pyrene by using Suzuki-Miyaura reaction and Scholl reaction.

Acknowledgments

It is with my utmost gratitude and honor that I acknowledge those individuals who have guided and sometimes pushed me through this process.

First and foremost, I would like to thank my major professor, Dr. Bradley L. Merner, for giving me the opportunity to pursue a Ph.D. under his direction and for opening doors I never knew imaginable. He has given me support, guidance, and opportunities from day one, and has pushed me to think and reason for myself at a level I did not know I could achieve. Thank you for everything Dr. Merner, I certainly would not be here without you.

I would like to give thanks to all my committee members: Dr. Byron Farnum, Dr. Rashad Karimov, and Dr. Stewart Schneller for their precious suggestions and helpful guidance during my research. I would also like to thank my external reader Dr. Cassabdra Porter for her participation in evaluating my work.

I also must thank Dr. Doug Goodwin, who has helped me a lot during the transition. Thank you for being willing to provide your assistance and advice throughout this entire difficult drawn-out process.

I also would like to thank the Auburn University Department of Chemistry and Biochemistry for the opportunity to learn from so many incredible professors and mentors both in classes and as a teaching assistant. Thanks to Dr. Melissa Boersma for her help and instruction in mass spectrometry. Also, a special thanks to Dr. Raj Pokkuluri for helping me to solve my crystal structures.

My deepest gratitude also belongs to my lab mates throughout my time in the Merner group. Kara Johnson, Nirob Saha, Sydney Jackson, Timothy (Hank) Barnes, Andrew Caskey, Jacob Istre, Taiwo Adepoju and Didimos Pulikkottil have all been a source of encouragement and have pushed me to grow as a scientist. Also, other friends within this department, Nan Shi, Jiaming Liu, Kun Ding, Jinyan Cui Tingting Qu and Hui Jin, I am so grateful for your friendship.

Finally, I am deeply and genuinely grateful to my family members, especially my parents and my sisters for their love and support. I must acknowledge and thank the most important people in my life. To my wife Qian, you have been steadfast in your support of me throughout this entire process, especially during the COVID-19 pandemic. Without your love and support, I would never cross the finish line. Thank you for being such a wonderful wife that I could ever ask for.

Content

List of Figures

List of Abbreviations

Δ	Heat
18-crown-6	1,4,7,10,13,16-Hexaoxacyclooctadecane
Å	Angstroms
Ac	Acetyl
Ac_2O	Acetic anhydride
Ar	Aromatic ring
Bpin	Boronic acid pinacol ester
$B_2(pin)_2$	Bis(pinacolato)diborane
Bpy	2,2'-Bipyridyl
CNB	Carbon nanobelt
CNTs	Carbon nanotubes
cod	1,5-Cyclooctadiene
CPP	Cycloparaphenylene
dba	Dibenzylideneacetone
DCM	Dichloromethane
dr	Diastereomeric ratio
DDQ	2,3-Dichloro-5,6-dicyano-1,4-benzoquinone
DMA	Dimethylacetamide
DMF	*N*,*N*-dimethylformamide
DMP	Dess-Martin periodinane
DMSO	Dimethyl sulfoxide
dppf	1,1'-Bis(diphenylphosphino)ferrocene
dtbpy	4,4'-Di-*tert*-bytyl-2,2'-bipyridine
equiv.	Equivalent
Et	Ethyl

EtOAc	Ethyl acetate
EtOH	Ethanol
FVP	Flash vacuum pyrolysis
G II	Grubbs second generation
H-G II	Hoveyda-Grubbs second generation
HRMS	High resolution mass spectrometry
i-Pr	Isopropyl
i-Pr_2NH	Diisopropylamine
i-PrOBpin	2-Isopropoxy-4,4,5,5-tetramethyl-1,3,2-dioxaborolane
LDA	Lithium diisopropylamide
LiHMDS	lithium hexamethyldisilazide
Me	Methyl
MeOH	Methanol
M.S.	Molecular sieves
n-BuLi	*n*-Butyllithium
Nap	Naphthalenide
NBS	N-bromosuccinimide
NIS	N-iodosuccinimide
NEt_3	Triethylamine
NMR	Nuclear magnetic resonance
OLED	Organic light emitting diode
PAH	Polycyclic aromatic hydrocarbon
PCC	Pyridinium chlorochromate
PhMe	Toluene
p-TsOH	*para*-Toluenesulfonic acid
pyr.	Pyridine
RCM	Ring-closing metathesis

Rf	Retention factor
SE	Strain energy
S-Phos	2-Dicyclohexylphosphino-2’6’-dimethoxybiphenyl
TBAF	Tetrabutylammonium fluride
TBDMSCl	*Tert*-butyldimethylsilyl chloride
TES	Triethylsilyl
THF	Tetrahydrofuran
Tf	triflyl
TfOH	Trifluoromethanesulfonic acid
Tf_2O	Trifluoromethanesulfonic anhydride
TLC	Thin layer chromatography
TMSA	Trimethylsilylacetylene
UV	Ultraviolet
UV/vis	Ultraviolet/visible

Chapter 1 Towards the Synthesis of Small and Highly Strained [*n*]Cycloparaphenylenes via a Cyclophane-based Approach

1 Introduction

1.1 Cycloparaphenylenes

Since the first observation and detailed structural analysis of carbon nanotubes (CNTs) in 1991 by Iijima,[1] the bottom-up chemical synthesis of CNT has been of considerable scientific interest because of the unique physical and chemical properties of these allotropes of carbon, as well as their potential applications in technology advancement.[2,3] Bottom-up synthetic approaches to these carbon-rich materials are particularly important, as it would yield one type of CNT product.

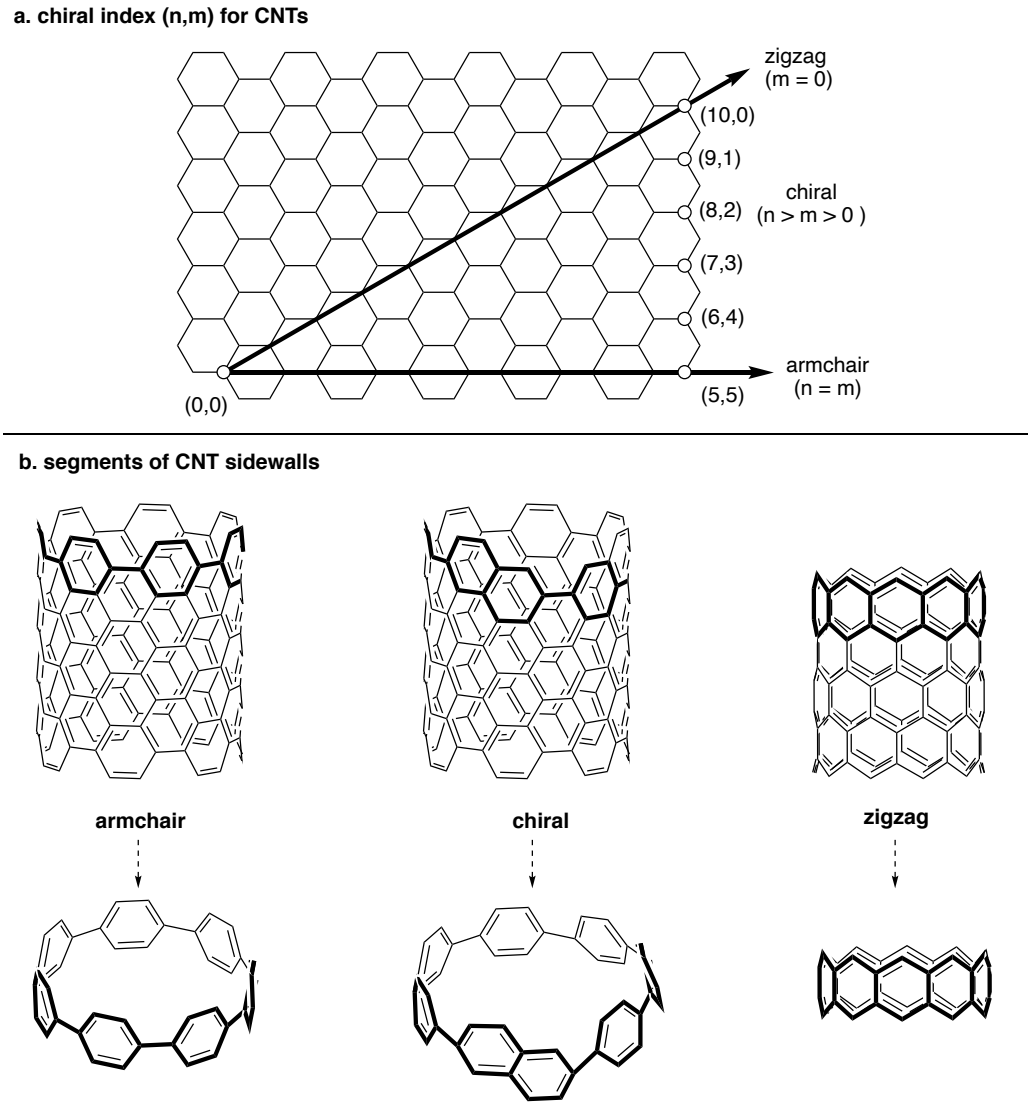

Figure 1. Carbon nanorings as segments of CNT sidewalls

Single-walled CNTs can be obtained and visualized by considering the hypothetical roll-up of a two-dimensional graphene sheets. The way in which the graphene sheet is wrapped gives rise to a particular CNT structure, which is assigned a chiral index, indicated by a pair of numbers (Figure 1). The CNT structure referred to a "zigzag" arises when m = 0, and these types of CNTs represent linear acenes (*eg.*, naphthalene, anthracene, tetracene, etc.). The "armchair" CNT structure is afforded when n = m, and such structures resemble phenylene-type PAHS. When n > m > 0 a "chiral" CNT is produced. The chiral index (n,m) can be used to deduce a variety of electrical, optical, magnetic, and mechanical properties of CNTs.[4] The smallest repeating subunits of the armchair and chiral CNTs, are macrocyclic segments known as carbon nanohoops (Figure 1).

Macrocyclic structures consisting of *n* benzene rings connected through *para* linkages are known as [*n*]cycloparaphenylenes ([*n*]CPPs). These, so-called carbon nanohoops can represent the shortest possible (macrocyclic) cross-section of an armchair carbon nanotube (Figure 2). As such, these benzenoid macrocyclic segments, represent diameter-defining templates from which CNTs and higher-order carbon nanostructures, such as carbon nanobelts (CNBs), can be assembled. Envisioned decades ago,[5] pre-dating the discovery of the fullerene and CNT allotropes of carbon, the [*n*]CPPs are inherently strained molecules and their chemical synthesis eluded many synthetic research groups for over 70 years.[6-13] The structure of [5]cycloparaphenylene (**2.1,** Figure 2) can be mapped onto a carbon nanobelt (**2.2**), a (5,5) armchair CNT (**2.3**) and C_{60} fullerene (**2.4**The first syntheses of [*n*]CPPs were reported in 2008 by Bertozzi and Jasti,[14] which was shortly followed by independent contributions from Itami[15] and Yamago,[16] respectively. In the following 13 years, there has been an ever-increasing level of interest in molecules of this type, as evidenced by the volume of publications describing their synthesis, structure and properties.[17] The smallest and most strained [*n*]CPP that has been synthesized to date, is [5]CPP (**2.1**) which has a strain energy of 119 kcal/mol.

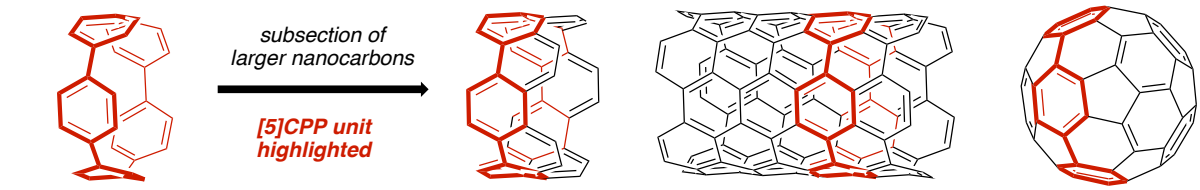

[5]cycloparaphenylene **2.1** | **carbon nanobelt** **2.2** | **[5,5] Armchair CNT** **2.3** | **C_{60}** **2.4**

Figure 2. [5]CPP subunit as it maps onto larger nanostructures and nanocarbons

1.2 Early attempts to synthesize [*n*]CPPs

Over the past 15 years, the [*n*]CPPs have moved from theoretical curiosities to synthetically accessible molecules, and in some cases, they have been prepared on gram scales. However, synthetic investigations of [*n*]CPPs started much earlier when Parekh and Guha attempted the synthesis of the smallest member of this class of compounds, [2]CPP (**3.4**) in 1934.[5] Their initial attempts to synthesize this highly strained compound involved a Cu-mediated partial desulfurization reaction of a compound which they believed to be *p*,*p*'-diphenylenetetrasulfide **3.2** (Figure 3). The hope was to employ sequential desulfurization reactions, the latter involving pyrolysis of dithiacyclophane **3.3** to afford [2]CPP (**3.4**). Given the enormous amount of strain energy present in the final target, a 2022 view of the Parekh and Guha approach would seem somewhat naïve, and borderline ridiculous; however this approach is significant as it marks the first known attempted synthesis of a CPP molecule. At that time of their report, the authors were only able to characterize **3.2** and **3.3** on the basis of elemental analysis. Later, they realized there is a possibility that they isolated higher-order oligomers such as **3.5**, **3.6** and **3.7**.[6,12]

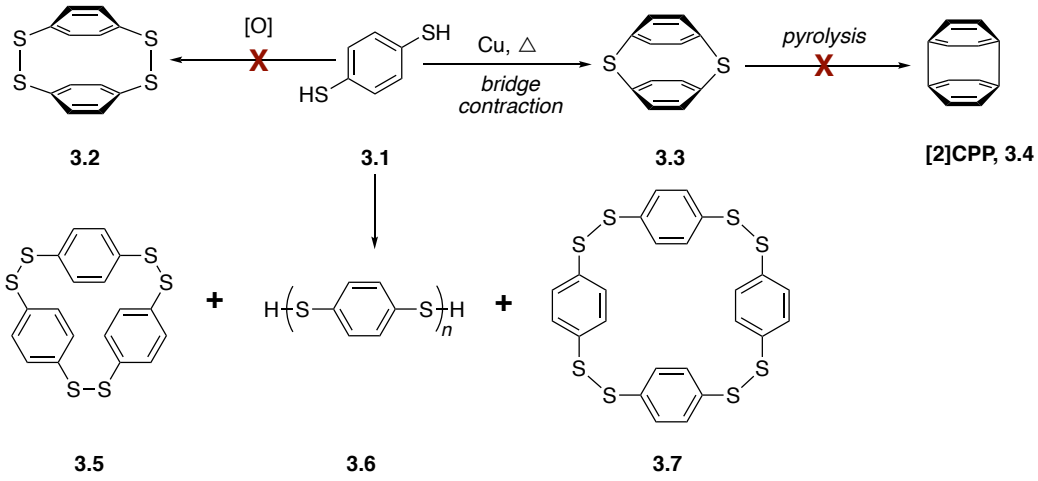

Figure 3. Parekh and Guha's attempted synthesis of [2]CPP

In 1984, Vögtle and co-workers synthesized [6] and [8]CPP precursors **4.1** and **4.2** in high yield,[8] but unfortunately, all attempts to convert these macrocycles into the desired carbon nanohoops through desulfurization reactions failed (Figure 4). A few years later, in 1993, Vögtle and co-workers published a paper entitled *"On the way to macrocyclic paraphenylenes*".[10] In this work, they attempted to install the remaining benzene rings of [8]CPP by engaging macrocycle **5.1**, which had been synthesized via a Wittig-based cyclooligomerization reaction, in a Diels-Alder reaction with phenyl vinyl sulfone (Figure 5).

Unfortunately, all attempts to transform enynes **5.1** and **5.2** into [8] and [12]CPP were reported to be unsuccessful.

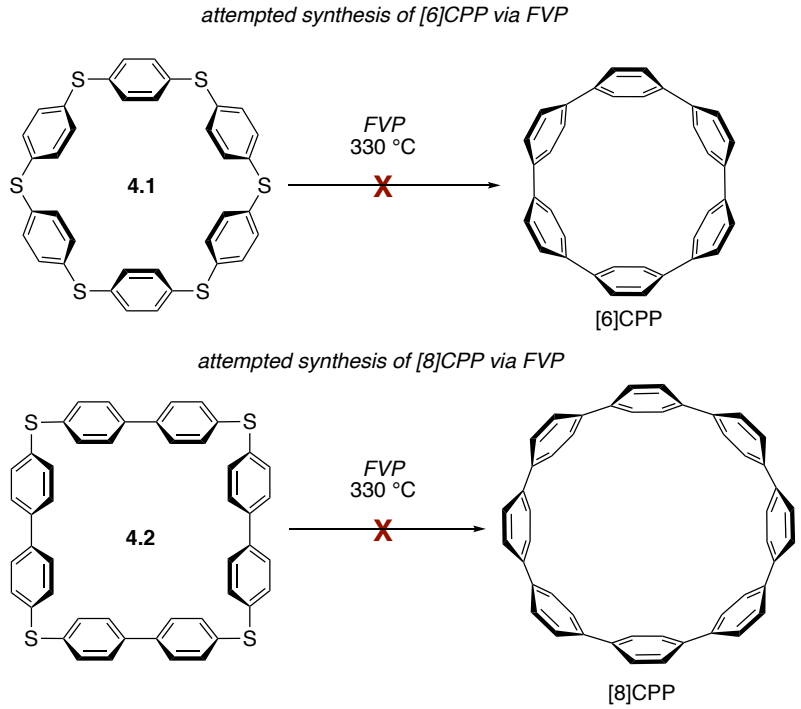

Figure 4. Vogtle's attempted preparation of [6]CPP and [8]CPP by desulfurization

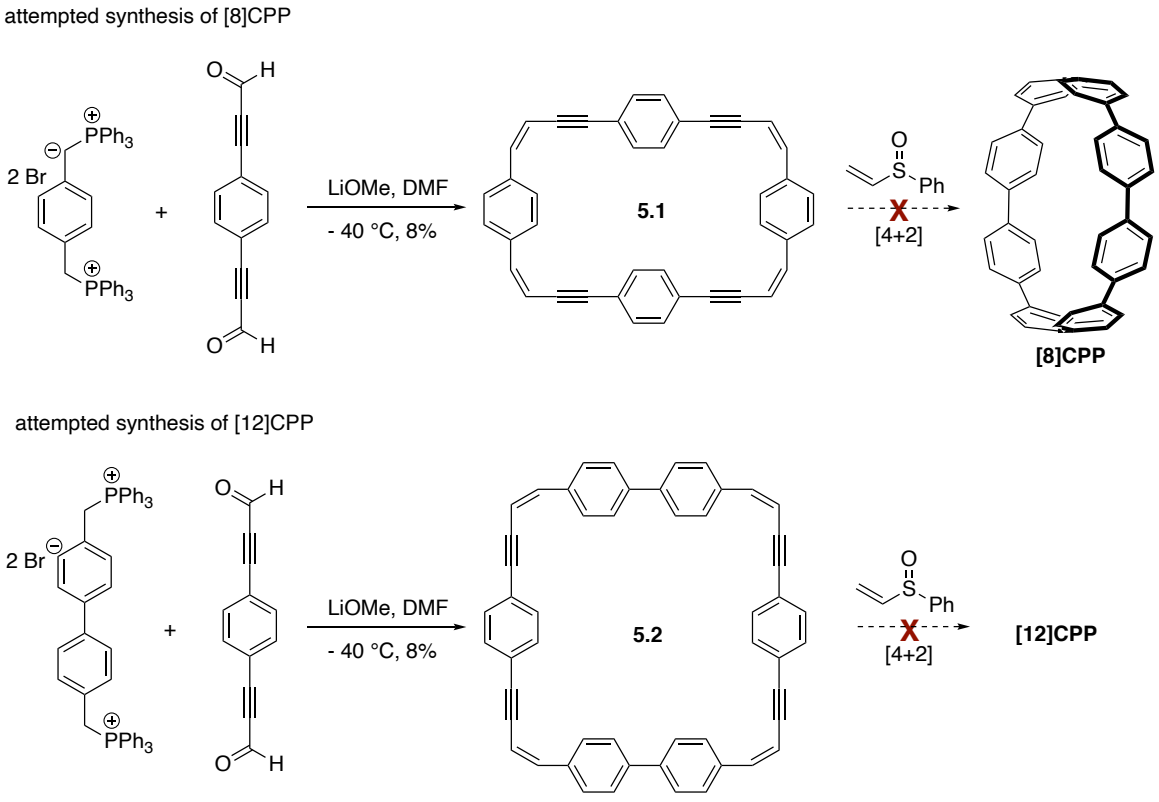

Figure 5. Vogtle's attempted preparation of [8]CPP and [12]CPP by Diels-Alder reaction

The third strategy explored by Vögtle was to assemble macrocycles containing cyclohexane rings as well as arenes.[7] These types of macrocycles (**6.2**, Figure 6) were expected to be less strained than the desired [*n*]CPPs as the sp^3 hybridized bridgehead carbon atoms can better accommodate the curvature of the macrocycle. Once such macrocycles had been assembled, the Vögtle synthesis plan called for aromatization of the cyclohexane units to form the remaining benzene rings of the carbon nanohoop targets. However, macrocycle formation under conditions of Kharasch coupling was in fact unsuccessful, giving liner oligomers **6.3** instead of the desired macrocycles.

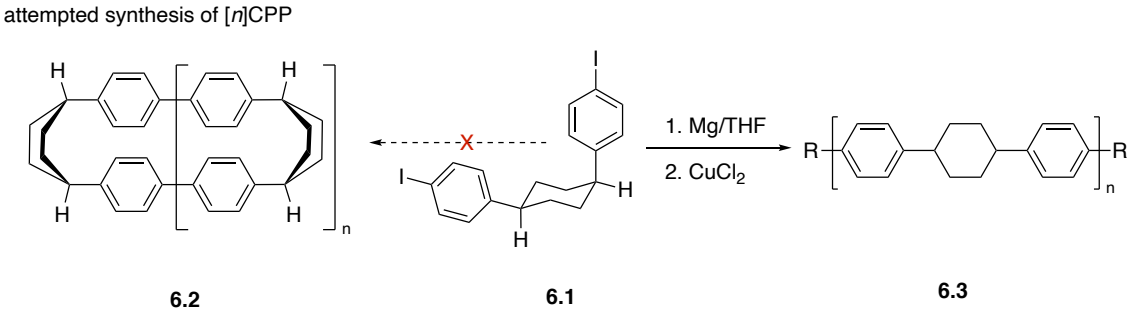

Figure 6. Failed cyclooligomerisation of 1,4-*syn*-diaryl cyclohexanes

1.3 Successful strategies for the synthesis of small [*n*]CPPs (*n*=9-5)

1.3.1 Unselective syntheses of [*n*]CPPs (n > 9)

The first synthesis of [*n*]CPPs was achieved by Bertozzi and Jasti in 2008, and it is a landmark in the history of CPP synthesis.[14] In this work, they started with monolithiation of 1,4-diiodobenzene **7.1** then subsequent addition of benzoquinone to generate a *syn*-1,4-diol **7.2**, which was then treated with NaH and MeI to form diiodide **7.3** in 34% yield over four steps. With one cross-coupling partner in hand, they next converted a portion of **7.3** to the corresponding bis(pinacolborane) **7.4** by double lithiation and addition to 2-isopropoxy-4,4,5,5-tetramethyl-1,3,2-dioxaborolane. With both cross-coupling precursors in hand, they used a 1:1 mixture of **7.3** and **7.4** to form macrocycles **7.5**, **7.6** and **7.7** through Suzuki-Miyaura cross-coupling reaction. Macrocycles **7.5**, **7.6** and **7.7** where then treated with lithium napthalenide at −78 °C afforded the corresponding cycroparaphenylenes **7.8**, **7.9** and **7.10** in moderate yields.

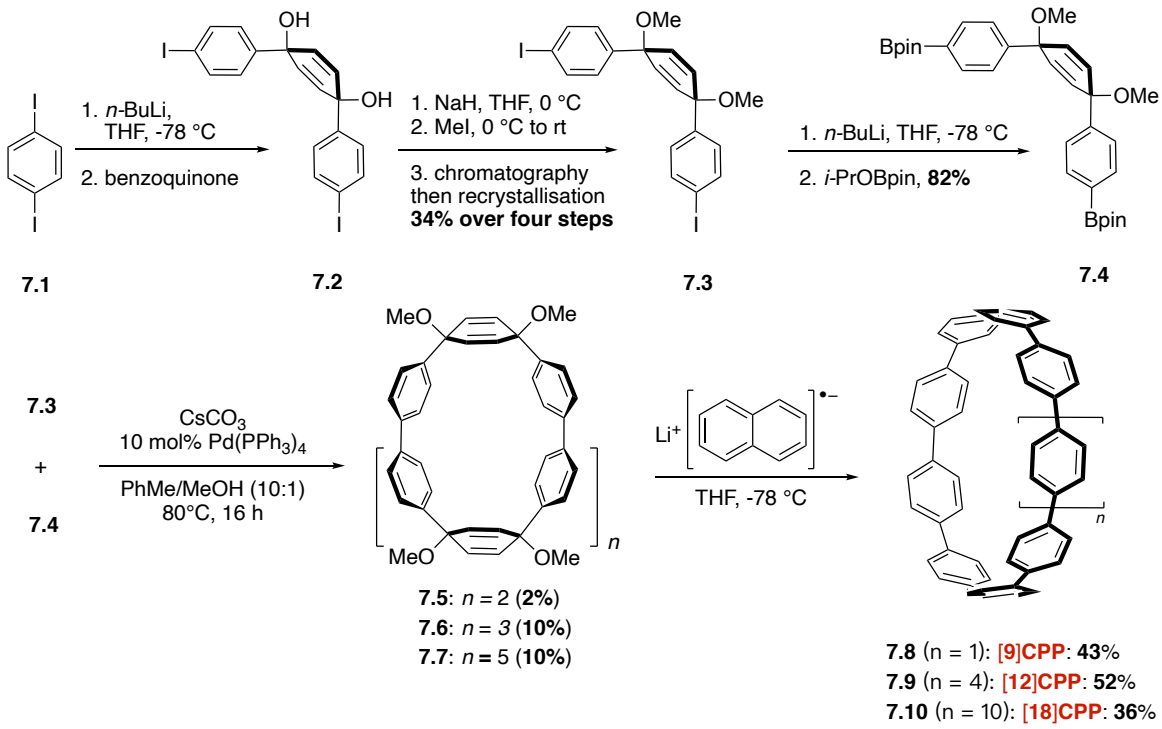

Figure 7. The first synthesis of CPPs, reported by Bertozzi and co-workers

The significance of the Bertozzi group's work was acknowledged by the community at large, with a review published in early 2009 reporting the potential applicability of the CPPs as starting materials for the "bottom-up" synthesis of carbon nanotubes.

1.3.2 Size-selective synthesis of [9]CPP

A few years later, in 2011, Itami and co-workers reported the synthesis of [9]CPP, which involved a nickel-mediated macrocyclization reaction (Figure 8).[17a] In this work, an L-shaped diphenylcyclohexane unit was used as starting material in a $[Ni(cod)_2]$/bpy catalyzed cyclotrimerization reaction to form the [9]CPP precursor **8.2**. Cyclic trimer **8.2** was then treated with $NaHSO_4 \cdot H_2O$ in refluxing *m*-xylene/DMSO under air to afford [9]CPP in 24% isolated yield. Also, during their synthesis, Itami and co-workers reported the first X-ray crystal structure of [9]CPP.

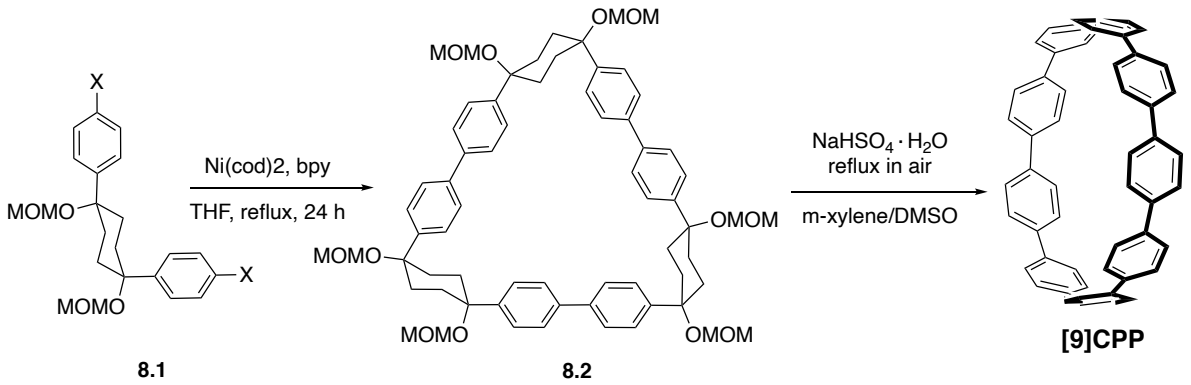

Figure 8. Highlights from Itami and co-workers synthesis of [9]CPP

1.3.3 Synthesis of [8]CPP

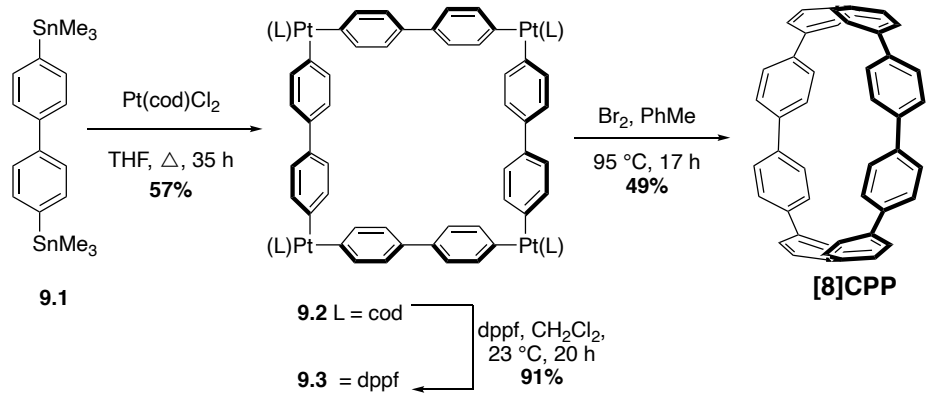

Figure 9. The synthesis of [8]CPP reported by Yamago and co-workers

In 2010, Yamago and co-workers reported a conceptually original synthetic route to [*n*]CPPs (Figure 9).[16] In this work, they treated 4,4'-bis(trimethylstannyl)biphenyl **9.1** with $Pt(cod)Cl_2$ to afford macrocycle **9.2**, then after ligand exchange, cod to dppf, [8]CPP precursor **9.3** was formed, reductive elimination of the aryl groups resulted in the formation of [8]CPP. This marked the first time [8]CPP had been synthesized, and this synthetic strategy was applicable to the syntheses of other [*n*]CPPs. While the use of a super-stoichiometric quantity of Pt has cost implications for scale-up, Yamago's route nevertheless is exceedingly concise and high yielding, given that [8]CPP was prepared in just three steps from **9.1** and 25% overall yield.

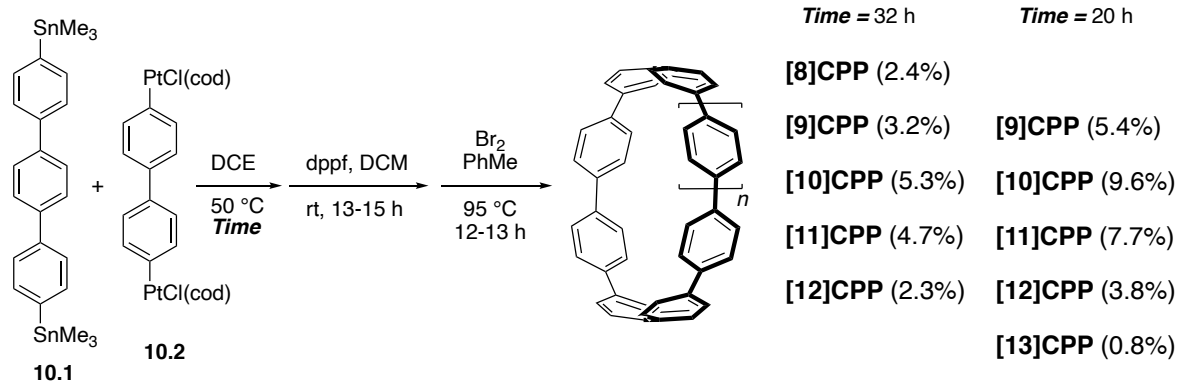

Figure 10. Yamago's platinum-mediated synthesis of [8-13]CPP

A year later, Yamago followed up his 2010 communication on the synthesis of [8]CPP with a full article that extended their platinum-mediated macrocyclization strategy to the synthesis of CPPs from n = 8 to 13 (Figure 10).[17b] In this work, bis(stannyl)terphenyl building block **10.1** was reacted with bis(platinum)biphenyl building block **10.2** to form the CPP precursors. Ligand exchange with dppf was then affected without separation of the intermediate. Oxidation with bromine gave desired CPPs. It was found that simply varying the reaction for the first step profoundly affected the product distribution. It is also notable that the process provides access to odd-numbered CPPs, as well as even numbered carbon nanohoops.

1.3.4 Synthesis of [7]CPP

A 2011 publication from Jasti and co-workers reported the first synthesis of [7]CPP, the smallest CPP isolated at that point.[17c] In this work, they used a strategy which was a variant of that employed in the first synthesis of [*n*]CPPs in 2008. As shown in Figure 11, this strategy relies on orthogonal Suziki-Miyaura coupling reactions, and the key is the exploitation of the enhanced reactivity of aryl bromides with respect to aryl chlorides. Oxidative dearomatization of silyl-protected bromophenol **11.1** with hypervalent iodine in the presence of water generated hydroxyketone **11.2**. Deprotonation of hydroxyketone **11.2** with NaH followed by the addition of aryllithium gave the desired *syn*-1,4-diol **11.3**. This diol was treated with NaH and MeI to form dimethyl ether **11.4**. To prepare for a Suzuki-Miyaura coupling reaction, a portion of **11.4** was converted into boronate **11.5** through lithium-halogen exchange followed by treatment with (isopropoxy)pinacolborane. The union of **11.4** and **11.5** via Suzuki-Miyaura cross-coupling under comparatively mild conditions, gave 6-ring linear precursor **11.6**, with the two chlorides remaining untouched. Use of Buchwald's S-Phos ligand under forcing conditions

afforded **11.7** in 12% yield. Finally, reductive aromatization with lithium naphthalenide gave [7]CPP, for which an X-ray crystal was also obtained to confirm the structure.

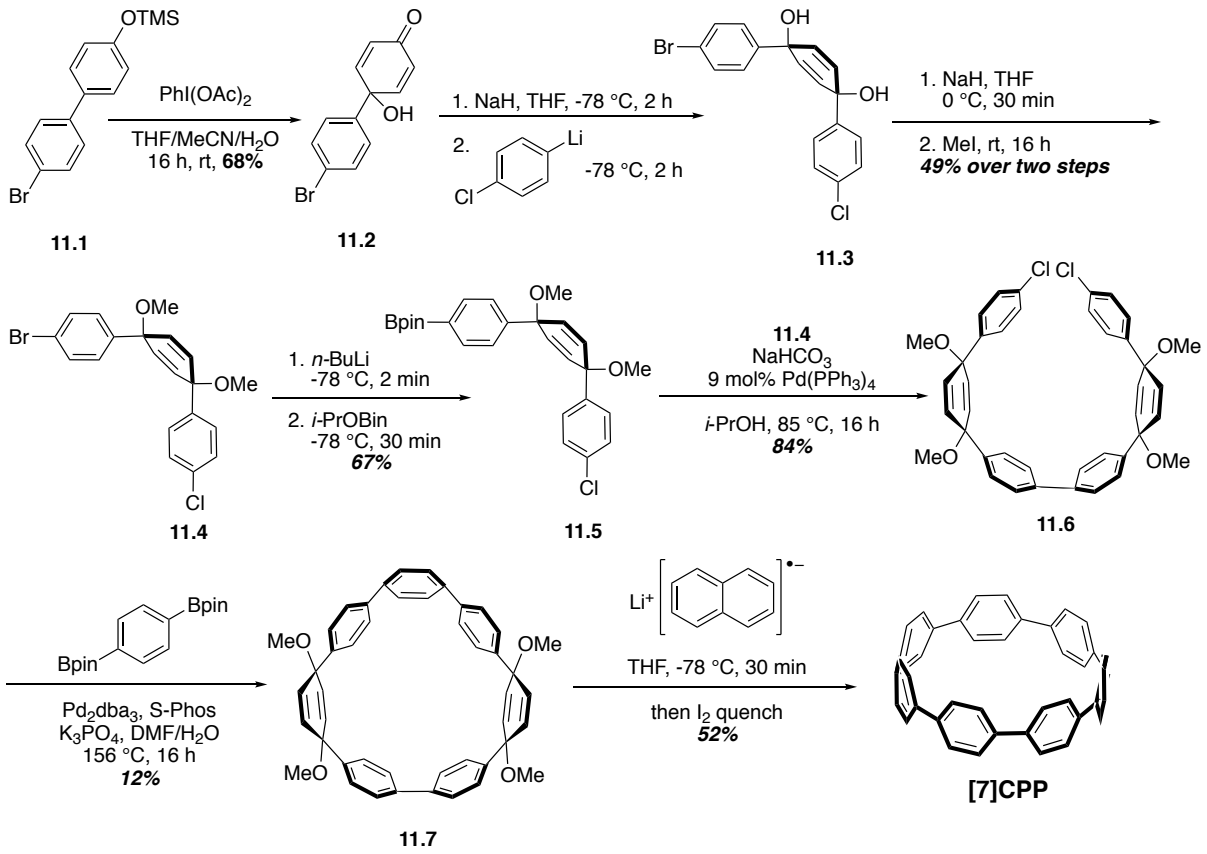

Figure 11. Jasti's synthesis of [7]CPP

1.3.5 Synthesis of [6]CPP

The record for the synthesis of the smallest and most strained [*n*]CPP was broken by Jasti and co-workers in 2012 with the synthesis of [6]CPP (Figure 12).[17g] The key tactic employed in this synthesis was to use an oxidative dearomatization reaction with hypervalent iodine that had employed in Jasti's prior synthesis of [7]CPP. However, in the instance of [6]CPP, this tactic was utilize at two stages in the synthesis. The synthesis began with the deprotonation of hydroxyketone **11.2** with NaH, subsequent addition of TBS-protected aryllithium gave diol **12.1**, followed by the methylation with NaH and MeI to afford dimethyl ether **12.2** in 52% yield over four steps. Removal of the silyl-protecting group of **12.2** with TBAF proceeded smoothly to generate phenol **12.3**, which was then treated with hypervalent iodine in the presence of H_2O to give hydroxyketone **12.4** in 71% yield. Hydroxyketone **12.4** was then treated with (4-bromophenyl)lithium under similar conditions as those for ketone **11.2** to generate dibromide

12.6 in 51% yield. Macrocyclic ring-closure was affected by the same dual intermolecular/intramolecular Suzuki-Miyaura strategy employed for the synthesis of [7]CPP to form macrocycle **12.7** in 12% yield. Finally, **12.7** was subjected to reductive aromatization in the presence of sodium naphthalenide to afford [6]CPP in 48% yield.

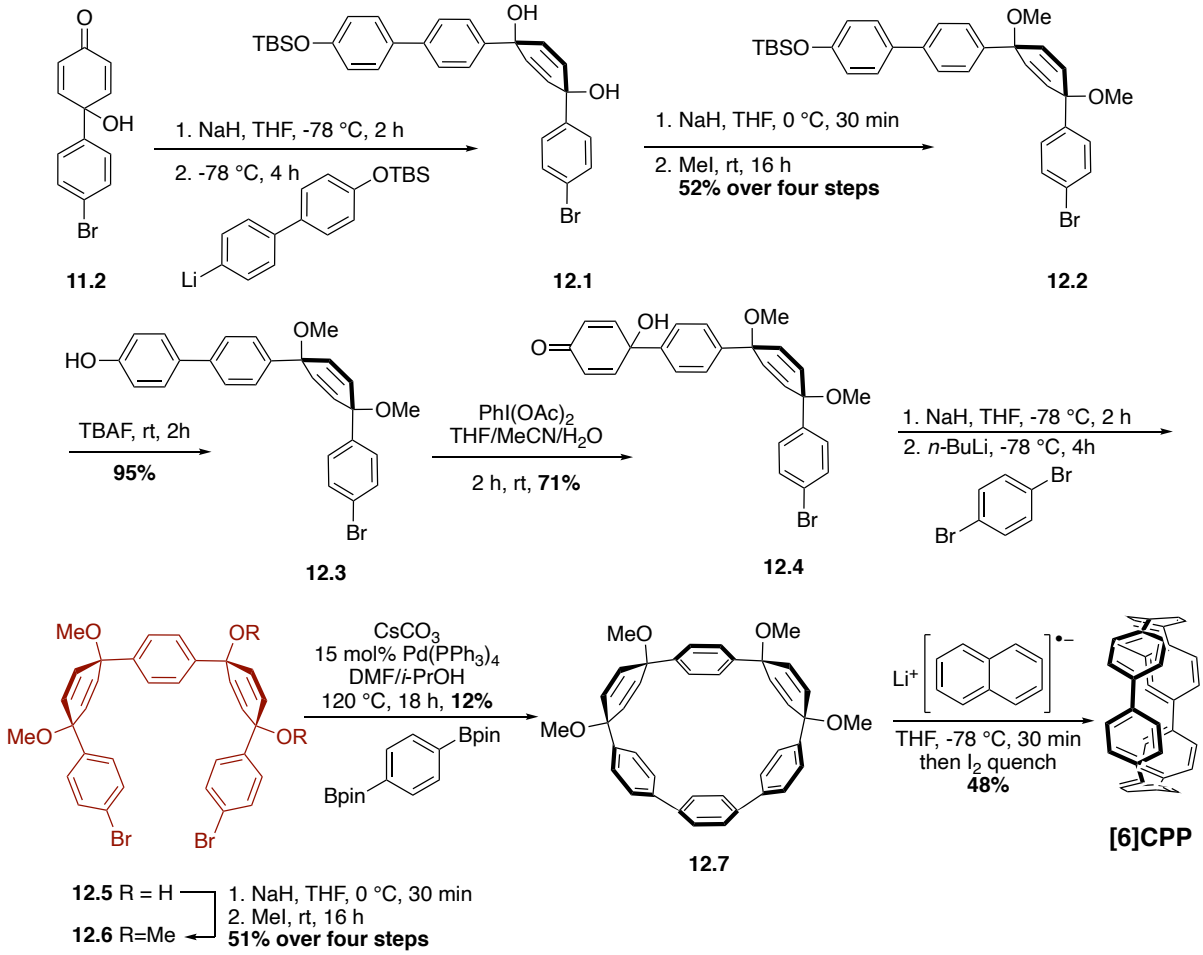

Figure 12. Jasti's synthesis of [6]CPP

1.3.6 Synthesis of [5]CPP

The record set by Jasti and co-workers in 2012 for the synthesis of the smallest [*n*]CPP (*n* = 6) fell on January 27, 2014, when Yamago and co-workers reported the first synthesis of [5]CPP (Figure 13, A).[17i] In order to overcome the intimidating strain energy of this structure, the Yamago group adopted a hybrid approach that incorporated concepts from previous syntheses reported by Itami and Jasti. Namely, a Ni-mediated macrocyclization reaction, followed by reductive aromatization of a 1,4-cyclohexadiene-1,4-diol unit after macrocyclization, with the latter proving to be highly innovative and considerably milder than

the previously reported conditions from Jasti and co-workers. In this work, like the synthesis of [7]CPP, the first step involves dearomatization of the TMS-protected biphenyl derivative **11.1** with $PhI(OAc)_2$ to affored 4-(bromophenyl)-4-hydroxycyclohexa-2,5-dienone (**11.2**, Figure 13). The resulting hydroxyketone **11.2** was then treated with sodium hydride followed by *in situ* generated 4-lithio-4'-(*tert*-butyldimethylsilyloxy)biphenyl, to afford diol **12.1**. The resultant product was treated with TESCl to afford a protected *syn*-1,4-diol, and subsequently treated with LiOH to cleave phenolic TBS group to afford **13.1** in 92% yield over four steps. Treatment **13.1** with $PhI(OAc)_2$ gave hydroxy ketone **13.2**, which was successively treated with sodium hydride and in *situ* generated 4-lithio-4'-(*tert*-butyldimethylsilyloxy)biphenyl to afford diol **13.3**, followed by TESCl to afford macrocyclization precursor **13.4** in 53% overall yield. Treatment of **13.4** with $Ni(cod)_2$ and 2,2'-bypyridine (bpy) in refluxing THF for 15 hours afforded the cyclized product **13.5** in 63% yield. Removal of the TES groups upon treatment with TBAF afforded tetraol **13.6** in quantitative yield, and the resultant diol was subjected to reductive aromatization ($SnCl{\bullet}H_2O$ in THF at 60 °C) to afford [5]CPP in 58% yield, for the very first time.

Just few weeks later, Jasti and co-workers also published a paper on the synthesis of [5]CPP, in which a palladium-catalyzed, oxidative boronate coupling was employed as the key macrocyclization step (Figure 13, B).[17k] Similar to the Yamago approach, the Jasti synthesis commenced with biaryl **11.1**, and followed a similar sequence to afford **13.7**, albeit using a different macrocyclization precursor. Macrocycle **13.8** was first observed as a minor by-product during the synthesis of [12]CPP. It was later realized that **13.8** is potentially a precursor of [5]CPP, and Jasti and co-workers optimized their reaction conditions to facilitate the formation of **13.8**. It was discovered that high dilution and using 1.0 equiv. of KF promoted intramolecular boronate coupling to give **13.8** in 52% yield. Based on Jasti's previous work, reductive aromatization of **13.8** was expected to furnish [5]CPP. However, when **13.8** was treated with excess sodium naphthalenide at −78 °C, a stable dianion was formed, which did afford [5]CPP as intended. Instead, the dianion was quenched with MeOH, and reduced macrocycle **13.9** was isolated in 88% yield. Subsequent treatment of **13.9** with LDA effected smooth elimination of two equivalents of MeOH, giving [5]CPP in 69% yield.

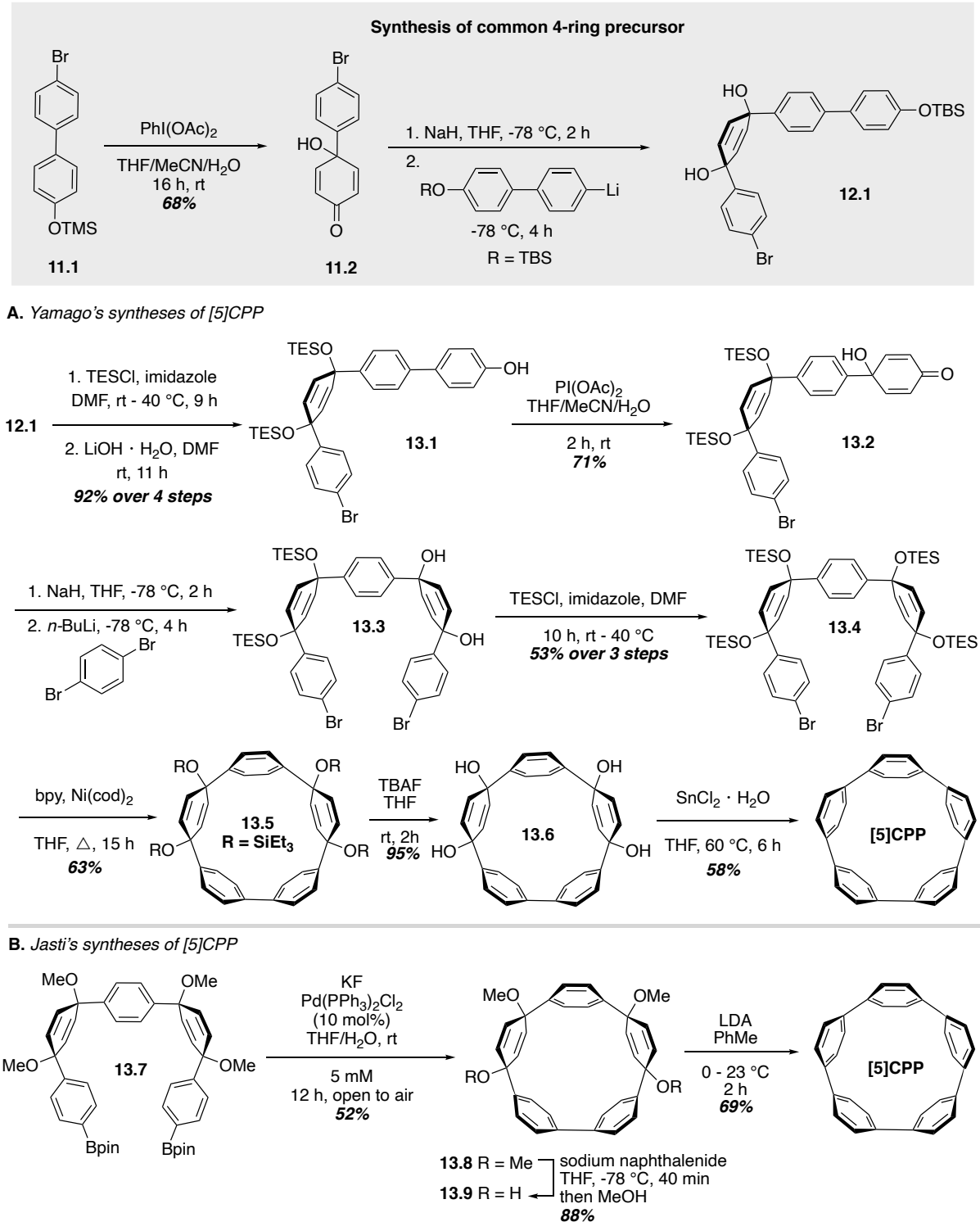

Figure 13. Yamago and Jasti's syntheses of [5]CPP

2 Common synthetic approaches to [n]CPPs

As we all can see from the previous work, despite their (relatively) simple structure, composed of only benzene rings held together by biaryl bonds at the *para*-positions, the synthesis of CPPs has been a significant challenge due to the difficulty in assembling the highly strained macrocyclic structure. After numerous endeavors, carried out over more than a half-century, the synthesis of [*n*]CPPs was achieved by the three groups mentioned above, using three different synthetic approaches. It should be noted nearly all other syntheses of [*n*]CPPs follow an approach similar to the three highlighted in Figure 14. The Jasti and Itami approaches make use of L-shaped subunits that consist of a central *syn*-1,4-dimethoxycyclohexa-2,5-diene and or *syn*-1,4-dihydroxycyclohexane as “masked” benzene rings (Figure 14A and 14B). The incorporation of *syn*-configured, 1,4-diol precursors provide the appropriate curvature to enable macrocyclization during subunit assembly, and subsequently, these pre-arene units can be subjected to a strain-building aromatization step to afford the desired cycloparaphenylenes. The second route employs a Pt-based molecular square with 4,4’-biphenylene sides and platinum vertices (Figure 14C), which is later subjected to reductive elimination to afford a cycloparaphenylene.

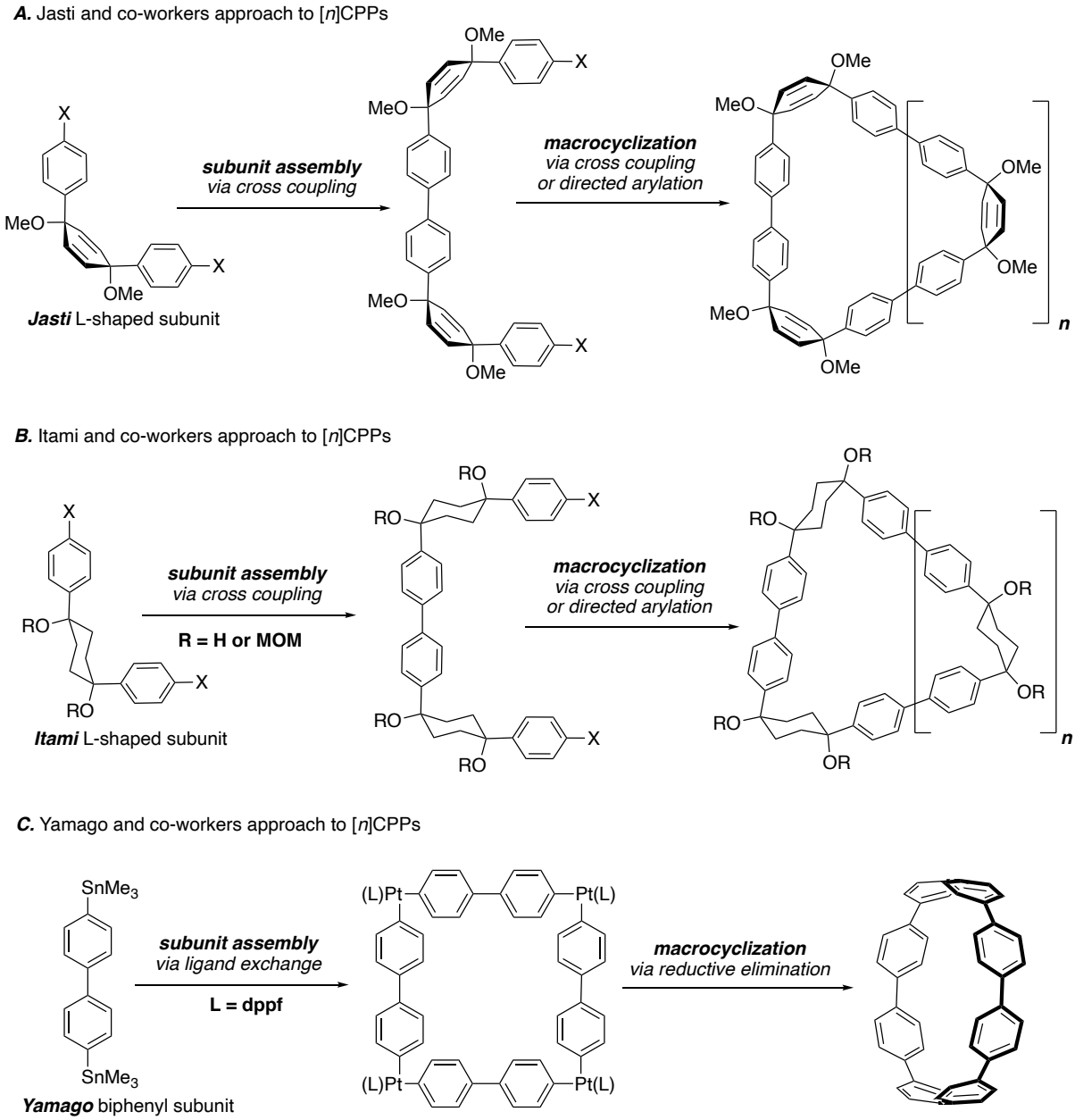

Figure 14. Generalized approaches to [*n*]CPPs

3 Timeline of the development of strained [*n*]CPP syntheses

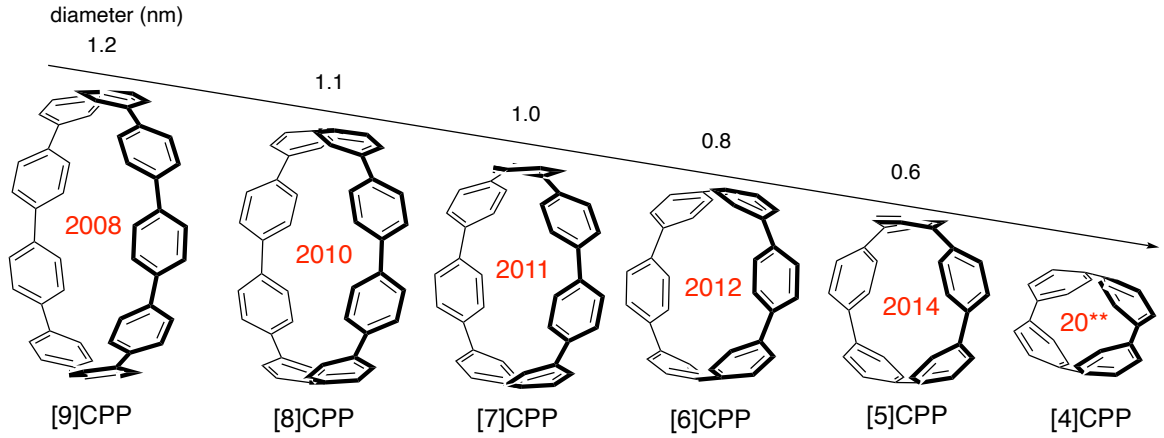

Figure 15. Timeline of the development of CPPs

The first and most strained [*n*]CPP to be synthesized, was [9]CPP, which was reported by Bertozzi and co-workers in late 2008 using a shotgun, Suzuki coupling-based macrocyclization. Using a subunit akin to Jasti's L-shaped subunit (Figure 14A) for macrocyclization, [9], [12] and [18]CPP were produced during this seminal report. Essentially, the next three smallest homologs, [8], [7], and [6]CPP, respectively, were synthesized one year apart from each other (Figure 15). The development of slightly modified macrocyclization strategies were necessary to accomplish the synthesis of the increasingly strained carbon nanohoops, and it took nearly two years move from [6] to [5]CPP. As described above, two similar approaches were reported by Yamago and Jasti, which relied on modified macrocyclization and aromatization protocols. It has been over seven years since the synthesis of [5]CPP was reported, and to the best of my knowledge, no synthesis or approach to [4]CPP has been reported at the time of preparing this thesis. The main objectives of this project are to develop a novel, cyclophane-based approach to both [5] and [4]CPP. The synthesis of [5]CPP will be pursued initially validate the proposed synthetic strategy and develop the necessary skeletal building reactions that will be employed in the assembly of [4]CPP and its synthetic precursors.

4 A novel cyclophane-based approach to [*n*]CPPs (n = 4 and 5)

One of the major areas of interest in the Merner laboratory is the synthesis of strained macrocyclic systems from unstrained macrocyclic precursors. A new synthetic strategy that employs a relatively unstrained, 1,4-diketo-bridged macrocycle as precursor to a strained 1,4-

arene-bridged (bent *para*-phenylene) macrocycle was reported by Merner and co-workers in 2015 (Figure 16A).[18]

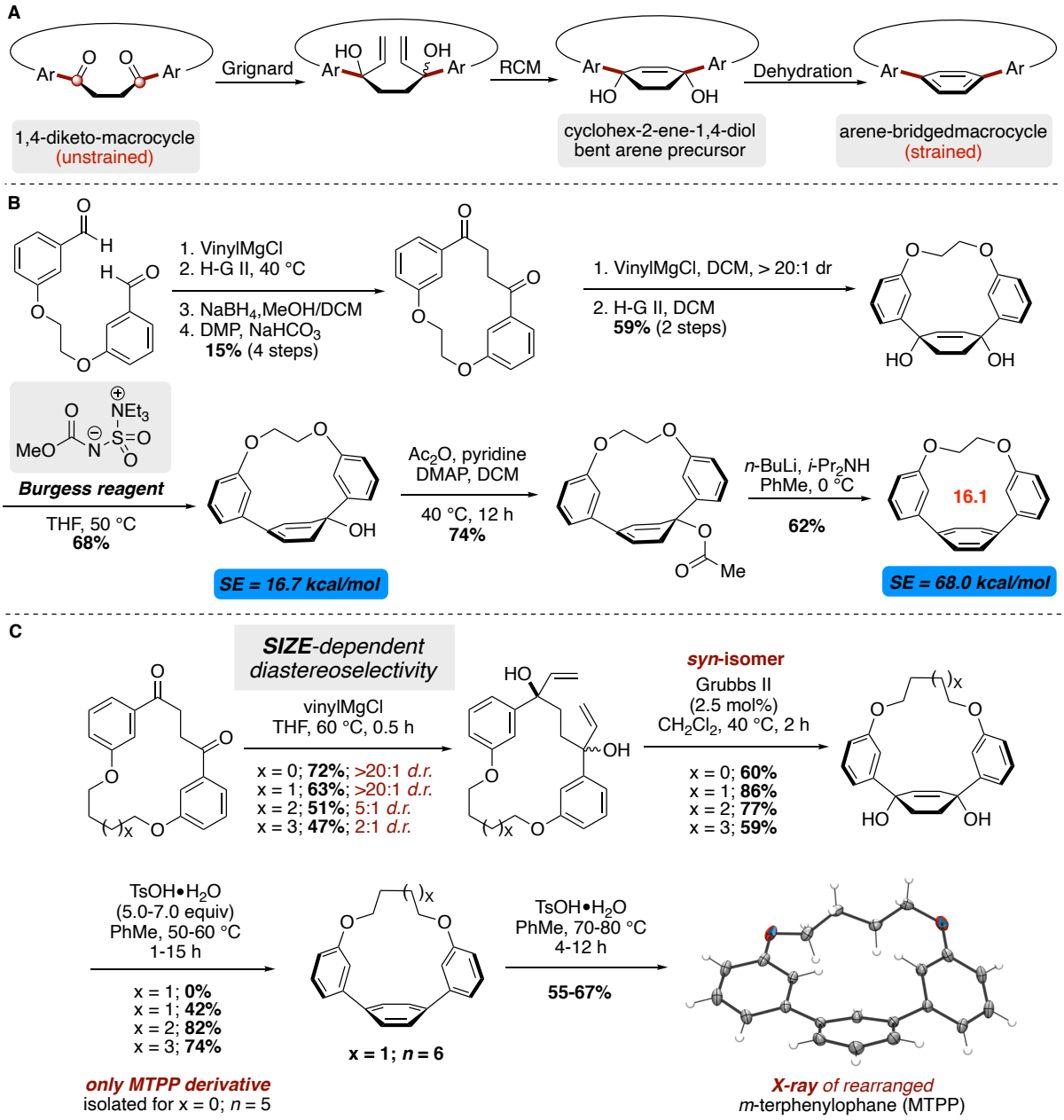

Figure 16. Synthesis of strained benzenoid macrocycles

This approach utilizes a streamlined synthesis of macrocyclic 1,4-diketones, which can be subsequently transformed into strained benzenoid macrocycles and represents a new approach for the synthesis of benzenoid segments of CNTs. This strategy was employed during the synthesis of a highly strained *p*-terphenyl-containing macrocycle in 2016 (Figure 16B). The central *para*-phenylene ring of **16.1** is predicted to be more strained (SE = 43

kcal/mol) than a *para*-phenylene monomer unit of [4]CPP (SE = 36 kcal/mol).[19] Moreover, this highly strained *para*-phenylene unit still retains its aromatic character.

In the same year, Merner and co-workers reported a detailed investigation of aromatization protocols for converting different macrocyclic cyclohex-2-ene-1,4-diols into highly strained *para*-phenylene units. These findings demonstrate that 1,4-diketones are suitable surrogates to strained arene unites[20] (Figure 16C). The success of our research program, directed towards the synthesis of highly strained benzenoid systems, instills great confidence that the syntheses of [5] and [4]CPP will succumb to the proposed cyclophane-based approaches.

Synthetically, the biggest challenge for the generation of [*n*]CPPs is the formation of macrocycle which usually contains high levels of intrinsic ring strain, mostly resulting from the connection of benzene rings in *para*-positions. It has been 8 years since chemists synthesized [5]CPP in 2014, 8 years gap suggests that [4]CPP is much more challenging than other CPPs syntheses and looks like will need both modified macrocyclization and aromatization strategies to the formation of this highly strained cycloparaphenylenes. The strain introduced at the last step of the synthesis of compound **16.1** (Figure 16B) is 51kcal/mol which indicates that this method may be utilized for introducing the strain energy into the aromatization step of [4]CPP synthesis. A novel strategy for the synthesis of strained benzenoid macrocyclic systems aimed at the development of synthetic tools for a bottom-up approach to carbon nanohoops and nanobelts has been developed in our laboratory over the past 8 years. The approach utilizes a streamlined synthetic protocol to furnish gram-scale quantities of macrocyclic 1,4-diketones, that can be viewed as [*n*.4]metacyclophanes, which can be further transformed into highly strained benzenoid macrocycles, using ring-closing metathesis and dehydration reactions, respectively. One of the main advantages of this approach is that it avoids cross-coupling reactions in the production of biaryl bonds, which have been problematic in macrocyclization reactions. Furthermore, using the 1,4-diketo-bridging group as an arene convertible unit, helps relieve strain within the macrocyclic backbone of the desired sub-targets, en route to highly strained benzenoid macrocycles. The syntheses reported to date for [5]CPP, the smallest and most strained CPP to be synthesized, seem unsuitable for the preparation of a macrocyclic precursor to [4]CPP.

5 Retrosynthetic analysis of [*n*]CPP (n = 4 and 5)

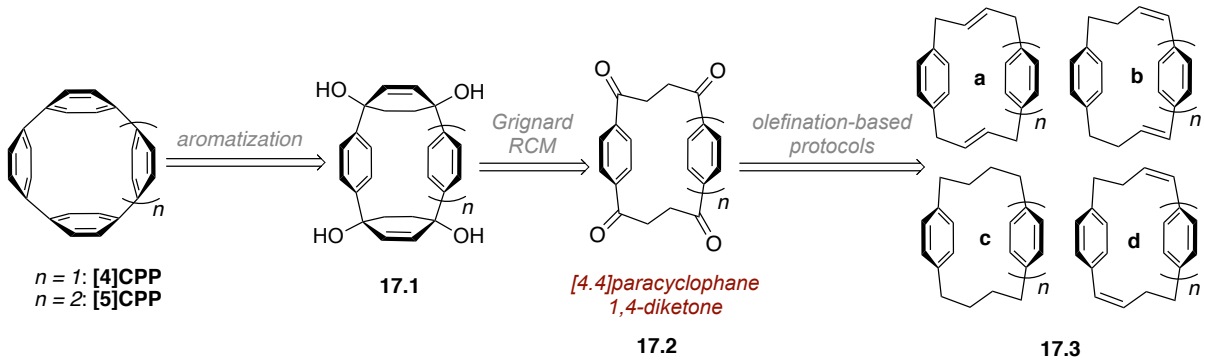

Figure 17. Retrosynthetic analysis of CPPs

The retrosynthetic analysis of this strategy is described in Figure 17, it was envisaged that CPPs could be accessed from macrocyclic precursor tetraol **17.1**, which includes two pre-arene unites and two or three arene units. Two pre-arene units could be simplified to [4.4]paracyclophane 1,4-diketone **17.2**, which can be prepared through olefination-based approaches from either one of macrocyclic **17.3** (a-d) by oxidizing benzylic or allylic position.

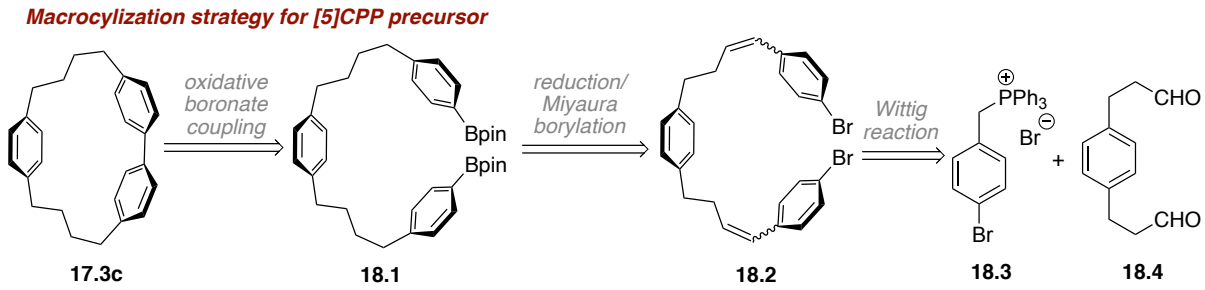

Figure 18. Retrosynthetic analysis of [5]CPP precursor **17.3c** (n =2)

6 Attempt synthesis of [5]CPP

Macrocycle **17.3c** (*n* = *2*) is representative of the targets that will be synthesized and the strategies that will be pursued, and thus will be the focus of the remaining discussion of my disconnective analysis. Cyclophane **17.3c** (*n* = *2*) can be brought back to bis-boronate **18.1**, which, in the forward sense, can be subjected to an oxidative boronate coupling reaction that has proven to be a powerful synthetic tool for macrocyclization. Bis-boronate **18.1** can be formed from dibromide **18.2** through reduction and Miyaura borylation. Compound **18.2** can be synthesized from two compounds that are easy to prepare via a Wittig reaction.

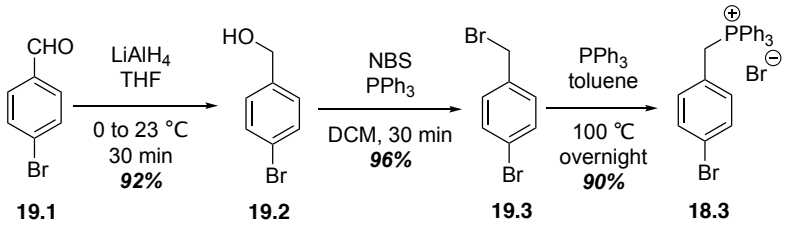

Figure 19. Synthesis of phosphonium salt **18.3**

The synthesis macrocycle **17.3c** (*n* = *2*) commenced with the preparation of two key building blocks, phosphonium salt **18.3** and dialdehyde **18.4**. The inner salt **18.3** was synthesized from 4-bromobenzaldehyde over three steps (Figure **19**). First, 4-bromobenzaldehyde **19.1** was being reduced by $LiAlH_4$ to afford primary alcohol **19.2** in 92% yield, followed by the Appel reaction with NBS and PPh_3 gave 1-bromo-4(bromomethyl)benzene **19.3** in 96% yield. Treatment **19.3** with PPh_3 in toluene afforded inner salt **18.3** in 90% yield.

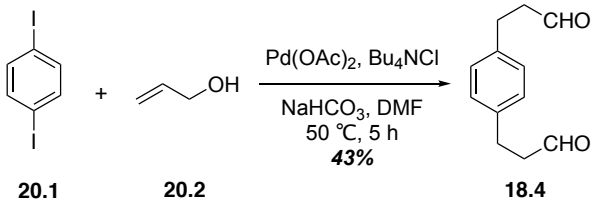

Figure 20. Synthesis of dialdehyde **18.4**

The dialdehyde **18.4** is being prepared via the Pd-catalyzed allylic alkylation 1,4-diiodobenzene **19.1** and allylic alcohol **19.2** in the presence of base and phase transfer catalyst (Figure **20**). Then the Wittig reaction was conducted using inner salt **18.3 and** dialdehyde **18.4** in the presence of 18-crown-6 and KOH to generate diene **18.2** in 98% yield as a mixture (*Z*,*Z*/*E*,*E*/*Z*,*E*) of isomers (**Figure 21**). After reducing the olefins with Pd/C, dibromo **21.1** was converted to diboronate ester **18.1** through lithium-halogen exchange followed by subsequent trapping of the reactive species with (isopropoxy)pinacolborane in 59% yield. Using a palladium-catalyzed oxidative boronate homocoupling performed under air at room temperature, macrocycle **17.3c** (n = 2) was prepared in 51% yield.

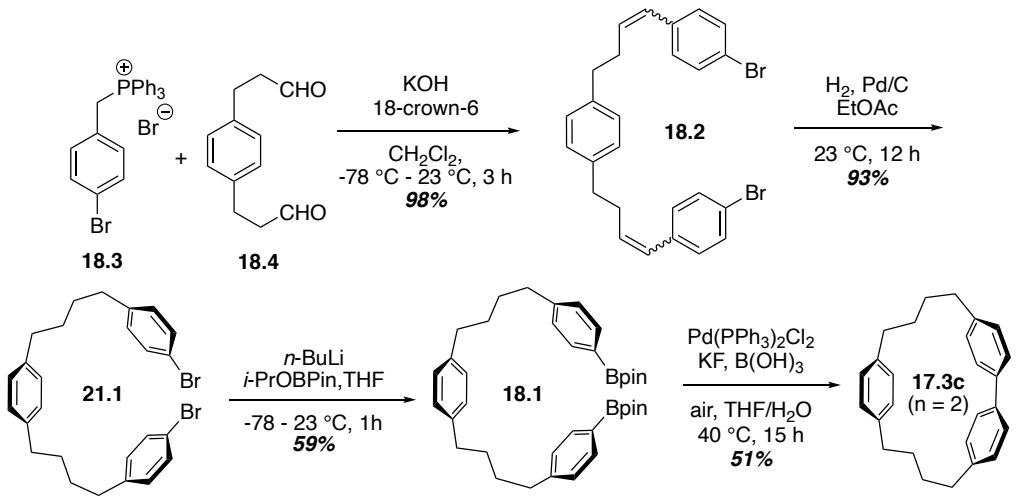

Figure 21. Synthesis of macrocycle **17.3c** (n = 2)

Unfortunately, the attempted global benzylic oxidation of macrocycle **17.3c** (n = 2) in the presence of $FeCl_3 \cdot H_2O$/*t*-BuOOH did not afford tetraketone **17.2** (n = 2), but rather gave diketone **22.1** in 20% yield after 4days (Figure 22).

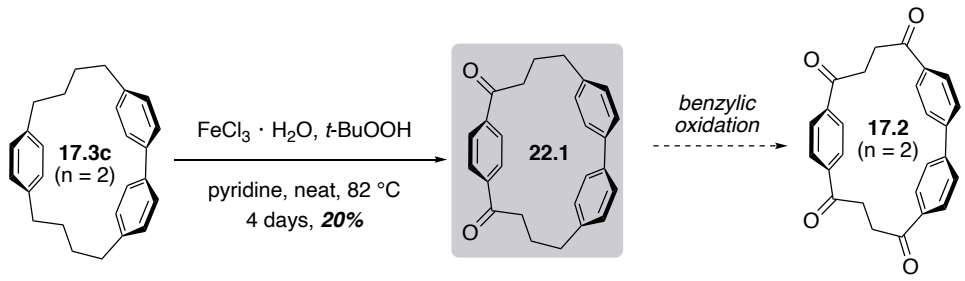

Figure 22. Attempted benzylic oxidation of macrocycle **17.3c** (n =2)

Starting from compound **17.3c** (n = 2), several sets of benzylic oxidation conditions have been attempted to data (Figure 23), however, successful passage to the desired tetraketone **17.2** (n = 2) has not been possible. It appears that the activity of benzylic positions at compound **17.3c** (n = 2) is less than linear ones due to the configuration of the molecule.

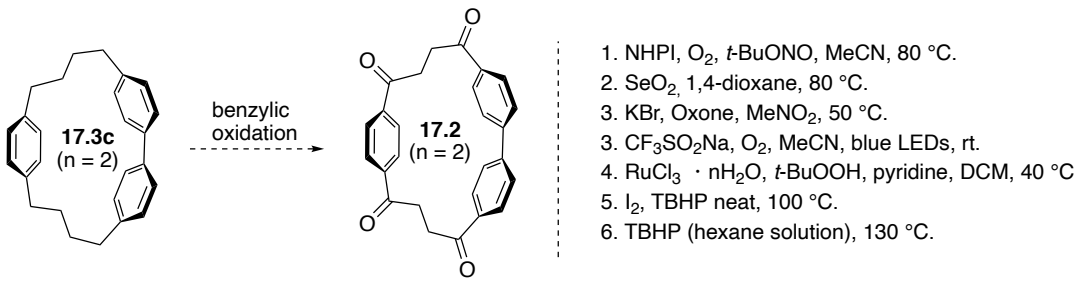

Figure 23. Attempted benzylic oxidation

Not only benzylic oxidation reactions but a serious of the benzylic bromination reactions also have been attempted on compound **17.3c** (n = 2) (Figure 24). Unfortunately, no desired tetrabrominated compound was obtained.

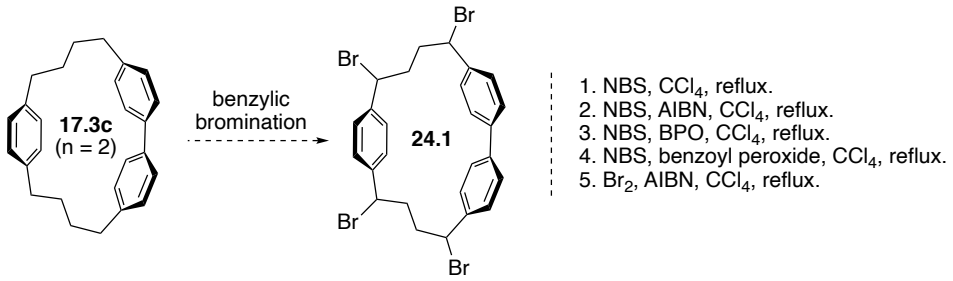

Figure 24. Attempted benzylic bromination

It is unclear at this juncture as to why oxidation of the remaining benzylic positions of **17.3c** (n = 2) has not been successful. One possibility is that the introduction of the ketone functional group at the desired positions may increase the strain energy within the macrocyclic framework of **17.3c** (n = 2). Furthermore, the arene unit that bridges these positions in **17.3c** (n = 2) is different from the biaryl, arene unit, which has the desired ketone units adjacent to the arenes. To avoid the strain energy, a different [5]CPP precursor has been synthesized.

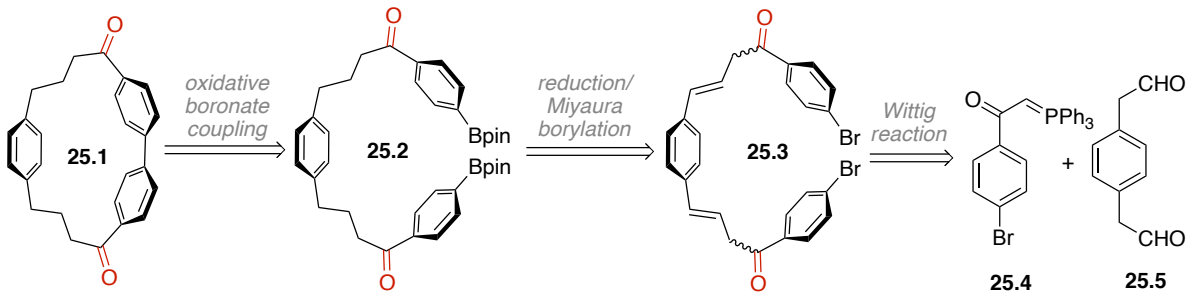

Figure 25. Retrosynthetic analysis of [5]CPP precursor **25.1**

The retrosynthetic analysis of this strategy is described in Figure 25, diketone **25.1** can be brought back to bis-boronate **25.2**, which, in the forward sense, can be subjected to an oxidative boronate coupling reaction. Bis-boronate **25.2** can be formed from dibromide **25.3** through reduction and Miyaura borylation. Same as the previous strategy, compound **25.3** can be synthesized from two compounds that are easy to prepare via a Wittig reaction from phosphoris ylide **25.4** and aldehyde **25.5**.

The synthesis of diketone **25.1** commenced with the preparation of two key building blocks, phosphoris ylide **25.4** and dialdehyde **25.5**, both of these compounds are accessible from commercially available chemicals. The synthesis of ylide was followed a typical procedure (Figure 26), bromination of 4'-bromoacetophenone **26.1** gave 2-bromo-4'-bromoacetophenone **26.2** in 90% yield, followed by treatment with PPh_3 in DCM afforded the inner salt **26.3** in 95%, under basic condition, the inner salt will convert to phosphoris ylide **25.4** which is more stable at ambient.

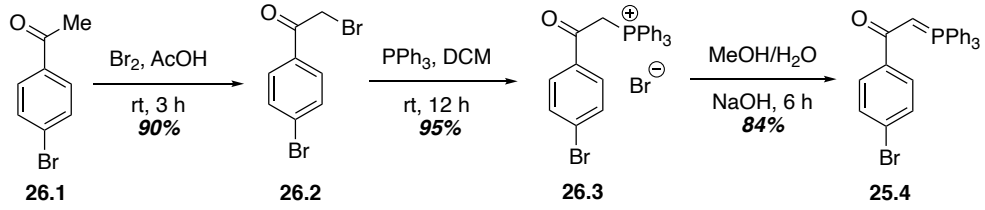

Figure 26. Synthesis of phosphoris ylied **25.4**

Another Witting reaction reactant dialdehyde **25.5** was synthesized over three-steps from commercially available chemical *p*-phenylenediacetic acid **27.1** through an esterification-reduction-oxidation sequence in 61% overall yield.

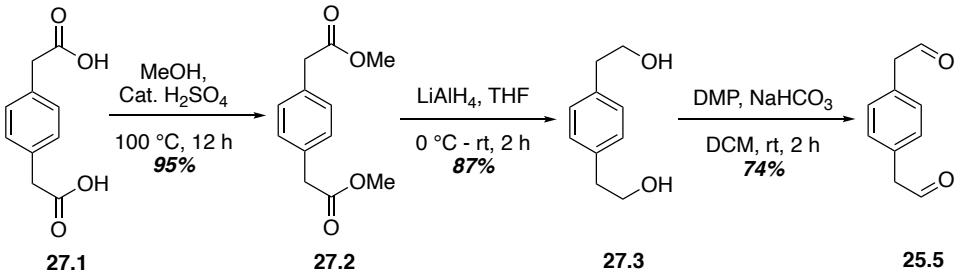

Figure 27. Synthesis of dialdehyde **25.5**

Treatment phosphoris yield **25.4** with dialdehyde **25.5** to afford dienone **25.3** as a mixture of olefin isomers in 90% yield (Figure 28). Catalytic hydrogenation of the olefin units in **25.3** was achieved in 84% yield to furnish dibromo-diketone **28.1**, which was subsequently subjected to Miyaura borylation to afford bis-boronate **25.2** in 52% yield. Employing the same palladium-catalyzed oxidative boronate coupling reaction as described above, gave macrocycle **25.1** in 55% yield.

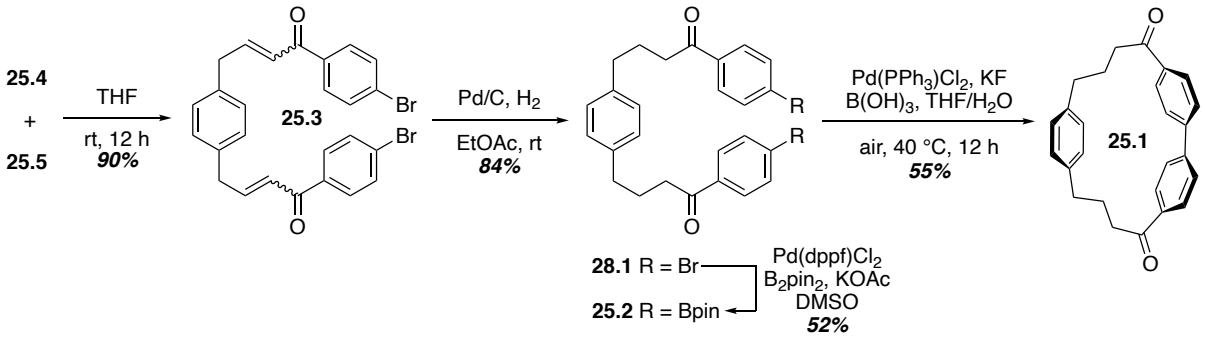

Figure 28. Synthesis of macrocycle **25.1**

So far, the most advanced stage compounds are diketones **22.1** and **25.1**, to understand the reactivity of benzylic positions of **25.1**, a series of benzylic oxidation of **25.1** was attempted by my colleague, unfortunately, no desired product was achieved.

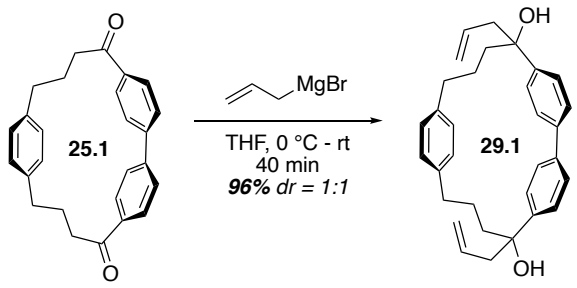

Figure 29. Grignard addition on **25.1**

Alternatively, we tried to convert the sp^2 carbonyl carbon to sp^3 carbon to reduce the molecule strain. From the most advanced stage diketone **25.1**, Allyl Grignard addition gave allylic diol compound **29.1** in 96% yield with a mixture of two diastereomers (dr = 1:1) (Figure 29).

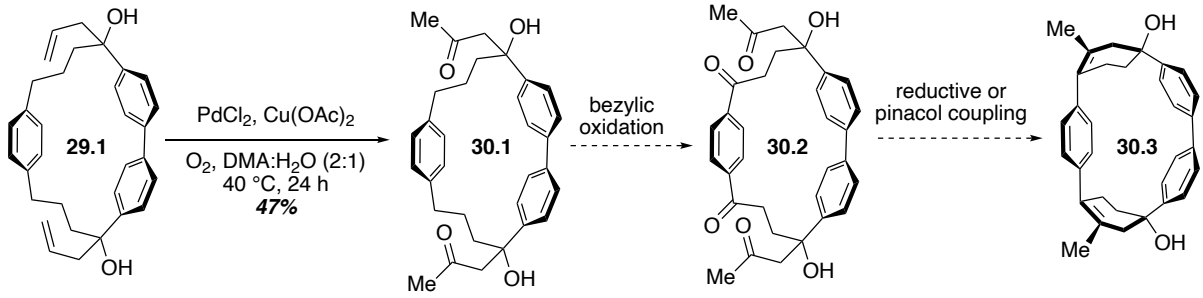

Figure 30. Wacker-Tsuji oxidation of **29.1** and end-game strategy for the synthesis of [5]CPP

A Wacker-Tsuji oxidation reaction was conducted on compound **29.1**, the desired diketone-diol compound **30.1** was observed from crude NMR (Figure 30). At this stage, benzylic oxidation of **30.1** will give the coupling precursor tetraketone-diol compound **30.2**, Intermolecular reductive coupling or pinacol coupling of compound **30.2** will give [5]CPP derivative precursor macrocycle **30.3**, then, late-stage dehydrative aromatization of these two precursors will form [5]CPP derivative. Unfortunately, the story ends here, due to the time constraints and other ongoing projects, no further experiments were carried out on this material.

7 Attempt synthesis of [4]CPP

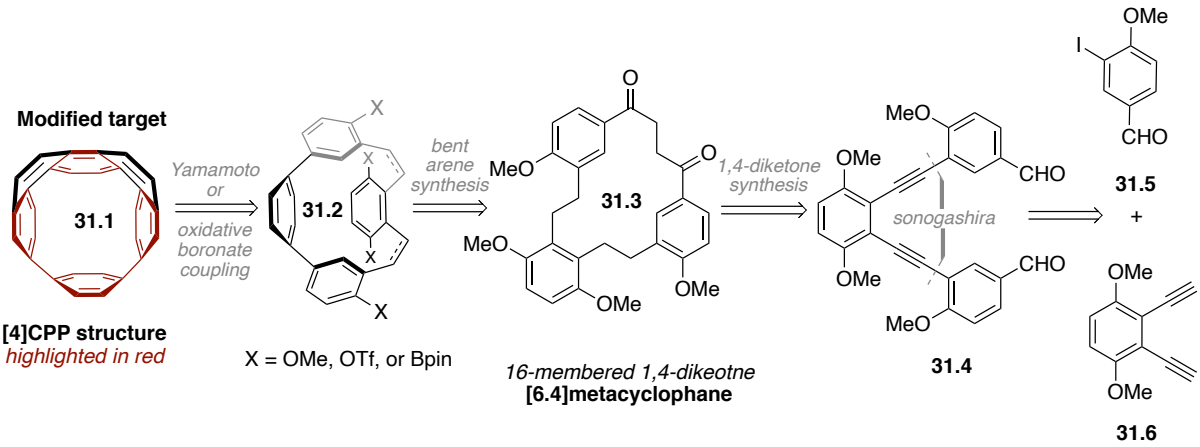

Figure 31. Retrosynthetic strategy of modified [4]CPP **31.1**

Along with the syntheses of [5]CPP, we also tried to synthesize a modified [4]CPP compound. Retrosynthetically, the modified [4]CPP target **31.1** (highlight in red, Figure 31) could be accessed from macrocycle **31.2** via a Yamamoto or oxidative boronate coupling. Macrocycle was expected to be generated from 1,4-diketone **31.3** through a stepwise Grignard and ring-closing metathesis strategy. 1,4-diketone could be further disconnected to dialdehyde **31.4** which could be assembled through a Sonogashira reaction from two easily accessed compounds **31.5** and **31.6**.

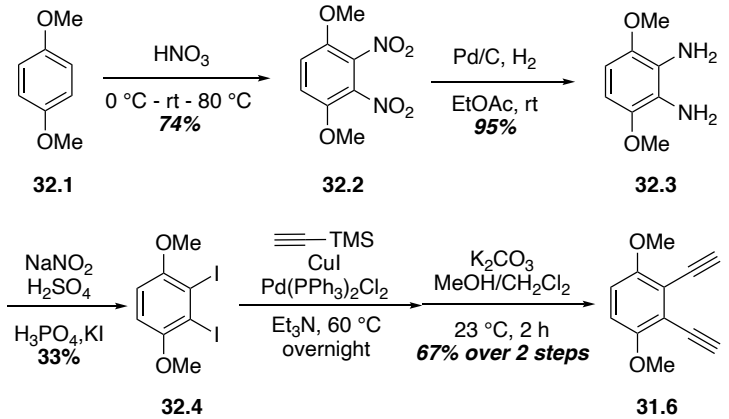

Figure 32. Synthesis of starting material **31.6** for Sonogashira reaction

The synthetic approach to modified [4]CPP commenced with the synthesis of starting material for Sonogashira reaction, as shown in Figure 32, dinitration of 1,4-dimethoxybenzene **32.1** gave 2,3-dinitro-1,4-dimethoxybenzene **32.2** in 74% isolated yield. Catalytic

hydrogenation with H_2 and Pd/C afforded the diamine **32.3** in 95% yield. Tetrazotation and subsequent Sandmeyer reaction gave 1,4-dimethoxy-2,3-diiodobenzene **32.4** in 33% yield. And we found that careful control of temperature and addition rate was crucial for reproducible results. Sonogashira cross-coupling with ethynyltrimethylsilane followed by desilylation gave 2,3-diethynyl-1,4-dimethoxybenzene **31.6** in 67% over two steps.

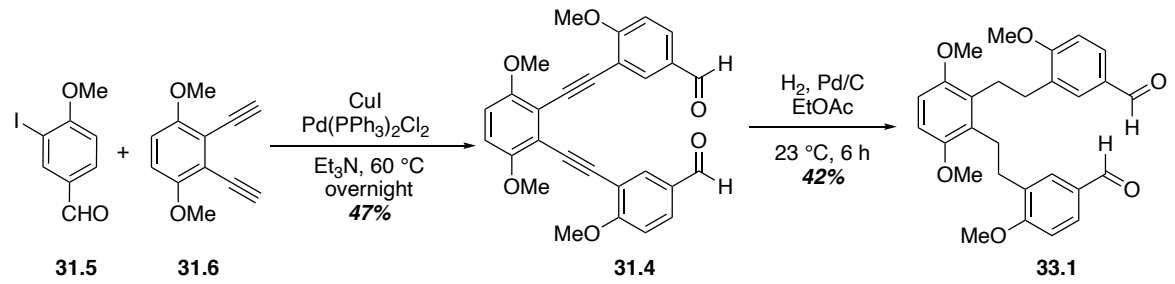

Figure 33. Sonogashira reaction and reduction of compound **31.4**

Subsequently, another Sonogashira reaction of alkyne **31.6** and aryl iodide **31.5** led to dialdehyde **31.4** in 47% yield, which then was reduced to dialdehyde **33.1**. This reduction step has to be monitored closely by TLC because the aldehyde groups on compound **31.4** could be easily over-reduced to methyl groups.

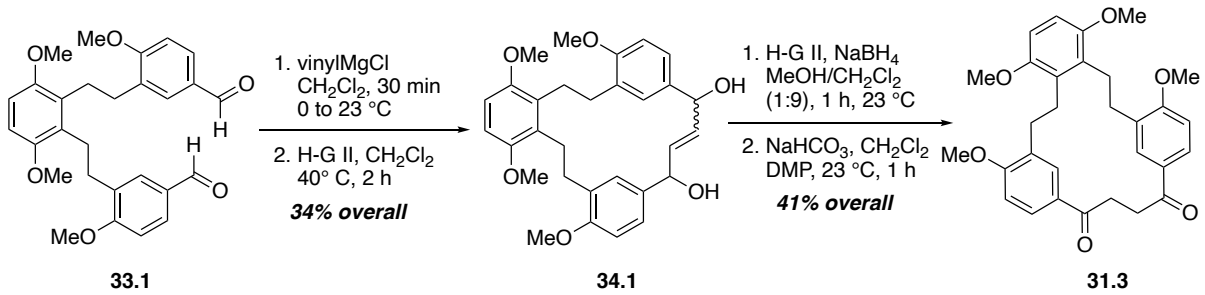

Figure 34. The syntheses of compound **31.3**

After reduction of the alkynes, a rapid protocol for the conversion of dialdehydes into macrocyclic 1,4-diketones was applied to dialdehyde **33.1**, Grignard reaction of **33.1** with vinylMgCl followed by a macrocyclic ring-closing metathesis (RCM) reaction gave macrocyclic diol **34.1** in 34% yield over two steps. Diol **34.1** was then subjected to transfer hydrogenation conditions and oxidized by Dess-martin periodinane to macrocyclic diketone **31.3** in 41% overall yield.

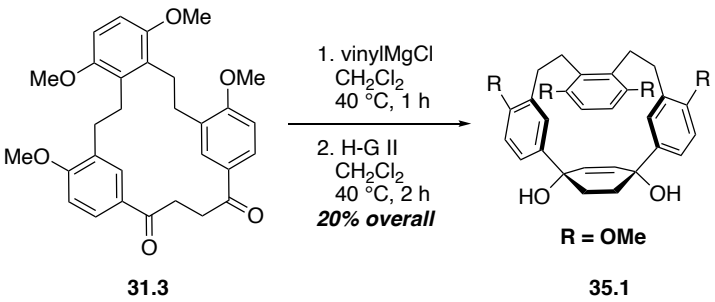

Figure 35. RCM reaction of **31.3**

The Grignard reaction of **31.3** with vinylMgCl afforded allylic diol as a 3:1 mixture of *syn*/*anti* diastereomers, with only the major diastereomer undergoing cyclization when treated with the HG-II catalyst to afford **35.1** in 20% overall yield.

Direct aromatization of **35.1** was accomplished using Burgess reagent-mediated dehydrative aromatization reaction to afford the *p*-phenylene unit **31.2** in 60% yield. Unfortunately, the demethylation of compound **31.2** was unsuccessful. No further reactions were carried out at this stage due to the lack of compound **31.2**. However, the syntheses of **31.1** and **31.2** leave these portions of the projects in a great place for a new graduate student to take over.

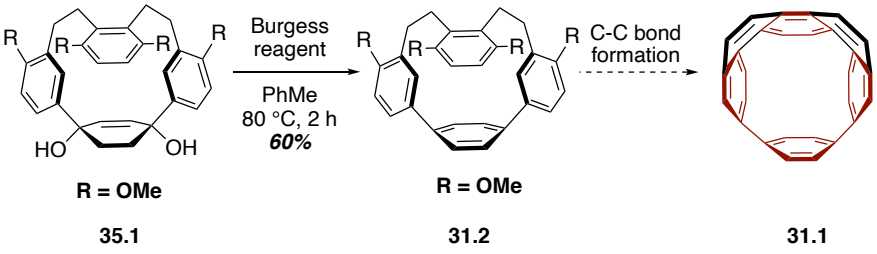

Figure 36. Aromatization of **35.1**

8 Conclusion

Highly strained hydrocarbons have captivated synthetic and physical organic chemists for decades because of their challenging structures and unique properties. [5]CPP still remains as the smallest carbon nanohoop to be synthesized. The next big advancement for this field of chemical synthesis will be the synthesis of [4]CPP. The Merner lab has developed a suitable strategy for assembling the macrocyclic framework of [4]CPP and they have also developed

an aromatization strategy capable of synthesizing a benzene ring that is more strained than a monomer unit of [4]CPP.

Reference

[1] S. Iijima, *Nature* **1991**, *354*, 56.

[2] M. Dresselhaus, G. Dresselhaus, P. Avouris, Carbon Nanotudes: *Synthesis Properties, Applications, Springer, Berlin*, **2001**.

[3] a) P. Avouris, Z. Chen, V. Perebeinos, *Nat. Nanotechnol.* **2007**, *2*, 605; b) P. Avouris, M. Freitag, V. perebeinos*, Nat. Photonics* **2008**, *2*, 341; c) V. Sgobba, D. M. Guldi, *Chem. Soc. Rev.* **2009**, *38*, 165.

[4] M. S. Dresselhaus, G. Dresselhaus, R. Saito, *Carbon* **1995**, *33*, 883.

[5] V. C. Parekh, P. C. Guha, *J. Indian Chem. Soc*., **1934**, *11*, 95.

[6] D. T. M. Wong and C. S. Marvel, *J. Polym. Sci., Polym. Chem. Ed.,* **1976**, *14*, 1637.

[7] Y. Miyahara, T. Inazu, and T. Yoshino, *Tetrahedron Lett*. **1983**, *24*, 5277.

[8] J. Franke, and F. Vogtel, *Tetrahedron Lett*. **1984**, *25*, 3445.

[9] J. E. McMurry, G. J. Haley, J. R. Matz, J. C. Clardy and J. Mitchell, *J. Am. Chem. Soc*. **1986**, *108*, 515.

[10] R. Friederich, M. Nieger, and F. Vogtel*, Chem. Ber.,* **1993**, *126*, 1723.

[11] S. Kammermeier, P. G. Jones and R. Herges, *Angrew. Chem. Int. Ed.,* **1996**, *35*, 2669.

[12] O. M. Yaghi, H. Li, and T. L. Groy, *Z. Kristallogr. -New Cryst. Struct.,* **1997**, *212*, 453.

[13] M. Machon, S. Reich, J. Maultzsch, H. Okudera, A. Simon, R. Herges and C. Thomsen, *Phys. Rev. B: Condens. Matter mater. Phys.,* **2005**, *72*, 155402.

[14] R. Jasti, J. Bhattacharjee, J. B. Neaton, C. R. Bertozzi, *J. Am. Chem. Soc.* **2008**, *130*, 17646.

[15] H. Takaba, H. Omachi, Y. Yamamoto, J. Bouffard, K. Itami, *Angew. Chem., Int. Ed.,* **2009**, *48*, 6112.

[16] S. Yamago, Y. Watanabe, T. Iwamoto, *Angew. Chem., Int. Ed.,* **2010**, *49*, 757.

[17] a.) Y. Segawa, P. Senel, S. Matsuura, H. Omachi, K. Itami, *Chem. Lett.* **2011**, *40*, 423. b.) T. Iwamoto, Y. Watanabe, Y. Sakamoto, T. Suzuki and S. Yamago, *J. Am. Chem. Soc.* **2011**, *133*, 8354. c.) T. Sisto, M. Golder, E. S. Hirst, R. Jasti, *J. Am. Chem. Soc.* **2011**, *133*, 15800. d.) Y. Ishii, Y. Nakanishi, H. Omachi, S. Matsuura, K. Matsui, H. Shinohara, Y. Segawa, K. Itami, *Chem. Sci.,* **2012**, *3*, 2340. e.) E. Darzi, T. Sisto, R. Jasti, *J. Org. Chem*. **2012**, *77*, 6624. f.) T. Sisto, R. Jasti, Synlett **2012**, *23*, 483. g.) J. Xia, R. Jasti, *Angew. Chem., Int. Ed.,* **2012**, *51*, 2474. h.) E. Kayahara, T. Iwamoto, T. Suzuki, S. Yamago, *Chem. Lett.* **2013**, *42*, 621. i.) E. Kayahara, V. K. Patel, S. Yamago. *J. Am. Chem. Soc.* **2014**, *136*, 2284. j.) F. Sibbel, K. Matsui, Y. Segawa, A. Studer, K. Itami, *Chem. Commun.,* **2014**, *50*, k.) P. Evans, E. Darzi, R. Jasti, *Nature Chem.* **2014**, *6*, 404. l.) J. Lin, E. Darzi, R. Jasti, I. Yavuz, K. N. Houk, *J. Am. Chem. Soc.* **2019**, *141*, 17646.

[18] N. K. Mitra, R. Meudom, J. D. Gorden, B. L. Merner, *Org. Lett.* **2015**, *17*, 2700.

[19] N. K. Mitra, H, Corzo, B. L. Merner, *Org. Lett.* **2016**, *18*, 3278.

[20] N. K. Mitra, R. Meudom, H, Corzo, J. D. Gorden, B. L. Merner, *J. Am. Chem. Soc.* **2016**, *138*, 3235.

Chapter 2 Synthesis of hexa-substituted pyrenes and their application to curved polycyclic aromatic hydrocarbon

9 Introduction

Pyrene ($C_{16}H_{10}$) is a fascinating fluorophore and one of the most promising starting materials for developing improved optoelectronic materials. Many important hydrocarbon materials contain pyrene units within their structures. These include, coronene, C_{70} fullerene (ADD), and armchair carbon nanonanotubes (CNTs, Figure 37). Pyrene's unique photophysical properties have inspired many scientists across the chemical disciplines since it was first discovered by Laurent in 1837 as a residue of the distillation of coal tar.[1] Since then, this polycyclic aromatic hydrocarbon (PAH) has been the subject of tremendous investigation.[2]

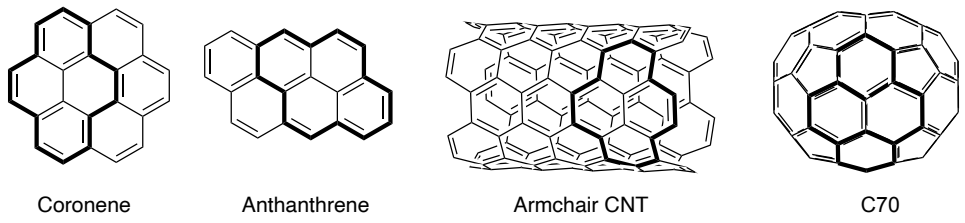

Figure 37. Pyrene unit in different PAHs

Pyrene is also prepared via several pyrolytic processes. For instance, by pyrolysis of acetylene and hydrogen,[3] in the destructive distillation of soft coal tar, by the zinc-dust distillation of thebenol and thebenin,[4] and from petroleum by the catarol process.[5] The first chemical synthesis of pyrene was reported by Weitzenbock in 1913 (Figure 38).[6]

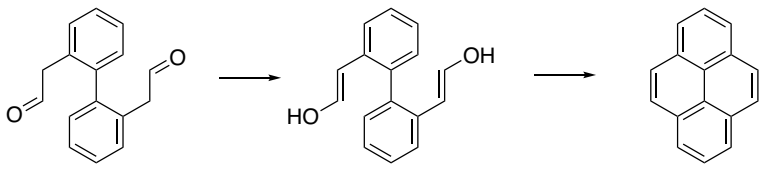

Figure 38. Synthesis of pyrene by Weitzenbock

Electrophilic aromatic substitution reactions of pyrene have been well studied and multiple procedures for bromination, nitration, acylation, alkylation, and formylation have been reported. While numerous protocols have been described, there are still several

regioselectivity issues for pyrene substitution chemistry. Since pyrene is such a valuable building block in the development of new electronic materials, access to regioselectivily functionalized and substituted pyrene derivatives is highly desirable. The electrophilic aromatic substitution of pyrene normally occurs at the 1-, 3-, 6-, and 8-positions (Figure 39), owing to increased electron density at these carbon atoms.[7-10] The exception to this, is when bulky or sterically hindered electrophiles are employed in these reactions. For example, *tert*-butylation of pyrene takes place at the 2 or 2 and 7-positons, due to an unfavorable steric interaction that arises between the incoming electrophile and the proton at the 10 position.[11] This type of steric clash is known as a *peri*-interaction in the world of polycyclic aromatic hydrocarbons.

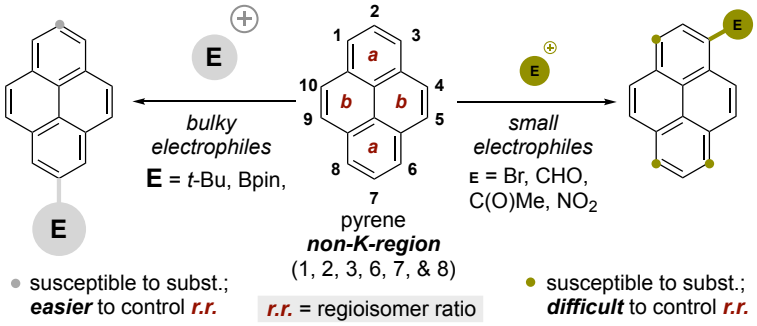

Figure 39. General approaches to mono-functionalize pyrene

The preparation and purification of mono-substituted pyrene is relatively easy, allowing the introduction of simple, unfunctionalized pyrene units into designed molecular architectures that can possess interesting optoelectronic properties. However, the selective preparation of disubstituted pyrene derivatives is considerably more challenging, but highly desirable with respect to pyrene-based materials synthesis. The following sections will discuss the incorporation of disubstituted pyrene building blocks in the controlled synthesis of linear or cyclic oligomers as well as pyrene-based polymers.

9.1 The synthesis of mono-substituted pyrene derivatives

The most common chemical reactions used to prepare mono-substituted pyrene derivatives are bromination, formylation and acylation, for selective substitution of the 1-position, while alkylation and borylation have been used to substitute the 2-position of pyrene selectively. In the case of electrophilic bromination, no Lewis acid catalyst is required as is the case for benzene. In fact, pyrene can be exhaustively brominated to afford 1,3,6,8-tetrabromopyrene

by heating a solution of pyrene with over 4 equivalents of bromine in nitrobenzene (Figure 40, A).[12] After substitution of the 1-position has taken place, there are three possible di-substituted pyrenes that can form. The 1,3-disubstiution pattern is the lowest yielding substitution product as substitution of the 1-posiiton (initially) seems to attenuate the nearby 3-positon. Subsequent substitution of the 6- or 8-positions to afford 1,6 and 1,8-disubstitution seems to take place at identical rates, as equal amounts of these isomers are formed; however, separation of these isomers can be problematic. Bromopyrene derivatives are important starting materials for cross-coupling reactions, and thus desirable for the synthesis of new, conjugated pyrene-based materials. The discussion below will describe how selective bromination reactions can be employed in the synthesis of polyfunctionalized pyrene derivatives.

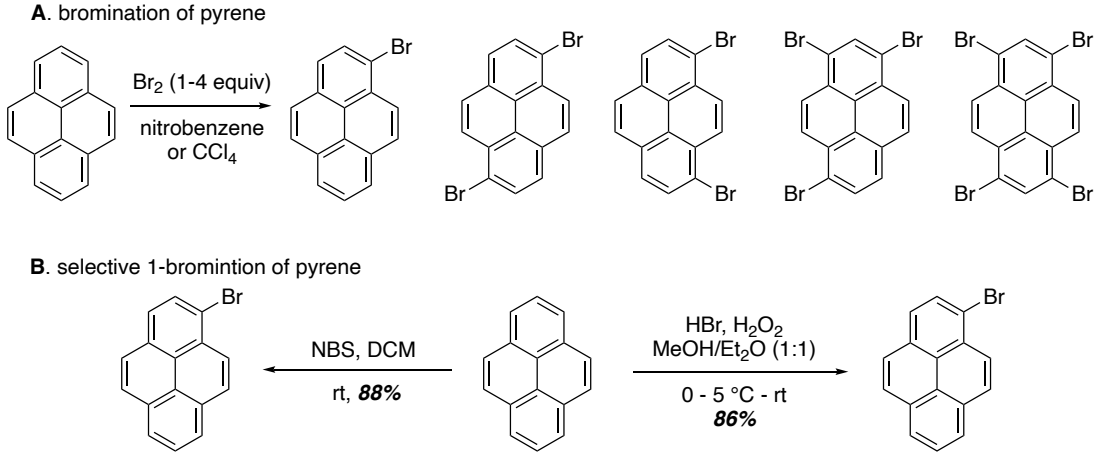

Figure 40. Bromination of pyrene

In recent years, more reagents were developed to exclusively obtain 1-bromopyrene in high yields. For example, with NBS as the bromination reagent,[13] DCM as the solvent, 1-bromopyrene was obtained in 88% yield as a light-yellow solid. When using HBr and H_2O_2 as the bromination reagent,[14] MeOH/Et_2O (1:1) as the solvent, 1-bromopyrene was obtained in 86% yield (Figure 40).

1-Acetylpyrene can be synthesized via a Friedel-Crafts acylation reaction.[15] Monoacetylation can be achieved when pyrene is treated with acetic anhydride in the presence of boron trifluoride dimethyl sulfide complex to give **40.1** in 88% yield (Figure 41).[16] Acetylation of pyrene under the conditions of aluminum trichloride and acetyl chloride in dichloromethane, requires low temperatures and carefully controlled reagent equivalents. Even a slight excess of reagent and increase in temperature will lead to bis-acetylation. Thus, it is not surprising to find that this method leads to lower yields of **40.1,** (*e.g.*, 65%, Figure 41).

In later sections, selective acetylation reactions of functionalized pyrene derivatives will be discussed.

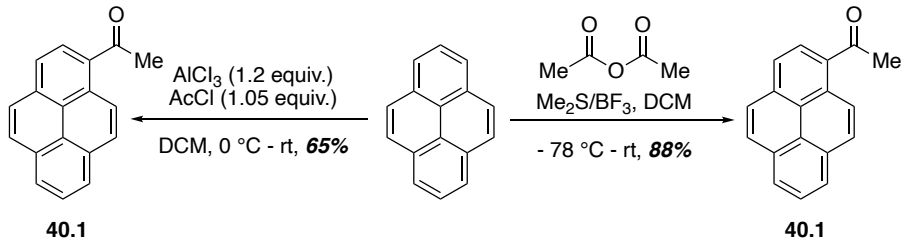

Figure 41. Acylation of pyrene

Monoformylation of pyrene, to afford 1-formylpyrene, can be achieved using either the Rieche or Vilsmeyer formylation reaction in high yields (Figure 42, A).[17] Unlike acetylation, over formylation is not a concern for this reaction, even when it is employed to more highly substituted pyrene derivatives. For example, Merner and co-workers have reported that formylation of 4,5-dimethoxypyrene only takes place at either the 1 or 3-position of pyrene with variable regioselectivity (Figure 42, B).[18] Even under forcing conditions, a second formylation reaction does not take place. Again, the introduction of the formyl group seems to attenuate further substitution of pyrene.

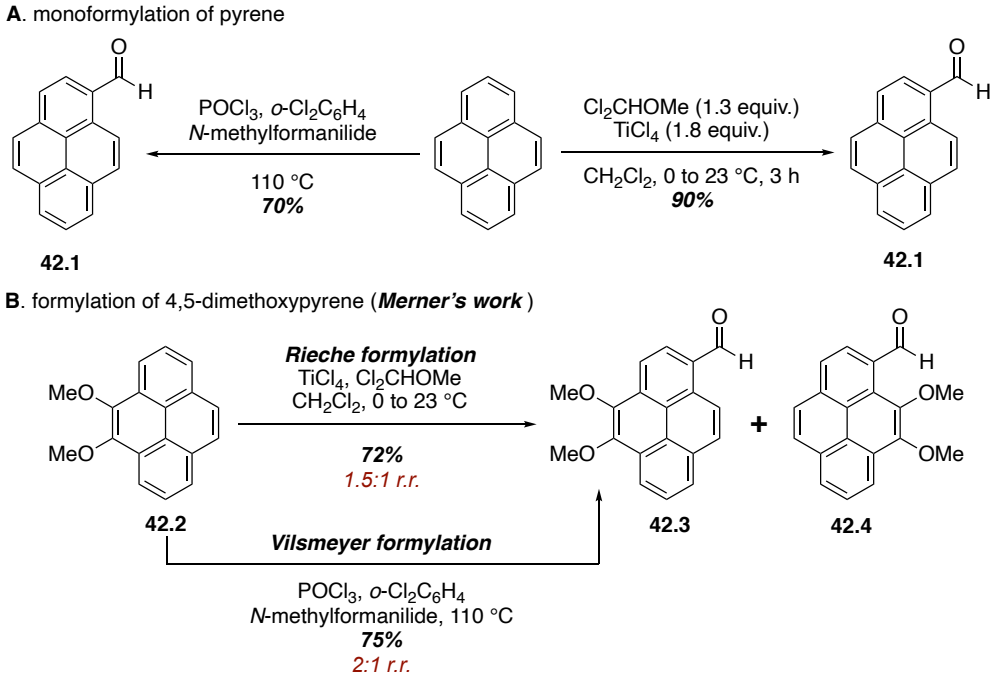

Figure 42. Formylation of pyrene

Substitution at less hindered 2- or 2- and 7-position is limited to bulky substituents. Only a few direct methods to achieve substitution at these positions have been reported to date.[7] The most straightforward way is the direct Ir-catalyzed borylation of the C-H bonds at 2 and 7-positions, giving 2-(Bpin)pyrene and 2,7-bis(Bpin)pyrene (Figure 43).[19] This one-step, high-yielding synthesis provides a direct entry point for the preparation of 2- and 2,7-substituted pyrene derivatives that can be employed in cross-coupling reactions.

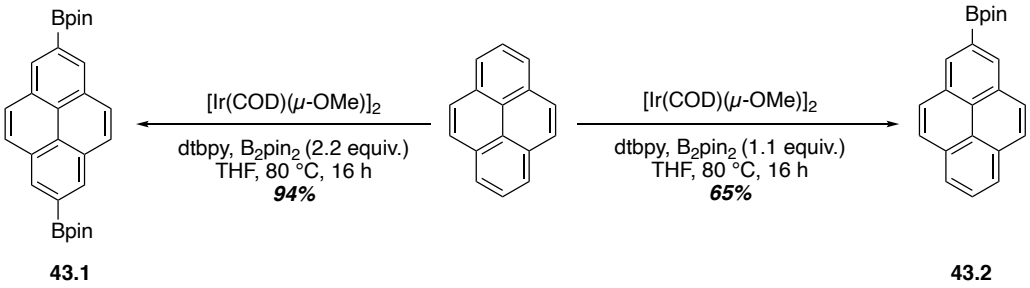

Figure 43. Borylation of pyrene

Mono-*tert*-butylation of pyrene with *tert*-butylchloride in the presence of $AlCl_3$ at 0 ºC will install a *tert*-butyl group at 2-position (Figure 44).[20] This procedure is well known, and while **44.1** can be prepared in 71% yield, unreacted pyrene and 2,7-di-*tert*-butylpyrene is formed as a by-product. If the latter (**44.2**) is desired, it can be synthesized in a 84% yield by simply adding an excess of *tert*-butylchloride.

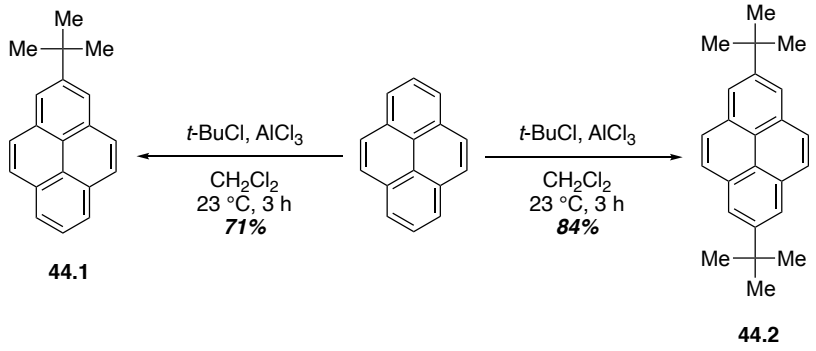

Figure 44. Friedel-Crafts alkylation (*tert*-Butylation) of pyrene

After *tert*-butylation, this bulky group blocks the adjacent 1 and 3-positions of pyrene from further substitution, permitting functionalization/electrophilic substitution at the 6 and 8-positions. For instance, treating 2-*tert*-butylpyrene **44.1** with 1 equivalent bromine in DCM at -78 ºC to affords 1-bromo-7-*tert*-butylpyrene in 72% yield. If increase the number of equivalents

of bromine is increased to 2 equivalents, under the same reaction condition 1,3-dibromo-7-*tert*-butylpyrene can be formed in high yield (**45.2**, 89%) (Figure 45).[21]

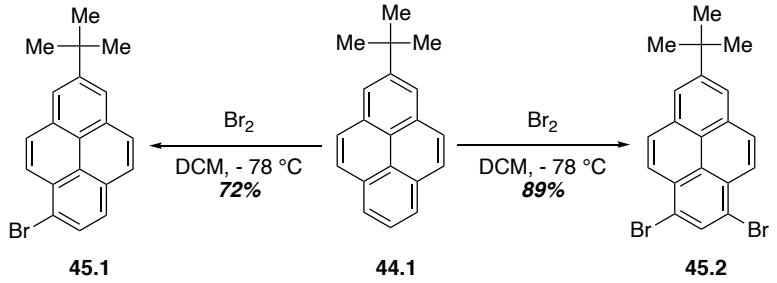

Figure 45. Bromination of 2-(*tert*-butyl)pyrene

9.2 1,6- and 1,8-Disubstituted pyrene

Disubstitution of the 1,3; 1,6; or 1,8-positions of pyrene typically yields a complex mixture of these three possible substitution patterns, which are difficult to separate. For example, dibromination of pyrene results (predominately) in a mixture of 1,6- dibromopyrene (**46.2**) and 1,8-dibromopyrene (**46.1**), which can only be isolated by several fractional recrystallizations based on the subtle differences in solubility of the two regioisomers (Figure 46).[22] Nonetheless, the tedious separation of 1,6-dibromopyrene with 1,8-dibromopyrene forms two valuable pyrene building blocks for coupling reactions. As you can see from Figure 46, pure 1,8-dibromopyrene (**46.1**) and 1,6-dibromopyrene (**46.2**) can be used in Sonogashira coupling reactions, resulting in disubstituted ethynyl pyrene derivatives (**46.3** and **46.5**) which can be used for other coupling reactions. Moreover, dibromopyrene compounds (**46.1** and **46.2**) can direct subject to Suzuki-Miyaura reactions or apply in Miyaura borylation reactions which resulted in bis(4,4,5,5-tetramethyl-1,3,2-dioxaborolan-2-yl)pyrene **46.4** and **46.6** which can be applied for further cross-coupling reactions.

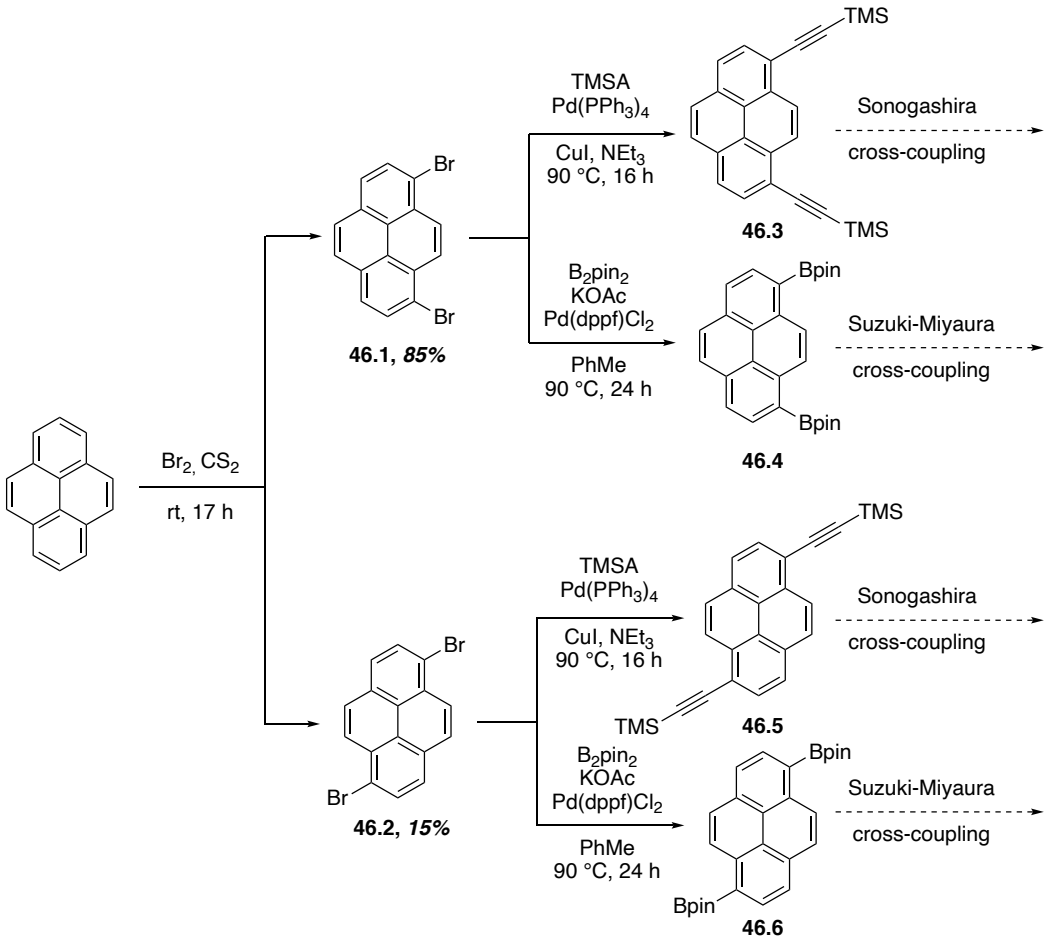

Figure 46. 1,6- and 1,8-dibromination of pyrene

To address this separation issue, and to selectively synthesize a 1,8-dibromopyrene derivative, Bodwell and co-workers developed a new bromination protocol in 2011.[23] In this work, the 4 and 5 positions of pyrene, which, along with the 9 and 10 positions are known as the K-region, were first substituted to sterically hinder the 3 and 6 positions, thereby enabling regioselective substitution at the 1 and 8 positions. This was accomplished by first oxidizing a single K-region of pyrene upon treatment with $RuCl_3 \cdot H_2O/NaIO_4$ to furnish the 4,5-dione **47.1** in 45% yield (Figure 47). Reduction of **47.1** with sodium dithionite gave 4,5-dihydroxypyrene **47.2**, which was immediately *O*-alkylated to generate 4,5-dibutyloxypyrene (**47.3**). Treating **47.3** with 2.2 equivalents of bromine in dichloromethane at room temperature for just 5 minutes results in the (completely) regioselective formation of **47.4** in 95% yield. With a selective approach to 1,8-dibromopyrene **47.4** in hand, Bodwell and co-workers were able to demonstrate the synthetic value of this type of cross-coupling substrate by synthesizing a new pyrene-based macrocycle. A Sonogashira reaction of **47.4** with trimethylsilyl acetylene, followed by the deprotection with TBAF affords bis-alkyne **47.6** in 83% yield. Oxidative coupling of the **47.6** gave predominantly the cyclic trimer derivative **47.7** in 28% yield. These

alkynylated pyrene macrocycles were found to have unique electronic property, the absorption spectra of **47.7** shows complex absorption bands with appreciable intensity at longer wavelengths. And the ethynyl and alkoxyl substituents on the pyrene systems break the symmetry and allow the coupling of the ground- and excited-state wave functions

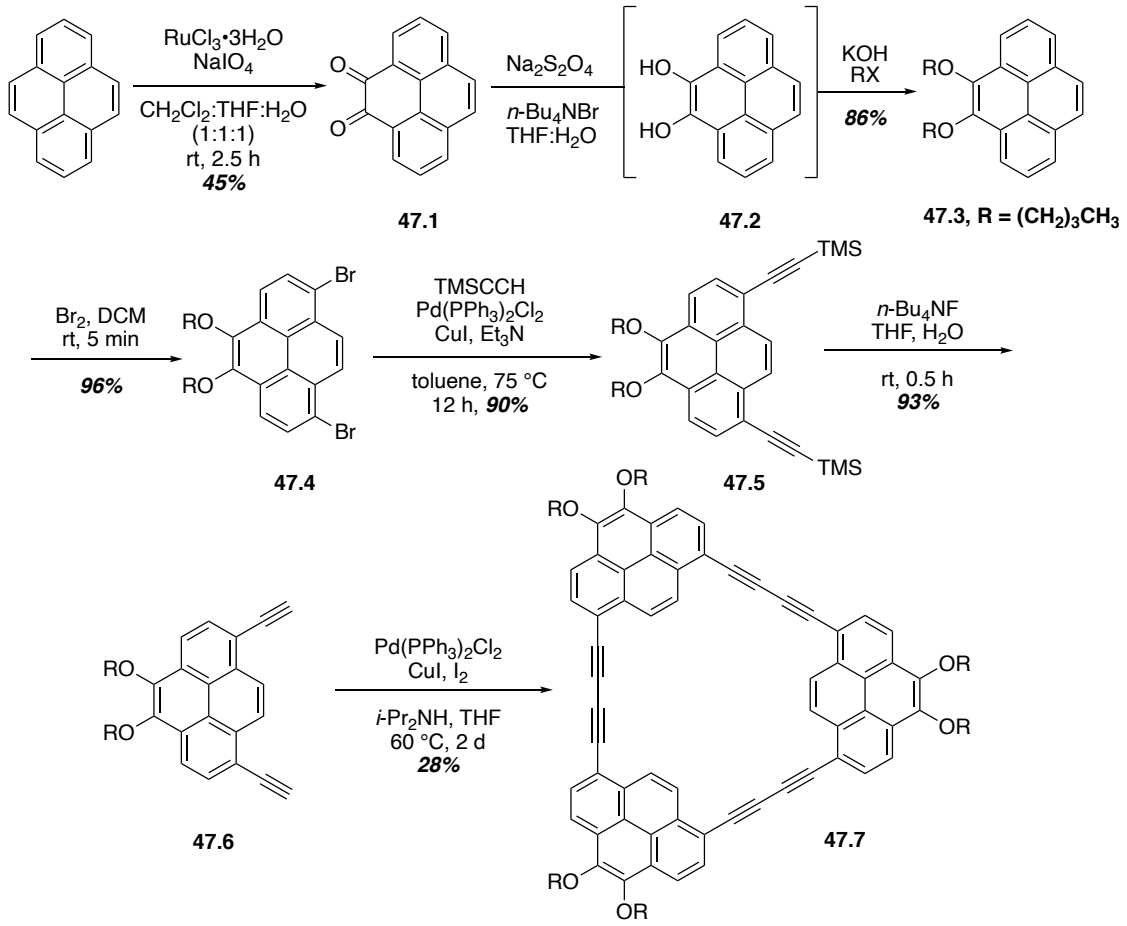

Figure 47. Synthesis of 1,8- diethynylpyrenes

In the same work, Bodwell and co-workers deomonstarted that **47.4** could be mono-alkynylated upon Sonogashira coupling of with 2-methylbut-3-yn-2-ol (1.1 equiv) to afford ynol **48.1** in 68% yield. An *in situ* deprotection followed by self-Sonogashira reaction of the ynol units gave afforded tetra- and trimerization products **48.2** and **48.3** in 30% and 23% yield respectively (Figure 48). The sections below will discuss how this pre-functionalization of pyrene's K-region inspired the development of new strategies for regioselective, polysubstitution of pyrene.

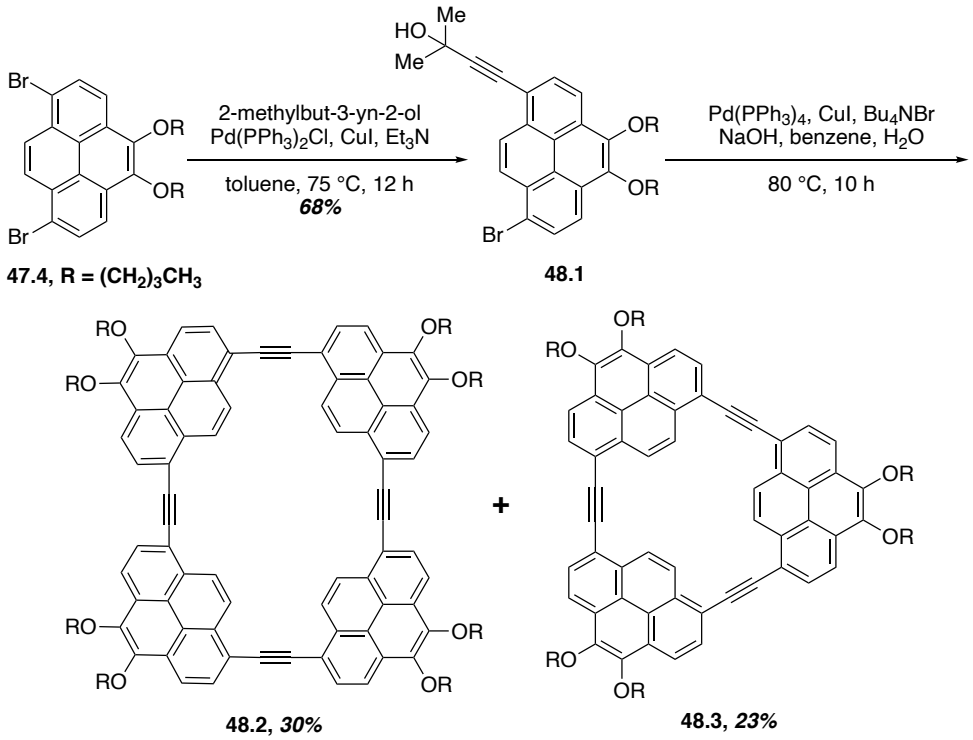

Figure 48. Synthesis of macrocycles

9.3 1,3-Disubstituted pyrene

As previously mentioned, the electrophilic substitution of pyrene occurs at the 1,3,6,8-positions, however, the formation of 1,3-disubstituted pyrene is not trivial since the 1,6- and 1,8-disubstituted pyrenes are preferentially formed. In order to selectively substitute the 1 and 3 positions of pyrene, the 7 position must first be substituted, to block the adjacent nucleophilic carbon atoms. In 2008, Müllen and co-workers reported an approach to 1,3-dibromo-7-*tert*-butylpyrene (Figure 49).[24] In this work, they used a *tert*-butyl group as a positional protecting group and low-temperature reaction conditions to form a 1,3-disubstituted pyrene in high yield. Pyrene was first mono-*tert*-butylated to generated 2- *tert*-butylpyrene **44.1**, which was then treated with bromine in dichloromethane at −78 ºC to give 1,3-dibromo-7-*tert*-butylpyrene (**45.2**) in 89% yield. Compound **45.2** is not only widely used to prepare polymer as blue-emitter for single-layer OLEDs, but also a useful building block that has been employed in numerous cross-coupling reactions such as Suzuki-Miyaura, Heck, Sonagashira, and Yamamoto reactions. For example, in the syntheses of oxygen-doped PAHs work Bonifazi and co-workers reported in 2020,[25] Suzuki-Miyaura cross coupling between **45.2** and 4-*tert*-butyl-2-methoxyphenylboronic acid, using [$Pd(PPh_3)_4$] as a catalyst, gave access to the phenol-bearing pyrene **49.2** in excellent yield after demethylation with BBr_3 in dichloromethane. A final oxidative Pummerer ring closure with CuO in $PhNO_2$ under reflux condition yielded the O-

doped PAH **49.3** in 83% yield.[14] And this unique O-embedded PAH exhibites a semiconducting behavior which indicate this is an attractive approach to fabricate nanographene with semiconducting properties and relatively high conductivity.

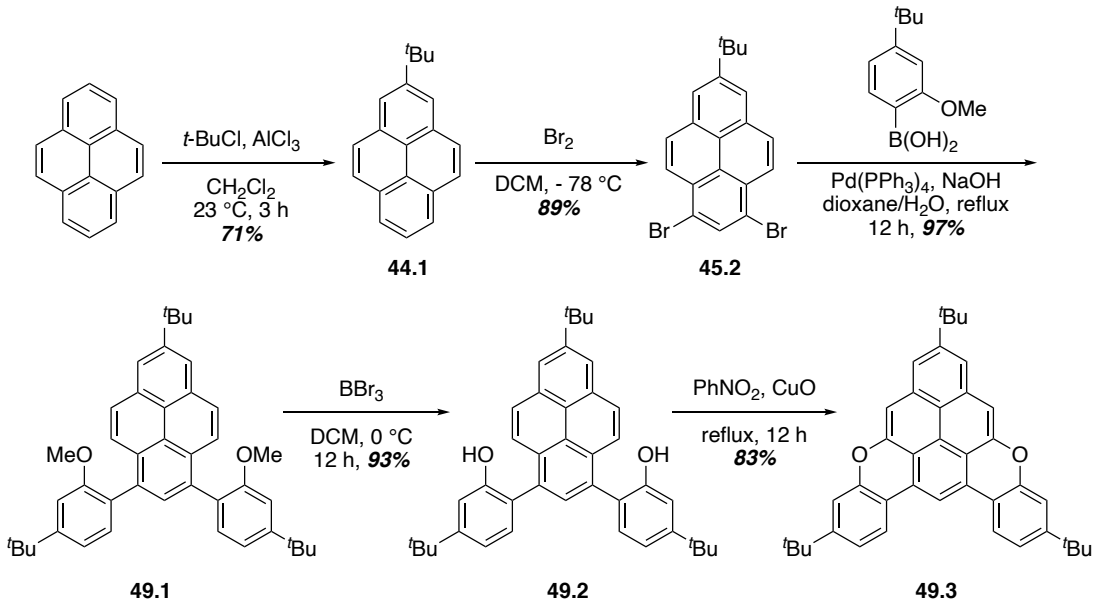

Figure 49. Synthesis of 1,3-dibromo-*tert*-butylpyrene **45.2**

9.4 2,7-Disubstituted pyrenes

Despite the increasing interest in and demand for 2,7-disubstituted pyrenes, only a few examples have been reported in the literature. Substitution of pyrene at the 2 and 7 positions is a long-standing problem since these positions are not directly accessible by electrophilic substitution of pyrene itself with substituents that can be used in future skeletal building reactions. The exception to this of course is the borylation procedure mentioned above. To be more specific, the difficulty in synthesizing the desired pyrene derivatives results from the presence of nodal planes in both the HOMO and the LUMO (Figure 50), which lie perpendicular to the molecule and pass through the 2- and 7- positions. Most of the contributions of the HOMO can be observed at the 1-, 3-, 6-, and 8-positions. Therefore, the electrophilic substitution of pyrene happens at those positions.

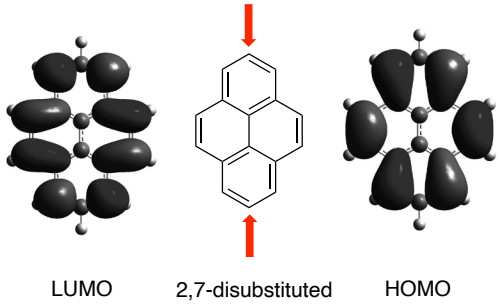

Figure 50. LUMO (left) and HOMO (right) of pyrene

To address this issue several different strategies have been employed to substitute the 2 and 7 positions, but all of these involve indirect routes to pyrene derivatives, or temporary dearomatization of the pyrene core. For example, the reduction of pyrene to 4,5,9,10-tetrahydropyrene (**51.1**), with H_2 and Pd/C, enables bromination at the (former) 2 and 7 positions (Figure 51) to give **51.2** in 55% yield. Subsequent mono-lithiation of **51.2** at −78 ºC, followed by quenching the resulting anion with octyl chloroformate to yield the ester **5.3** in 72% yield. The ester **51.3** was then oxidized/re-aromatized with DDQ to give compound 2,7-disubstituted pyrene derivative **51.4** in 63% yield. Compound **51.4** was later used as a starting material in cross-coupling reaction.[26]

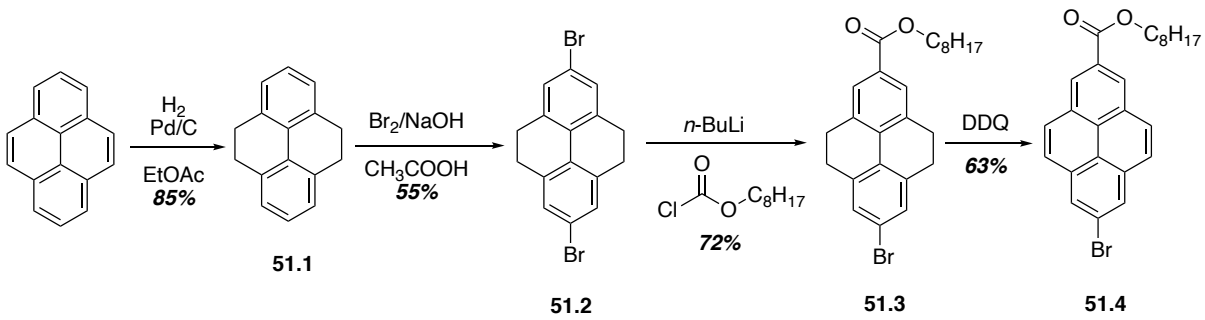

Figure 51. Synthetic approach to 2,7-disubstituted pyrene **51.4**

Another important example of the utilization of dibromide **51.2** is from Yamago and co-workers in their 2014 synthesis of a pyrene-based carbon nanohoop.[27] In this work, a cyclic tetramer of 2,7-pyrenylene, *i.e.*, [4]cyclo-2,7-pyrenylene or [4]CPY (**52.4**), was synthesized from pyrene in six steps in 18% overall yield (Figure 52). Following the approach described in Figure 51, **51.2** was synthesized from pyrene and subjected Yamago's platinum-square-based strategy for assembling macrocyclic precursors to carbon nanohoops. Compound **51.2** was converted to the 2,7-bis(trimethylstannyl)-4,5,9,10-tetrahydropyrene (**52.1**) in 85% yield. Subsequent reaction of **52.1** with [Pt(cod)Cl_2] in THF afforded platinum complex **52.2** in 56% yield, which, upon heating, in the presence of PPh_3 at 100 ºC, underwent a reductive

elimination affording [4]cyclo-4,5,9,10-tetrahydro-2,7-pyrenylene (**52.3)** in 51% yield. Finally, [4]CPY (**52.4**) was synthesized upon dehydrogenation of **52.3**, with Pd/C in 1,2-dichlorobenzene at 150 ºC, in nearly quantitative yield. This synthesis marked the first time that an all pyrene-containing carbon nanohoop had been prepared. The structure of **52.4** can be viewed as a pi-extended [8]CPP, which, at the time, was important in view of the growing interest in synthesizing carbon nanobelts. This work by Yamago inspired some of the chemistry that has been developed in this chapter.

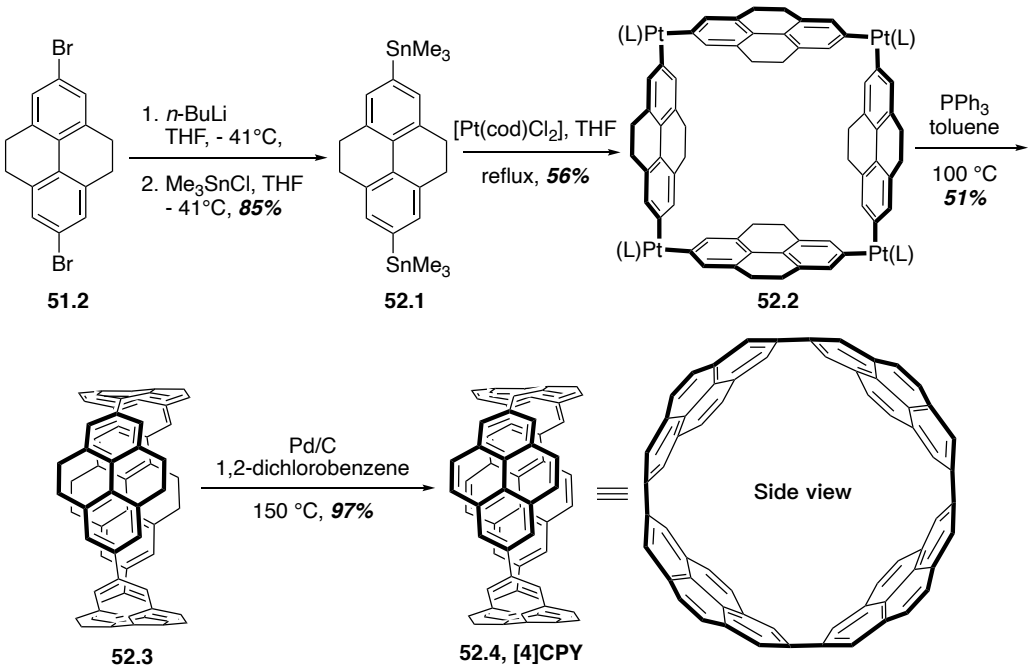

Figure 52. Yamago's synthesis of [4]CPY

Marder and co-workers have also reported on the synthesis of 2,7-functionalized pyrene derivatives.[19] In their work, a regiospecific direct C-H borylation of pyrene with an iridium-based catalytic method was developed (Figure 53). Treatment of pyrene with in situ prepared $[Ir(OMe)COD]_2$, 4,4'-di-*tert*-butyl-2,2'-bipyridine (dtbpy) and B_2pin_2 gave 2,7-bis-(Bpin)-pyrene **43.1** in 95% yield. Compound **43.1** is not only a useful as a direct cross-coupling partner, but also, due to recent developments in organoboron chemistry, this compound can be converted into multiple functional groups. For example, oxidizing compound **43.1** with H_2O_2 in the presence of NaOH gave 2,7-dihydroxypyrene (**53.1**) in 89%. Treatment of **53.1** with Tf_2O and pyridine in hexane gave compound **53.2** in 60% yield. Compound **43.1** could also be converted to 2,7-dibromopyrene (**53.3**) by the action of 6.0 equivalents of $CuBr_2$ at 90 ºC for 16 hours in MeOH/H_2O/THF (70% yield, Figure 53). At this point, a Sonogashira reaction could be conducted on both compounds **53.2** and **53.3**. Treatment compound **53.2** with trimethylsilylacetylene (TMSA) with $Pd(PPh_3)_2Cl_2$, CuI in DMF/Et_3N at 80 ºC for 16 hours

formed compound **53.4** in 51% yield. By using almost identical reaction conditions, compound **53.3** was obtained from compound **53.4** in 44% yield.

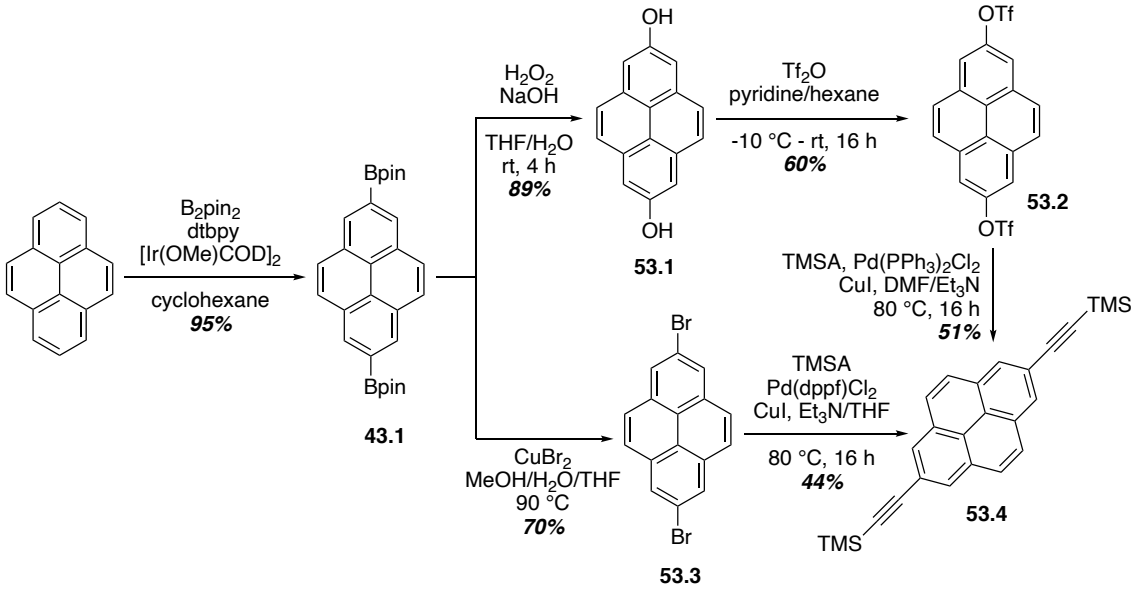

Figure 53. 2,7-difunctionalization of pyrene

In 2013, Sutherland and co-workers developed another strategy to synthesize 2,7-disubstituted pyrenes.[28] In this work, they started from pyrene-4,5-diketone **47.1**, which was prepared via the oxidation of the pyrene K-region (Figure 54). From here, two different compounds were prepared. The first, involved reduction of **47.1** with zinc and in situ protection with the tertbutyldimethylsilyl (TBDMS) chloride afforded bis-silyl ether **54.1** in 45%. Iridium-catalyzed borylation of **54.1**, using the conditions developed by Marder and co-workers, afforded 2,7-bispinacol borane **54.2** in 98% yield. Similarly, following the Bodwell procedure described above, 4,5-dimethoxypyrene (**42.2**) was synthesized in 92% yield, and the same borylation strategy was employed to give **54.4** in 63% yield.

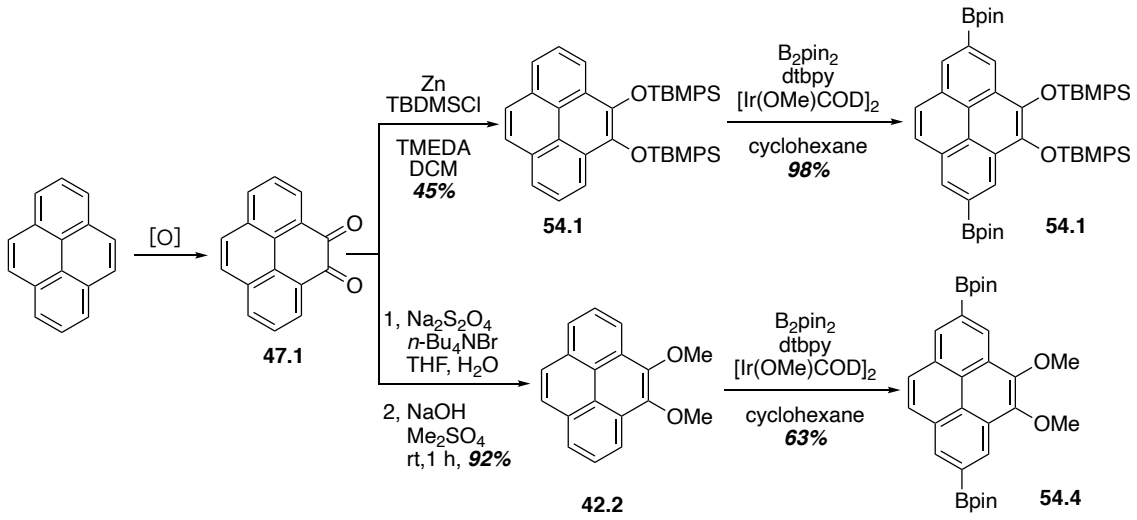

Figure 54. Synthesis of 2,7-disubstituted pyrene for cross-coupling reactions

In the same year, Müllen and co-workers reported another paper that described the efficient synthesis of 2,7-disubstituted pyrenes **55.4** and **55.5** (Figure 55).[29] This approach is based on the pyrene-4,5,9,10-tetraone **55.1**, which can be prepared from pyrene through oxidation of both K-regions on gram-scale (27%). The tretraketone **55.1** can then be subjected to direct bromination or iodination with NBS or NIS, with halogenation taking place at the 2,7-positions. Reduction with $Na_2S_2O_4$, followed by methylation affords hexa-substituted pyrenes **55.4** and **55.5** in 82% and 78% yield, respectively.

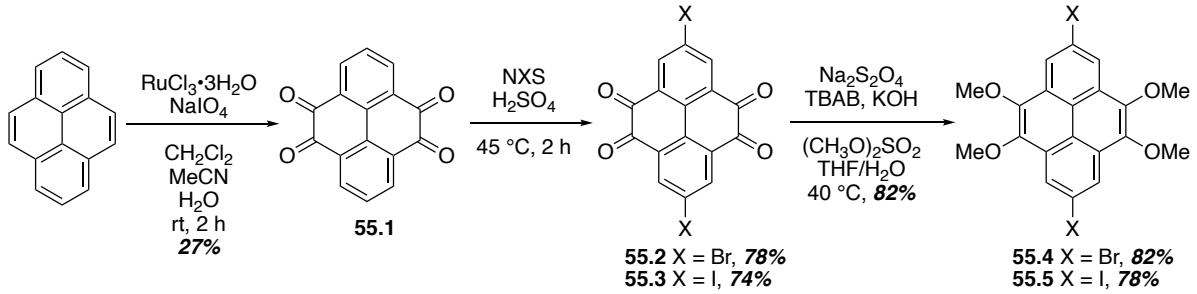

Figure 55. Syntheses of 2,7-disubstituted pyrene

10 Importance of regioselectively substituted pyrenes as building blocks for pi-extended PAHs and carbon nanobelts

As described above, the substitution of chemistry is limited to either functionalization of the 1, 3, 6, and 8 positions or the 2 and 7 positions, in a single synthetic operation. Moreover, selective substitution of the most nucleophilic carbons of pyrene (*i.e.,* the 1, 3, 6, and 8 positions) requires functionalization of the K-region prior to substituting these carbon atoms.

At this stage the 1 and 8 positions can be selectively substituted. While there have been numerous reports for using the later strategy (pre-functionalization of the K-region) to synthesize 1,8- or 2,7-disubstituted pyrenes, at the time of this work, a general strategy that enables the introduction of cross-coupling handles or functional groups suitable for future skeletal building reactions, had not been reported. Thus, the development of new methods that enable functionalization/substitution of the 1, 2, 7, and 8 positions would be highly valuable for the development of new pyrene-based materials, particularly macrocyclic systems that can be converted into carbon nanobelts.

In the work described by Bodwell and co-workers above, after installing two methoxy groups at the 4,5-positions of pyrene, they were able to selectively dibrominate the 1,8-positions and use these aryl bromide handles in the synthesis of 1,8-pyrenylene macrocycles (**47.4**, Figure 47). Yamago and co-workers were able to synthesize a, cyclic tetramer of pyrene, *i.e.*, [4]cyclo-2,7-pyrenylene (**52.4**, Figure 52), from pyrene over six steps. Inspired by Bodwell and Yamago's work, we designed a strategy that combined these two methods to facilitate the synthesis of functionalized macrocyclic pyrene systems that could be converted into fully conjugated, functionalized carbon nanobelts (concept, Figure 56). The remaining sections of this chapter will discuss the selective substitution chemistry that has been developed in our laboratory.

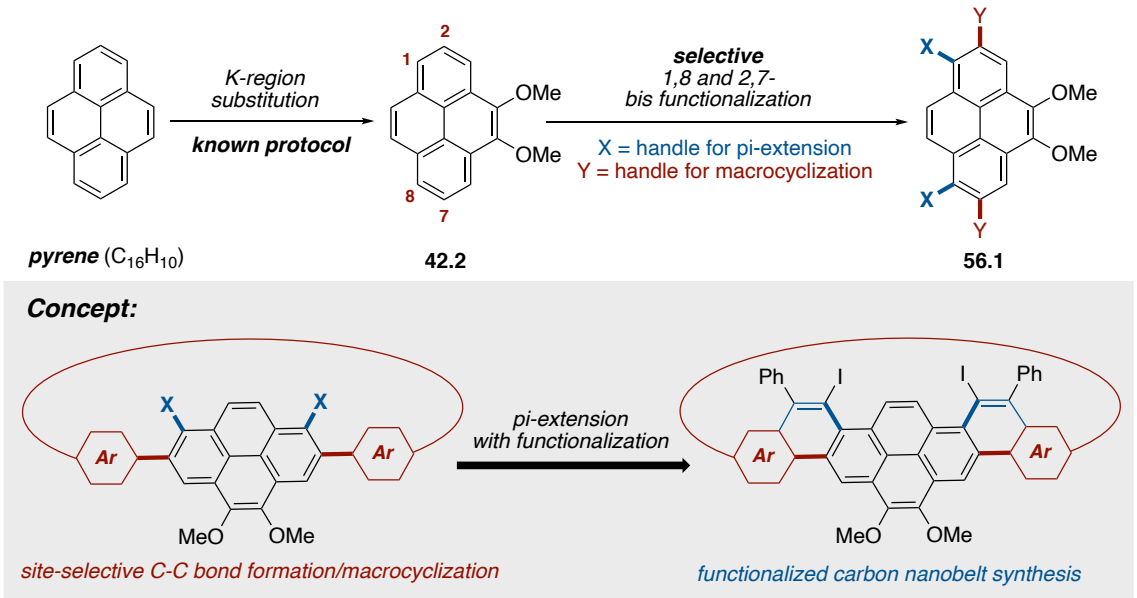

Figure 56. General strategy of selective 1,8 and 2,7-bis-functionalization of pyrene and the application of these building blocks to macrocycle synthesis

11 A novel strategy to synthesize 2,7,4,5-tetrasubstituted pyrene derivatives

In 2018, Merner and co-workers reported a strategy for regioselective substitution of non-symmetric tetra- and pentasubstituted pyrenes.[18] In this work, they described a monoformylaiton (see Figure 57), monobromination and monacylation strategies that allowed for the selective introduction of these substituents. In the case of the bromination and acylation reactions, these substitutions were performed sequentially afford tetrasubstituted pyrene **57.2** in 70% overall yield.

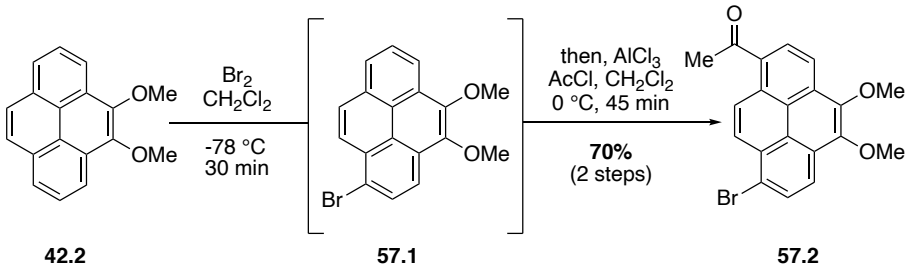

Figure 57. Synthesis of pentasubstituted pyrene **57.2**

As described above, formylation of 4,5-dimethoxypyrene yielded a separable mixture of isomeric aldehydes **42.3** and **42.4**. Dakin oxidation of **42.3** gave hydroxypyrene **58.1**, which was directly allylated and then subjected to a Claisen rearrangement at 190 °C in *N*,*N*-diethylaniline to furnish **58.2** in 32% overall yield (Figure 58, A). This approach is significant in that it facilitates primary, C-2 alkylation of pyrene, which is not possible via direct substitution. A similar strategy was used to prepare brominated derivative **58.4** (Figure 58, b).

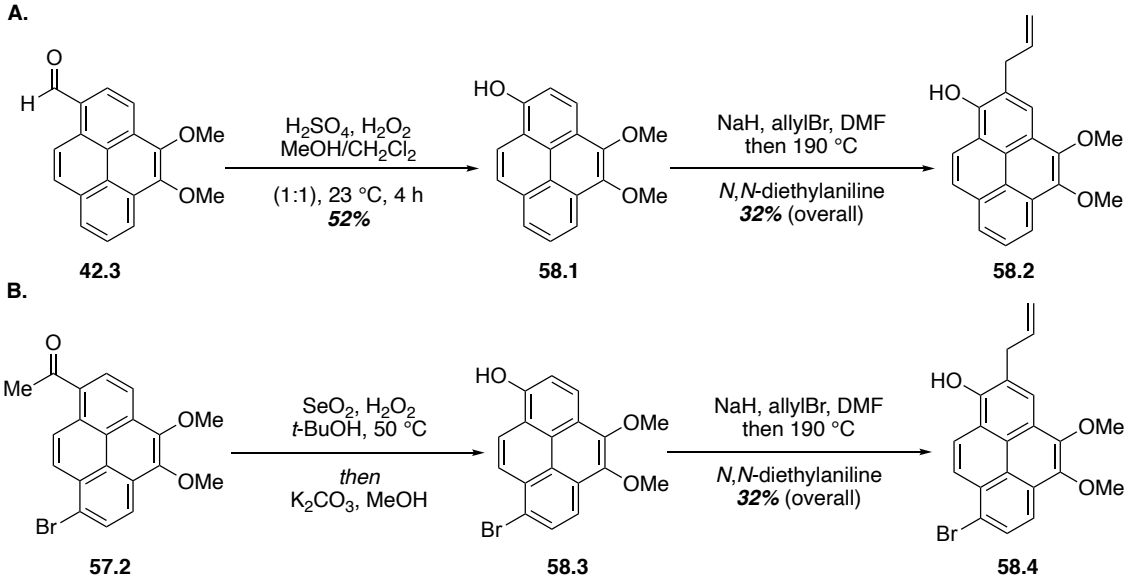

Figure 58. Synthesis of tetra- and pentasubstituted pyrenes **58.2** and **58.4**

With this precedent available in our laboratory, I sought to apply this strategy to the synthesis of 1,8-dihydroxypyrene **59.4** (Figure 59). Indeed, 4,5-dimethoxypyrene, which was prepared on a 5-10 gram scale using the Bodwell protocol (see Appendix **I** for details), could be bis-acylated under Friedel-Crafts acylation conditions to afford diketone **59.1** in 76% yield (Figure 59). While this approach works well on a 100-200 milligram scale, it proved to be problematic on larger scales. Success of this reaction requires higher dilution, and the order of addition for the reagents is crucial. 4,5-Dimethoxypyrene must be added as a 0.01mM solution in dichloromethane to dilute solution of acetyl chloride and aluminum chloride at 0 °C. If the reaction is warmed above 0 °C, dealkylation of the methoxy groups occurs, and presumably, condensation products via a Lewis-Acid mediated aldol reaction occur. Nonetheless, Bayer-Viliger oxidation of the diketone to afford the diacetate ester **59.2** occurs in the presence of hydrogen peroxide and catalytic selenium dioxide in 84% yield. While **59.2** was difficult to purify, it could be subjected to hydrolysis in the presence of potassium carbonate in methanol. The intended product of this reaction, 4,5-dimethoxypyrene-1,8-diol (**59.4**) was not isolated, but rather the oxidation product, pyren-1,8-dione (**59.3**) was. As will be discussed below, the **59.4** was highly susceptible to air oxidation.

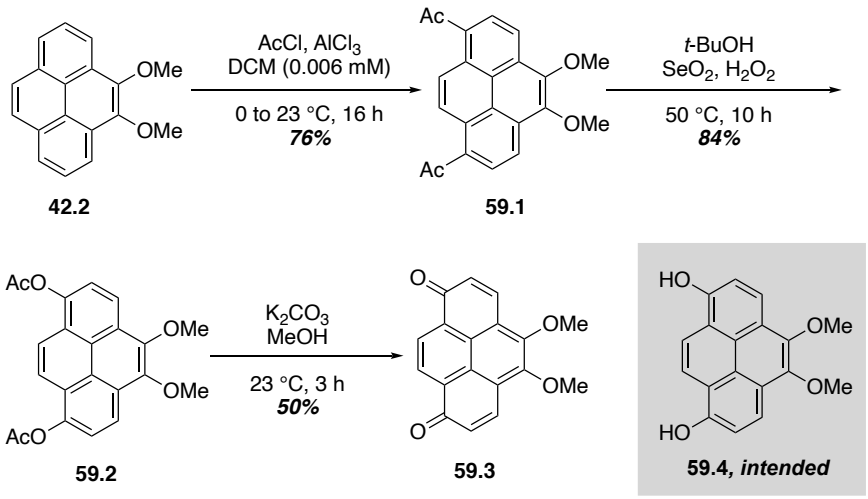

Figure 59. Synthesis of diketone-dimethoxypyrene via Baeyer-Villiger reaction

In order to address the scalability of the Friedel-Crafts acylation reaction of 4,5-dimethoxy (**42.2**) en route to diketone **59.3**, an alternative approach was pursued. Bromination of **42.2** with bromine in dichloromethane gave **60.1** in 90% yield on 10 gram scale (Figure 60). Two different protocols to convert **60.1** to bis-boronate ester **60.2** were attempted. The first involves lithium-halogen exchange, followed by subsequent quenching of the reactive species with (isopropoxy)pinacolborane to form bis-boronate ester **60.2** in 65% yield. The second

method employs a Miyaura borylation. Treatment **60.1** with $Pd(dppf)Cl_2$, B_2pin_2 and KOAc in dioxane at 80 ºC gave **60.2** in 78% after 12 h. Standard oxidation conditions, basic hydrogen peroxide, of **60.2** afforded pyrene-1,8-dione **60.2** in 90% yield. Using this sequence, over 10 g of **11.3** could be prepared in a single pass through the synthesis.

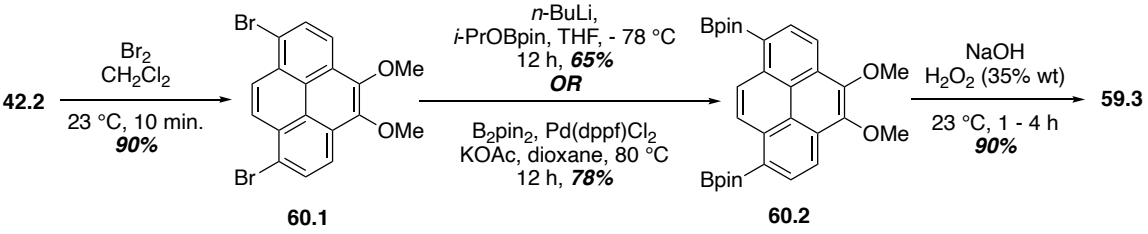

Figure 60. Synthesis of diketone-dimethoxypyrene via Miyaura borylation reaction

With a gram-scale synthesis of **59.3** in hand, I next sought to functionalize this oxidized pyrene derivative. Bromination of **59.3** with NBS in DMF gave 2,7-dibromopyrene-1,8-dione (**61.1**) in 90% yield. The simple three line ^1H NMR spectrum of **61.2** did not unequivocally confirm the regiochemistry of **61.2**; however, crystals suitable for X-ray analysis were obtained upon recrystallization from ethyl acetate/hexanes, which confirmed that **61.1** does undergo standard enone-type bromination. Reduction of the diketone under traditional hydride reducing conditions (*i.e.,* $NaBH_4$, Dibal-H, or $LiAlH_4$) were low yielding, and appeared to not go to completion. However, it was later determined that the afforded reduction product undergoes air oxidation upon work up and standing in a flask at room temperature. Thus, it was necessary to directly reduce **61.1**, and alkylate the resulting diol immediately. This was accomplished upon treatment of **61.1** with $Na_2S_2O_4$ in MeOH/DCM to afford **61.2**, which was immediately converted to 2,7-dibromo-1,4,5,8-dimethoxypyrene (**61.3**) in 75% yield over two steps

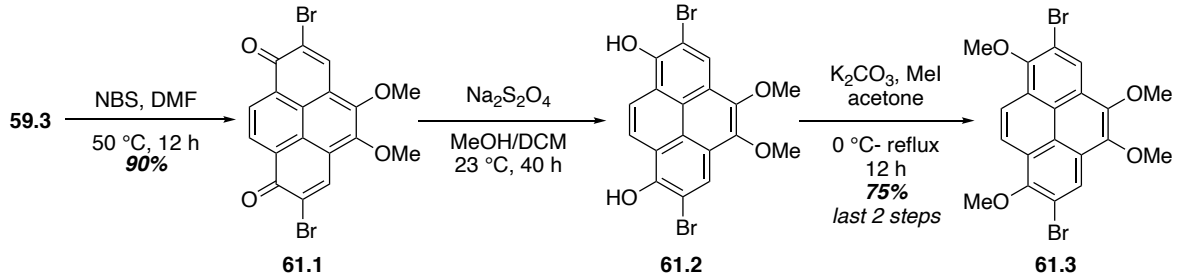

Figure 61. Synthesis of 2,7-functionalized pyrene derivatives

11.1 The application of 2,7-dibromo-1,4,5,8-tetramethoxypyrene 61.3 to cross-coupling reactions and subsequent pi-extension.

With an approach to hexasubstituted pyrene **61.3** in hand, an attempt to functionalize the vinyl bromide units of **61.1** was first attempted. Surprisingly, dibromo-diketone **61.1** proved to be resistant to Suzuki cross-coupling with boronic acids and boronate esters under conditions reported to be compatible with bromoenones (Figure 62).

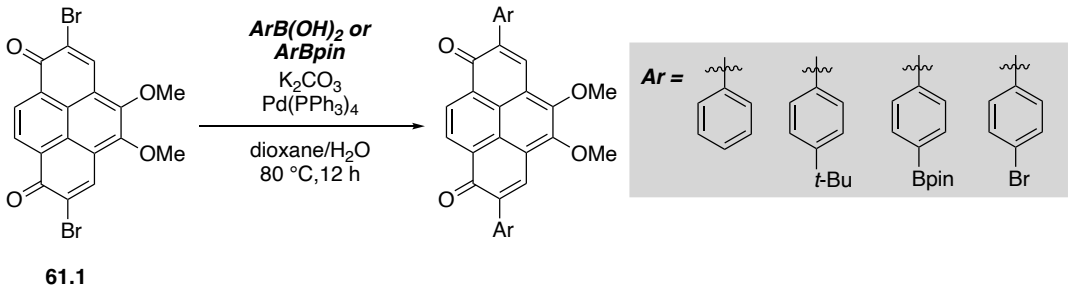

Figure 62. Attempted Suzuki cross-coupling reactions of compound **61.1**

While dibromide **61.1** was not a good candidate for cross coupling under Suzuki reaction conditions, hexasubstituted pyrene **61.3** was. A variety of aryl and heteroaryl boronic acids were initially examined under the reaction conditions presented in Figure 63. All of the boronic acids employed resulted in high yielding Suzuki reactions with dibromide **61.3**, including sterically hindered, *ortho*-substituted boronic acids such as 2-methylphenyl (**63.7**), 2-chlorophenyl (**63.5**), and *ortho*-biphenyl boronic acids (**63.2** and **63.9**). In the case of the latter, these substrates could be used directly in future pi-extension reactions (see below), while **63.5** and **63.8** contain functional group handles that should enable future C-C bond forming reactions.

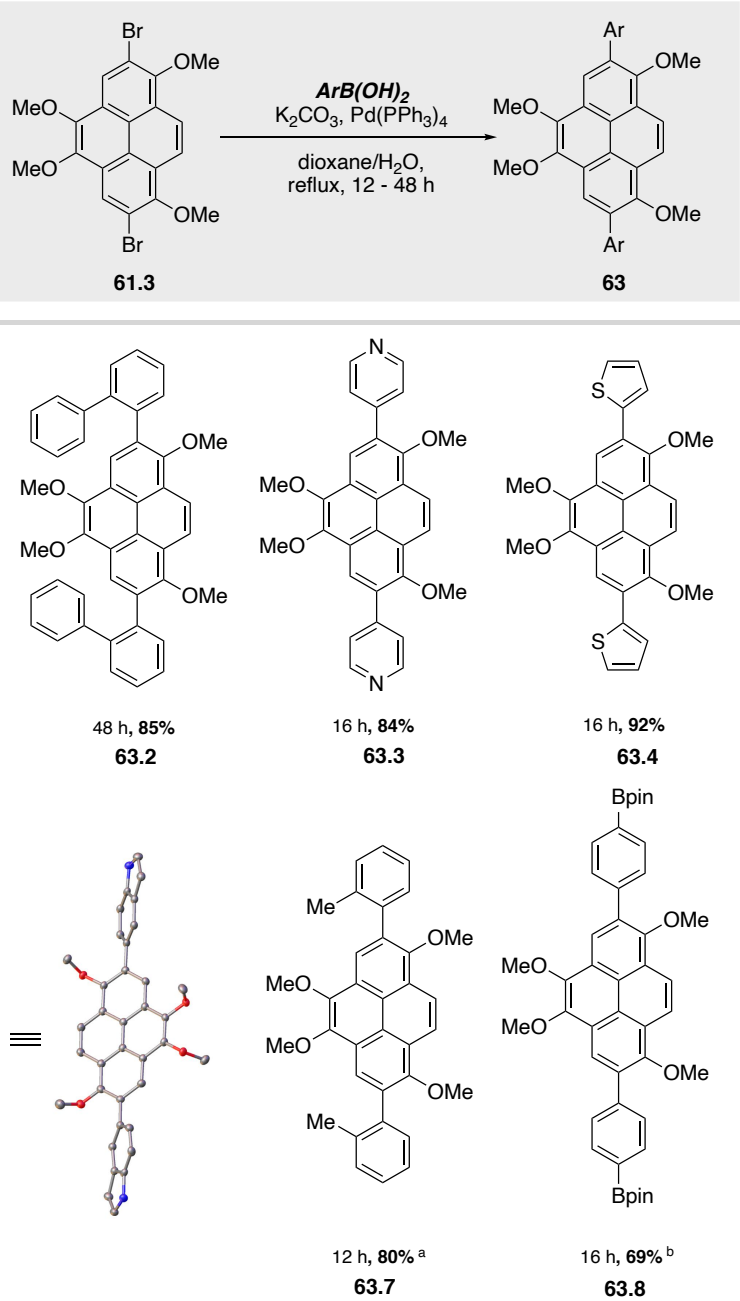

reaction conditions: 2,7-dibromo-1,4,5,8-tetramethoxypyrene (0.02 mmol, 1.0 eq.), boronic acid (0.07 mmol, 3.5 eq.), K_2CO_3 (0.08 mmol, 4.0 eq.),$Pd(Ph_3)_4$ (10 mol%), 1,4-dioxane (0.2 mL), H_2O (0.05 mL), reflux, 12 - 48 h. [a]2,7-dibromo-1,4,5,8-tetramethoxypyrene (0.02 mmol, 1.0 eq.), boronic acid (0.07 mmol, 3.5 eq.),K_2CO_3 (0.2 mmol, 10.0 eq.), $Pd(Ph_3)_4$ (10 mol%), EtOH/toluene (1:1, 0.2 mL), H_2O (0.1 mL), reflux, 12 - 48 h. [b]2,7-dibromo-1,4,5,8-tetramethoxypyrene (0.02 mmol, 1.0 eq.), 1,4-bid(4,4,5,5-tetramethyl-1,3,2-dioxaborolan-2-yl)benzene (0.06 mmol, 3.0 eq.), K_3PO_4 (0.08 mmol, 4.0 eq.), $Pd(Ph_3)_4$ (10 mol%), DMF (0.15 mL), 100 °C, 16 h.

Figure 63. Substrates scope of Suzuki reaction of compound **61.3**

11.2 Pi-extension reaction on compounds 63.2 and 63.9

Compound **63.2** and compound **63.9** are potential pi-extension reaction candidates, we expected to form two new C-C bonds at 3,6-positions on pyrene (Figure 64, **64.1**). Treatment **63.2** with $FeCl_3$ in DCM/$MeNO_2$ at 0 ºC did not form the desired product **64.1**, unexpectedly,

the cyclization occurred at 1,4-positions gave compound **64.2** in 54% with the loss of two methoxy groups. Recrystallization of **64.2** from DMA/MeOH produced crystals suitable for X-ray crystallographic analysis, which confirmed the regioselectivity of the Scholl reaction product.

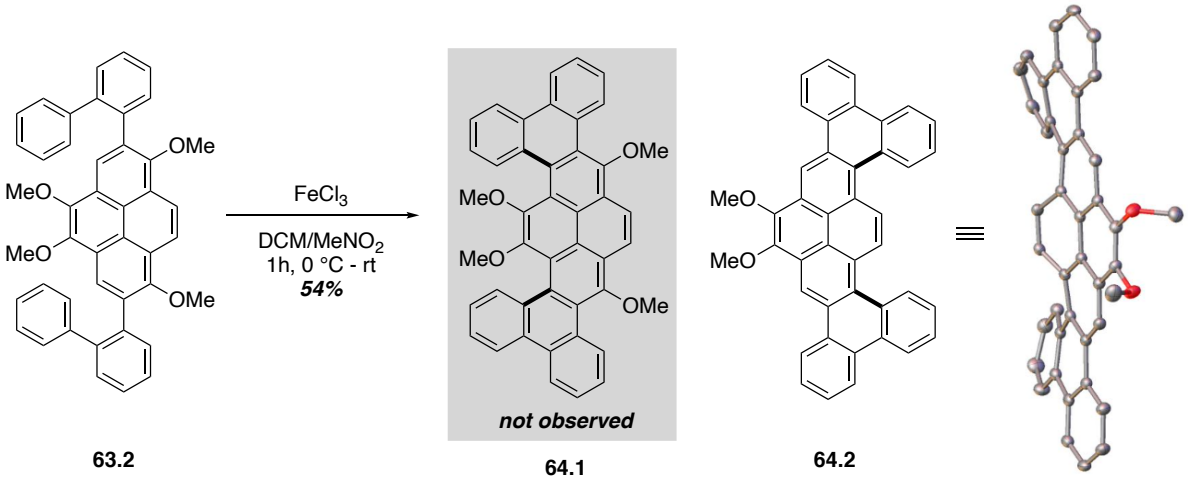

Figure 64. Pi-extension reaction of compound **63.2**

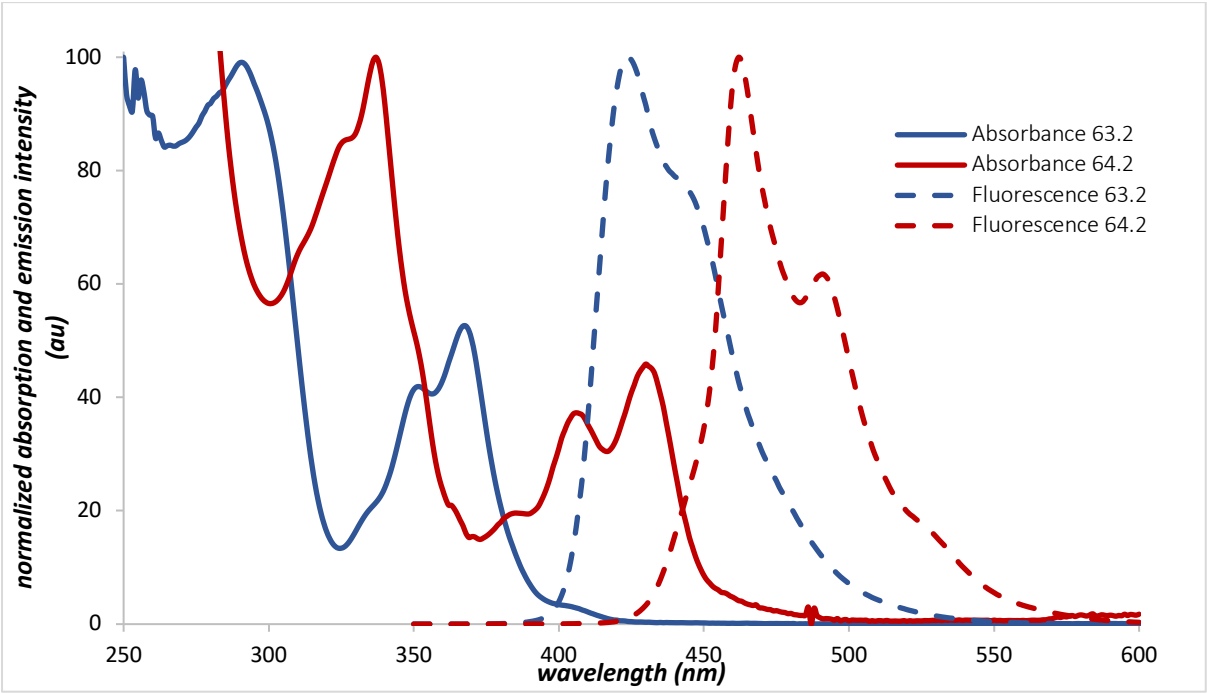

Figure 65. Normalized UV-Vis absorption and emission spectrum of the solution of **63.2** (blue, 1.4 X 10^{-5} M) and **64.2** (red, 1.3 X 10^{-5} M) in DCM at room temperature

A comparison of the photophysical properties of compound **64.2** to the starting material **63.2** shows that there is a red shift in the UV-vis spectra and a distinct red shift in emission spectra. (Figure 65)

To confirm this unexpected result, another Scholl reaction was conducted on compound **63.9** (Figure 66). Treatment **63.9** with $FeCl_3$ in $DCM/MeNO_2$ at 0 ºC again, the same demethylated Scholl reaction product (**66.2**) was obtained.

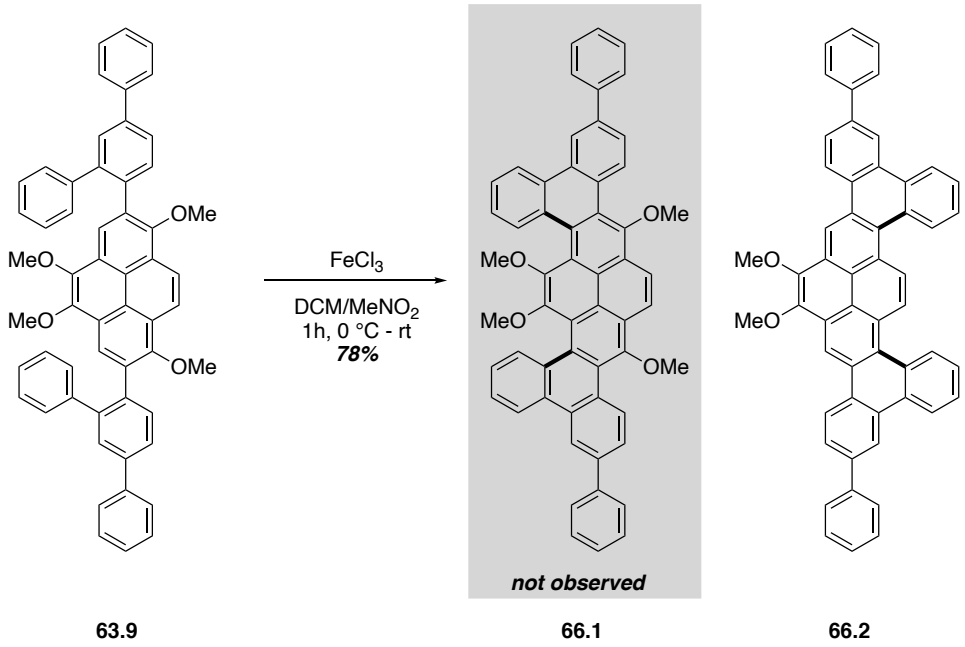

Figure 66. Pi-extension reaction of compound **63.9**

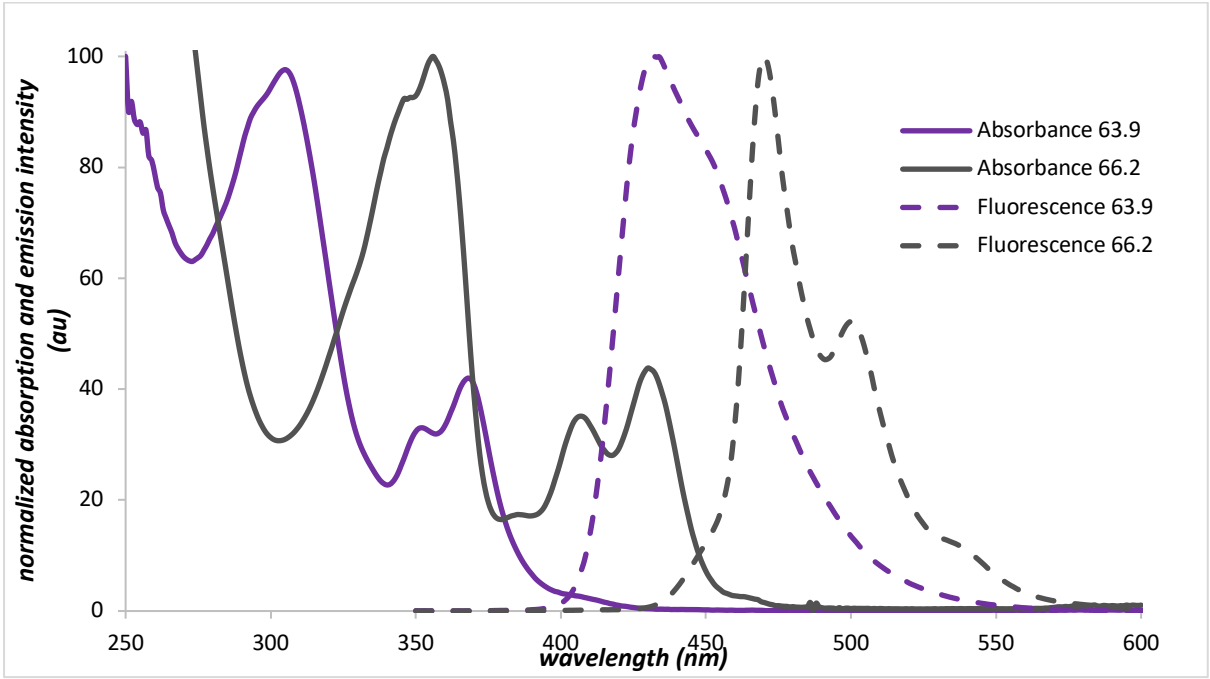

Figure 67. Normalized UV-Vis absorption and emission spectrum of the solution of **63.9** (purple, 8.7 X 10^{-6} M) and **66.2** (grey, 9.4 X 10^{-6} M) in DCM at room temperature

The comparison of the photophysical properties of compound **63.9** to the starting material **66.2** has basically the same trend. A slight red shift in UV-vis and red shift in emission spectra. (Figure 67)

11.3 The possible reaction mechanism of pi-extension reaction

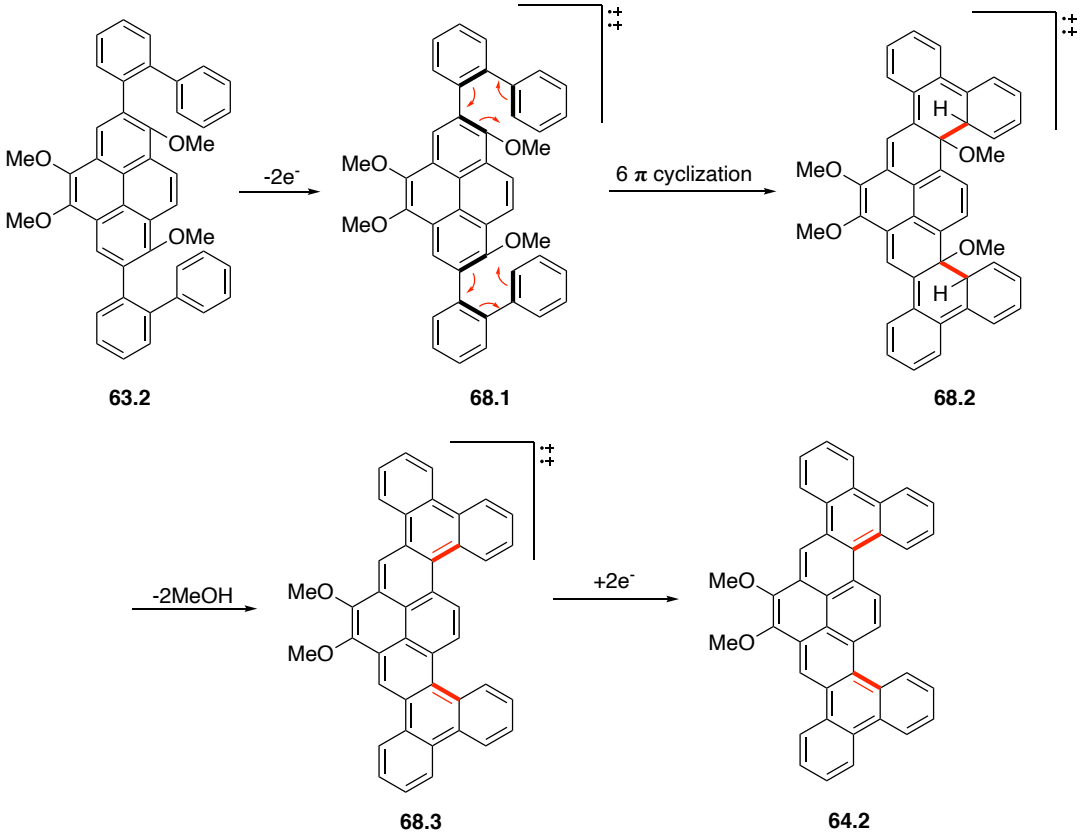

Figure 68. Possible reaction pathway for the regioselective pi-extension reaction

The possible mechanism of this regioselective pi-extension reaction is shown in Figure 68. Compound **63.2** was oxidized by $FeCl_3$ to diradical cation compound **68.1**, followed by the 6π cyclization to form intermediate **68.2** which can eliminate methanol to generate radical cation compound **68.3**. compound **68.3** then aromatized to the product **64.2**. In 2012, Hilt and co-workers reported a work that investigated the regioselectivity in Scholl reactions for the synthesis of oligoarenes.[30] In this work, they presented a comprehensive explanation for the highly regioselective Scholl reaction leading to the formation of tribenzo[*fg*,*ij*,*rst*]pentaphene derivatives by joint experimental and quantum chemical investigations. According to Hilt's work, $FeCl_3$ was only an oxidant here and did not get involved in the elimination of the methanol step.

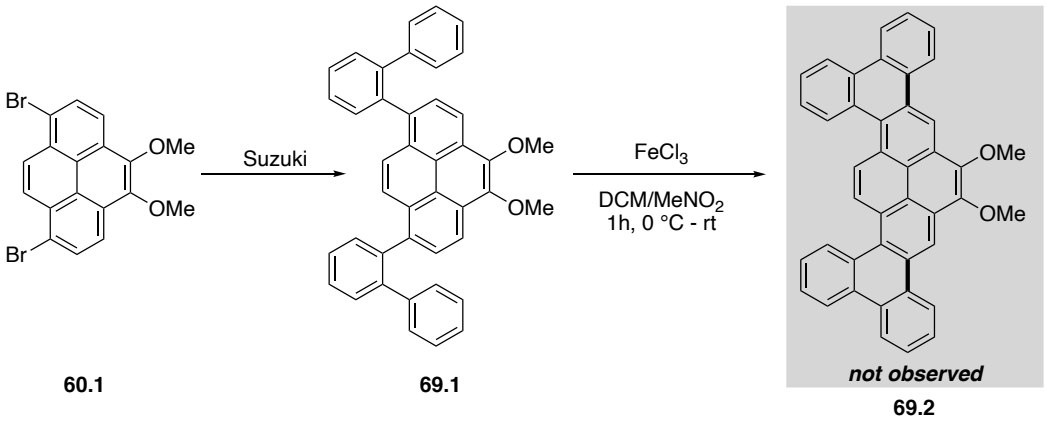

60.1 **69.1** **69.2**

Figure 69. Suzuki-Miyaura reaction and attempted pi-extension reaction of compound **69.1**

To test this regioselective, a Suzuki-Miyaura reaction was conducted on compound **60.1** to form another pi-extension reaction precursor compound **69.1**, treatment with $FeCl_3$ in DCM/$MeNO_2$ at 0 ºC again, no desired compound was observed after 1 hour (Figure 69). This suggests two methoxy groups at 1,8-position of compound **63.2** are the directing group in this regioselective Scholl reaction.

11.4 The synthesis and application of 2,7-dibromo-4,5-dimethoxypyrene-1,8-bis(trifluoromethanesulfonate)

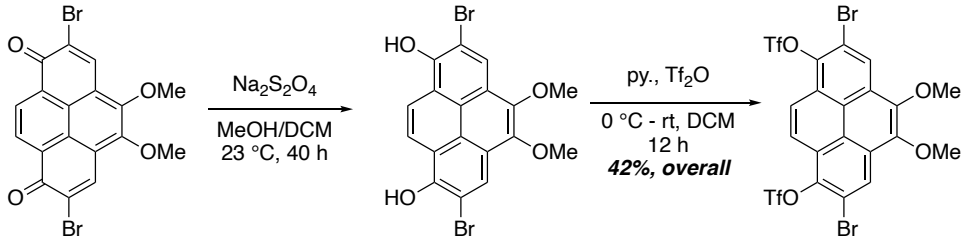

61.1 **61.2** **70.1**

Figure 70. The synthesis of compound **70.1**

Not only compound **61.3** can be made from compound **61.1**, but a reduction of **61.3** followed by treatment with Tf_2O in the presence of pyridine also gave compound **70.1** in 42% yield over two steps (Figure 70). Compound **70.1** also is a good partner for the Suzuki-Miyaura cross-coupling reaction, hopefully, we can apply two kinds of Suzuki-Miyaura cross-coupling reactions on this compound to install two different aryl groups.

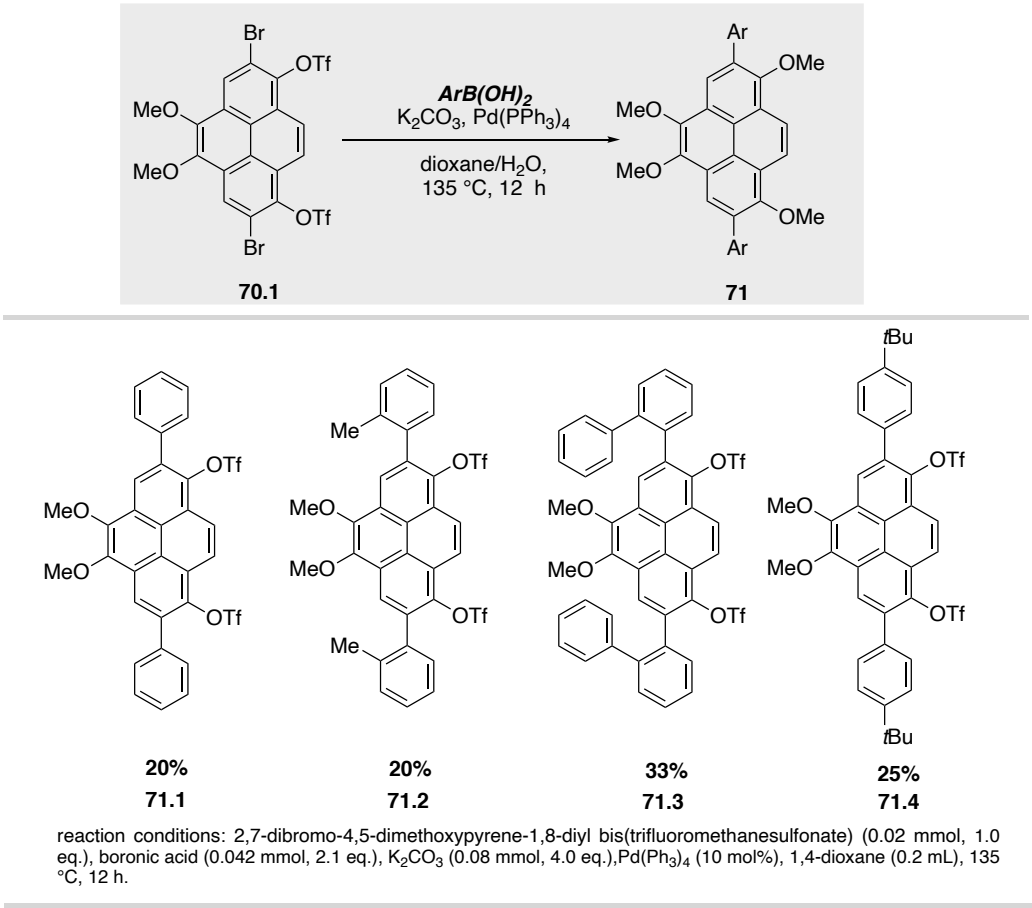

Figure 71. Selective Suzuki-Miyaura cross-coupling of compound **70.1**

I started with the investigation of selective Suzuki-Miyaura cross-coupling reaction on compound **70.1**, the result is summarized in Figure 71. Variety of boronic acids were tested under the typical Suzuki-Miyaura cross-coupling condition, such as phenylboronic acid, 2-methylphenylboronic acid, 2-biphenylboronic acid, and 4-*tert*-butylphenylboronic acid. Unfortunately, the selectivity of these reactions was not very satisfactory, most of the reactions observed the tri- and tetra-reacted Suzuki-Miyaura product, so far, the best result we got is 33% yield with 2-biphenylboronic acid.

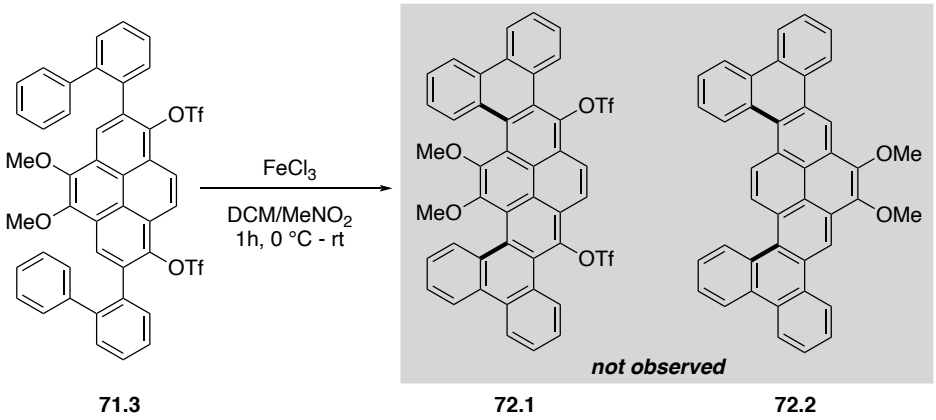

Figure 72. Pi-extension reaction of compound **71.3**

Compound **71.3** was subjected to Scholl reaction conditions (Figure 72), unlike the previous result, the cyclization did not happen in the presence of triflate groups.

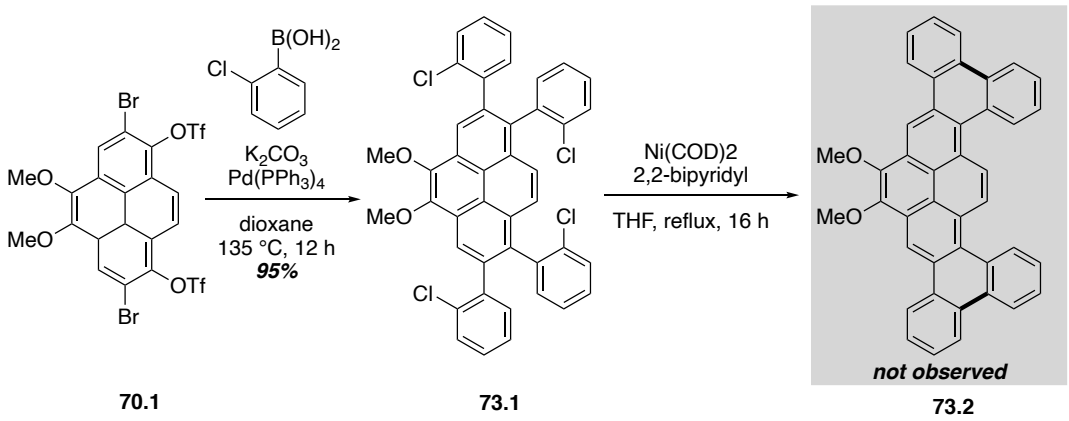

Figure 73. Non-selective Suzuki-Miyaura cross-coupling of compound **70.1** and Yamamoto coupling

Since selective Suzuki-Miyaura cross-coupling of the compound **70.1** was low yielding, we applied another Suzuki-Miyaura cross-coupling reaction to react with both bromine and triflate (Figure 73). Treatment **70.1** with 2-chlorophenylboronic acid under typical condition, tetrakis(2-chlorophenyl)-4,5-dimethoxypyrene **73.1** was obtained nearly quantitative yield. Compound **73.1** is also a good candidate to test the unexpected Scholl result through a Yamamoto coupling reaction. Unfortunately, no desired product was observed after treating **73.1** with $Ni(COD)_2$ and 2,2-bipyridine in THF and reflux for 16 hours.

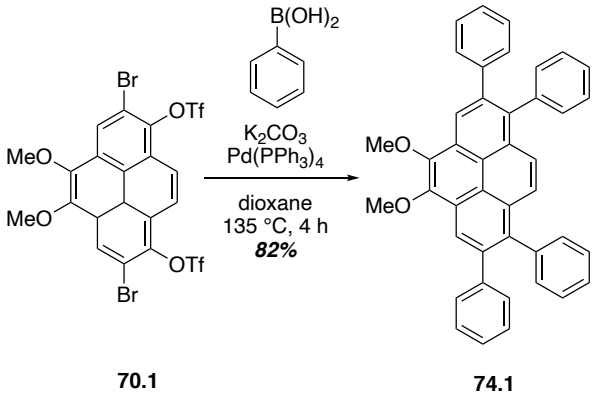

Figure 74. Non-selective Suzuki-Miyaura cross-coupling reaction of compound **70.1**

Inspired by the reaction in Figure 73, another Suzuki-Miyaura cross-coupling reaction was conducted on compound **23.1** with phenylboronic acid (Figure 74). Under the same condition, tetrakisphenyl-4,5-dimethoxypyrene was formed in 82% after 4 hours. As you can see, compound **74.1** is the precursor of unexpected Scholl reaction product **64.2**.

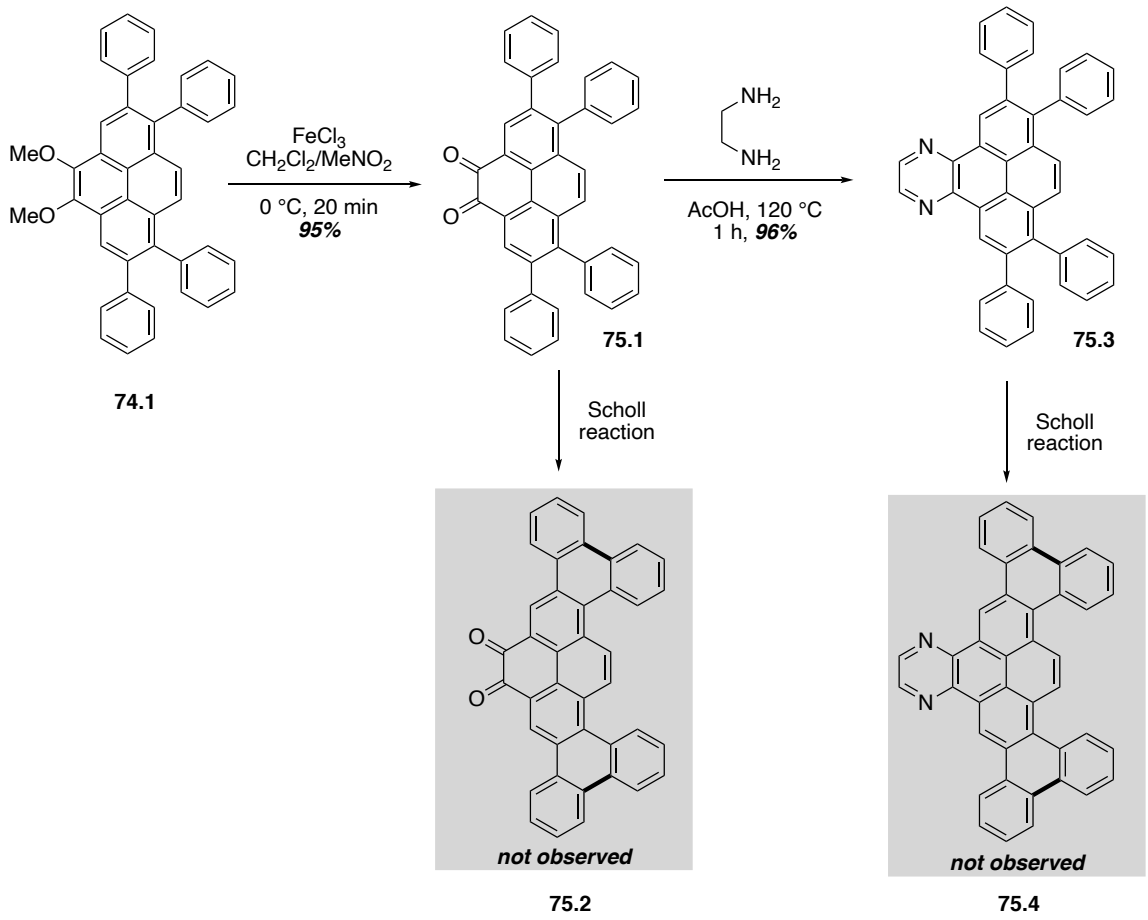

Figure 75. Attempted Scholl reaction of compound **74.1**

Treatment compound **74.1** with $FeCl_3$ in DCM/$MeNO_2$, monitored by TLC, no desired product was observed. Instead, oxidized compound 1,2,7,8-tetraphenylpyrene-4,5-dione **75.1** was generated in nearly quantitative yield. Under standard Scholl reaction condition this compound could not be cyclized to **75.2**. But dione **75.1** could be easily reacted with ethane-1,2-diamine to form pyrazine compound **75.3** in 96% yield. I also tried Scholl reaction on this pyrazine compound, but again, no cyclized compound was observed.

12 Conclusion

Substitution chemistry of pyrenes is typically limited to reaction at the 1-,3-,6-, and 8-positions, due to the nodal plane on both HOMO and LUMO. However, our high-yielding methodology provides rapid access to 2,7-functionalized pyrene is expected to be particularly useful in the synthesis of conjugated rigid-rod systems and other organic frameworks. And the highly regioselective Scholl reaction will be useful to evaluate future syntheses of oligoarene and graphene materials and other complex polyarene architectures.

Reference

[1] Laurent, A. *Ann. Chim. Phys.* **1837**, *66*, 136.

[2] Graebe, C. *Liebigs Ann.* **1871**, *158*, 285.

[3] Meyer, R. *Chem. Ber*. **1912**, *45*, 1609.

[4] Freund, M. *Chem. Ber*. **1897**, *30*, 1383.

[5] Steiner, H. *J. Inst. Pet.* **1947**, *33*, 410.

[6] Weitzenbock, R. *Mh. Chem.* **1913**, *34*, 193.

[7] Vollmann, H.; Becker, H.; Corell, M.; Streeck, H. *Liebigs Ann.* **1937**, *531*, 1.

[8] Altschuler, L; Berliner, E. *J. Am. Chem. Soc.* **1966**, *88*, 5837.

[9] Dewar, M. J. S.; Dennington, R. D. *J. Am. Chem. Soc.* **1989**, *111*, 3804.

[10] Hites, R. A. *Calculated Molecular Properties of Polycyclic Aromatic Hydrocarbons*; Elsevier: New York, 1987.

[11] Miyazawa, A.; Yamato, T.; Tashiro, M. *Chem. Express* **1990**, *5*, 381.

[12] Idaik, K, R.; Licha, T.; Lukeš, V.; Rapta, P.; Frydel, J.; Schaffer, M.; Taeuscher, E.; Beckert, R.; Dunsch, L, *J Fluoresc* **2014**, *24*, 153.

[13] 1) Đordević, L.; Milano, D.; Demitri, N.; Bonifazi D. *Org. Lett*. **2020**, *22*, 4283; 2) He, X.; Wang, X.; Tse, Y. S.; Ke, Z.; Yeung, Y. *ACS Catal*. **2021**, *11*, 12632; 3). He, X.; Wang, X.; Tse, Y. S.; Ke, Z.; Yeung, Y. *Angew. Chem. Int. Ed*. **2018**, *57*, 12869.

[14] 1) Chidirala, S.; Ulla, H.; Valaboju, A.; Kiran, M. R.; Mohanty, M. E.; Satyanarayan, M. N.; Umesh, G.; Bhanuprakash, K.; Rao, V. J. *J. Org. Chem.* **2016**, *81*, 603; 2). Wang, Y.; Li, X.; Li, F.; Sun, W.; Zhu, C.; Cheng, Y. *Chem. Commun.,* **2017**, *53*, 7505.

[15] George, S. R. D.; Frith, T. D. H.; Thomas, D. S.; Harper, J. B. *Org. Biomol. Chem.,* **2015**, *13*, 9035.

[16] Kiselyov, A. S.; Harvey. *Tetrahedron Letters* **1995**, *36*, 4005.

[17] 1) Nelsen, D. L.; Anding , B. J.; Sawicki, J. L.; Christianson, M. D.; Arriola, D. J.; Landis, C. R.; *ACS Catal*. **2016**, *6*, 7398; 2) Zeng, Z.; Torriero, A. A. J.; Bond, A. M.; Spiccia L. *Chem. Eur. J.* **2010**, *16*, 9154; 3) Yamato, T.; Miyazawa, A.; Tashiro, M. *J. Chem. Soc. Perkin Trans*. **1993**, 3127; 4) Zeng, Z.; Spiccia L. *Chem. Eur. J.* **2009**, *15*, 12941.

[18] Dmytrejchuk, A. M.; Jackson, S. N.; Meudom, R.; Gorden, J. D.; Merner, B. L. *J. Org. Chem.* **2018**, *83*, 10660.

[19] Crawford, A, G.; Liu, Z.; Mkhalid, I. A. I.; Thibault, M.; Schwarz, N.; Alcaraz, G.; Steffen, A.; Collings, J. C.; Batsanov, A. S.; Howard, J. A. K.; marder, T. B. *Chem. Eur. J.* **2012**, *18*, 5022.

[20] Lorbach, D.; Keerthi, A.; Figueira-Duarte, T. M.; Baumgarten, M.; Wagner, M.; Müllen, K. *Angew. Chem. Int. Ed*. **2016**, *55*, 418.

[21] 1) Wang, C.; Ichiyanagi, H.; Sakaguchi, K.; Feng, X.; Elsegood, M. R. J.; Redshaw, C.; Yamato, T. *J. Org. Chem.* **2017**, *82*, 7176; 2) Feng, X.; Hu, J.; Tomiyasu, H.; Tao, Z.; Redshaw, C.; Elsegood, M. R. J.; Horsburgh, L.; Teat, S. J.; Wei, X.; Yamato, T. *RSC Adv.,* **2015**, *5*, 8835.

[22] Zych, D.; Slodek, A. *RSC Adv.,* **2019**, *9*, 24015.

[23] Venkataramana, G.; Dongare, P.; Dawe, L. N.; Thompson, D. W.; Zhao, Y.; Bodwell, G. J. *Org. Lett*. **2011**, *13*, 2240.

[24] Figueira-Duarte, T. M.; Simon, S. C.; Wagner, M.; Drtezhinin, S. I.; Zachariasse, K. A.; Müllen, K. *Angew. Chem. Int. Ed*. **2008**, *47*, 10175.

[25] Đordević, L.; Valentini, C.; Demitri, N.; Mézière, C.; Allain, M.; Sallé, M.; Folli, A.; Murphy, D.; Mañas-Valero, S.; Coronado, E.; Bonifazi, D. *Angew. Chem. Int. Ed*. **2020**, *59*, 4106.

[26] Rausch, D.; Lambert, C. *Org. Lett.* **2006**, *8*, 5037.

[27] Iwamoto, T.; Kayahara, E.; Yasuda, N.; Suzuki, T.; Yamago S. *Angew. Chem.* **2014**, *126*, 6548.

[28] Keller, S. N.; Veltri, N. L.; Sutherland, T. C. *Org. Lett.* **2013**, *15*, 4798.

[29] Kawano, S.; Baumgarten, M.; Chercka, D.; Enkelmann, V.; Müllen, K. *Chem. Commun.,* **2013**, *49*, 5058.

[30] Danz, M.; Tonner, R.; Hilt, G. *Chem. Commun.,* **2012**, 48, 377.

Appendix

General Experimental Conditions

All reactions required dry condition were run in flame or oven-dried (120 ºC) glassware and cooled under a positive pressure of ultra high pure nitrogen or argon gas. All chemicals were used as received from commercial sources, unless otherwise stated. Anhydrous reaction solvents were purified and dried by passing HPLC grade solvents through activated columns of alumina (Glass Contour SDS). All solvents used for chromatographic separations were HPLC grade (hexanes, ethyl acetate, dichloromethane, chloroform, methanol, and acetone). Chromatographic separations were performed using flash chromatography, as originally reported by Still and co-workers, on silica gel 60 (particle size 43-60 μm). Reaction progress was monitored by thin layer chromatography (TLC), on glass-backed silica gel plates (pH = 7.0). TLC plates were visualized using a handheld UV lamp (254 nm) and stained using an aqueous ceric ammonium molybdate (CAM) solution. Plates were dipped, wiped clean, and heated from the back of the plate. ^{1}H and ^{13}C nuclear magnetic resonance (NMR) spectra were recorded at 500 or 600 MHz, calibrated using residual undeuterated solvent as an internal reference (CHCl3, δ 7.27 and 77.2 ppm), reported in parts per million relative to trimethylsilane (TMS, δ 0.00 ppm), and presented as follows: chemical shift (δ, ppm), multiplicity (s = single, d = doublet, dd = doublet of doublets, ddd = doublet of doublet of doublets, dt = doublet of triplets, t = triplet, m = multiplet, p = pentet), coupling constants (*J*, Hz). High-resolution mass spectrometric (HRMS) data were obtained using an electrospray ionization (ESI).

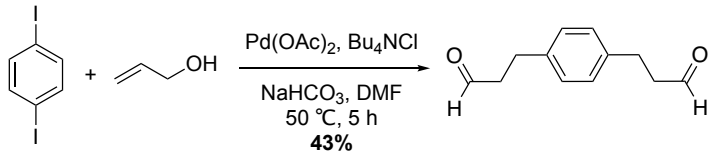

3,3'-(1,4-phenylene)dipropanal: $NaHCO_3$ (1.28 g, 15.2 mmol, 5.00 equiv.), 1,4-diiodobenzene (1.00 g, 3.04 mmol, 1.0 equiv.), Bu_4NCl (1.68 g, 6.08 mmol, 2.0 equiv.), and $Pd(OAc)_2$ (28 mg, 0.12 mmol, 4 mol%) were dissolved in anhydrous and degassed DMF (10 mL). Allyl alcohol (528 mg, 9.12 mmol, 3.0 equiv.) was added. The reaction mixture was heated for 5 h at 50 ºC. After cooling to room temperature, H_2O (20 mL) and Et_2O (25 mL) were added. The organic layer was separated and the aqueous phase was extracted with Et_2O (3 X 20 mL). The combined organic layers were washed with brine (50 mL) and dried over $MgSO_4$. The solvent was removed under reduced pressure and the residue was purified

by flash chromatography on silica gel to afford title compound as a white solid. (248 mg, 43%). ^{1}H NMR (500 MHz, $CDCl_3$) δ 9.83 (s, 2H), 7.13 (s, 4H), 2.94 (t, *J* = 7.5 Hz, 4H), 2.77 (t, *J* = 7.5 Hz, 4H).

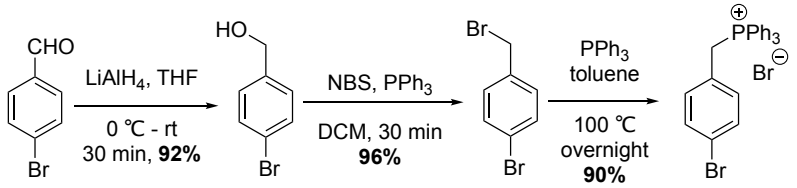

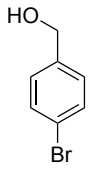

(4-bromophenyl)methanol : To a stirred solution of LDA (324 mg, 8.1 mmol, 1.5 equiv.) in dry THF (10 mL) was added dropwise a solution of 4-bromobenzaldehyde (1.0 g, 5.4 mmol, 1.0 equiv.) in dry THF (15 mL) at 0 ºC. After 30 min, the reaction was quenched by addition with 40% KOH solution at 0 ºC. The precipitate was filtered off and washed with Et_2O. The combined filtrates were dried over $MgSO_4$ and solvent was removed under reduced pressure and the residue was purified by flash chromatography on silica gel to afford title compound as a colorless oil. (919 mg, 92%). ^{1}H NMR (500 MHz, $CDCl_3$) δ 7.50 (d, *J* = 7.4 Hz, 2H), 7.26 (d, *J* = 7.4 Hz, 2H), 4.67 (d, *J* = 5.0 Hz, 2H), 1.66 (s, 1H).

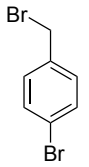

1-bromo-4-(bromomethyl)benzene : To the stirred solution of alcohol (800 mg, 4.35 mmol, 1.0 equiv.) in dry DCM (20 mL), triphenylphosphine (1.71g, 6.53 mmol, 1.5 equiv.) and N-bromosuccinimide (1.16 g, 6.53 mmol, 1.5 equiv.) were added. After consumed all the starting material, the solvent was removed under reduced pressure, the crude product was purified by flash chromatography on silica gel to afford title compound. (1.03 g, 96%). ^{1}H NMR (500 MHz, $CDCl_3$) δ 7.48 (d, *J* = 8.4 Hz, 2H), 7.28 (d, *J* = 8.4 Hz, 2H), 4.44 (s, 2H).

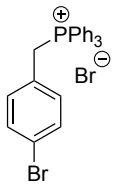

(4-bromobenzyl)triphenylphosphonium bromide : Benzylbromide (200 mg, 0.81 mmol, 1.0 equiv.) and triphenylphosphine (212 mg, 0.81 mmol, 1.0 equiv.) were added to toluene (2 mL), and the mixture was heated at 100 ºC for 12 h. The resulting precipitate was collected by filtration and washed with hexane. the title product was obtained. (371 mg, 90%).

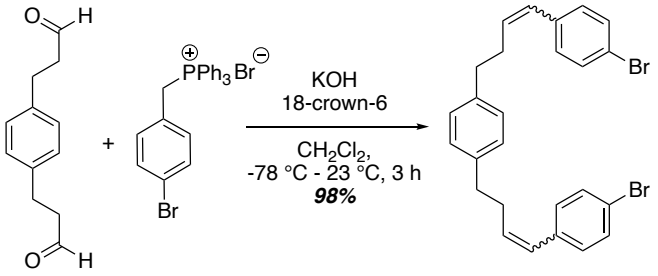

1,4-bis((*Z*)-4-(4-bromophenyl)but-3-en-1-yl)benzene and **1-((*E*)-4-(4-bromophenyl)but-3-en-1-yl)-4-((*Z*)-4-(4-bromophenyl)but-3-en-1-yl)benzene**: A solution of aldehyde (60 mg, 0.32 mmol, 1.0 equiv.), (4-bromobenzyl)-triphenylphosphonium bromide (338 mg, 0.66 mmol, 2.1 equiv.) and 18-crown-6 (17 mg, 0.064 mmol, 0.2 equiv.) in DCM (2 mL) was cooled to -78 ºC. To solution was added freshly powdered KOH (81 mg, 1.44 mmol, 4.5 equiv.) and the solution was stirred at -78 ºC for 2 h then wormed up to 23 ºC and stirred for 1 h. Then the reaction mixture was diluted with DCM (10 mL) and filtered. The filtrate was washed with sat. NH_4Cl (15 mL), dried over $MgSO_4$ and solvent was removed under reduced pressure and the residue was purified by flash chromatography on silica gel to afford the title compound as a white solid. (142 mg, 90%). **(*Z,Z*) isomer**: ^{1}H NMR (500 MHz, $CDCl_3$) δ 7.42 (d, *J* = 7.7 Hz, 4H), 7.10 (s, 4H), 7.07 (d, *J* = 7.7 Hz, 4H), 6.36 (d, *J* = 11.8 Hz, 2H), 5.73 (dt, *J* = 12.6, 7.1 Hz, 2H), 2.74 (t, *J* = 7.7 Hz, 4H), 2.60 (t, *J* = 7.6 Hz, 4H). **(*Z,E*) isomer**: ^{1}H NMR (500 MHz, $CDCl_3$) δ 7.42 (t, *J* = 7.5 Hz, 4H), 7.19 (d, *J* = 8.1 Hz, 2H), 7.17 – 7.10 (m, 4H), 7.07 (d, *J* = 7.9 Hz, 2H), 6.36 (dd, *J* = 14.1, 7.2 Hz, 2H), 6.25 (dt, *J* = 15.5, 6.8 Hz, 1H), 5.73 (dd, *J* = 12.0, 6.8 Hz, 1H), 2.76 (dt, *J* = 15.9, 5.9 Hz, 4H), 2.60 (q, *J* = 7.6 Hz, 2H), 2.51 (q, *J* = 7.3 Hz, 2H).

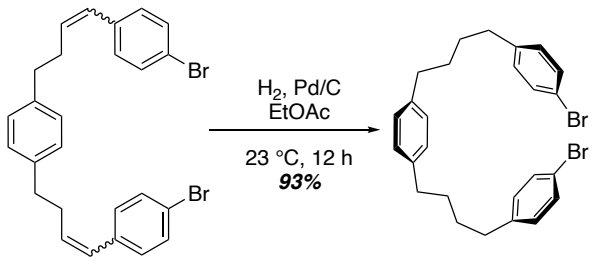

1,4-bis(4-(4-bromophenyl)butyl)benzene : A suspension of olefin (70 mg, 0.14 mmol, 1.0 equiv.) and 10% Pd/C (18 mg) in EtOAc (3 mL) was stirred under a balloon of hydrogen for 12 h at room temperature. Then the reaction mixture was diluted with EtOAc (10 mL) and filtered through a pad of celite. The filtrate was evaporated, and the residue was purified by flash chromatography on silica gel to afford the title compound as a colorless oil. (65 mg, 93%). ^{1}H NMR (500 MHz, $CDCl_3$) δ 7.38 (d, *J* = 8.1 Hz, 4H), 7.07 (s, 4H), 7.04 (d, *J* = 8.1 Hz, 4H), 2.63 – 2.54 (m, 8H), 1.66 – 1.62 (m, 8H).

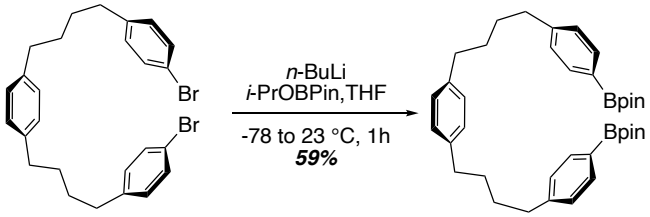

1,4-bis(4-(4-(4,4,5,5-tetramethyl-1,3,2-dioxaborolan-2-yl)phenyl)butyl)benzene : A solution of aryl-Br (95 mg, 0.19 mmol, 1.0 equiv.) in THF (2 mL) was added *n*-BuLi (1.5 M in THF, 0.33 mL, 2.5 equiv.) at -78 ºC. after stirred 1 h at -78 ºC, *i*-PrOBpin (89 mg, 0.48 mmol, 2.5 equiv.) was added dropwise in 10 min. The mixture was then warmed up to room temperature and stirred overnight. 2 mL Sat. NH_4Cl was added to quench the reaction, the mixture was extracted with DCM (3 X 5 mL), dried over $MgSO_4$ and solvent was removed under reduced pressure and the residue was purified by flash chromatography on silica gel to afford title compound as a colorless oil. (66 mg, 59%). ^{1}H NMR (500 MHz, $CDCl_3$) δ 7.73 (d, *J* = 7.7 Hz, 4H), 7.19 (d, *J* = 7.6 Hz, 4H), 7.06 (s, 4H), 2.65 (t, *J* = 7.1 Hz, 4H), 2.59 (t, *J* = 7.2 Hz, 4H), 1.68 – 1.62 (td, *J* = 10.4, 9.4, 3.9 Hz, 8H), 1.35 (s, 24H).

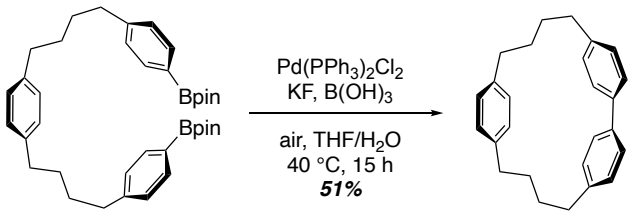

1,2,7(1,4)-tribenzenacycloundecaphane : Diboronic ester (237 mg, 0.4 mmol, 1.0 equiv.) was added to a 500 mL flask with bis(triphenylphosohine)palladium(II) dichloride (16 mg, 0.02 mmol, 5 mol%) and boric acid (143 mg, 2.3 mmol, 5.0 equiv.). the solid were dissolved in THF (392 mL) and the mixture was stirred vigorously for 10 min. KF (27 mg, 0.46 mmol, 1.0 equiv.) was added to the mixture followed by the addition of H_2O (40 mL). the reaction was stirred at room temperature open to the atmosphere for 12 h. The THF was removed under vacuum and the resulting solution was extracted with DCM (3 X 50 mL). The combined organic layers were washed with deionized water (3 X 50 mL) and brine (50 mL) then dried over $MgSO_4$ and solvent was removed under reduced pressure and the residue was purified by flash chromatography on silica gel to afford title compound as a colorless solid. (70 mg, 51%). ^{1}H NMR (500 MHz, $CDCl_3$) δ 7.49 (d, *J* = 7.4 Hz, 4H), 7.16 (d, *J* = 7.3 Hz, 4H), 6.20 (s, 4H), 2.64 (s, 4H), 2.04 (t, *J* = 6.0 Hz, 4H), 1.55 (d, *J* = 7.5 Hz, 4H), 1.29 (t, *J* = 7.2 Hz, 4H).

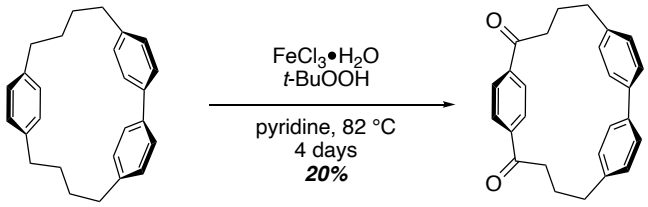

1,2,7(1,4)-tribenzenacycloundecaphane-6,8-dione : Macrocycle (5 mg, 0.015 mmol, 1.0 equiv.) was added to the solution of $FeCl_3{\cdot}6H_2O$ (0.4 mg, 0.0015 mmol, 10 mol%) in pyridine (0.1 mL). After the addition of TBHP (70% in H_2O, 9.6 mg, 0.075 mmol, 5.0 equiv.), the reaction mixture was heated to 82 ºC for 4 days. The mixture was then cooled to room temperature and transfer into a 1 N solution of HCl (2 mL) in order to remove the pyridine. The organic phase was extracted with EtOAc (3 X 5 mL), then dried over $MgSO_4$ and solvent was removed under reduced pressure and the residue was purified by flash chromatography on silica gel to afford title compound as a colorless solid. (1 mg, 20%). ^{1}H NMR (500 MHz, $CDCl_3$) δ 7.41 (s, 4H), 7.19 (d, *J* = 7.2 Hz, 4H), 7.01 (d, *J* = 7.2 Hz, 4H), 2.79 (t, *J* = 6.1 Hz, 4H), 2.59 – 2.51 (m, 4H), 2.46 – 2.39 (m, 4H).

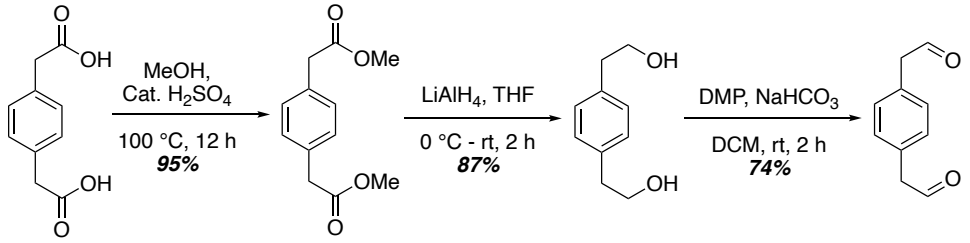

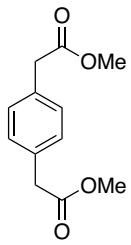

dimethyl 2,2'-(1,4-phenylene)diacetate: In a clean flask, acid (1.0 g, 5.15 mmol, 1.0 equiv.) and MeOH (5 mL) were added. A catalytic amount of H_2SO_4 was transferred through pipet. Then the flask was heated at 100 ºC for 12 h. After detaching the reaction, it was cooled to room temperature and purified by flash chromatography on silica gel to afford title compound as a white solid. (1.09 g, 95%).

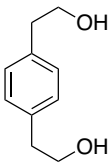

2,2'-(1,4-phenylene)bis(ethan-1-ol) : Under argon, a round bottom flask was charged with a stirring bar, $LiAlH_4$ (103 mg, 2.58 mmol, 5.0 equiv.) in dry THF (5 mL). then the mixture was cooled to 0 ºC and a solution of diester (100 mg, 0.52 mmol, 1.0 equiv.) in dry THF (1 mL) was added dropwise. After addition, the

reaction was stirred warm up to room temperature. After 2 h, the mixture was quenched with sat. Na_2SO_4 solution (5 mL) and filtered through celite. The filtrate was diluted with DCM then washed with brine (3 X 10 mL). dried over $MgSO_4$ and solvent was removed under reduced pressure and the residue was purified by flash chromatography on silica gel to afford title compound as a white solid. (75 mg, 87%)

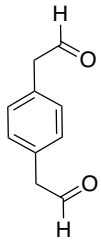

2,2'-(1,4-phenylene)diacetaldehyde : Diol (163 mg, 1 mmol, 1.0 equiv.) was dissolved in DCM (45 mL), followed by the sequential addition of NaHCO3 (252 mg, 3.0 mmol, 3.0 equiv.) and Dess-Martin periodinane (1,27 g, 3.0 mmol, 3.0 equiv.). After 30 min., $Na_2S_2O_3$ (20 mL) and $NaHCO_3$ (20 mL) was added to the mixture. The payers were separated and the aqueous phase was extracted with DCM (3 X 50 mL), dried over $MgSO_4$ and solvent was removed under reduced pressure and the residue was purified by flash chromatography on silica gel to afford title compound as a white solid. (120 mg, 74%). ^{1}H NMR (500 MHz, $CDCl_3$) δ 9.77 (s, 2H), 7.24 (s, 4H), 3.72 (d, *J* = 2.3 Hz, 4H).

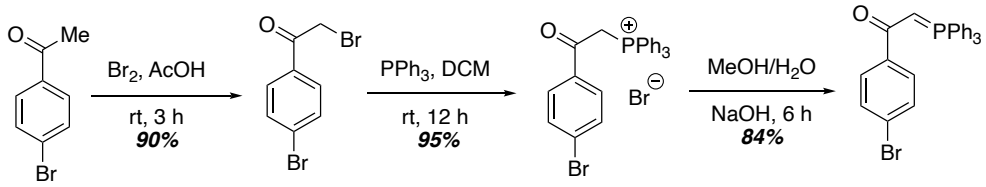

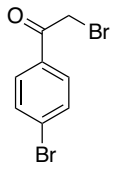

2-bromo-1-(4-bromophenyl)ethan-1-one : To a stirred solution of 4-bromoacetophenone (3.0 g, 15 mmol, 1.0 equiv.) in acetic acid (23 mL) was added dropwise bromine (0.775 mL, 15 mmol, 1.0 equiv.). The solution was allowed to a stir at room temperature for a future 3 h, until a color change from dark brown to yellow had occurred. The solution was then diluted with EtOAc (50 mL), and washed with $Na_2S_2O_3$ solution (2M, 2 X 50 mL), Sat. $NaHCO_3$ (2 X 50 mL), and water (2 X 50 mL). Then dried over $MgSO_4$ and solvent was removed under reduced pressure to give a white solid. (3.7 g, 90%). ^{1}H NMR (500 MHz, $CDCl_3$) δ 7.87 (d, *J* = 8.6 Hz, 2H), 7.66 (d, *J* = 8.6 Hz, 2H), 4.41 (s, 2H).

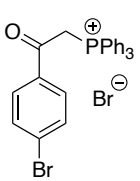

(2-(4-bromophenyl)-2-oxoethyl)triphenylphosphonium bromide: Bromekeotne (1.0 g, 3.6 mmol, 1.0 equiv.) and triphenylphosphine (943 mg, 3.6 mmol, 1.0 equiv.) were added to toluene (6 mL), and the mixture was heated at 100 ºC for 12 h. The resulting precipitate was collected by filtration and washed with hexane. the title product was obtained. (1.8 g, 95%).

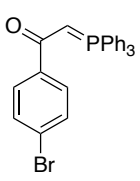

1-(4-bromophenyl)-2-(triphenyl-λ^5-phosphanylidene)ethan-1-one: The phosphonium salt (920 mg, 1.75 mmol, 1.0 equiv.) was added to a mixture of H_2O and MeOH (v/v = 1:1, 6 mL) and the reaction mixture was stirred at room temperature for 2 h, followed by the addition of 1.6 M NaOH to PH = 7-8, the reaction was stirred at room temperature for 3 h. After flash filtration of the suspension formed, the precipitate was washed with water and dried without further purification. (673 mg, 84%)

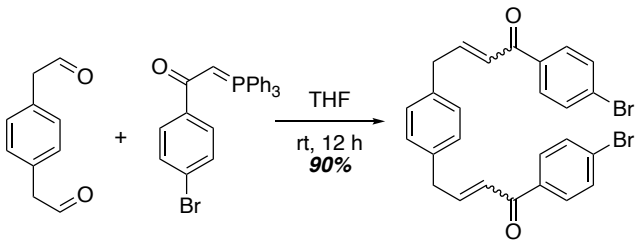

4,4'-(1,4-phenylene)bis(1-(4-bromophenyl)but-2-en-1-one): To a solution of stabilized ylide (603 mg, 1.31 mmol, 3.0 equiv.) in THF (5 mL) was added to a dialdehyde (71 mg, 0.44 mmol, 1.0 equiv.) solution. The mixture was stirred at room temperature for 12 h. After removing the solvent, the residue was purified by flash chromatography on silica gel to afford title compound as a white solid. (206 mg, 90%). ^{1}H NMR (500 MHz, $CDCl_3$) δ 7.90 – 7.85 (m, 1H), 7.78 – 7.74 (m, 2H), 7.67 – 7.57 (m, 4H), 7.38 – 7.33 (m, 1H), 7.23 – 7.13 (m, 3H), 6.81 (ddt, *J* = 15.0, 13.2, 1.6 Hz, 1H), 6.60 – 6.49 (m, 1H), 6.47 – 6.41 (m, 1H), 3.89 (dd, *J* = 6.7, 1.3 Hz, 2H), 3.65 – 3.61 (m, 2H).

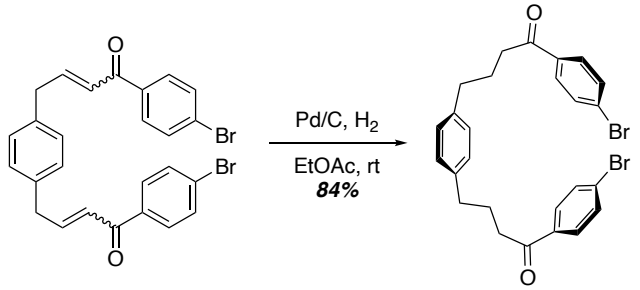

4,4'-(1,4-phenylene)bis(1-(4-bromophenyl)butan-1-one): A suspension of olefin (100 mg, 0.19 mmol, 1.0 equiv.) and 10% Pd/C (30 mg) in EtOAc (3 mL) was stirred under a balloon of hydrogen for 12 h at room temperature. Then the reaction mixture was diluted with EtOAc (10 mL) and filtered through a pad of celite. The filtrate was evaporated, and the residue was purified by flash chromatography on silica gel to afford the title compound as a colorless oil. (79 mg, 84%). ^{1}H NMR (500 MHz, $CDCl_3$) δ 7.78 (d, *J* = 8.5 Hz, 4H), 7.59 (d, *J* = 8.5 Hz, 4H), 7.13 (s, 4H), 2.94 (t, *J* = 7.3 Hz, 4H), 2.69 (t, *J* = 7.5 Hz, 4H), 2.07 (p, *J* = 7.3 Hz, 4H).

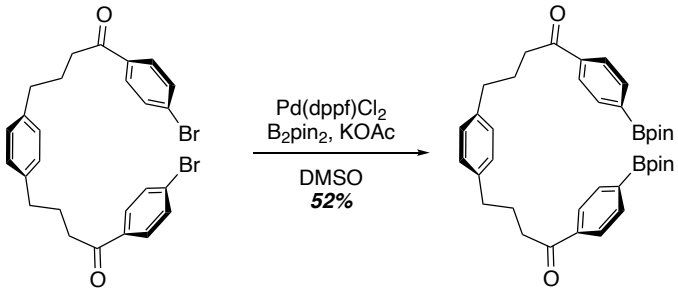

4,4'-(1,4-phenylene)bis(1-(4-(4,4,5,5-tetramethyl-1,3,2-dioxaborolan-2-yl)phenyl)butan-1-one): A flask was charged with Pd((dppf)C_{l2} (10 mg, 5 mol%), KOAc (80 mg, 0.8 mmol, 4.0 equiv.) and B_2pin_2 (111 mg, 0.44 mmol, 2.2 equiv.) was back filled with nitrogen. DMSO (2 mL) and aryl-Br (100 mg, 0.2 mmol, 1.0 equiv.) were added. After being stirred at 80 ºC for 12 h, the mixture was extracted with EtOAc (3 X 10 mL) and water (3 X 10 mL), dried over $MgSO_4$ and solvent was removed under reduced pressure and the residue was purified by flash chromatography on silica gel to afford title compound as a white solid. (65 mg, 52%). ^{1}H NMR (500 MHz, $CDCl_3$) δ 7.95 – 7.83 (m, 8H), 7.13 (s, 4H), 3.00 (t, *J* = 7.3 Hz, 4H), 2.70 (t, *J* = 7.6 Hz, 4H), 2.07 (p, *J* = 7.4 Hz, 4H), 1.36 (s, 24H).

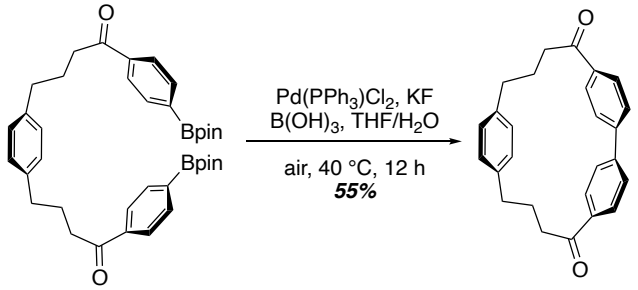

1,2,7(1,4)-tribenzenacycloundecaphane-3,11-dione: Diboronic ester (100 mg, 0.16 mmol, 1.0 equiv.) was added to a 500 mL flask with bis(triphenylphosohine)palladium(II) dichloride (12 mg, 0.02 mmol, 10 mol%) and boric acid (50 mg, 0.8 mmol, 5.0 equiv.). the solid were dissolved in THF (140 mL) and the mixture was stirred vigorously for 10 min. KF (10 mg, 0.02, 1.0 equiv.) was added to the mixture followed by the addition of H_2O (14 mL). the reaction was stirred at room temperature open to the atmosphere for 12 h. The THF was removed under vacuum and the resulting solution was extracted with DCM (3 X 50 mL). The combined organic layers were washed with deionized water (3 X 50 mL) and brine (50 mL) then dried over $MgSO_4$ and solvent was removed under reduced pressure and the residue was purified by flash chromatography on silica gel to afford title compound as a colorless solid. (32 mg, 55%).

^{1}H NMR (500 MHz, $CDCl_3$) δ 7.67 – 7.55 (m, 8H), 6.30 (s, 4H), 2.87 – 2.79 (m, 4H), 2.18 (t, *J* = 7.3 Hz, 4H), 1.73 (p, *J* = 7.0 Hz, 4H).

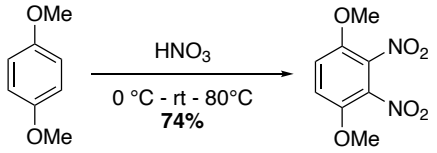

1,4-dimethoxy-2,3-dinitrobenzene: 1,4-dimethoxybenzene (1.0 g, 7.25 mmol, 1.0 equiv.) was added to 10 mL of HNO_3 in ice bath during 30 min. After 1h in ice bath and another 1 h at room temperature, the yellow mixture was heated up to 100 ºC. after 1 h, the mixture was quenched with ice water. The mixture was filtrated and the residue was washed with water. After dried in air, the crude product was recrystallized in glacial acetic acid to afford title compound as a yellow crystal. (1.2 g, 74%)

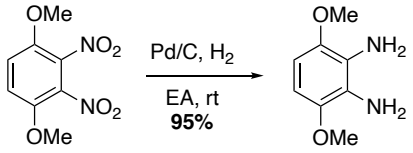

3,6-dimethoxybenzene-1,2-diamine: To a stirred solution of nitrobenzene (293 mg, 1.29 mmol, 1.0 equiv.) in EtOAc (2 mL), 10% Pd/C (14 mg) was added under H_2 atmosphere (1 balloon pressure). The reaction was stirred for 12 h then filtered through a pad of celite to remove the catalyst. After evaporation of the solvent under reduced pressure, the title compound was obtained and used for the next step directly.

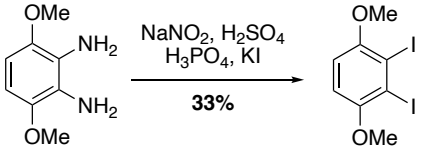

2,3-diiodo-1,4-dimethoxybenzene: A solution of diamino compound (131 mg, 0.78 mmol, 1.0 equiv.) in ice cold concentrated H_2SO_4 (2 mL) was added over 10 min at 0 ºC to a stirred solution of nitrosyl sulfuric acid (prepared from 280 mg $NaNO_2$ and 2 mL concentrated H_2SO_4 according to Fierz-David and Blangey) resulting in a red solution. Stirring was continued at 0

ºC for an additional 20 min., Phosphoric acid (85%, 4 mL) was added slowly to the solution and the temperature was kept below 10 ºC and then stirred for an additional 20 min. The resulting yellow inhomogeneous slurry was poured into a violently stirred solution of KI (687 mg, 3.51 mmol, 4.5 equiv.) in ice water (10 mL). This gave a deep red solution and some gas evolution. This solution was stirred at room temperature for 2 h and then heated to 40 ºC for 30 min., the solution was extracted with DCM (3 X 50 mL) and the combined organic phases were washed with sodium bisulfite (30 mL) and dried over $MgSO_4$ and solvent was removed under reduced pressure and the residue was purified by flash chromatography on silica gel to afford title compound as a white solid. (100 mg, 33%).

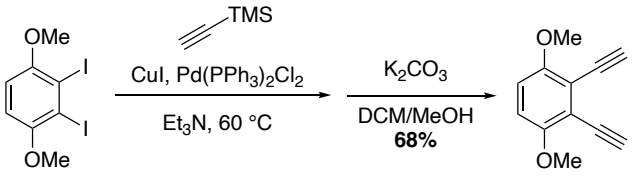

2,3-diethynyl-1,4-dimethoxybenzene: To a solution of aryl iodide (89 mg, 0.23 mmol, 1.0 equiv.), CuI (4.4 mg, 0.023 mmol, 10 mol%) and $Pd(PPh_3)Cl_2$ (8 mg, 5 mol%) in Et_3N (1 mL) was added trimethylsilylacetylene (57 mg, 0.58 mmol, 2.5 equiv.) dropwise. Then the resulting mixture was heated under nitrogen atmosphere at 60 ºC for 12 h. After the mixture was cooled to room temperature, the solid was removed by filtration. The filtrate was treated with water and extracted with DCM and dried over $MgSO_4$ and solvent was removed under reduced pressure. The residue was dissolved in MeOH (4 mL) and added K_2CO_3 (100 mg, 0.69 mmol, 3.0 equiv.), the resulting mixture was stirred at room temperature and monitored by TLC to establish the consumption of starting material. After the solid was removed by filtration, the filtrate was extracted with DCM and water, dried over $MgSO_4$ and solvent was removed under reduced pressure and the residue was purified by flash chromatography on silica gel to afford the title compound as a white solid. (29 mg, 67%). ^1H NMR (500 MHz, $CDCl_3$) δ 6.87 (s, 2H), 3.88 (s, 6H), 3.59 (s, 2H).

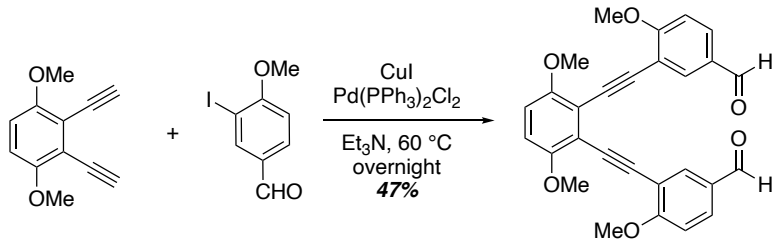

3,3'-((3,6-dimethoxy-1,2-phenylene)bis(ethyne-2,1-diyl))bis(4-methoxybenzaldehyde):

To a solution of aryl iodide (170 mg, 0.65 mmol, 2.5 equiv.), CuI (5 mg, 0.026 mmol, 10 mol%) and $Pd(PPh_3)Cl_2$ (9 mg, 5 mol%) in Et_3N (1 mL) was added 2,3-diethynyl-1,4-dimethoxybenzene (48 mg, 0.26 mmol, 1.0 equiv.). Then the resulting mixture was heated under nitrogen atmosphere at 60 ºC for 12 h. After the mixture was cooled to room temperature, the solid was removed by filtration. The filtrate was treated with water and extracted with DCM and dried over $MgSO_4$ and solvent was removed under reduced pressure, dried over $MgSO_4$ and solvent was removed under reduced pressure and the residue was purified by flash chromatography on silica gel to afford the title compound as a yellow solid. (55 mg, 47%). ^1H NMR (500 MHz, $CDCl_3$) δ 9.81 (s, 2H), 8.08 (d, *J* = 2.1 Hz, 2H), 7.84 (dd, *J* = 8.6, 2.1 Hz, 2H), 7.02 (d, *J* = 8.6 Hz, 2H), 6.86 (s, 2H), 3.92 (s, 6H), 3.91 (s, 6H).

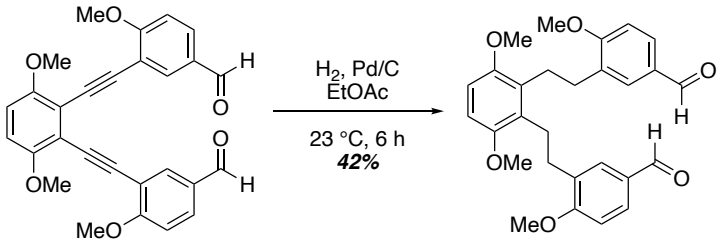

3,3'-((3,6-dimethoxy-1,2-phenylene)bis(ethane-2,1-diyl))bis(4-methoxybenzaldehyde):

To a stirred solution of nitrobenzene (100 mg, 0.22 mmol, 1.0 equiv.) in EA (10 mL), 10% Pd/C (24 mg) was added under H_2 atmosphere (1 balloon pressure). The reaction was stirred for 6 h then filtered through a pad of celite to remove the catalyst. After evaporation of the solvent under reduced pressure the residue was purified by flash chromatography on silica gel to afford the title compound as a white solid. (43 mg, 42%). ^1H NMR (500 MHz, $CDCl_3$) δ 9.87 (s, 2H), 7.73 (d, *J* = 7.0 Hz, 4H), 6.94 (d, *J* = 8.6 Hz, 2H), 6.71 (s, 3H), 3.79 (s, 12H), 3.01 – 2.91 (m, 4H), 2.82 (dd, *J* = 10.3, 6.2 Hz, 4H).

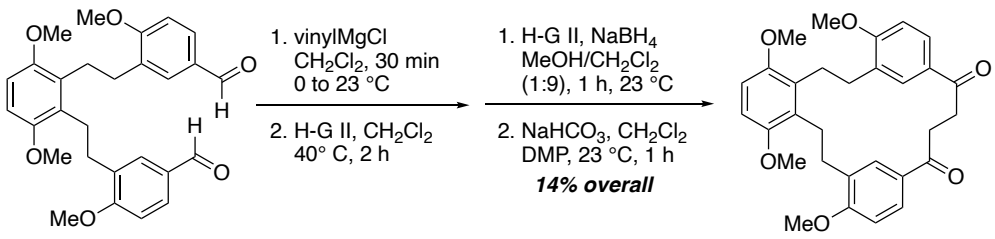

$1^6,4^3,4^6,7^6$-tetramethoxy-1,7(1,3),4(1,2)-tribenzenacycloundecaphane-8,11-dione:
Vinylmagnesium chloride (1.7 M in THF, 0.1 mL, 0.16 mmol, 2.5 equiv.) was added to a stirred solution of the dialdehyde (30 mg, 0.06 mmol, 1.0 equiv.) in DCM (2mL). After 10 min., the reaction was poured into water (5 mL) and further diluted with 1 M HCl (4 mL). The resulting mixture was extracted with DCM (3 X 5 mL). the combined organic extracts were washed with sat. $NaHCO_3$ (10 mL) and water (10 mL), dried over $MgSO_4$, filtered, and concentrated under reduced pressure. The pale yellow residue was dissolved in DCM (2 mL), heated to 40 ºC, followed by the addition of Hoveyda-Grubbs second-generation catalyst (1.5 mg). After 1 h, the reaction mixture was concentrated under reduced pressure. The black residue was dissolved in 1:9 methanol/DCM (1 mL), and sodium borohydride (14 mg, 0.36 mmol, 6.0 equiv.) was added. After 3 h, the reaction was poured into water (5 mL) and further diluted with 1 M HCl (2 mL). the layers were separated and the aqueous phase was extracted with DCM (3 X 5 mL). The combined organic extracts were washed with water (5 mL), dried over $MgSO_4$, filtered and concentrated under reduced pressure. Then the residue was dissolved in DCM (2.5 mL), followed by the sequential addition of $NaHCO_3$ (10 mg, 0.12 mmol, 2.0 equiv.) and Dess-Martin periodinane (50 mg, 0.12 mmol, 2.0 equiv.). after 1 h, the reaction was poured into water (5 mL). the layers were separated and the aqueous phase was extracted with DCM (3 X 5 mL). The combined organic extracts were washed with water (5 mL), dried over $MgSO_4$, filtered and concentrated under reduced pressure. The residue was purified by flash chromatography on silica gel to afford title compound. (4 mg, 14%). ^{1}H NMR (500 MHz, $CDCl_3$) δ 8.01 (dd, *J* = 8.7, 2.3 Hz, 2H), 7.93 (d, *J* = 2.3 Hz, 2H), 7.02 (d, *J* = 8.7 Hz, 2H), 6.76 (s, 2H), 3.96 (s, 6H), 3.85 (s, 6H), 3.16 (s, 4H), 2.97 (tdq, *J* = 10.1, 7.5, 4.3, 3.8 Hz, 8H).

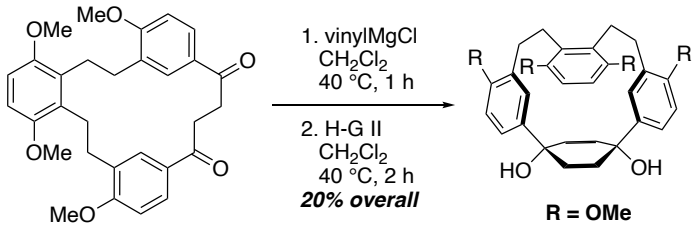

$1^6,4^3,4^6,7^6$-tetramethoxy-1,3(1,3),6(1,2)-tribenzena-2(1,4)-cyclohexanacyclooctaphan-22-ene-$2^1,2^4$-diol: 1,4-diketone (20 mg, 0.04 mmol, 1.0 equiv.), as a solution in DCM (2 mL) was added to a stirred 40 ºC solution of vinylmagnesium chloride (1.7 M in THF, 0.06 mL, 0.1 mmol, 2.5 equiv.). After 10 min, the reaction was poured into water (2 mL) and further diluted with 1 M HCl (2 mL). the resulting mixture was extracted with DCM (3 X 3 mL). The organic extracted were combined and washed with $NaHCO_3$ (3 mL) and brine (3 mL), then dried over $MgSO_4$ and concentrated under reduced pressure. The solid residue was dissolved in DCM

(1 mL) followed by addition of Grubbs' second-generation (0.6 mg, 2.5 mol%), the mixture was stirred at 40 ºC for 2 h. Then the solvent was removed under reduced pressure and the residue was purified by flash chromatography on silica gel to afford the title compound (4 mg, 20% overall). ^{1}H NMR (500 MHz, $CDCl_3$) δ 7.57 (dd, *J* = 8.5, 2.4 Hz, 2H), 7.44 (d, *J* = 2.4 Hz, 2H), 6.94 (d, *J* = 8.5 Hz, 2H), 6.75 (s, 2H), 3.88 (s, 6H), 3.86 (s, 6H), 3.20 (td, *J* = 12.3, 11.4, 4.8 Hz, 2H), 2.95 (td, *J* = 14.7, 13.5, 4.7 Hz, 2H), 2.79 – 2.68 (m, 4H), 2.16 – 2.09 (m, 2H), 2.00 – 1.91 (m, 2H).

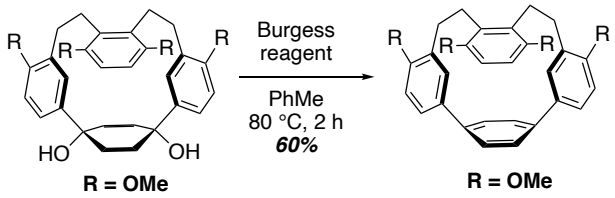

R = OMe **R = OMe**

1^6,4^3,4^6,7^6-tetramethoxy-1,3(1,3),2(1,4),6(1,2)-tetrabenzenacyclooctaphane : Burgess reagent (13 mg, 0.05 mmol, 4.0 equiv.) was added to a stirred solution of diol (7 mg, 0.014 mmol, 1.0 equiv.) in toluene (1 mL) at 80 ºC. after 2 h, the reaction was cooled to room temperature, water (3 mL) was added and the resulting mixture was stirred for 5min. The layers were separated and the mixture was extracted with DCM (3 X 3 mL). The organic extracted were combined and washed brine (3 mL), then dried over $MgSO_4$ and concentrated under reduced pressure. The residue was purified by flash chromatography on silica gel to afford the title compound. (4 mg, 60%). ^{1}H NMR (500 MHz, $CDCl_3$) δ 7.44 (dd, *J* = 8.1, 2.3 Hz, 2H), 7.36 (s, 4H), 6.88 (d, *J* = 8.2 Hz, 2H), 6.69 (s, 2H), 5.95 (d, *J* = 2.4 Hz, 2H), 3.88 (s, 6H), 3.82 (s, 6H), 2.72 – 2.61 (m, 8H).

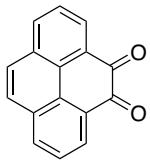

Pyrene-4,5-dione: To a solution of pyrene (10.00 g, 49.5 mmol) in dichloromethane (200 mL) and THF (200 mL) were added $RuCl_3$•$3H_2O$ (1.29 g, 4.95 mmol), N-methylimidazole (0.21 g, 2.5 mmol) and H_2O (250 mL). $NaIO_4$ (47.40 g, 221.5 mmol) was added in small portions over 20 min. The resulting slurry was stirred at room temperature for 2.5 h and the organic solvents were removed under reduced pressure. Dichloromethane (200 mL) and H_2O (200 mL) were added to dissolve the solids, and the layers were separated. The aqueous phase was extracted with dichloromethane (3 X 200 mL), and the combined organic layers were washed with H_2O (3 X 200 mL), dried over $MgSO_4$ and concentrated under reduced pressure to afford a dark-orange solid. The crude product was purified by flash chromatography to afford Pyrene-4,5-dione as

bright-orange crystals (4.2 g, 52% brsm). Rf (CH_2Cl_2) = 0.32. ^{1}H NMR (500 MHz, $CDCl_3$) δ 8.49 (dd, *J* = 7.5, 1.3 Hz, 2 H), 8.18 (dd, *J* = 7.9, 1.3 Hz, 2H), 7.85 (s, 2H), 7.76 (t, *J* = 7.7 Hz, 2H); ^{13}C NMR (126 MHz, $CDCl_3$) δ 180.66, 135.95, 132.26, 130.39, 130.31, 128.64, 128.19, 127.46;

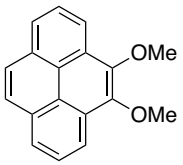

4,5-dimethoxypyrene: To a solution of pyrene-4,5-dione (3.30 g, 14.2 mmol) in THF (65 mL) and H_2O (65 mL) were added tetra-*n*-butylammonium bromide (1.37 g, 4.26 mmol) and $Na_2S_2O_4$ (7.43 g, 42.7 mmol). After 5 min, a solution of NaOH (6.80 g, 170 mmol) in H_2O (65 mL) was added to the reaction followed by Me_2SO_4 (8.95 g, 71 mmol). The red-colored reaction mixture was stirred at room temperature for 1 h. the reaction mixture was diluted with EtOAc (65 mL), the layers were separated and the aqueous phase was extracted with EtOAc (2 X 30 mL). The combined organic extracts were washed with water (50 mL) followed by brine (40 mL). the organic phase was dried over $MgSO_4$ and the solvent was removed under reduced pressure. The crude product was purified by flash chromatography to afford 4,5-dimethoxypyrene as a colorless solid (3.0 g, 81%). Rf (40% CH_2Cl_2/hexanes) = 0.5. ^{1}H NMR (500 MHz, $CDCl_3$) δ 8.50 (dd, *J* = 7.9, 1.1 Hz, 2H), 8.16 (dd, *J* = 7.6, 1.1 Hz, 2H), 8.08 (s, 2H), 8.05 (t, *J* = 7.7 Hz, 2H), 4.23 (s, 6H); ^{13}C NMR (126 MHz, $CDCl_3$) δ 145.00, 131.29, 128.55, 127.52, 126.21, 124.64, 123.05, 119.49, 61.35; HRMS (ESI) calculated for $C_{18}H_{15}O_2$([M+H]$^+$) m/z = 263.1066, found 263.1064.

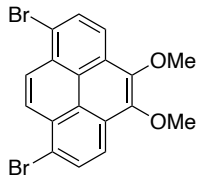

1,8-dibromo-4,5-dimethoxypyrene: Bromine (1.34 g, 8.37 mmol) in CH_2Cl_2 (10 mL) was added dropwise to a solution of 4,5-dimethoxypyrene (1.00 g, 3.81 mmol) in CH_2Cl_2 (30 mL) over 5 min at room temperature. After complete addition of bromine, stirring was continued at room temperature for 5 min. the reaction mixture was poured into sodium bisulfite solution (25 mL) and the layers were separated. The organic phase was washed with water (30 mL) followed by brine (30 mL) and dried over $MgSO_4$, the solvent was removed under reduced pressure. The crude product was purified by flash chromatography to afford 1,8-dibromo-4,5-dimethoxypyrene (1.45 g, 91%). Rf (40% CH_2Cl_2/hexanes) = 0.6; ^{1}H NMR (500 MHz, $CDCl_3$) δ 8.54 (s, 2H), 8.37 (d, *J* = 8.5 Hz, 2H), 8.29 (d, *J* = 8.4 Hz, 2H), 4.2 (s, 6H); ^{13}C NMR (126 MHz, $CDCl_3$) δ 144.65, 131.00, 129.67, 128.34, 127.69, 123.68, 120.90, 120.29, 61.38; HRMS (ESI) calculated for $C_{18}H_{13}O_2Br_2$([M+H]$^+$) m/z = 418.9276, found 418.9276.

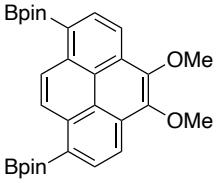

2,2'-(4,5-dimethoxypyrene-1,8-diyl)bis(4,4,5,5-tetramethyl-1,3,2-dioxaborolane): a flask with a condenser was charged with 1,8-dibromo-4,5-dimethoxypyrene (1.00 g, 2.39 mmol), $Pd(dppf)Cl_2$ (88 mg, 0.12 mmol, 5mol%), B_2pin_2 (1.82 g, 7.17 mmol), KOAc (0.94 g, 9.56 mmol) and 1,4-dioxane (12 mL) under nitrogen atmosphere, and the mixture degassed with nitrogen for 20 min and stirred at 80 ºC for 20 h. after cooled to room temperature, the mixture was filtered through a pad of celite and the solvent was removed under reduced pressure. The residue was purified by flash chromatography to afford 2,2'-(4,5-dimethoxypyrene-1,8-diyl)bis(4,4,5,5-tetramethyl-1,3,2-dioxaborolane) (0.96 g, 78%) as white solid. Rf (15% EtOAc/hexanes) = 0.3; ^{1}H NMR (500 MHz, $CDCl_3$) δ 9.31(s, 2H), 8.57 (d, *J* = 7.8 Hz, 2H), 8.49 (d, *J* = 7.9 Hz, 2H), 4.22 (s, 6H), 1.51 (s, 24H); ^{13}C NMR (126 MHz, $CDCl_3$) δ 145.59, 136.11, 134.10, 130.68, 128.49, 122.81, 118.54, 84.05, 61,39, 25.25; HRMS (ESI) calculated for $C_{30}H_{37}O_6B_2([M+H]^+)$ m/z = 512.2770, found 512.2760.

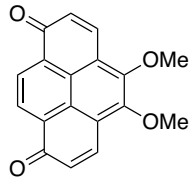

4,5-dimethoxypyrene-1,8-dione: 2,2'-(4,5-dimethoxypyrene-1,8-diyl)bis(4,4,5,5-tetramethyl-1,3,2-dioxaborolane) (1.00 g, 1.95 mmol) and NaOH (0.46 g, 11.65 mmol) were dissolve in THF (100 mL) and an aqueous solution of H_2O_2 (1.32 g, 11.65 mmol, 35 wt%) was added to this mixture. After stirring at room temperature for 4 h, the solution was acidified to pH 1-2 by using 1M HCl solution. The product was extracted with EtOAc (3 X 100 mL) and dried with $MgSO_4$, the solvent was removed under reduced pressure. The crude product was purified by flash chromatography to afford 4,5-dimethoxypyrene-1,8-dione (0.51 g, 90%) as a dark red solid. Rf (30% EtOAc/hexanes) = 0.2. ^{1}H NMR (500 MHz, $CDCl_3$) δ 8.57 (s, 2H), 8.06 (d, *J* = 10.0 Hz, 2H), 6.67 (d, *J* = 10.0 Hz, 2H), 4.12 (s, 6H); ^{13}C NMR (126 MHz, $CDCl_3$) δ 185.23, 154.32, 155.39, 131.97, 129.28, 128.79, 126.01, 124.20, 62.8; HRMS (ESI) calculated for $C_{18}H_{13}O_4([M+H]^+)$ m/z = 293.0808, found 293.0807.

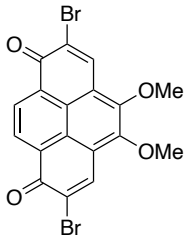

2,7-dibromo-4,5-dimethoxypyrene-1,8-dione: In a round-bottom flask, covered with aluminum foil, were mixed 4,5-dimethoxypyrene-1,8-dione (1.00 g, 3.42 mmol), NBS (1.83 g, 10.27 mmol) and DMF (12 mL) in that order. The mixture was stirred at 50 ºC for 12 h. After cooled to room temperature, the mixture was diluted with CH_2Cl_2 (100 mL) and extracted with water (3 X 100 mL) and dried over $MgSO_4$, the solvent was removed under reduced pressure. The crude product was purified by flash chromatography to afford 2,7-dibromo-4,5-dimethoxypyrene-1,8-dione (1.38 g, 90%) as a red solid. Rf (30%

EtOAc/hexanes) = 0.5; ^{1}H NMR (500 MHz, $CDCl_3$) δ 8.64 (s, 2H), 8.47 (s, 2H), 4.14 (s, 6H); ^{13}C NMR (126 MHz, $CDCl_3$) δ 178.33, 154.02, 137.02, 131.58, 130.42, 126.79, 125.24, 124.44, 62.93; HRMS (ESI) calculated for $C_{18}H_{11}O_2Br_2$([M+H]$^+$) m/z = 448.9018, found 448.9018.

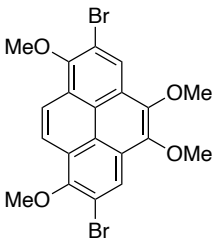

2,7-dibromo-1,4,5,8-tetramethoxypyrene: To a solution of 2,7-dibromo-4,5-dimethoxypyrene-1,8-dione (0.70 g, 1.56 mmol) in the mixture of MeOH (30 mL)/CH_2Cl_2 (10 mL), $Na_2S_2O_4$ (2.18 g, 12.5 mmol) was added under argon atmosphere and stirred for 40 h at room temperature. The reaction was monitored by TLC to confirm consumption of starting material. Upon completion, the reaction was quenched with 1 M HCl to pH = 2. Then the mixture was extracted with CH_2Cl_2 (3 X 100 mL) and dried over $MgSO_4$, the solvent was removed under reduced pressure to give a yellow crude product 2,7-dibromo-4,5-dimethoxypyrene-1,8-diol. The crude solid then dissolved in acetone (30 mL) under argon atmosphere, at 0 ºC, was added K_2CO_3 (2.15 g, 15.6 mmol) and iodomethane (0.87 g, 6.24 mmol). The solution was stirred for 30 min at 0 ºC and then refluxed for 12 h. After cooled to the room temperature, CH_2Cl_2 (100 mL) was added to the solution and extracted with water (3 X 100 mL) and dried over $MgSO_4$, the solvent was removed under reduced pressure. The crude product was purified by flash chromatography to afford 2,7-dibromo-1,4,5,8-tetramethoxypyrene (0.56 g, 72%) as a white solid. Rf (15% EtOAc/hexanes) = 0.5; ^{1}H NMR (600 MHz, $CDCl_3$) δ 8.61 (d, *J* = 0.8 Hz, 2H), 8.37 (d, *J* = 0.8 Hz, 2H), 4.18 (s, 3H), 4.14 (s, 3H); ^{13}C NMR (126 MHz, $CDCl_3$) δ 151.08, 143.79, 126.51, 125.58, 124.10, 123.22, 122.32, 116.31, 62.65, 61.38; HRMS (ESI) calculated for $C_{20}H_{17}O_4Br_2$([M+H]$^+$) m/z = 478.9488, found 478.9485.

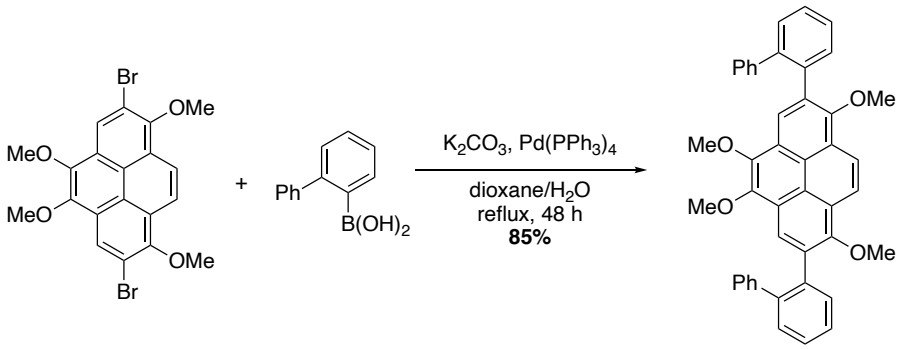

2,7-di([1,1'-biphenyl]-2-yl)-1,4,5,8-tetramethoxypyrene: To a mixture of 2,7-dibromo-1,4,5,8-tetramethoxypyrene (10 mg, 0.02 mmol), [1,1'-biphenyl]-2-ylboronic acid (14 mg, 0.07 mmol), potassium carbonate (11 mg, 0.08 mmol), and $Pd(PPh_3)_4$ (2.3 mg, 10 mol%), was

added 1,4-dioxane (0.2 mL) under nitrogen atmosphere. The mixture was degassed for 20 min then heated to 80 ºC for 48 h. After the reaction was cooled to room temperature, H_2O (1 mL) was added, and the mixture was extracted with EtOAc (3 X 5 mL). the combined organic layers were washed with brine (3 X 5 mL) and dried with $MgSO_4$, the solvent was removed under reduced pressure. The crude product was purified by flash chromatography to afford 2,7-di([1,1'-biphenyl]-2-yl)-1,4,5,8-tetramethoxypyrene (10 mg, 85%). Rf (10% EtOAc/hexanes) = 0.3. ^{1}H NMR (500 MHz, $CDCl_3$) δ 8.28 (s, 2H), 8.05 (s, 2H), 7.70 (dd, *J* = 7.4, 1.8 Hz, 2H), 7.61 – 7.47 (m, 6H), 7.22 (d, *J* = 7.3 Hz, 4H), 7.11 – 7.06 (m, 5H), 3.80 (s, 6H), 3.73 (s, 6H); ^{13}C NMR (126 MHz, $CDCl_3$) δ 151.69, 144.21, 141.95, 141.63, 137.38, 135.52, 131.96, 130.74, 129.63, 128.07, 128.04, 127.29, 126.50, 124.61, 124.41, 123,68, 123.55, 121.72, 61.86, 61.21; HRMS (ESI) calculated for $C_{44}H_{35}O_4$([M+H]$^+$) m/z = 627.2529, found 627.2505.

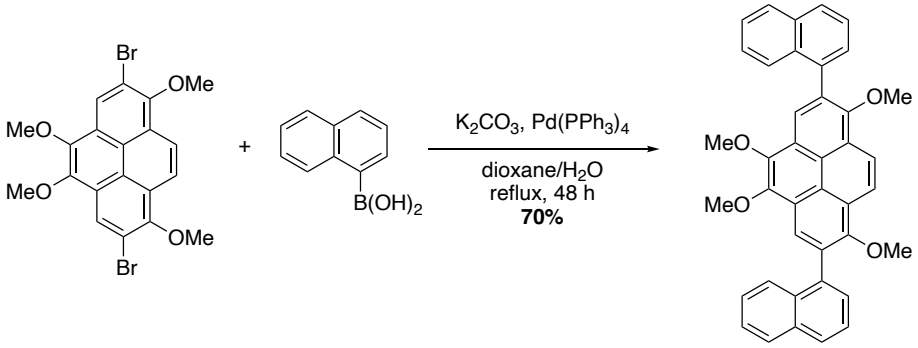

1,4,5,8-tetramethoxy-2,7-di(naphthalen-1-yl)pyrene: To a mixture of 2,7-dibromo-1,4,5,8-tetramethoxypyrene (10 mg, 0.02 mmol), naphthalen-1-ylboronic acid (12 mg, 0.07 mmol), potassium carbonate (11 mg, 0.08 mmol), and $Pd(PPh_3)_4$ (2.3 mg, 10 mol%), was added 1,4-dioxane (0.2 mL) under nitrogen atmosphere. The mixture was degassed for 20 min then heated to 80 ºC for 48 h. After the reaction was cooled to room temperature, H_2O (1 mL) was added, and the mixture was extracted with EtOAc (3 X 5 mL). the combined organic layers were washed with brine (3 X 5 mL) and dried with $MgSO_4$, the solvent was removed under reduced pressure. The crude product was purified by flash chromatography to afford 1,4,5,8-tetramethoxy-2,7-di(naphthalen-1-yl)pyrene (8 mg, 70%). Rf (5% EtOAc/hexanes) = 0.3. ^{1}H NMR (500 MHz, $CDCl_3$) δ 8.53 (d, *J* = 1.4 Hz, 2H), 8.45 (s, 2H), 8.01 (t, *J* = 8.6 Hz, 4H), 7.76 – 7.70 (m, 4H), 7.68 (dd, *J* = 8.2, 6.9 Hz, 2H), 7.55 (ddd, *J* = 8.1, 6.7, 1.2 Hz, 2H), 7.47 – 7.42 (m, 2H), 4.16 (s, 3H), 3.59 (s, 3H); ^{13}C NMR (126 MHz, $CDCl_3$) δ 152.37, 144.39, 137.35, 133.84, 132.46, 131.93, 128.41, 128.30, 128.27, 126.67, 126.63, 126.42, 126.07, 125.55,

125.06, 124.72, 124.12, 123.16, 122.14, 62.54, 61.35; HRMS (ESI) calculated for $C_{40}H_{31}O_4$([M+H]$^+$) m/z = 575.2217, found 575.2213.

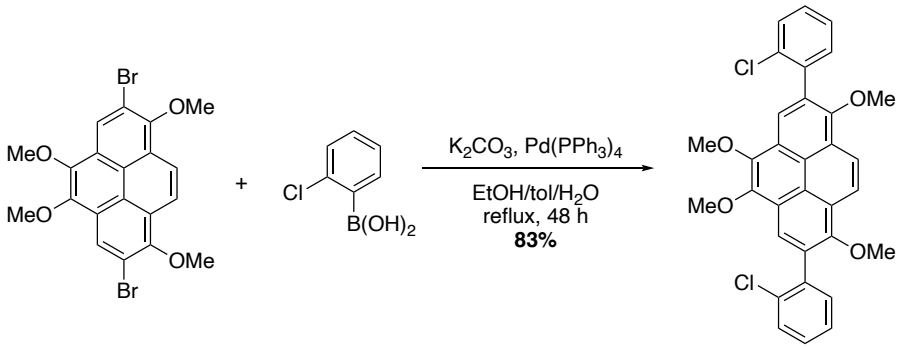

2,7-bis(2-chlorophenyl)-1,4,5,8-tetramethoxypyrene: To a mixture of 2,7-dibromo-1,4,5,8-tetramethoxypyrene (10 mg, 0.02 mmol), (2-chlorophenyl)boronic acid (10 mg, 0.06 mmol), potassium carbonate (28 mg, 0.2 mmol) , and $Pd(PPh_3)_4$ (2.3 mg, 10 mol%), was added EtOH (0.5 mL)/toluene (0.5 mL)/H_2O (0.25 mL) under nitrogen atmosphere. The mixture was degassed for 20 min then heated to 80 ºC for 48 h. After the reaction was cooled to room temperature, H_2O (1 mL) was added, and the mixture was extracted with EtOAc (3 X 5 mL). the combined organic layers were washed with brine (3 X 5 mL) and dried with $MgSO_4$, the solvent was removed under reduced pressure. The crude product was purified by flash chromatography to afford 2,7-bis(2-chlorophenyl)-1,4,5,8-tetramethoxypyrene (9 mg, 83%). Rf (5% EtOAc/hexanes) = 0.2. ^{1}H NMR (500 MHz, $CDCl_3$) δ 8.46 (s, 2H), 8.33 (s, 2H), 7.64 – 7.57 (m, 4H), 7.47 – 7.40 (m, 4H), 4.18 (s, 6H), 3.74 (s, 6H); ^{13}C NMR (126 MHz, $CDCl_3$) δ 151.82, 144.34, 138.19, 134.04, 132.42, 131.07, 129.88, 129.22, 126.74, 124.98, 124.73, 124.23, 122.36, 121.96, 62.49, 61.45; HRMS (ESI) calculated for $C_{32}H_{25}O_4Cl_2$([M+H]$^+$) m/z = 543.1124, found 543.1119.

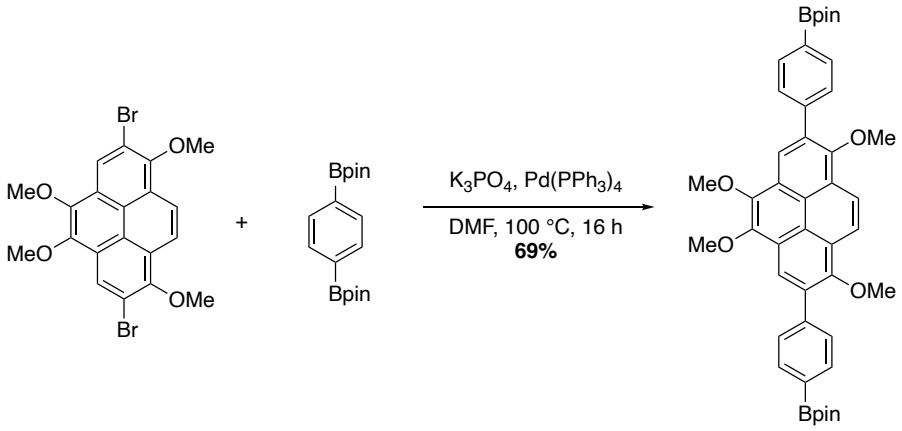

2,2'-((1,4,5,8-tetramethoxypyrene-2,7-diyl)bis(4,1-phenylene))bis(4,4,5,5-tetramethyl-1,3,2-dioxaborolane): To a solution of 2,7-dibromo-1,4,5,8-tetramethoxypyrene (35 mg, 0.07 mmol) in DMF (0.5 mL) under nitrogen atmosphere, K_3PO_4 (62 mg, 0.29 mmol), $Pd(PPh_3)_4$ (8.4mg, 10 mol%), and 1,4-bis(4,4,5,5-tetramethyl-1,3,2-dioxaborolan-2-yl)benzene (72 mg, 0.22 mmol) were added under nitrogen atmosphere. The mixture was degassed for 20 min then heated to 100 ºC for 16 h. After the reaction was cooled to room temperature, H_2O (10 mL) was added, and the mixture was extracted with EtOAc (3 X 10 mL). the combined organic layers were washed with brine (3 X 10 mL) and dried with $MgSO_4$, the solvent was removed under reduced pressure. The crude product was purified by flash chromatography to afford 2,2'-((1,4,5,8-tetramethoxypyrene-2,7-diyl)bis(4,1-phenylene))bis(4,4,5,5-tetramethyl-1,3,2-dioxaborolane) (35 mg, 69%). Rf (15% EtOAc/hexanes) = 0.5. ^{1}H NMR (500 MHz, $CDCl_3$) δ 8.46 (s, 2H), 8.43 (s, 2H), 8.01 (d, *J* = 7.6 Hz, 4H), 7.89 (d, *J* = 7.6 Hz, 4H), 4.18 (s, 6H), 3.70 (s, 6H), 1.42 (s, 24H); ^{13}C NMR (126 MHz, $CDCl_3$) δ 151.67, 144.37, 142.14, 135.08, 132.88, 129.37, 125.33, 125.01, 123.83, 122.02, 121.79, 84.09, 62.22, 61.37, 25.13; HRMS (ESI) calculated for HRMS (ESI) calculated for $C_{44}H_{49}O_8B_2$([M+H]$^+$) m/z = 727.3608, found 727.3600.

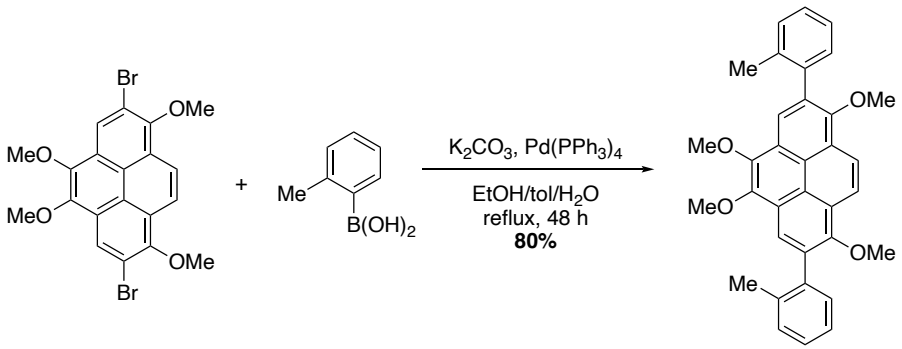

1,4,5,8-tetramethoxy-2,7-di-o-tolylpyrene: To a mixture of 2,7-dibromo-1,4,5,8-tetramethoxypyrene (10 mg, 0.02 mmol), o-tolylboronic acid (7 mg, 0.05 mmol), potassium carbonate (11 mg, 0.08 mmol), and $Pd(PPh_3)_4$ (2.3 mg, 10 mol%), was added EtOH (0.1 mL)/toluene (0.1 mL)/H_2O (0.05 mL) under nitrogen atmosphere. The mixture was degassed for 20 min then heated to 80 ºC for 48 h. After the reaction was cooled to room temperature, H_2O (1 mL) was added, and the mixture was extracted with EtOAc (3 X 5 mL). the combined organic layers were washed with brine (3 X 5 mL) and dried with $MgSO_4$, the solvent was removed under reduced pressure. The crude product was purified by flash chromatography to afford 1,4,5,8-tetramethoxy-2,7-di-o-tolylpyrene (8 mg, 80%). Rf (5% EtOAc/hexanes) = 0.3. ^{1}H NMR (500 MHz, $CDCl_3$) δ 8.46 (s, 1H), 8.29 (s, 1H), 7.49 (d, *J* = 7.2 Hz, 1H), 7.42 – 7.33 (m, 3H), 4.17 (s, 3H), 3.67 (s, 3H), 2.27 (s, 3H); ^{13}C NMR (126 MHz, $CDCl_3$) δ 151.73, 144.31,

139.22, 137.13, 133.24, 130.73, 130.17, 127.85, 125.72, 124.93, 124.57, 123.87, 122.18, 121.93, 62.18, 61.34, 20.47; HRMS (ESI) calculated for HRMS (ESI) calculated for $C_{34}H_{31}O_4$([M+H]$^+$) m/z = 503.2217, found 503.2226.

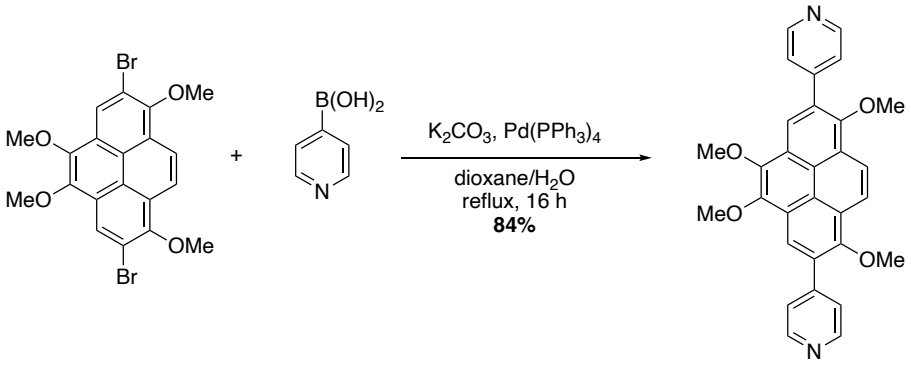

4,4'-(1,4,5,8-tetramethoxypyrene-2,7-diyl)dipyridine: To a mixture of 2,7-dibromo-1,4,5,8-tetramethoxypyrene (10 mg, 0.02 mmol), pyridine-4-ylboronic acid (9 mg, 0.07 mmol), potassium carbonate (11 mg, 0.08 mmol), and $Pd(PPh_3)_4$ (2.3 mg, 10 mol%), was added 1,4-dioxane (0.2 mL) and H_2O (0.005 mL) under nitrogen atmosphere. The mixture was degassed for 20 min then heated to 80 ºC for 16 h. After the reaction was cooled to room temperature, H_2O (1 mL) was added, and the mixture was extracted with EtOAc (3 X 5 mL). the combined organic layers were washed with brine (3 X 5 mL) and dried with $MgSO_4$, the solvent was removed under reduced pressure. The crude product was purified by flash chromatography to afford 4,4'-(1,4,5,8-tetramethoxypyrene-2,7-diyl)dipyridine (10 mg, 84%). Rf (15% EtOAc/hexanes) = 0.3. ^{1}H NMR (500 MHz, $CDCl_3$) δ 8.84 – 8.77 (m, 4H), 8.48 (s, 2H), 8.45 (s, 2H), 7.86 – 7.79 (m, 4H), 4.22 (s, 6H), 3.75 (s, 6H); ^{13}C NMR (126 MHz, $CDCl_3$) δ 151.83, 150.90, 150.26, 146.95, 144.38, 130.49, 125.82, 125.28, 124.71, 124.25, 122.26, 121.60, 121.35, 62.69, 61.38; HRMS (ESI) calculated for HRMS (ESI) calculated for $C_{30}H_{25}O_4N_2$([M+H]$^+$) m/z = 477.1809, found 477.1810.

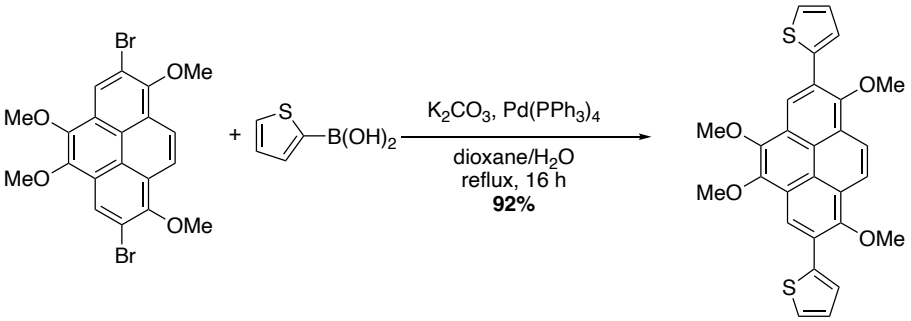

2,2'-(1,4,5,8-tetramethoxypyrene-2,7-diyl)dithiophene: To a mixture of 2,7-dibromo-1,4,5,8-tetramethoxypyrene (10 mg, 0.02 mmol), thiophen-2-ylboronic acid (9 mg, 0.07 mmol), potassium carbonate (11 mg, 0.08 mmol), and $Pd(PPh_3)_4$ (2.3 mg, 10 mol%), was added 1,4-dioxane (0.2 mL) and H_2O (0.005 mL) under nitrogen atmosphere. The mixture was degassed for 20 min then heated to 80 ºC for 16 h. After the reaction was cooled to room temperature, H_2O (1 mL) was added, and the mixture was extracted with EtOAc (3 X 5 mL). the combined organic layers were washed with brine (3 X 5 mL) and dried with $MgSO_4$, the solvent was removed under reduced pressure. The crude product was purified by flash chromatography to afford 4,4'-(1,4,5,8-tetramethoxypyrene-2,7-diyl)dipyridine (10 mg, 84%). Rf (1% EtOAc/hexanes) = 0.3. ^{1}H NMR (500 MHz, $CDCl_3$) δ 8.67 (s, 2H), 8.42 (s, 2H), 7.83 (dd, *J* = 3.6, 1.2 Hz, 2H), 7.51 (dd, *J* = 5.1, 1.1 Hz, 2H), 7.24 (dd, *J* = 5.1, 3.6 Hz, 2H), 4.22 (s, 6H), 3.98 (s, 6H); ^{13}C NMR (126 MHz, $CDCl_3$) δ 150.76, 144.32, 139.76, 127.44, 127.03, 126.68, 125.89, 125.55, 125.04, 123.62, 122.18, 119.70, 62.32, 61.37; HRMS (ESI) calculated for HRMS (ESI) calculated for $C_{28}H_{23}O_4S_2$([M+H]$^+$) m/z = 487.1030, found 477.1032.

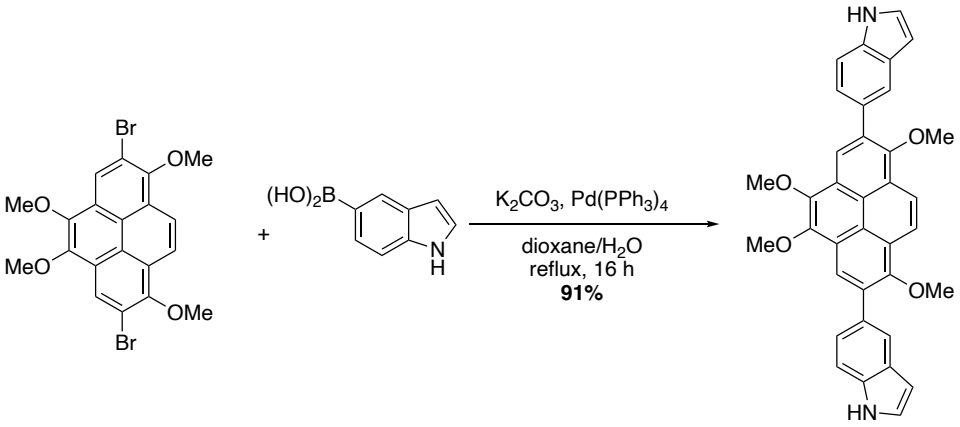

5,5'-(1,4,5,8-tetramethoxypyrene-2,7-diyl)bis(1H-indole) : To a mixture of 2,7-dibromo-1,4,5,8-tetramethoxypyrene (10 mg, 0.02 mmol), (1*H*-indol-5-yl)boronic acid (11 mg, 0.07 mmol), potassium carbonate (11 mg, 0.08 mmol), and $Pd(PPh_3)_4$ (2.3 mg, 10 mol%), was added 1,4-dioxane (0.2 mL) and H_2O (0.005 mL) under nitrogen atmosphere. The mixture was degassed for 20 min then heated to 80 ºC for 16 h. After the reaction was cooled to room temperature, H_2O (1 mL) was added, and the mixture was extracted with EtOAc (3 X 5 mL). the combined organic layers were washed with brine (3 X 5 mL) and dried with $MgSO_4$, the solvent was removed under reduced pressure. The crude product was purified by flash chromatography to afford 5,5'-(1,4,5,8-tetramethoxypyrene-2,7-diyl)bis(1H-indole) (10 mg, 91%). Rf (30% EtOAc/hexanes) = 0.2. ^{1}H NMR (500 MHz, DMSO-d_6) δ 11.29 (s, 2H), 8.48 (s, 2H), 8.40 (s, 2H), 8.03 (s, 2H), 7.63 (s, 4H), 7.49 (t, *J* = 2.8 Hz, 2H), 6.62 (t, *J* = 2.5 Hz, 2H),

4.18 (s, 6H), 3.65 (s, 6H). ^{13}C NMR (126 MHz, DMSO-d_6) δ 151.14, 143.53, 135.38, 133.89, 129.01, 127.99, 125.98, 124.25, 124.11, 122.86, 122.27, 121.75, 121.72, 120.98, 111.49, 101.59, 61.35, 61.02. HRMS (ESI) calculated for HRMS (ESI) calculated for $C_{36}H_{29}O_4N_2$([M+H]$^+$) m/z = 553.2122, found 553.2100.

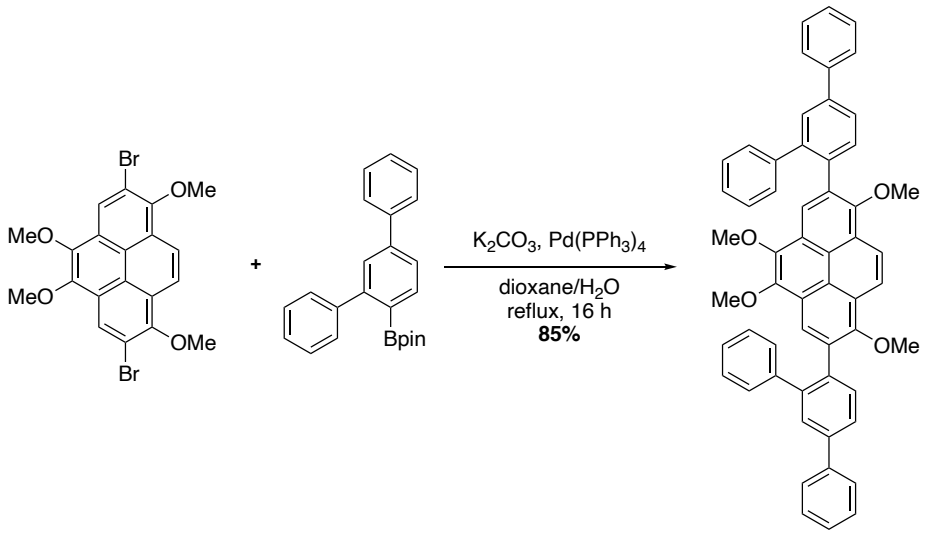

2,7-di([1,1':3',1''-terphenyl]-4'-yl)-1,4,5,8-tetramethoxypyrene: To a mixture of 2,7-dibromo-1,4,5,8-tetramethoxypyrene (20 mg, 0.04 mmol), 2-([1,1':3',1''-terphenyl]-4'-yl)-4,4,5,5-tetramethyl-1,3,2-dioxaborolane (60 mg, 0.16 mmol), potassium carbonate (23 mg, 0.16 mmol), and $Pd(PPh_3)_4$ (5 mg, 10 mol%), was added 1,4-dioxane (0.2 mL) and H_2O (0.005 mL) under nitrogen atmosphere. The mixture was degassed for 20 min then heated to 80 ºC for 16 h. After the reaction was cooled to room temperature, H_2O (1 mL) was added, and the mixture was extracted with EtOAc (3 X 5 mL). the combined organic layers were washed with brine (3 X 5 mL) and dried with $MgSO_4$, the solvent was removed under reduced pressure. The crude product was purified by flash chromatography to afford 2,7-di([1,1':3',1''-terphenyl]-4'-yl)-1,4,5,8-tetramethoxypyrene (28 mg, 85%) Rf (15% EtOAc/hexanes) = 0.2. ^{1}H NMR (500 MHz, $CDCl_3$) δ 8.32 (s, 2H), 8.09 (s, 2H), 7.83 (d, *J* = 1.7 Hz, 2H), 7.82 – 7.74 (m, 8H), 7.52 (t, *J* = 7.7 Hz, 4H), 7.44 – 7.39 (m, 2H), 7.33 – 7.28 (m, 4H), 7.12 (dt, *J* = 13.5, 6.8 Hz, 6H), 3.81 (d, *J* = 7.1 Hz, 12H); ^{13}C NMR (126 MHz, $CDCl_3$) δ 151.80, 144.24, 142.04, 141.96, 140.82, 136.41, 132.47, 132.18, 129.68, 129.51, 129.07, 128.13, 127.71, 127.36, 126.65, 125.92, 124.67, 124.47, 123.71, 123.61, 121.76, 61.99, 61.22.

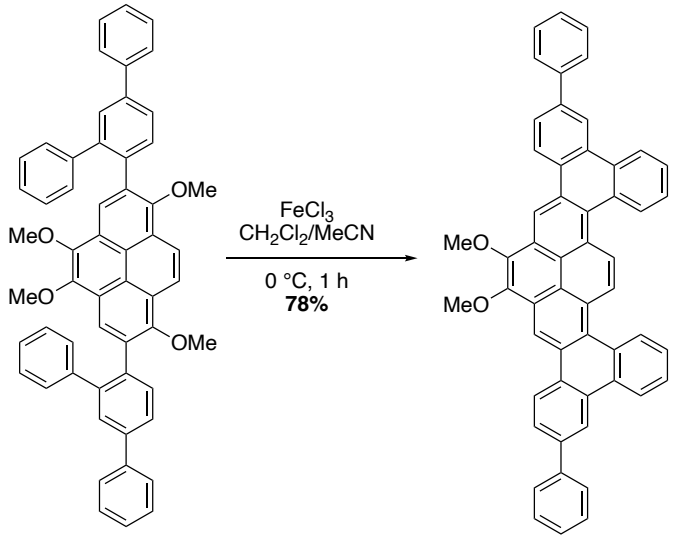

6,7-dimethoxy-2,11-diphenylpentabenzo[a,*c,m,o,rst*]pentaphene: A solution of iron(III) chloride (75 mg, 0.6 mmol) in dichloromethane/nitromethane (1 mL, 9:1) was added dropwise to a stirred 0 ºC solution of pyrene derivative (18 mg, 0.02 mmol) in dichloromethane (5 mL). During the addition, a gentle stream of nitrogen gas was passed through the reaction vessel, after which a nitrogen filled balloon was placed over the reaction. After 1 h, methanol (5 mL) and water (5 mL) were added to the reaction. The layers were separated and the aqueous phase extracted with dichloromethane (3 X 5 mL). the combined organic extracts were washed with brine (10 mL), dried over $MgSO_4$, filtered, and concentrated under reduced pressure. The residue was purified by flash chromatography to afford 6,7-dimethoxy-2,11-diphenylpentabenzo[*a,c,m,o,rst*]pentaphene (11 mg, 78%) Rf (15% EtOAc/hexanes) = 0.3. ^{1}H NMR (500 MHz, $CDCl_3$) δ 9.60 (s, 2H), 9.10 (d, *J* = 7.7 Hz, 2H), 9.06 (s, 2H), 9.01 (d, *J* = 8.6 Hz, 2H), 8.89 (d, *J* = 1.9 Hz, 2H), 8.80 (d, *J* = 7.7 Hz, 2H), 8.01 (d, *J* = 8.3 Hz, 2H), 7.87 (d, *J* = 7.5 Hz, 4H), 7.78 (dt, *J* = 15.6, 6.8 Hz, 4H), 7.58 (t, *J* = 7.6 Hz, 4H), 7.47 (t, *J* = 7.3 Hz, 2H), 4.43 (s, 6H); ^{13}C NMR (126 MHz, $CDCl_3$) δ 144.52, 141.15, 140.13, 130.93, 130.52, 130.43, 130.03, 129.31, 129.02, 128.05, 127.65, 127.60, 127.48, 127.27, 126.98, 126.68, 126.59, 126.43, 125.25, 124.78, 123.54, 123.33, 121.70, 113.60, 61.36.

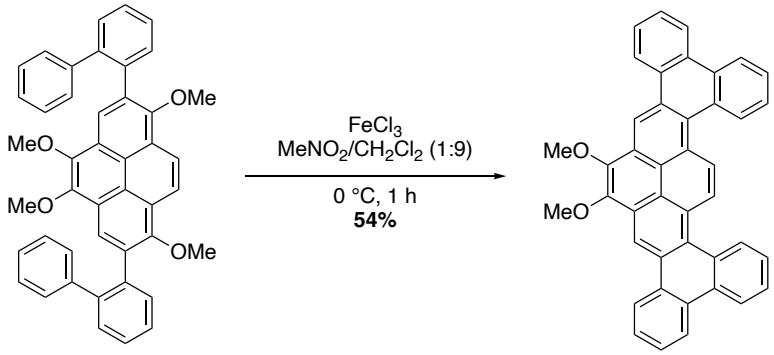

6,7-dimethoxypentabenzo[*a,c,m,o,rst*]pentaphene: A solution of iron(III) chloride (97 mg, 0.6 mmol) in dichloromethane/nitromethane (9:1) was added dropwise to a stirred 0 ºC solution of pyrene derivative (19 mg, 0.03 mmol) in dichloromethane (5 mL). During the addition, a gentle stream of nitrogen gas was passed through the reaction vessel, after which a nitrogen filled balloon was placed over the reaction. After 1 h, methanol (5 mL) and water (5 mL) were added to the reaction. The layers were separated and the aqueous phase extracted with dichloromethane (3 X 5 mL). the combined organic extracts were washed with brine (10 mL), dried over $MgSO_4$, filtered, and concentrated under reduced pressure. The residue was purified by flash chromatography to afford 6,7-dimethoxypentabenzo[*a,c,m,o,rst*]pentaphene (9 mg, 54%). Rf (5% EtOAc/hexanes) = 0.2. ^{1}H NMR (500 MHz, $CDCl_3$) δ 9.67 (s, 2H), 9.19 (d, *J* = 10.2 Hz, 4H), 9.03 (d, *J* = 7.0 Hz, 2H), 8.78 (dd, *J* = 16.0, 7.6 Hz, 4H), 7.88 – 7.73 (m, 8H), 4.42 (s, 6H); ^{13}C NMR (126 MHz, $CDCl_3$) δ 144.81, 131.19, 130.66, 130.50, 130.44, 130.06, 128.51, 127.90, 127.80, 127.57, 127.24, 127.00, 126.60, 125.57, 124.48, 123.80, 123.62, 123.50, 113.82, 61.55. HRMS (ESI) calculated for $C_{42}H_{27}O_2$([M+H]$^+$) m/z = 563.2005, found 563.1995.

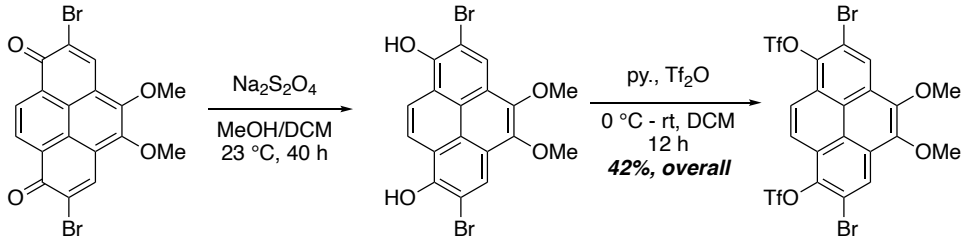

61.1 **61.2** **70.1**

2,7-dibromo-4,5-dimethoxypyrene-1,8-diyl bis(trifluoromethanesulfonate): To a solution of 2,7-dibromo-4,5-dimethoxypyrene-1,8-dione (1.19 g, 2.6 mmol) in the mixture of MeOH (45 mL)/CH_2Cl_2 (15 mL), $Na_2S_2O_4$ (3.68 g, 21.2 mmol) was added under argon atmosphere and stirred for 40 h at room temperature. The reaction was monitored by TLC to confirm the consumption of starting material. Upon completion, the reaction was quenched with 1 M HCl to pH = 2. Then the mixture was extracted with CH_2Cl_2 (3 X 200 mL) and dried over $MgSO_4$, the solvent was removed under reduced pressure to give a yellow crude product 2,7-dibromo-4,5-dimethoxypyrene-1,8-diol. Then (100 mg, 0.22 mmol) crude solid was dissolved in 1 mL DCM, and pyridine (70 mg, 0.88 mmol) was added. To this solution trifluoromethanesulfonic anhydride (149 mg, 0.53 mmol) was added dropwise at 0 ºC. the reaction mixture was allowed to warm to room temperature and stirred overnight. The mixture was quenched with 3M HCl and extracted with ethyl acetate. The organic layer was washed with Sat. $NaHCO_3$ solution,

brine, and dried over MgSO4. the solvent was removed under reduced pressure. The crude product was purified by flash chromatography to afford 2,7-dibromo-4,5-dimethoxypyrene-1,8-diyl bis(trifluoromethanesulfonate) (65 mg, 42%) as a white solid. Rf (30% EtOAc/hexanes) = 0.5; ^{1}H NMR (500 MHz, $CDCl_3$) δ 8.81 (s, 2H), 8.45 (s, 2H), 4.23 (s, 6H); ^{13}C NMR (126 MHz, $CDCl_3$) δ 144.67, 140.11, 129.61, 126.00, 125.26, 123.04, 122.71, 121.78, 120.16, 117.61, 116.35, 115.06, 61.59.

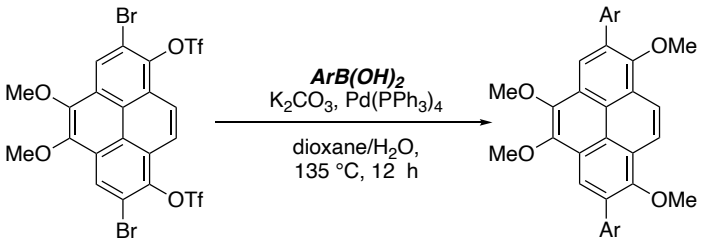

70.1 **71**

To a mixture of 2,7-dibromo-4,5-dimethoxypyrene-1,8-diyl bis(trifluoromethanesulfonate) (10 mg, 0.014 mmol), boronic acid (0.03 mmol), potassium carbonate 3M (0.1 mL), and $Pd(PPh_3)_4$ (2.3 mg, 10 mol%), was added 1,4-dioxane (0.2 mL) under nitrogen atmosphere. The mixture was degassed for 20 min then heated to 135 ºC for 12 h. After the reaction was cooled to room temperature, H_2O (1 mL) was added, and the mixture was extracted with EtOAc (3 X 5 mL). the combined organic layers were washed with brine (3 X 5 mL) and dried with $MgSO_4$, the solvent was removed under reduced pressure. The crude product was purified by flash chromatography to afford the corresponding product.

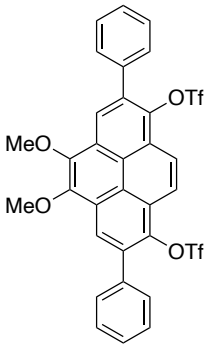

4,5-dimethoxy-2,7-diphenylpyrene-1,8-diyl bis(trifluoromethanesulfonate)

(2 mg, 20%), Rf (10% EtOAc/hexanes) = 0.1; ^{1}H NMR (500 MHz, $CDCl_3$) δ 8.68 (s, 2H), 8.14 (s, 2H), 7.72 – 7.66 (m, 4H), 7.53 – 7.47 (m, 4H), 7.47 – 7.40 (m, 2H), 4.14 (s, 6H).

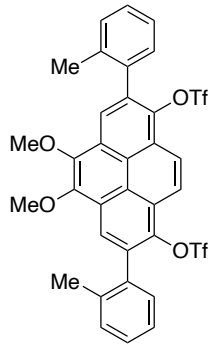

4,5-dimethoxy-2,7-di-*o*-tolylpyrene-1,8-diyl bis(trifluoromethanesulfonate)

(2 mg, 20%), Rf (15% EtOAc/hexanes) = 0.2; ^{1}H NMR (500 MHz, $CDCl_3$) δ 8.66 (s, 2H), 8.01 (s, 2H), 7.36 – 7.29 (m, 8H), 4.11 (s, 6H), 2.29 (s, 6H).

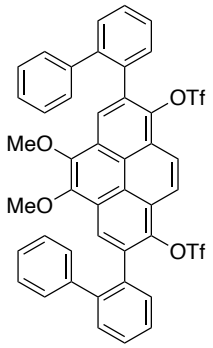

2,7-di([1,1'-biphenyl]-2-yl)-4,5-dimethoxypyrene-1,8-diyl bis(trifluoromethanesulfonate)

(4 mg, 33%), Rf (15% EtOAc/hexanes) = 0.1; ^{1}H NMR (500 MHz, $CDCl_3$) δ 8.45 (s, 2H), 7.72 (s, 2H), 7.52 – 7.42 (m, 8H), 7.37 – 7.31 (m, 4H), 7.23 (dd, *J* = 8.4, 7.0 Hz, 4H), 7.18 – 7.13 (m, 2H), 3.75 (s, 6H).

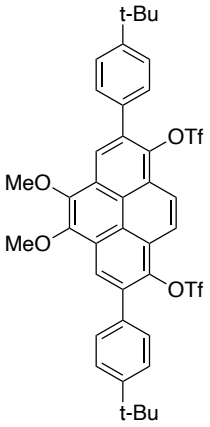

2,7-bis(4-(*tert*-butyl)phenyl)-4,5-dimethoxypyrene-1,8-diyl bis(trifluoromethanesulfonate)

(3 mg, 25%), Rf (10% EtOAc/hexanes) = 0.1; ^{1}H NMR (500 MHz, $CDCl_3$) δ 8.67 (s, 2H), 8.13 (s, 2H), 7.70 – 7.60 (m, 4H), 7.52 (d, J = 8.5 Hz, 4H), 4.12 (s, 6H), 1.39 (s, 18H).

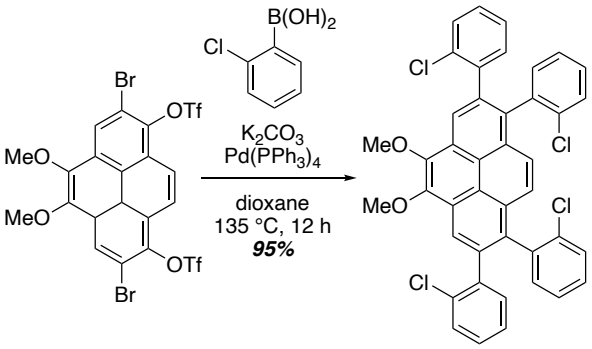

1,2,7,8-tetrakis(2-chlorophenyl)-4,5-dimethoxypyrene: To a mixture of 2,7-dibromo-4,5-dimethoxypyrene-1,8-diyl bis(trifluoromethanesulfonate) (20 mg, 0.03 mmol), boronic acid (24 mg, 0.15 mmol), potassium carbonate 3M (0.2 mL), and $Pd(PPh_3)_4$ (4 mg, 10 mol%), was added 1,4-dioxane (0.4 mL) under nitrogen atmosphere. The mixture was degassed for 20 min then heated to 135 ºC for 12 h. After the reaction was cooled to room temperature, H_2O (1 mL) was added, and the mixture was extracted with EtOAc (3 X 5 mL). the combined organic layers were washed with brine (3 X 5 mL) and dried with $MgSO_4$, the solvent was removed under reduced pressure. The crude product was purified by flash chromatography to afford 1,2,7,8-tetrakis(2-chlorophenyl)-4,5-dimethoxypyrene (21 mg, 95%) as a white solid. Rf (15% EtOAc/hexanes) = 0.5; ^{1}H NMR (500 MHz, $CDCl_3$) δ 8.52 (d, J = 5.4 Hz, 2H), 7.56 (s, 2H), 7.46 – 7.28 (m, 8H), 7.25 – 7.08 (m, 8H), 4.27 (s, 6H).

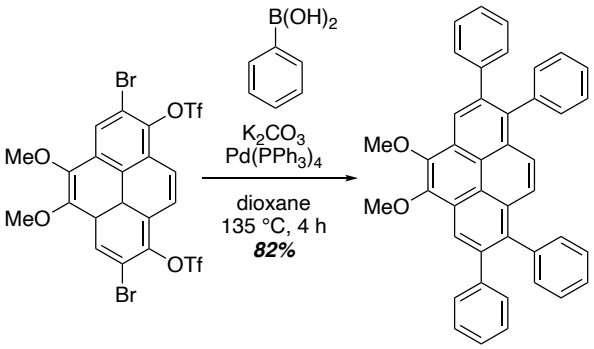

4,5-dimethoxy-1,2,7,8-tetraphenylpyrene: To a mixture of 2,7-dibromo-4,5-dimethoxypyrene-1,8-diyl bis(trifluoromethanesulfonate) (20 mg, 0.03 mmol), boronic acid (18 mg, 0.15 mmol), potassium carbonate 3M (0.2 mL), and $Pd(PPh_3)_4$ (4 mg, 10 mol%), was added 1,4-dioxane (0.4 mL) under nitrogen atmosphere. The mixture was degassed for 20 min then heated to 135 ºC for 4 h. After the reaction was cooled to room temperature, H_2O (1 mL) was added, and the mixture was extracted with EtOAc (3 X 5 mL). the combined organic layers were washed with brine (3 X 5 mL) and dried with $MgSO_4$, the solvent was removed under reduced pressure. The crude product was purified by flash chromatography to afford 4,5-dimethoxy-1,2,7,8-tetraphenylpyrene (21 mg, 95%) as a white solid. Rf (2% EtOAc/hexanes) = 0.2; ^{1}H NMR (500 MHz, $CDCl_3$) δ 8.59 (s, 2H), 7.84 (s, 2H), 7.36 – 7.19 (m, 20H), 4.27 (s, 6H); ^{13}C NMR (126 MHz, $CDCl_3$) δ 144.85, 142.44, 139.57, 139.26, 135.67, 131.82, 130.57, 129.46, 127.87, 127.75, 127.63, 126.76, 126.33, 126.20, 122.22, 121.08, 61.26.

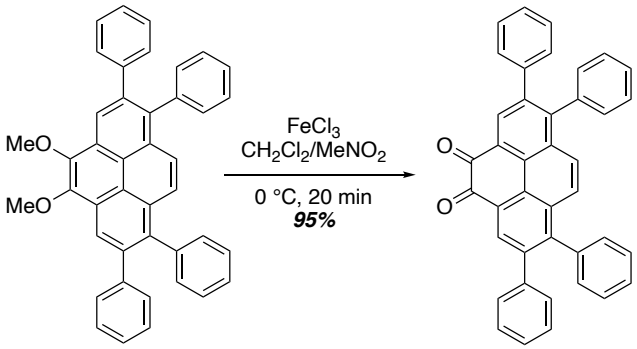

1,2,7,8-tetraphenylpyrene-4,5-dione: A solution of iron(III) chloride (81 mg, 0.5 mmol) in dichloromethane/nitromethane (9:1) was added dropwise to a stirred 0 ºC solution of 4,5-dimethoxy-1,2,7,8-tetraphenylpyrene (14 mg, 0.025 mmol) in dichloromethane (5 mL). During the addition, a gentle stream of nitrogen gas was passed through the reaction vessel, after which a nitrogen filled balloon was placed over the reaction. After 1 h, methanol (5 mL) and

water (5 mL) were added to the reaction. The layers were separated and the aqueous phase extracted with dichloromethane (3 X 5 mL). the combined organic extracts were washed with brine (10 mL), dried over $MgSO_4$, filtered, and concentrated under reduced pressure. The residue was purified by flash chromatography to afford 1,2,7,8-tetraphenylpyrene-4,5-dione (13 mg, 95%), Rf (10% EtOAc/hexanes) = 0.2; ^{1}H NMR (500 MHz, $CDCl_3$) δ 8.64 (s, 2H), 7.60 (s, 2H), 7.34 – 7.32 (m, 6H), 7.24 – 7.18 (m, 6H), 7.22 – 7.17 (m, 8H); ^{13}C NMR (126 MHz, $CDCl_3$) δ 180.60, 146.18, 141.20, 139.93, 137.61, 132.36, 131.15, 130.71, 129.87, 129.35, 128.15, 127.94, 127.75, 127.67, 127.14, 126.17.

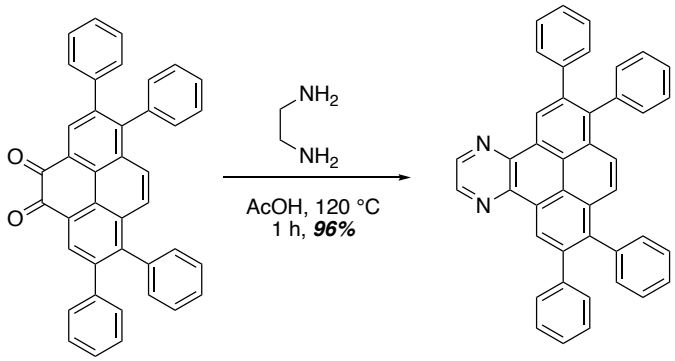

2,3,6,7-tetraphenylphenanthro[4,5-*fgh*]quinoxaline: To a vial was added a magnetic stir bar, 1,2,7,8-tetraphenylpyrene-4,5-dione (7 mg, 0.013 mmol), and diamine (2 mg, 0.033 mmol). Glacial acetic acid (0.1 mL) was added, the vial was well-sealed and heated to 125 ºC for 1 hour. The mixture was cooled to room temperature and poured into ice-cold water to removed acetic acid, then added 1 mL dichloromethane. The layers were separated and the aqueous phase was extracted with dichloromethane (3 X 1 mL). the combined organic extracts were washed with brine (2 mL), dried over $MgSO_4$, filtered, and concentrated under reduced pressure. The residue was purified by flash chromatography to afford 2,3,6,7-tetraphenylphenanthro[4,5-*fgh*]quinoxaline (7 mg, 96%) %), Rf (10% EtOAc/hexanes) = 0.3; ^{1}H NMR (600 MHz, $CDCl_3$) δ 9.55 (s, 2H), 9.00 (s, 2H), 7.84 (s, 2H), 7.39 – 7.29 (m, 16H), 7.29 – 7.15 (m, 4H).

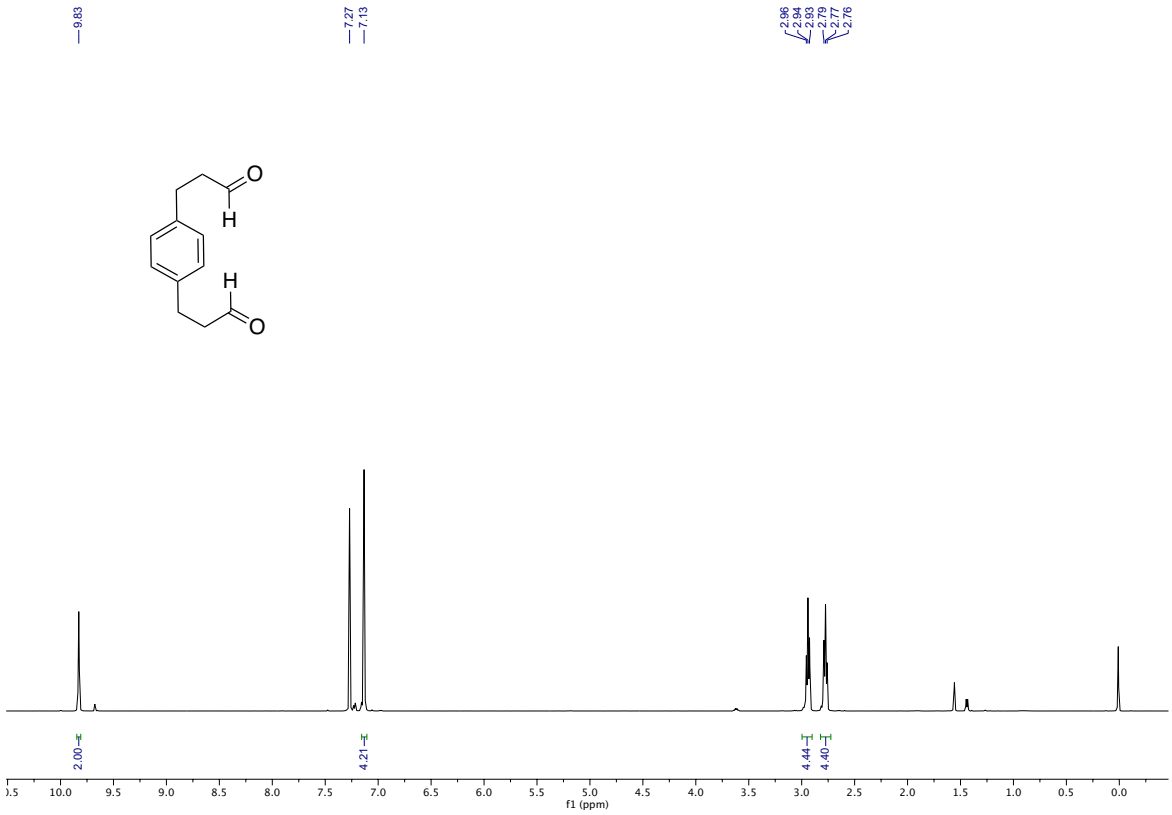
9.83
7.27
7.13
2.96
2.94
2.93
2.79
2.77
2.76
O
H
H
O
2.00
4.21
4.44
4.40
f1 (ppm)

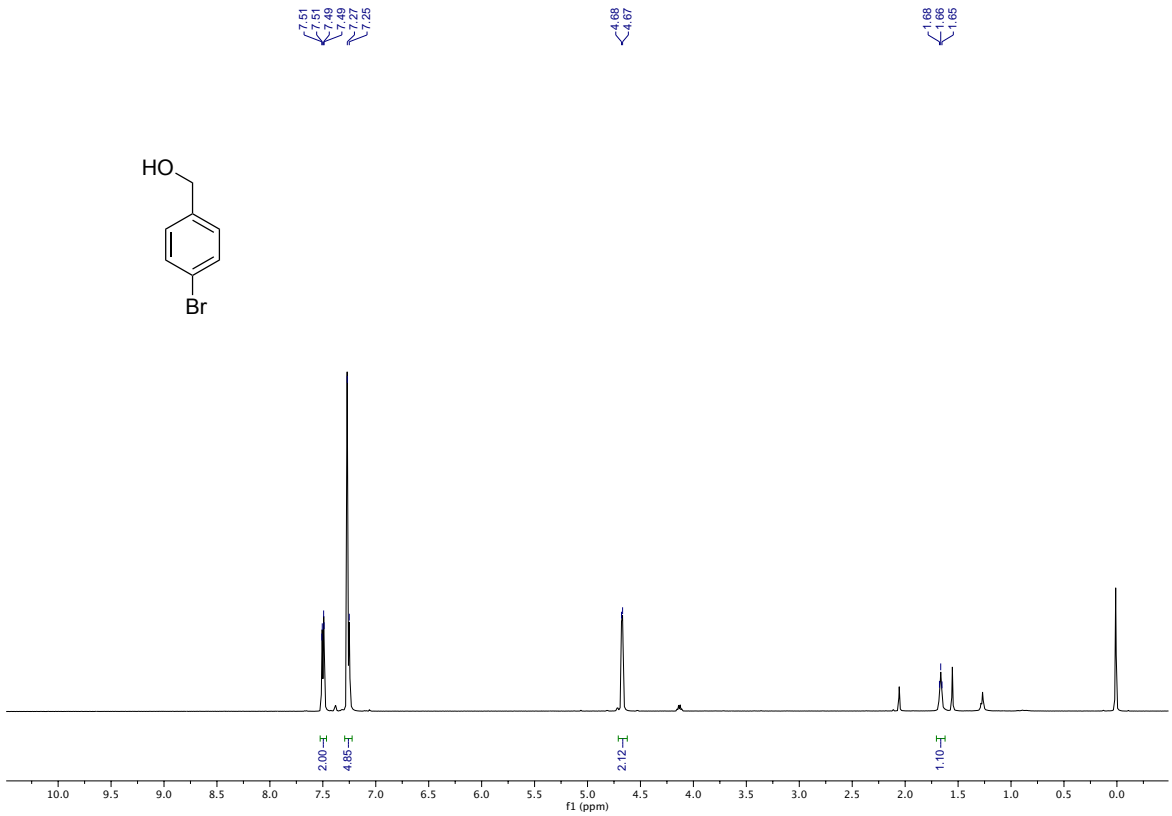
7.51
7.51
7.49
7.49
7.27
7.25
4.68
4.67
1.68
1.66
1.65
HO
Br
2.00
4.85
2.12
1.10
f1 (ppm)

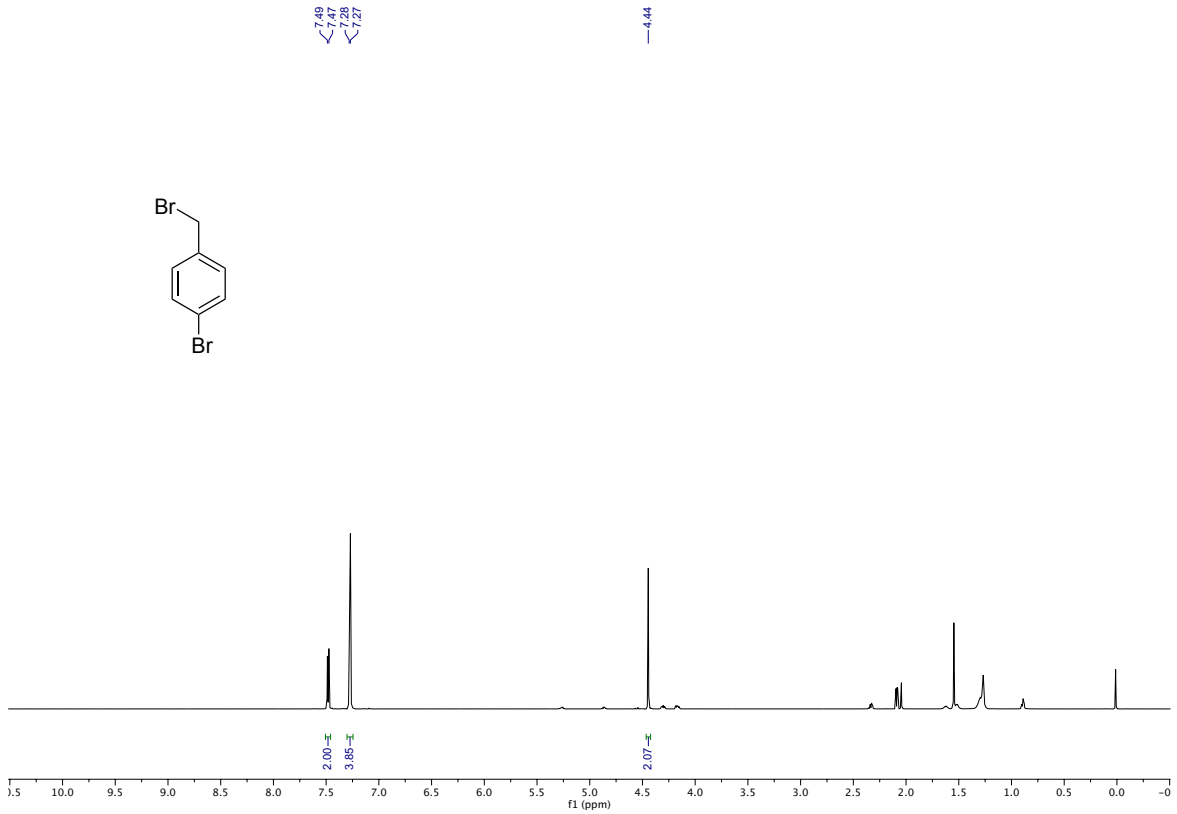
7.49
7.47
7.28
7.27
4.44
Br
Br
2.00
3.85
2.07
f1 (ppm)

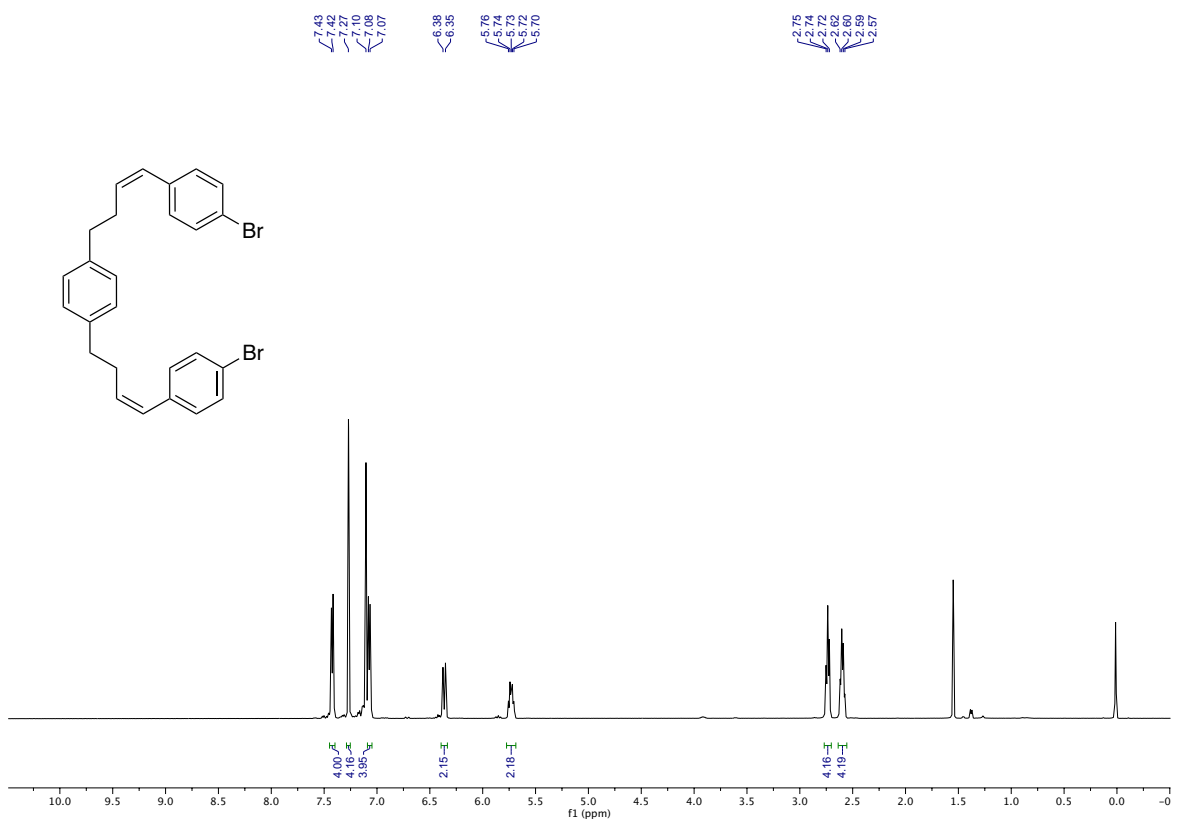
7.43
7.42
7.27
7.10
7.08
7.07
6.38
6.35
5.76
5.74
5.73
5.72
5.70
2.75
2.74
2.72
2.62
2.60
2.59
2.57
Br
Br
4.00
4.16
3.95
2.15
2.18
4.16
4.19
f1 (ppm)

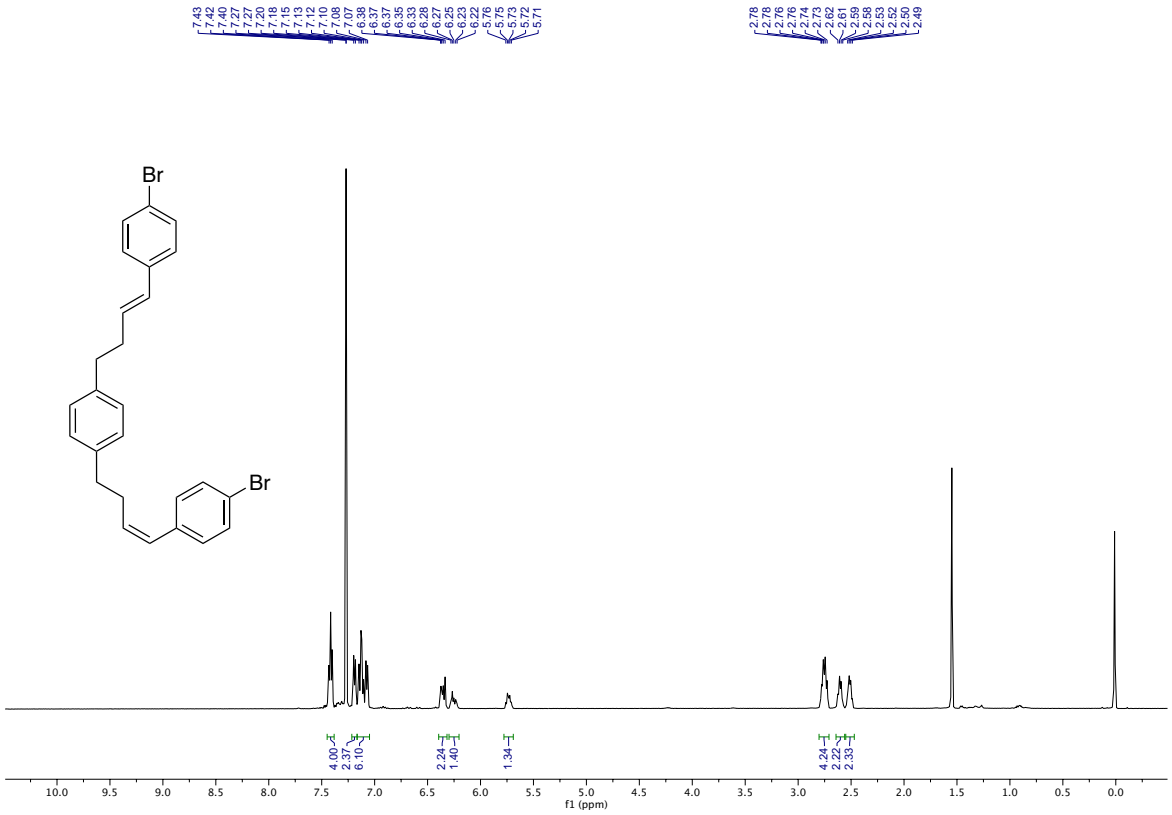
Br
Br
f1 (ppm)

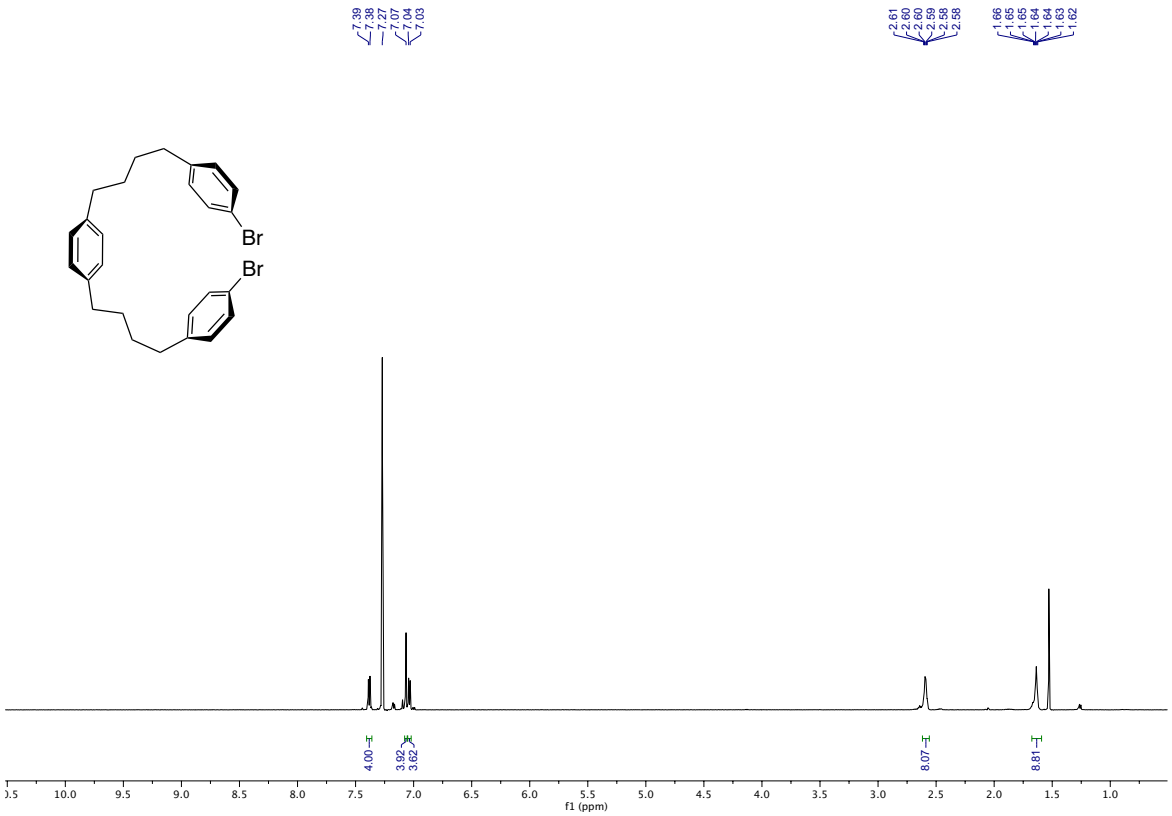
Br
Br
f1 (ppm)

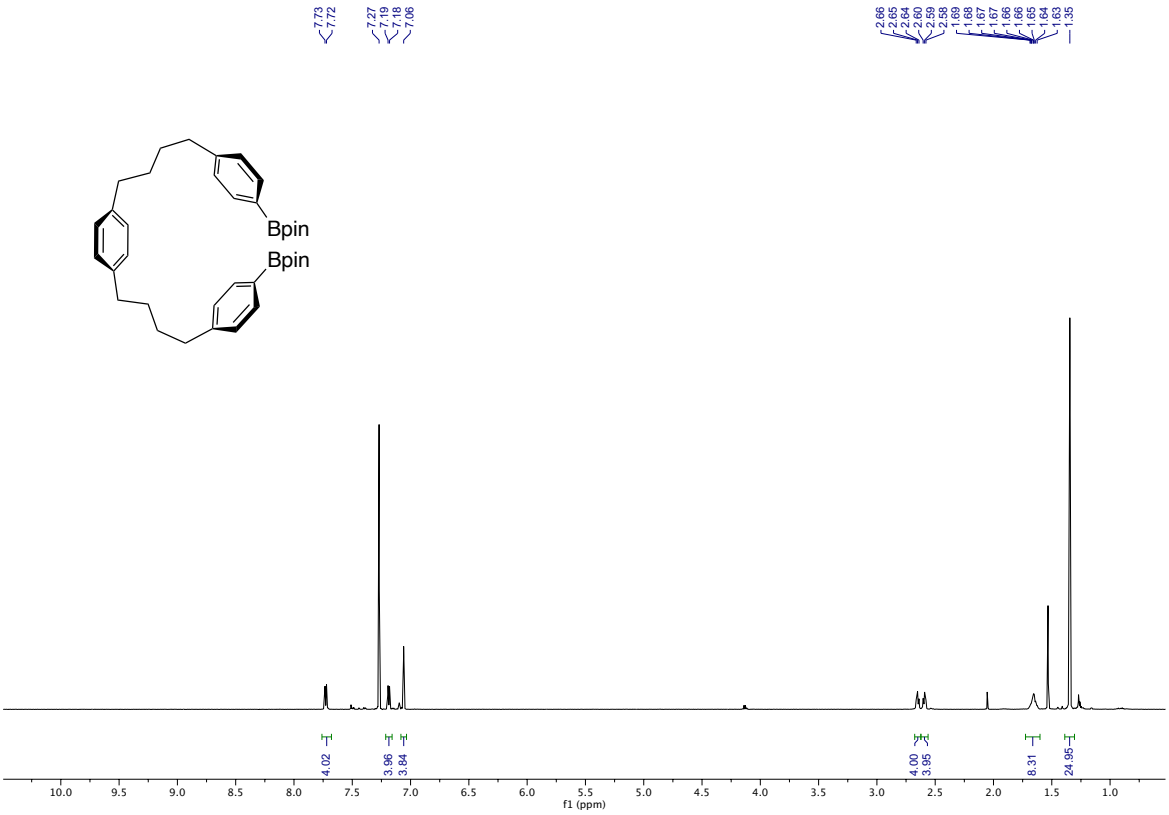
7.73
7.72
7.27
7.19
7.18
7.06
2.66
2.65
2.64
2.60
2.59
2.58
1.69
1.68
1.67
1.67
1.66
1.66
1.65
1.64
1.63
1.35
Bpin
Bpin
4.02
3.96
3.84
4.00
3.95
8.31
24.95
f1 (ppm)

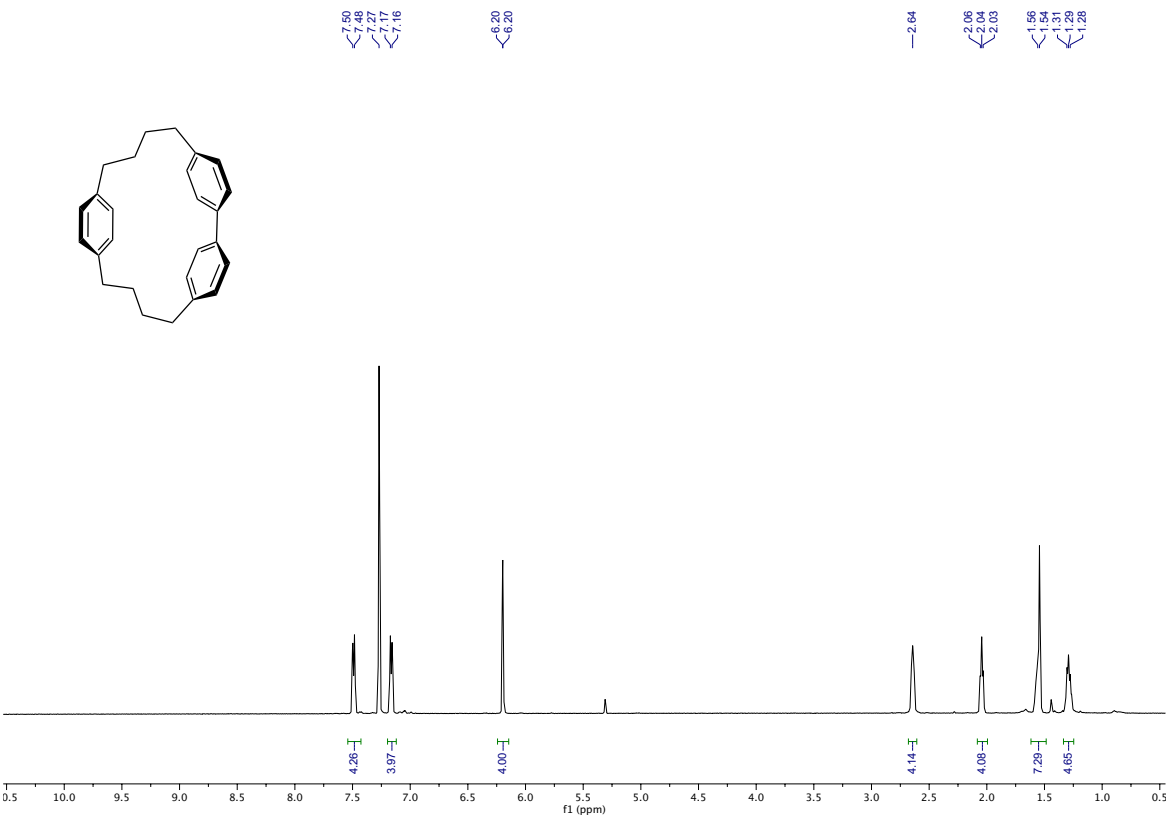
7.50
7.48
7.27
7.17
7.16
6.20
6.20
2.64
2.06
2.04
2.03
1.56
1.54
1.31
1.29
1.28
4.26
3.97
4.00
4.14
4.08
7.29
4.65
f1 (ppm)

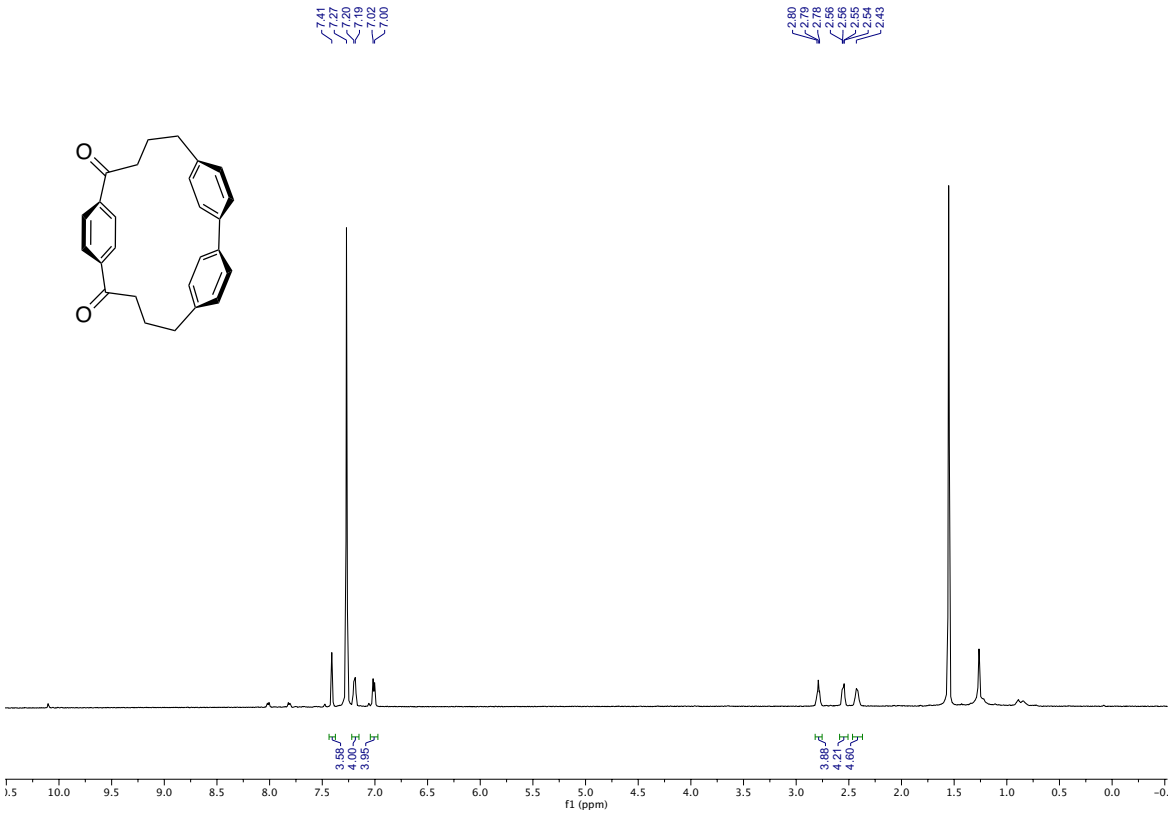
7.41
7.27
7.20
7.19
7.02
7.00
2.80
2.79
2.78
2.56
2.55
2.54
2.43
O
O
3.58
4.00
3.95
3.88
4.21
4.60
f1 (ppm)

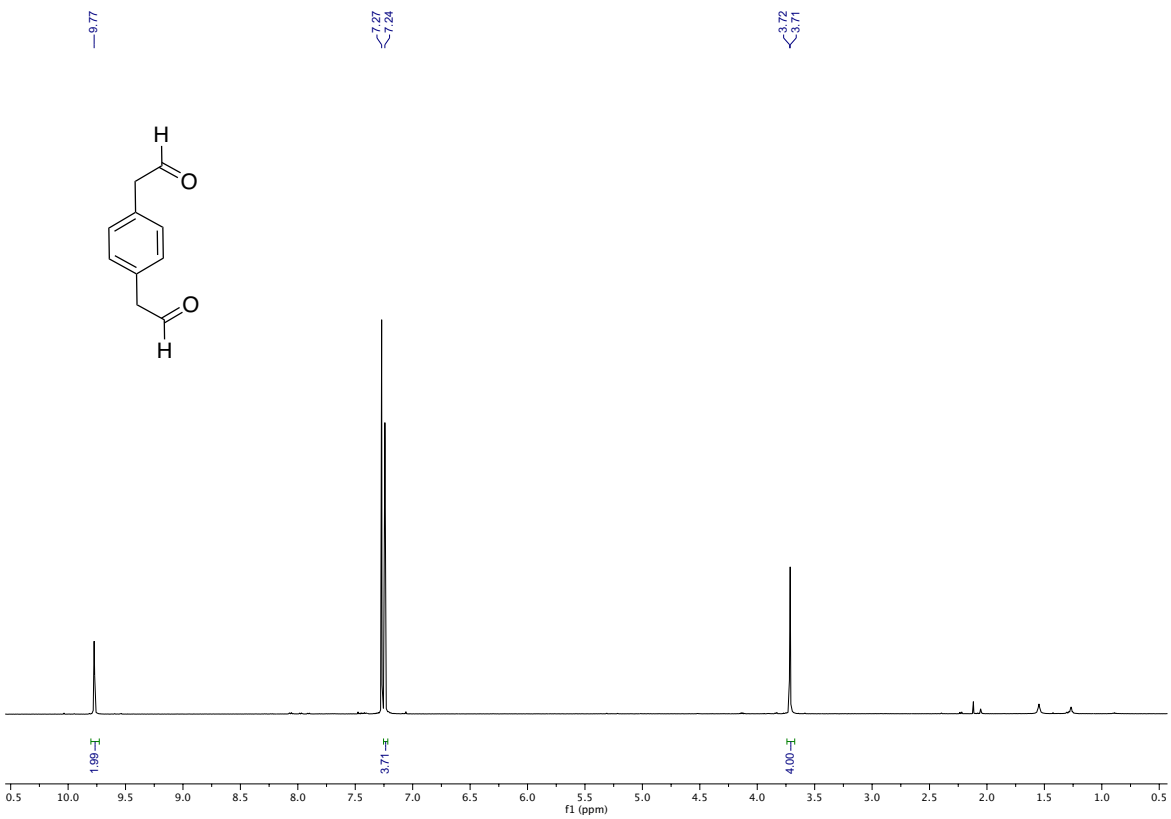
9.77
7.27
7.24
3.72
3.71
H
O
O
H
1.99
3.71
4.00
f1 (ppm)

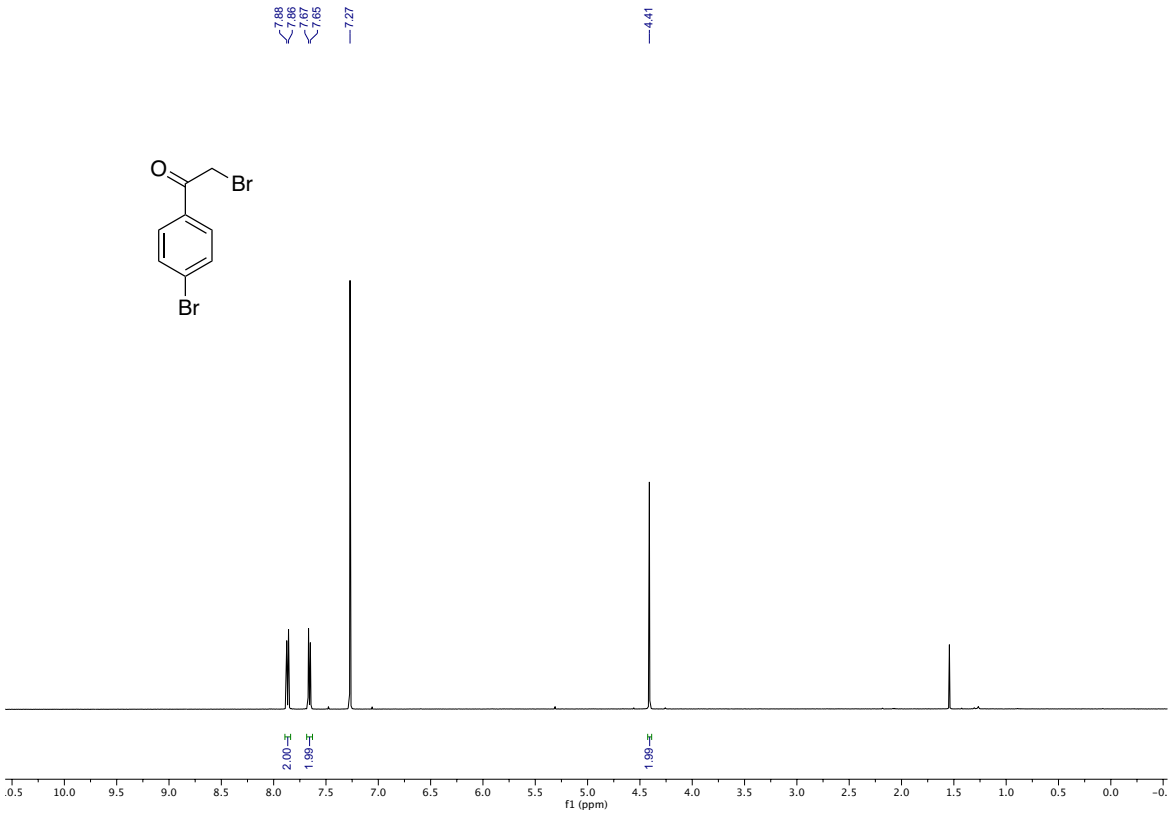
7.88
7.86
7.67
7.65
7.27
4.41
O
Br
Br
2.00
1.99
1.99
f1 (ppm)

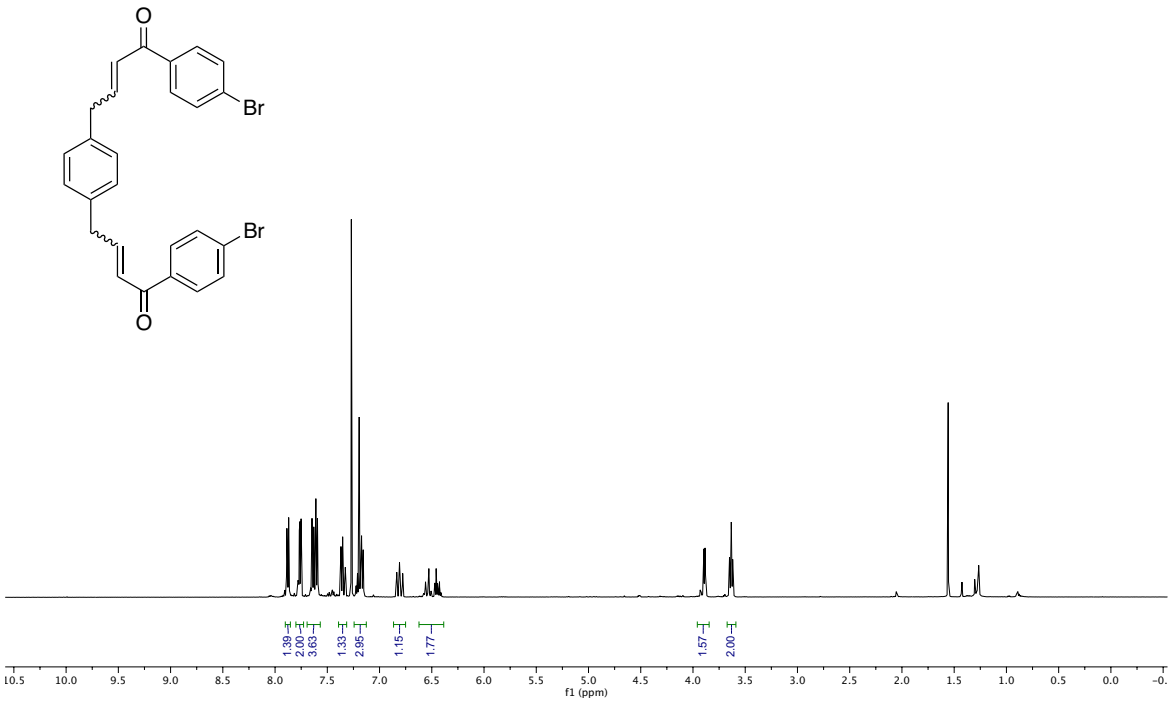
O
Br
Br
O
1.39
2.00
3.63
1.33
2.95
1.15
1.77
1.57
2.00
f1 (ppm)

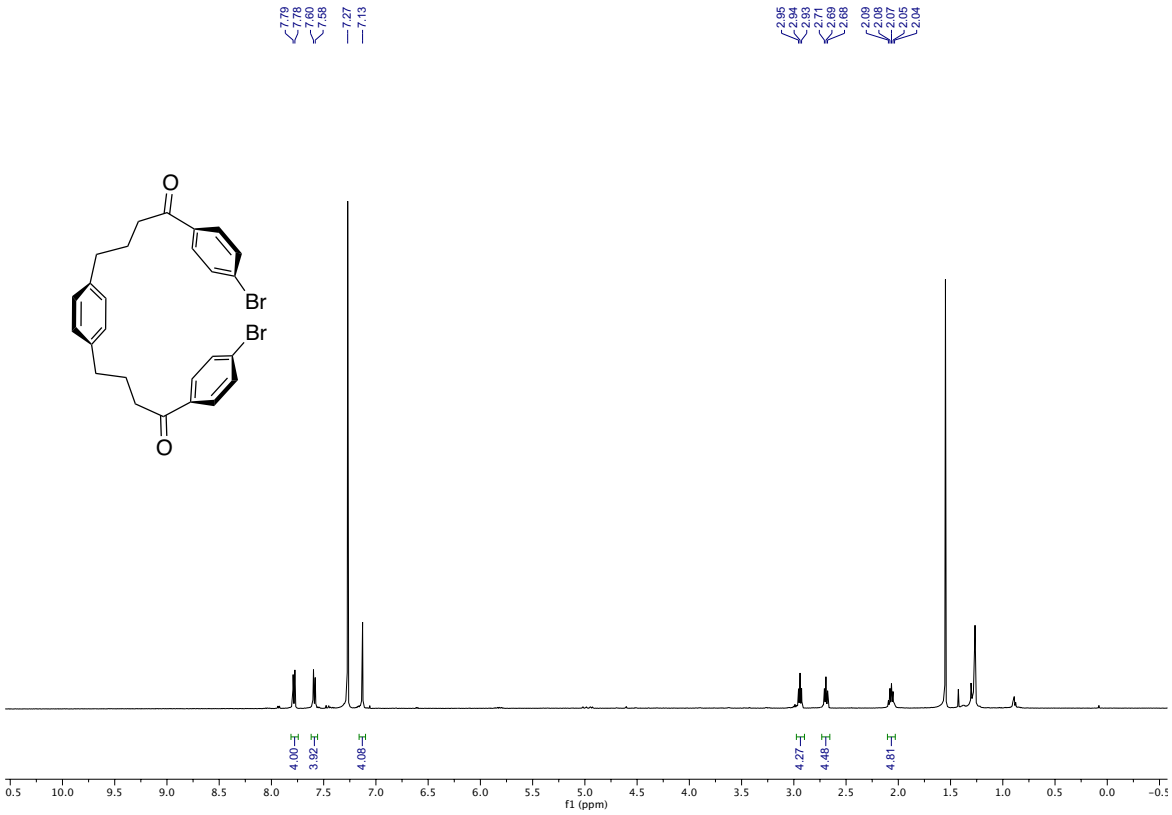
7.79
7.78
7.60
7.58
7.27
7.13
2.95
2.94
2.93
2.71
2.69
2.68
2.09
2.08
2.07
2.05
2.04
O
Br
Br
O
4.00
3.92
4.08
4.27
4.48
4.81
f1 (ppm)

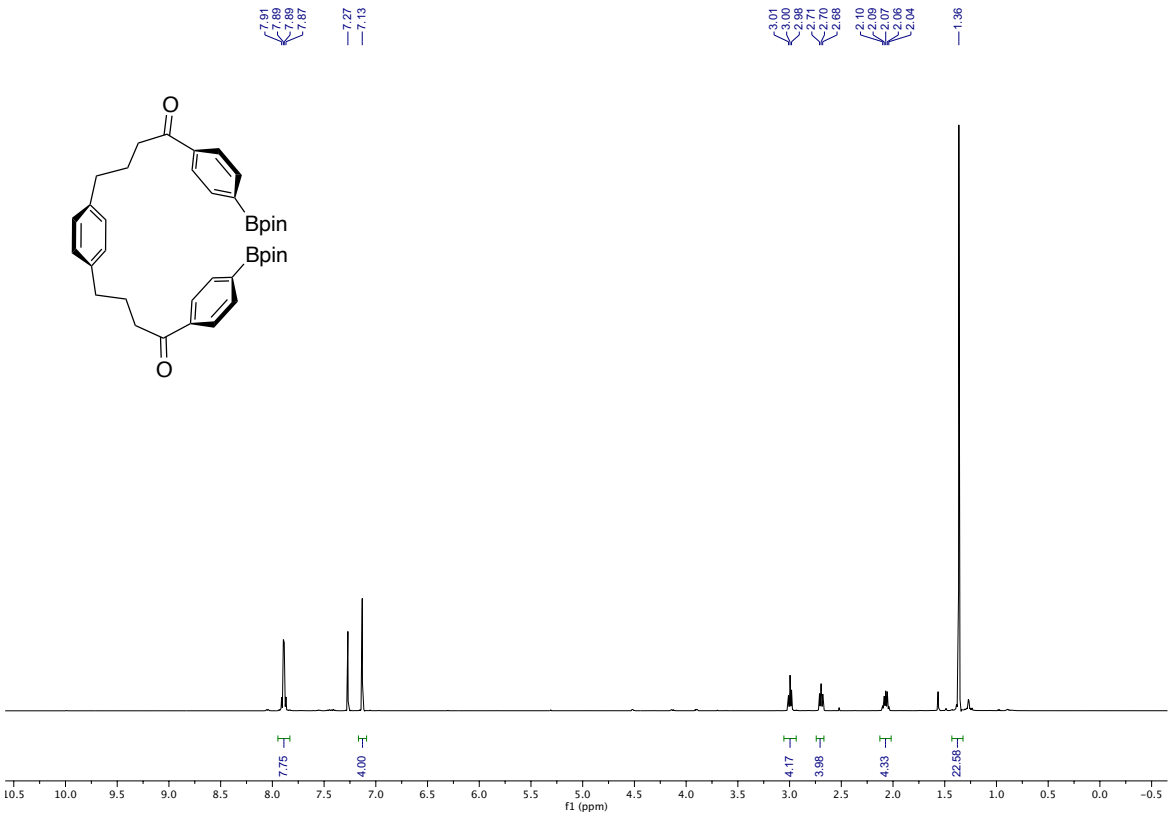
7.91
7.89
7.89
7.87
7.27
7.13
3.01
3.00
2.98
2.71
2.70
2.68
2.10
2.09
2.07
2.06
2.04
1.36
O
Bpin
Bpin
O
7.75
4.00
4.17
3.98
4.33
22.58
f1 (ppm)

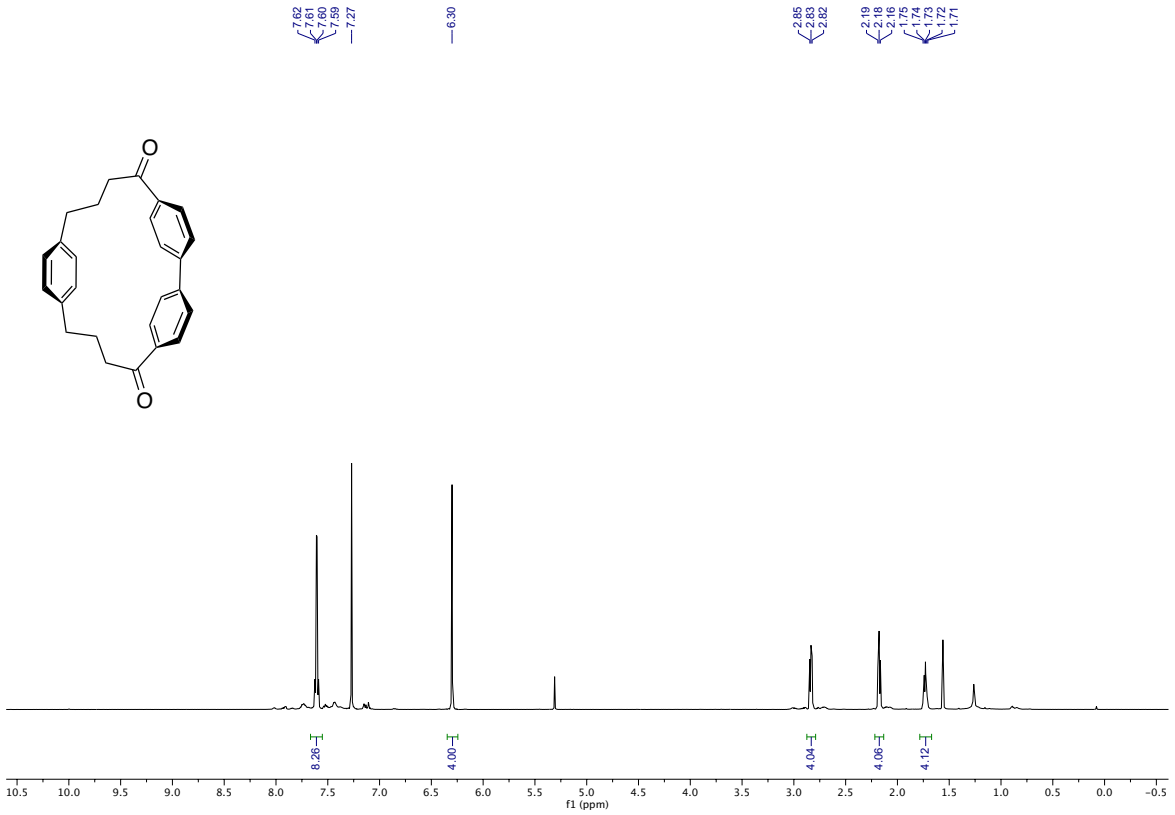
7.62
7.61
7.60
7.59
7.27
6.30
2.85
2.83
2.82
2.19
2.18
2.16
1.75
1.74
1.73
1.72
1.71
O
O
8.26
4.00
4.04
4.06
4.12
f1 (ppm)

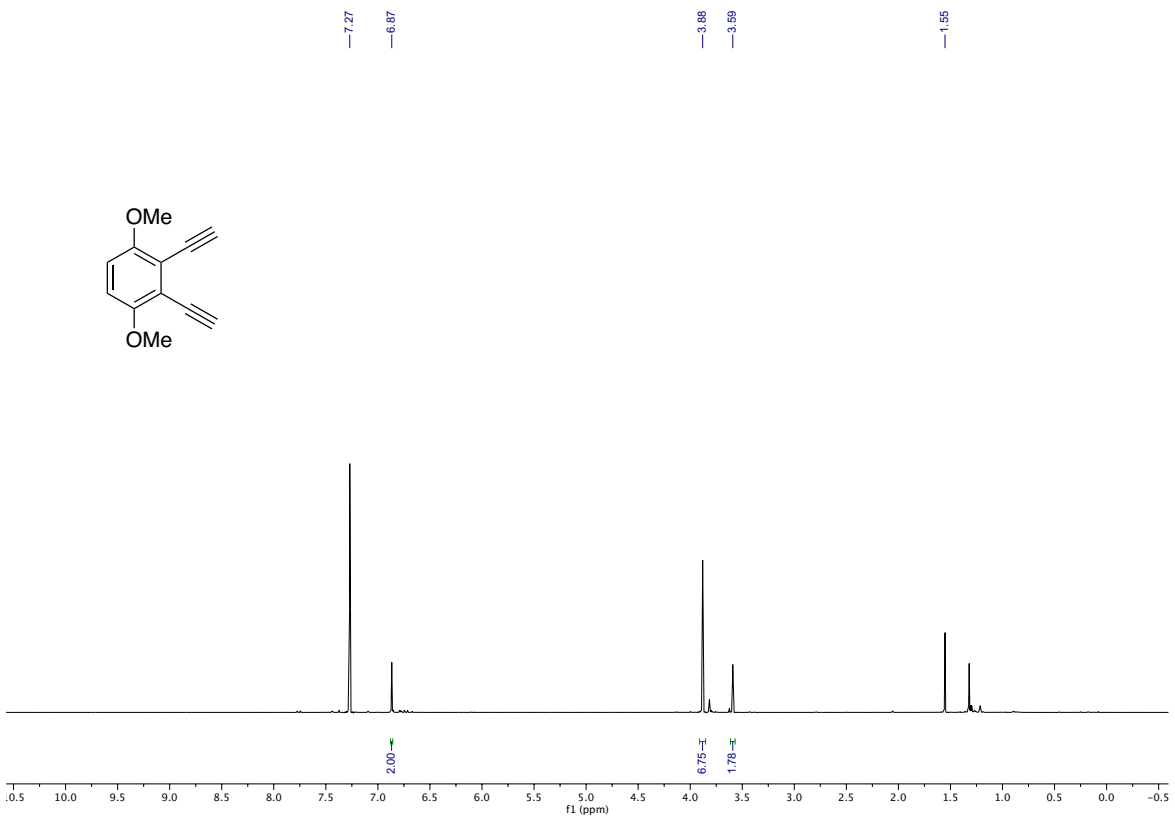
7.27
6.87
3.88
3.59
1.55
OMe
OMe
2.00
6.75
1.78
f1 (ppm)

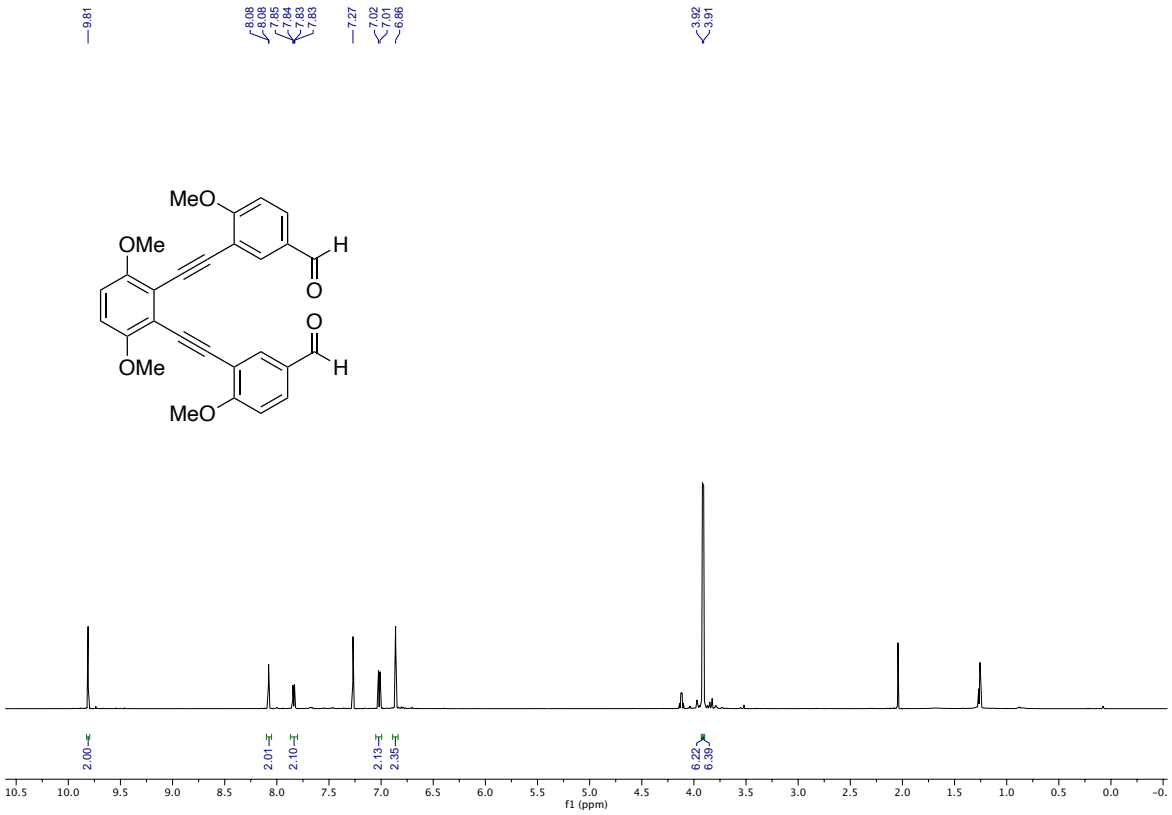
9.81
8.08
8.08
7.85
7.84
7.83
7.83
7.27
7.02
7.01
6.86
3.92
3.91
MeO
OMe
H
O
O
H
OMe
MeO
2.00
2.01
2.10
2.13
2.35
6.22
6.39
f1 (ppm)


9.87
7.74
7.73
6.95
6.93
6.71
3.79
2.97
2.96
2.94
2.83
2.83
2.82
2.61
OMe
MeO
O
H
H
OMe
O
MeO
2.00
3.93
2.25
2.67
12.49
4.68
4.51
f1 (ppm)

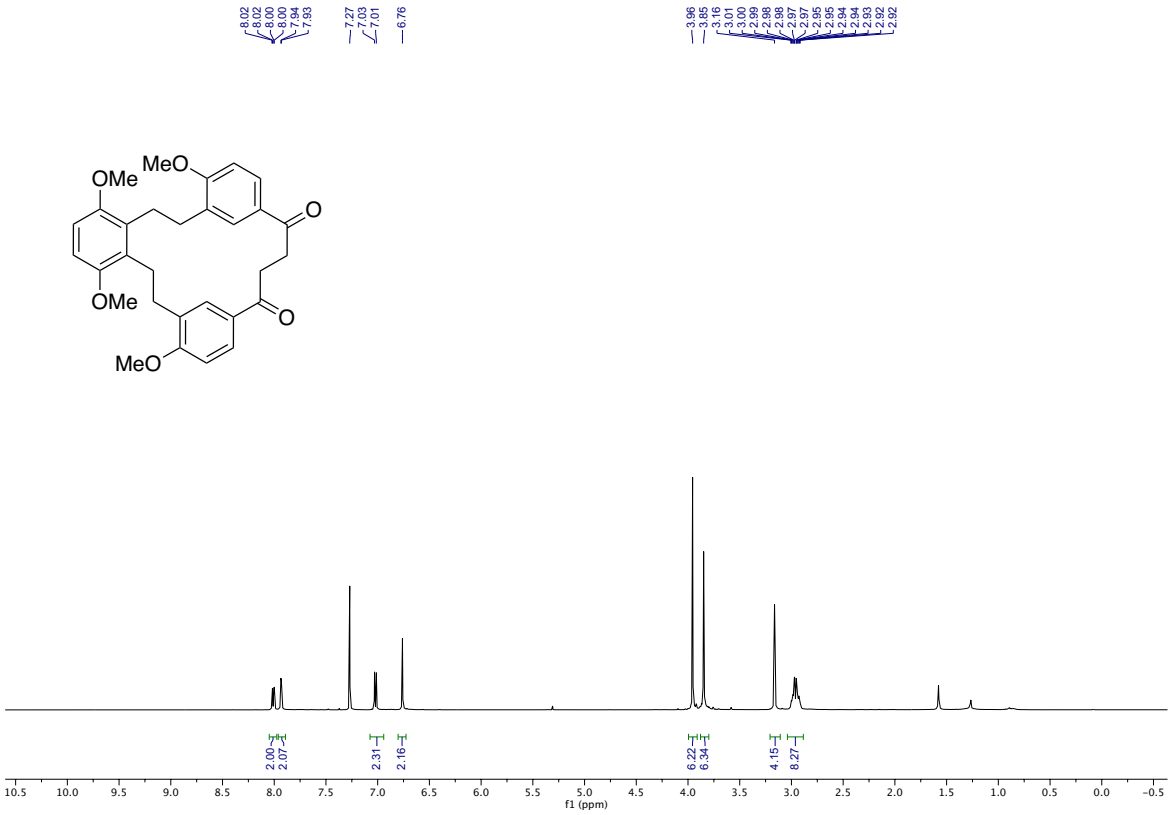
8.02
8.02
8.00
8.00
7.94
7.93
7.27
7.03
7.01
6.76
3.96
3.85
3.15
3.01
3.00
2.99
2.98
2.98
2.97
2.97
2.95
2.95
2.94
2.94
2.93
2.92
2.92
MeO
OMe
O
OMe
O
MeO
2.00
2.07
2.31
2.16
6.22
6.34
4.15
8.27
f1 (ppm)

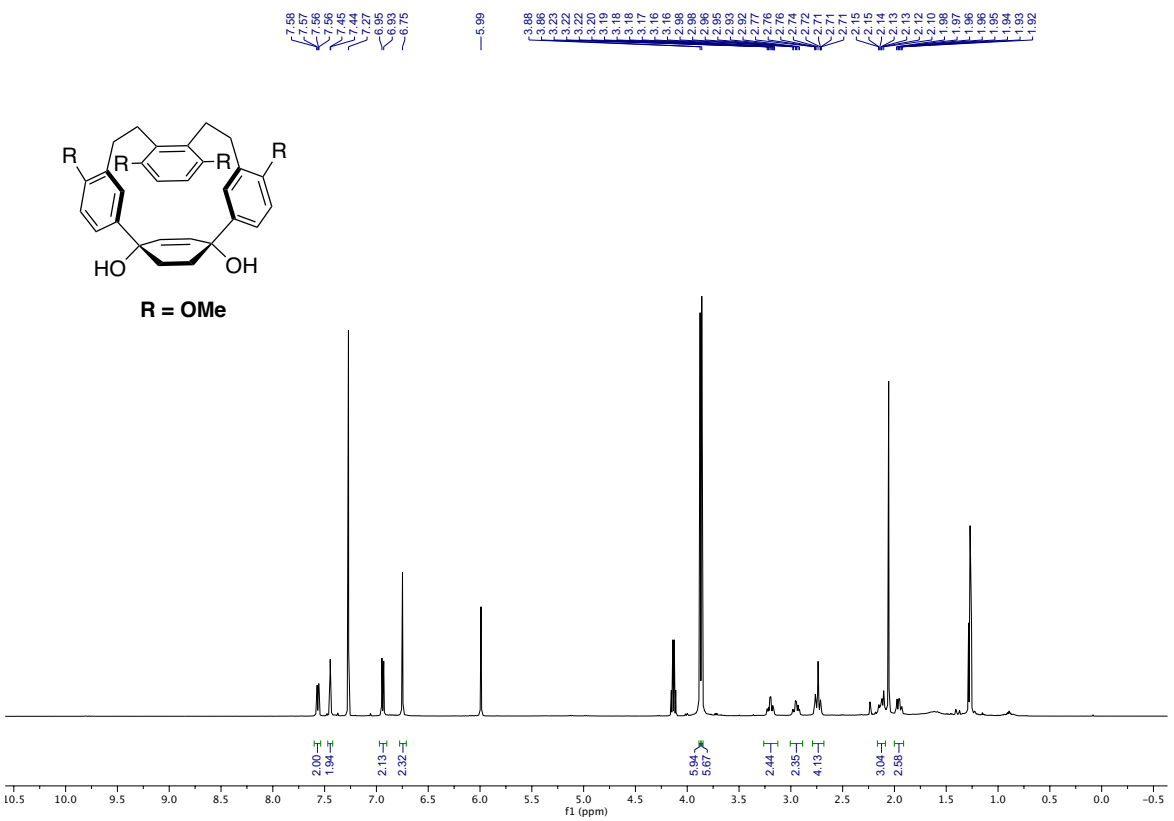
7.58
7.57
7.56
7.56
7.56
7.45
7.44
7.27
6.95
6.93
6.75
5.99
3.88
3.86
3.23
3.22
3.20
3.19
3.18
3.18
3.17
3.16
3.16
2.98
2.98
2.96
2.95
2.92
2.92
2.77
2.76
2.76
2.74
2.72
2.71
2.71
2.71
2.15
2.14
2.13
2.13
2.12
2.10
1.98
1.97
1.96
1.96
1.95
1.94
1.93
1.92
R
R
R
R
HO
OH
R = OMe
2.00
1.94
2.13
2.32
5.94
5.67
2.44
2.35
4.13
3.04
2.58
f1 (ppm)

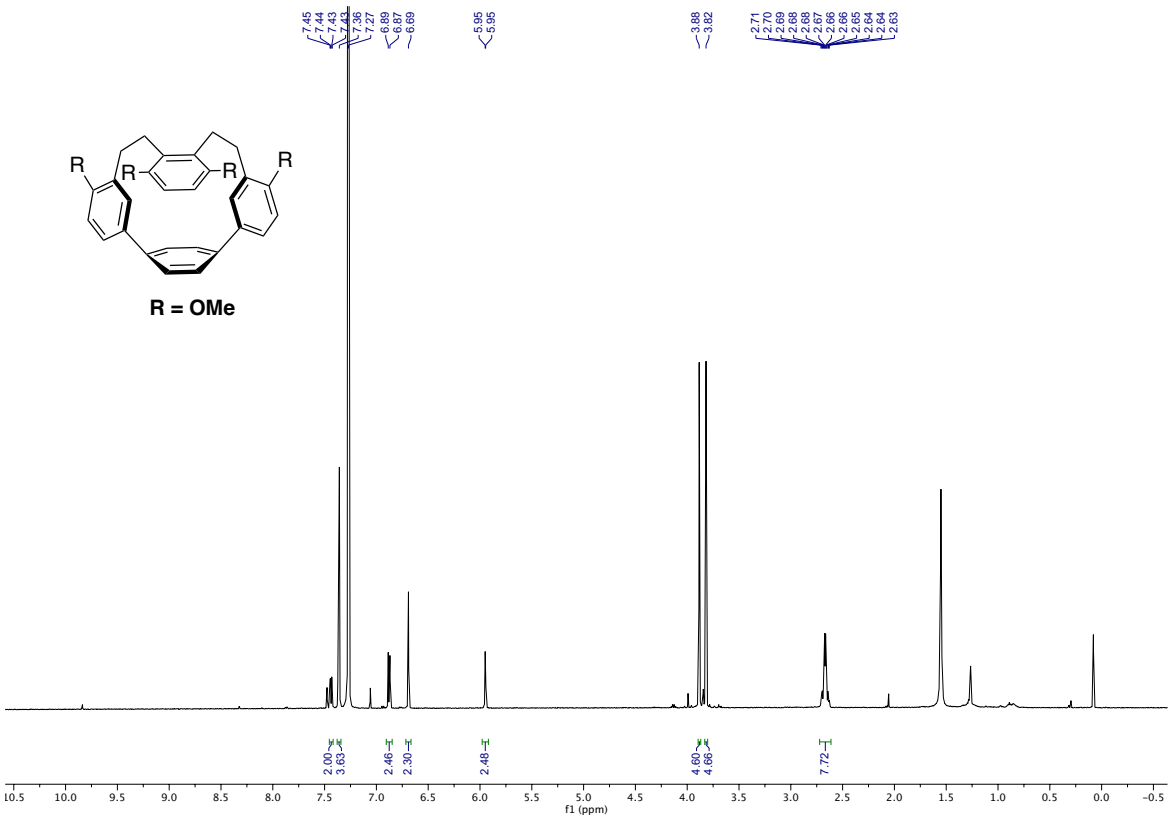
R
R
R
R
R = OMe
7.45
7.44
7.43
7.43
7.36
7.27
6.89
6.87
6.69
5.95
5.95
3.88
3.82
2.71
2.70
2.69
2.68
2.68
2.67
2.66
2.65
2.64
2.64
2.63
2.00
3.63
2.46
2.30
2.48
4.60
4.66
7.72
f1 (ppm)

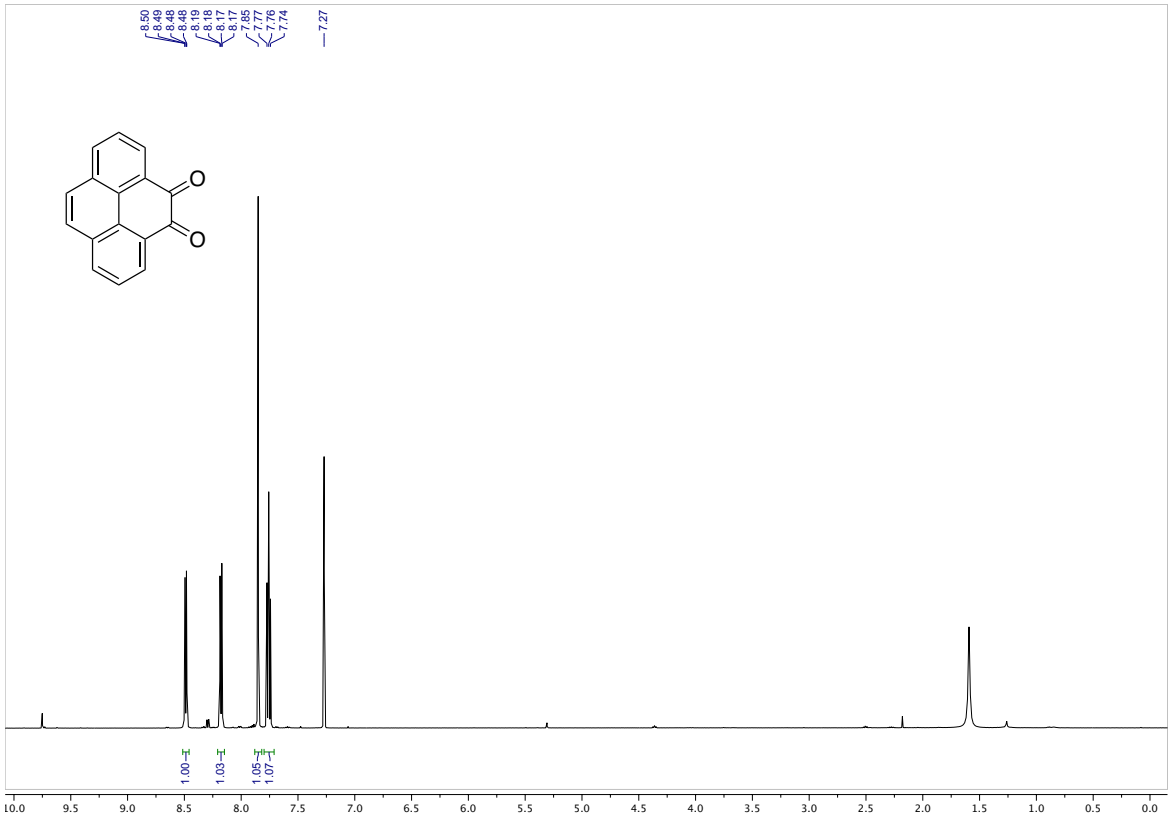
8.50
8.49
8.48
8.48
8.19
8.18
8.17
8.17
7.85
7.77
7.76
7.74
7.27
O
O
1.00
1.03
1.05
1.07

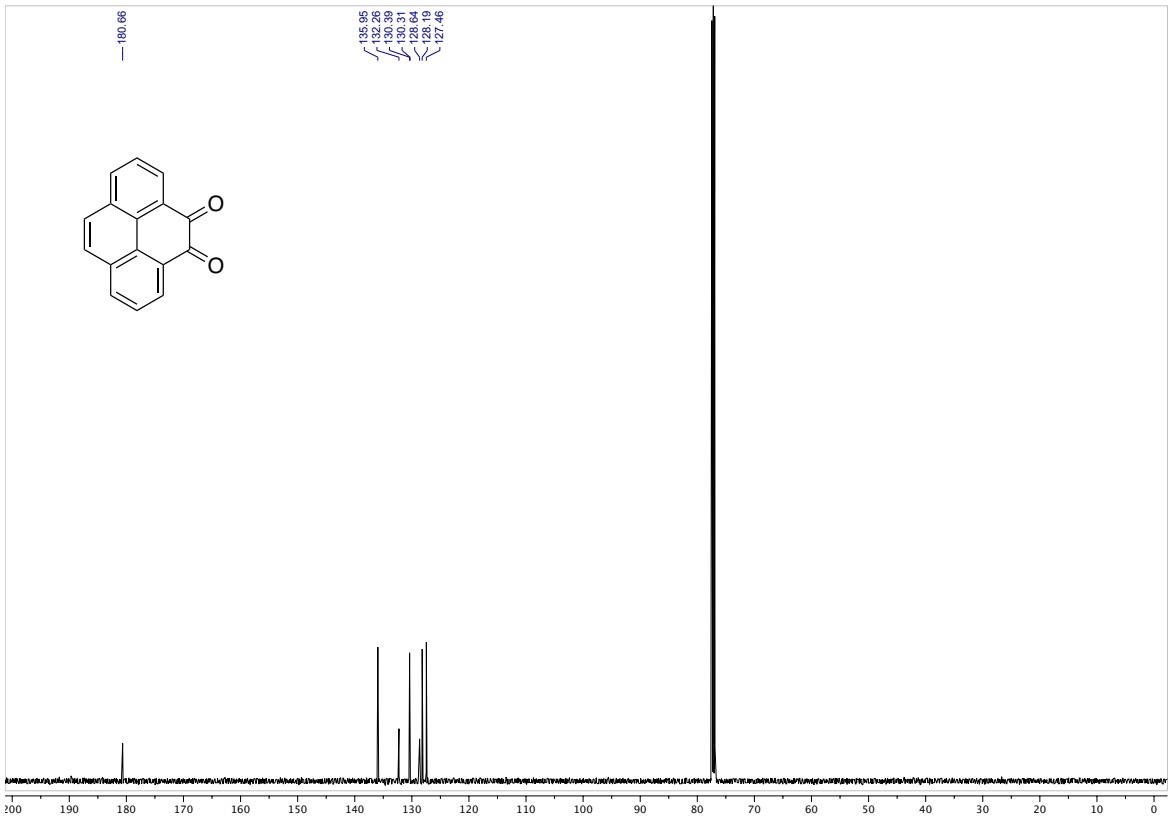
180.66
135.95
132.26
130.39
130.31
128.64
128.19
127.46
O
O

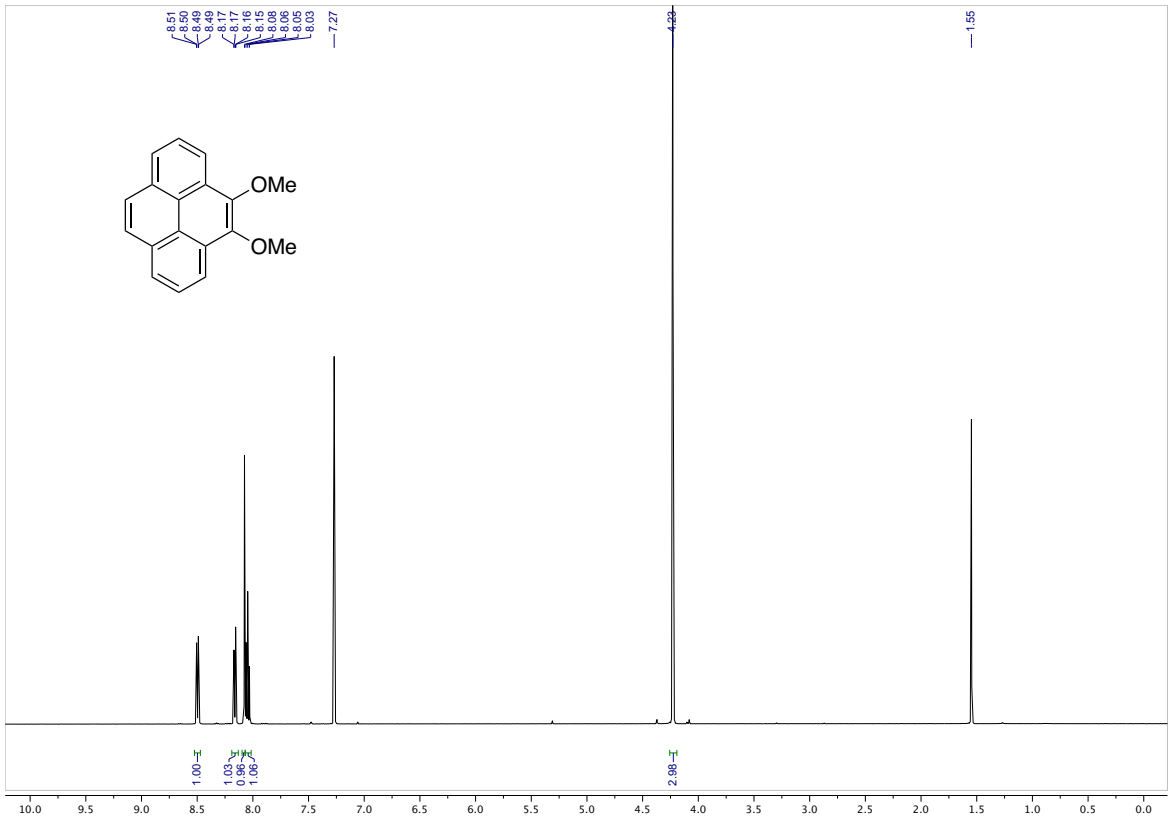
8.51
8.50
8.49
8.49
8.17
8.17
8.16
8.15
8.08
8.06
8.05
8.03
7.27
4.22
1.55
OMe
OMe
1.00
1.03
0.96
1.06
2.98

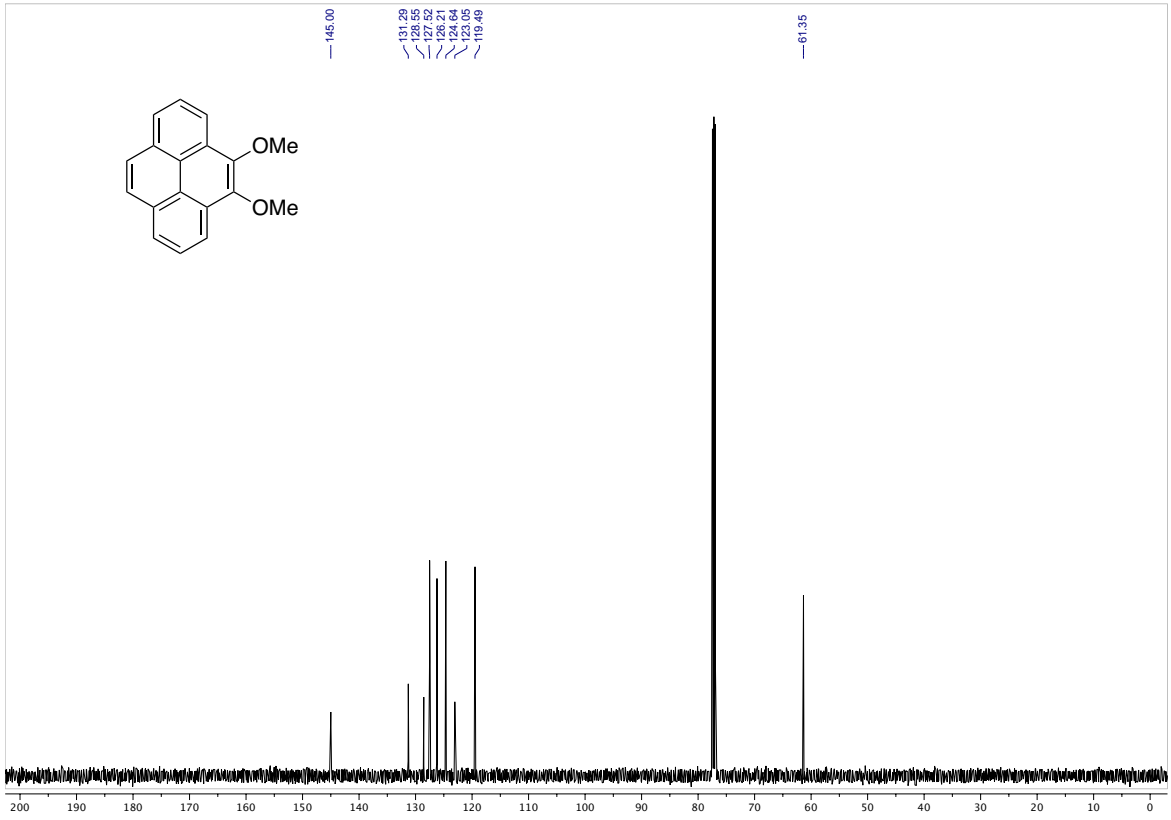
145.00
131.29
128.55
127.52
126.21
124.64
123.05
119.49
61.35
OMe
OMe
200
190
180
170
160
150
140
130
120
110
100
90
80
70
60
50
40
30
20
10
0

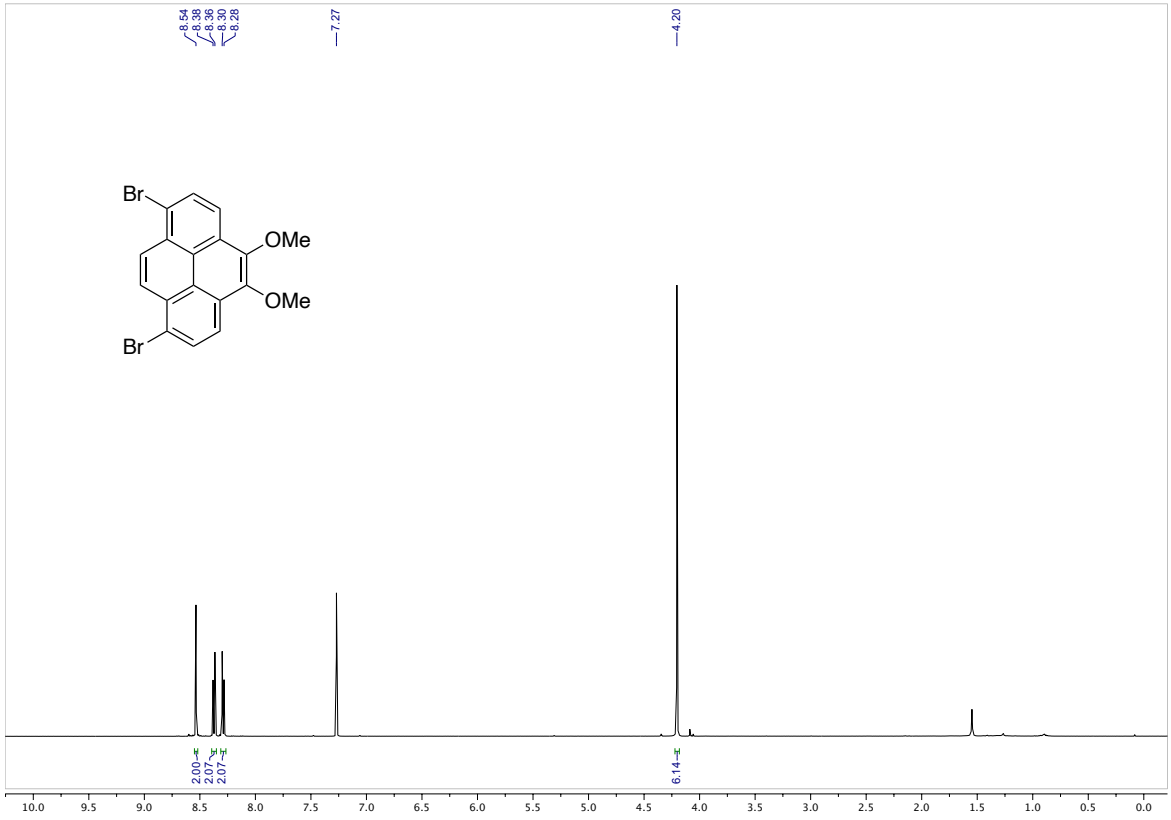
8.54
8.38
8.36
8.30
8.28
7.27
4.20
Br
OMe
OMe
Br
2.00
2.07
2.07
6.14
10.0
9.5
9.0
8.5
8.0
7.5
7.0
6.5
6.0
5.5
5.0
4.5
4.0
3.5
3.0
2.5
2.0
1.5
1.0
0.5
0.0

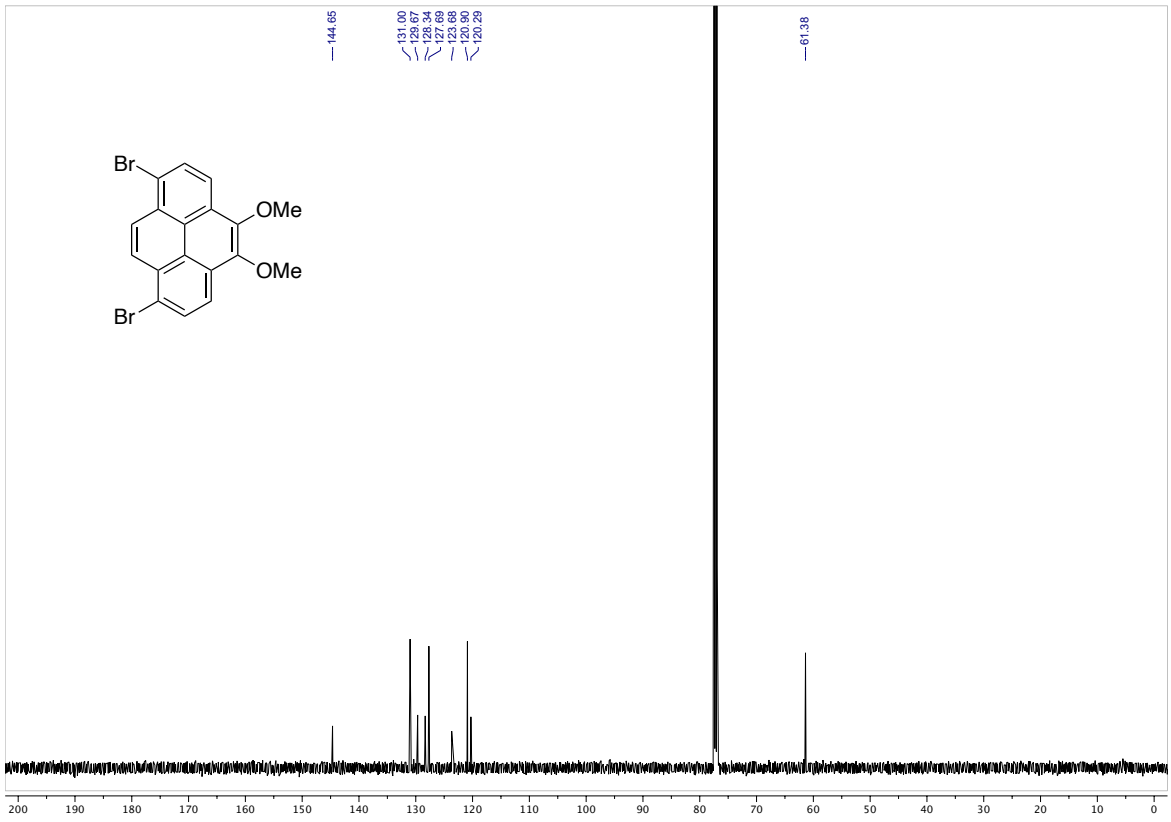
144.65
131.00
129.67
128.34
127.69
123.68
120.90
120.29
61.38
Br
OMe
OMe
Br
200
190
180
170
160
150
140
130
120
110
100
90
80
70
60
50
40
30
20
10
0

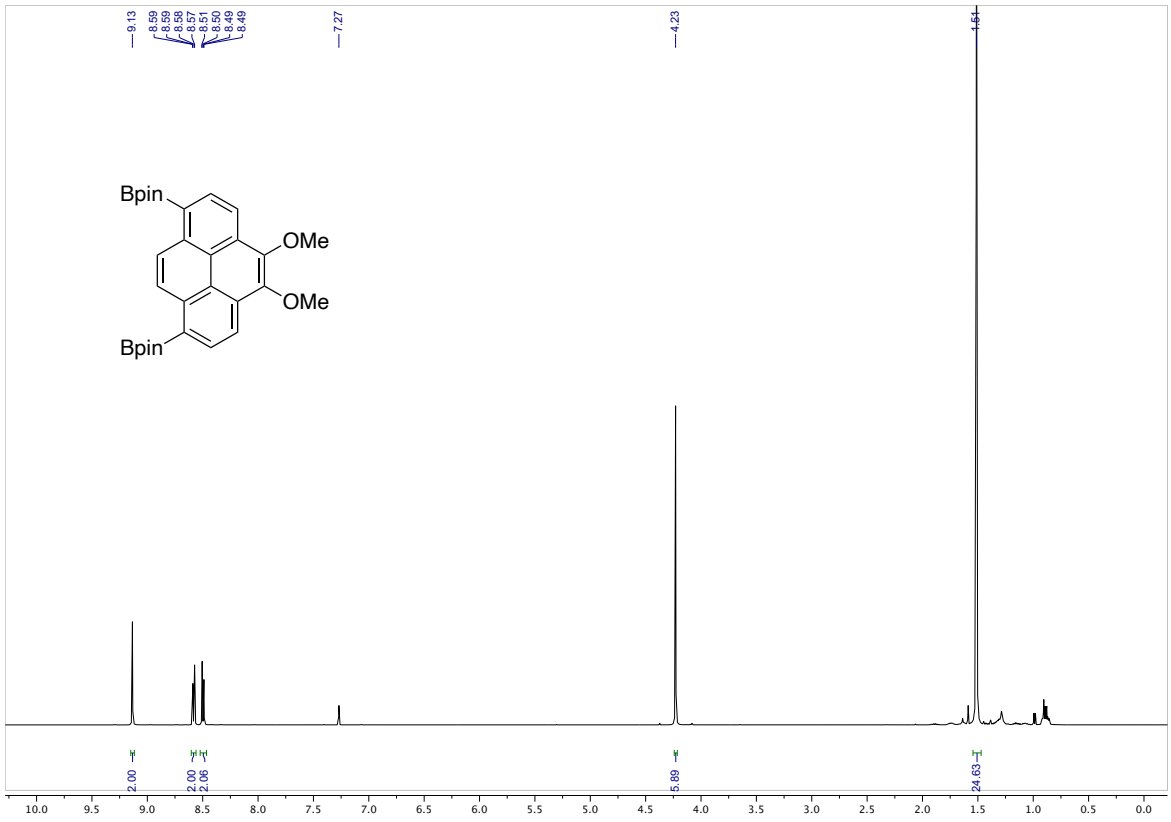
9.13
8.59
8.59
8.58
8.57
8.51
8.50
8.49
8.49
7.27
4.23
1.61
Bpin
OMe
OMe
Bpin
2.00
2.00
2.06
5.89
24.63
10.0
9.5
9.0
8.5
8.0
7.5
7.0
6.5
6.0
5.5
5.0
4.5
4.0
3.5
3.0
2.5
2.0
1.5
1.0
0.5
0.0

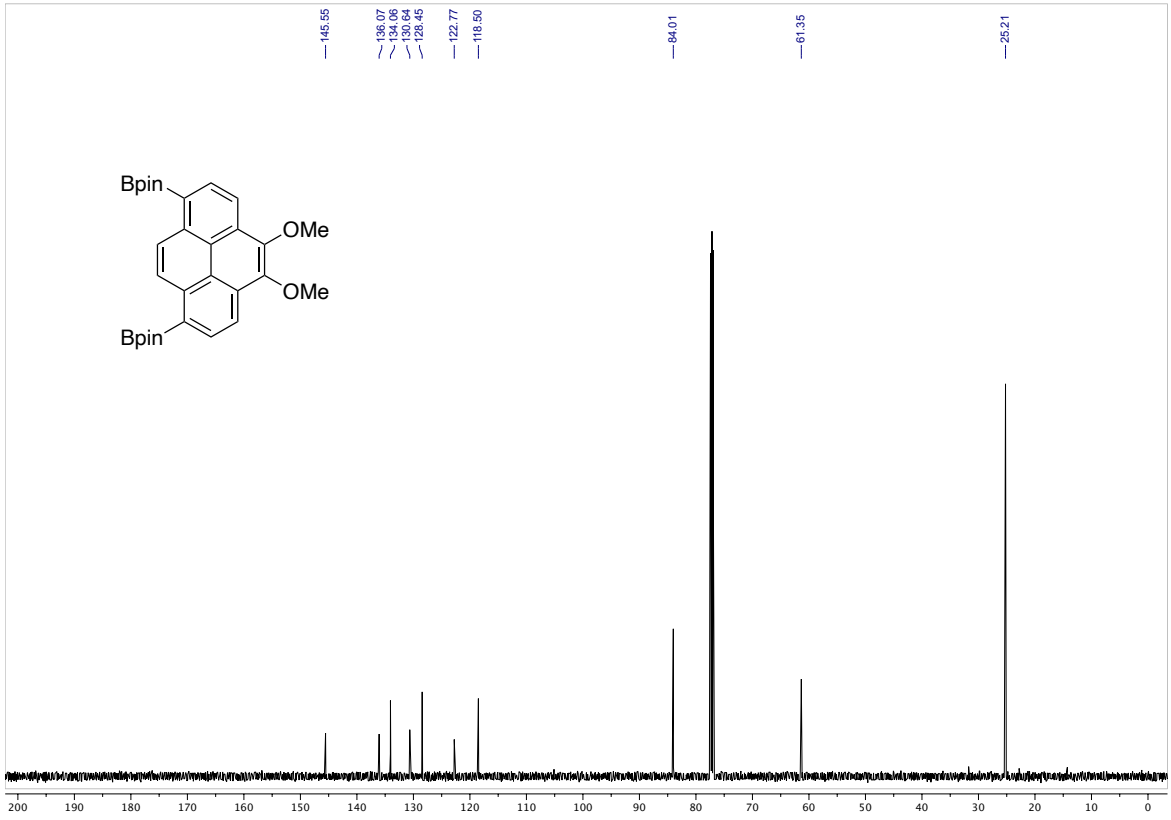
145.55
136.07
134.06
130.64
128.45
122.77
118.50
84.01
61.35
25.21
Bpin
OMe
OMe
Bpin
200
190
180
170
160
150
140
130
120
110
100
90
80
70
60
50
40
30
20
10
0

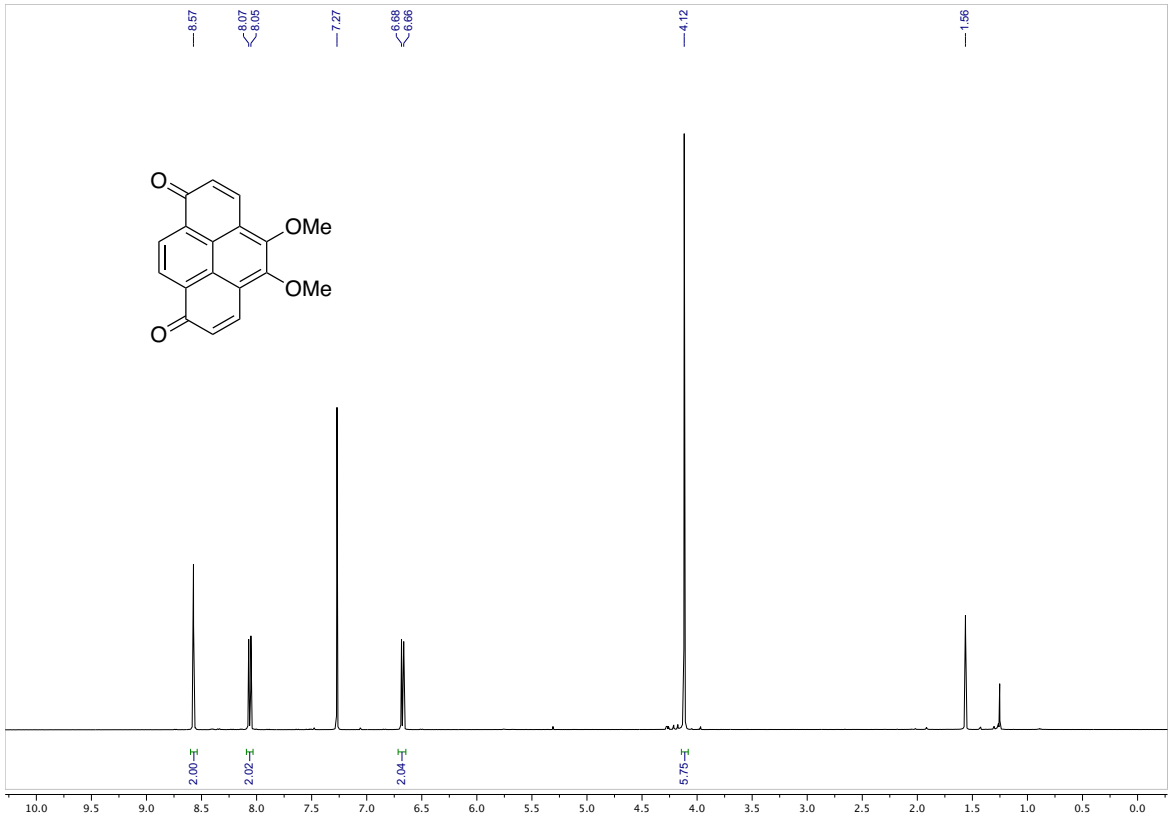
8.57
8.07
8.05
7.27
6.68
6.66
4.12
1.56
O
OMe
OMe
O
2.00
2.02
2.04
5.75
10.0
9.5
9.0
8.5
8.0
7.5
7.0
6.5
6.0
5.5
5.0
4.5
4.0
3.5
3.0
2.5
2.0
1.5
1.0
0.5
0.0

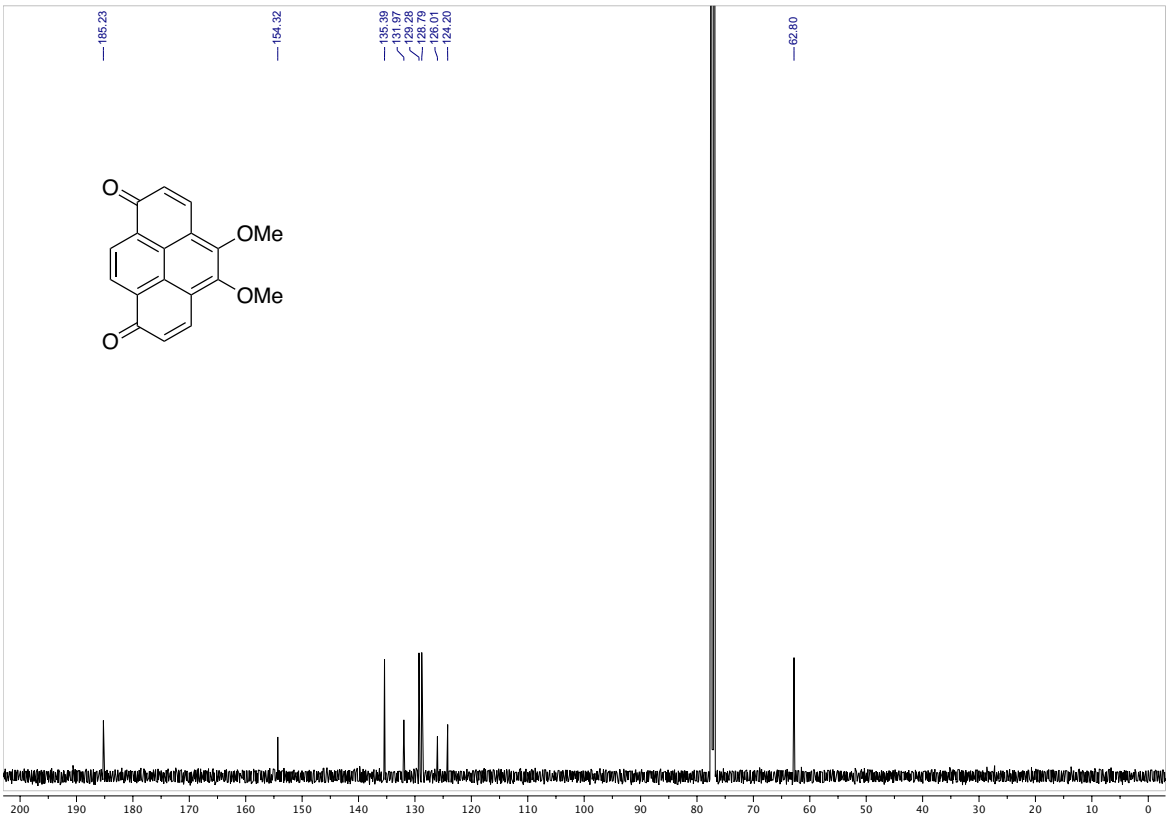
185.23
154.32
135.39
131.97
129.28
128.79
126.01
124.20
62.80
O
OMe
OMe
O
200
190
180
170
160
150
140
130
120
110
100
90
80
70
60
50
40
30
20
10
0

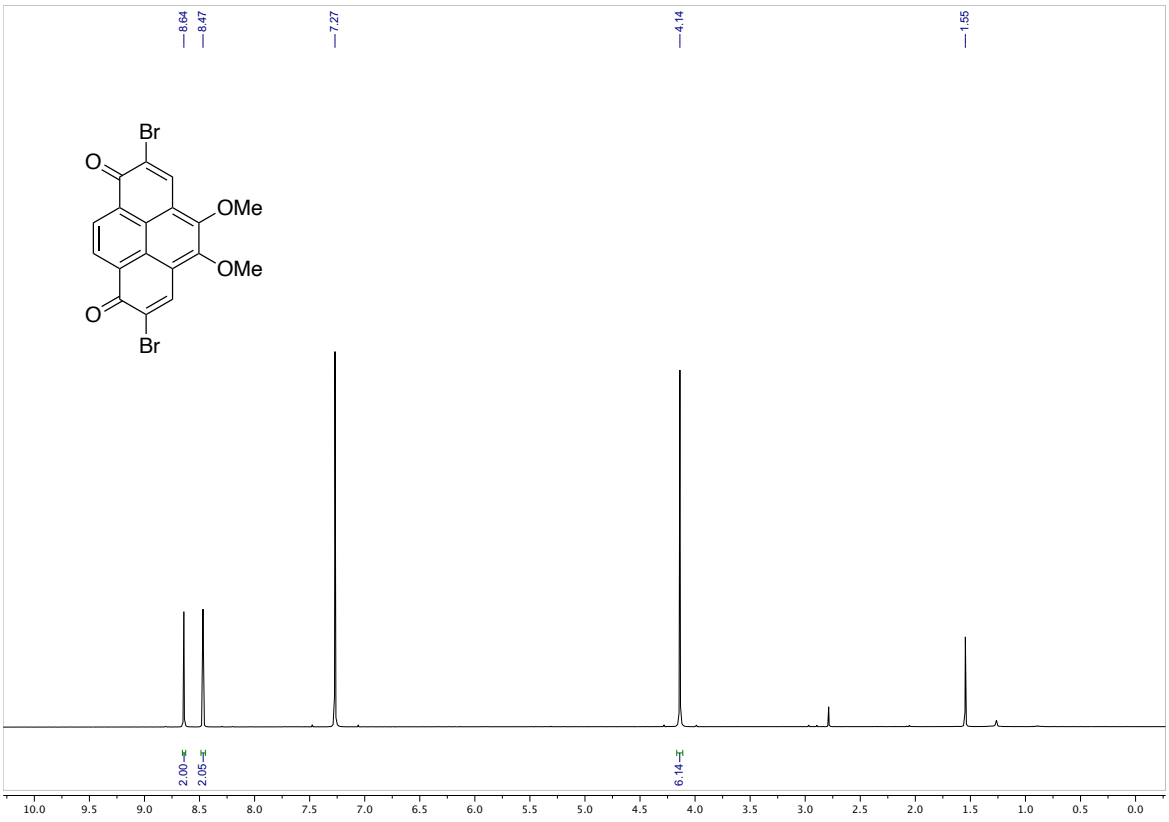
8.64
8.47
7.27
4.14
1.55
Br
O
OMe
OMe
O
Br
2.00
2.05
6.14
10.0
9.5
9.0
8.5
8.0
7.5
7.0
6.5
6.0
5.5
5.0
4.5
4.0
3.5
3.0
2.5
2.0
1.5
1.0
0.5
0.0

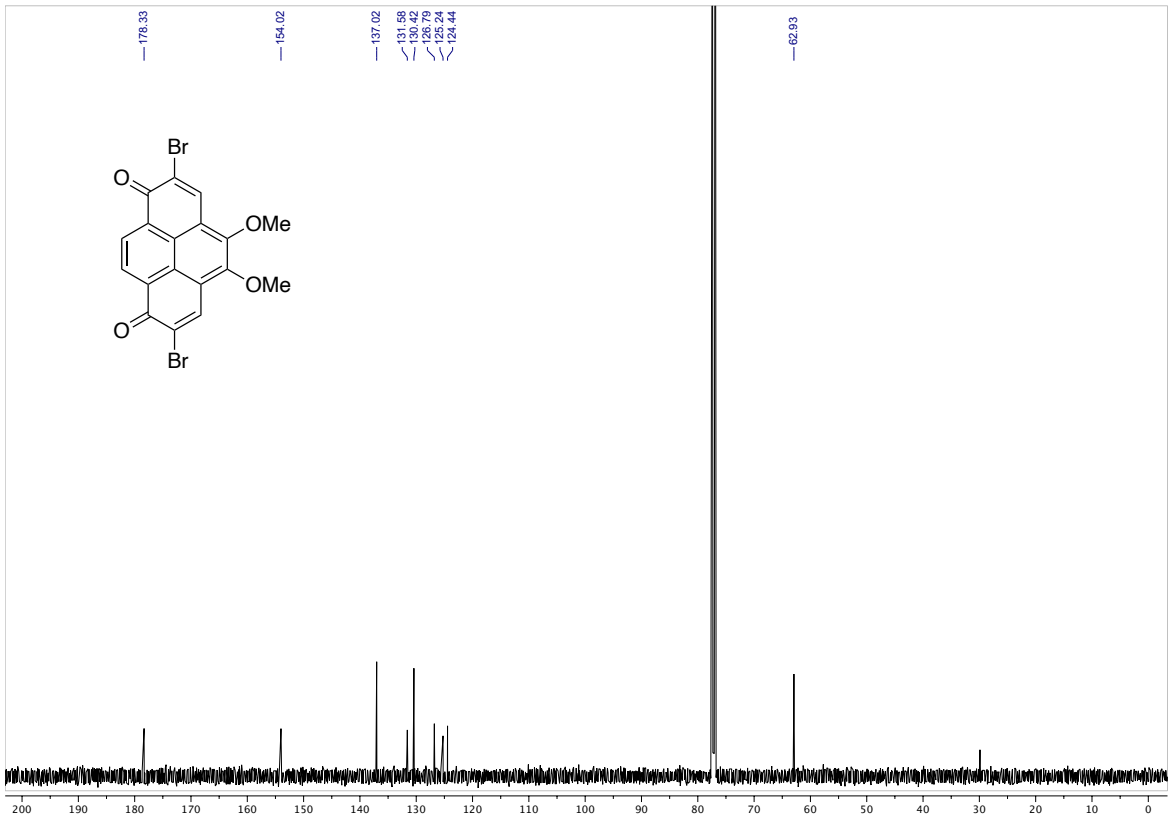
178.33
154.02
137.02
131.58
130.42
126.79
125.24
124.44
62.93
Br
O
OMe
OMe
O
Br
200
190
180
170
160
150
140
130
120
110
100
90
80
70
60
50
40
30
20
10
0

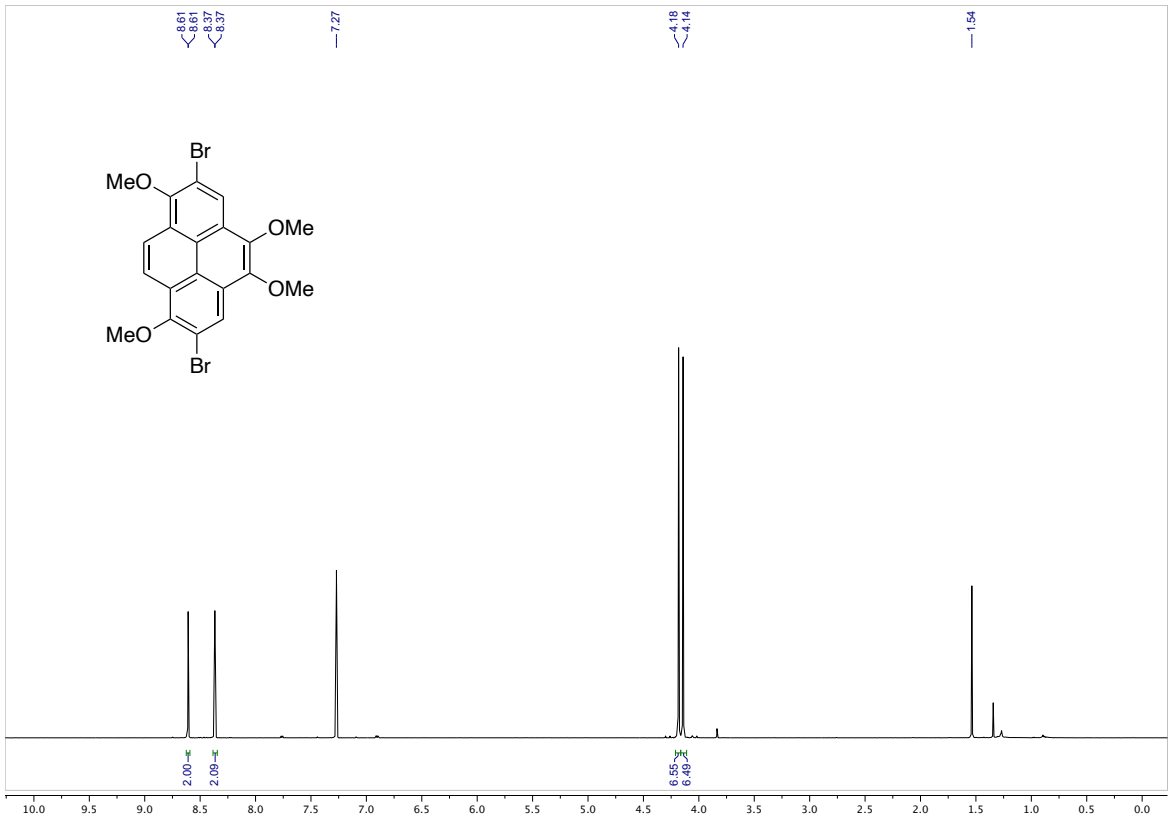
8.61
8.61
8.37
8.37
7.27
4.18
4.14
1.54
Br
MeO
OMe
OMe
MeO
Br
2.00
2.09
6.55
6.49
10.0
9.5
9.0
8.5
8.0
7.5
7.0
6.5
6.0
5.5
5.0
4.5
4.0
3.5
3.0
2.5
2.0
1.5
1.0
0.5
0.0

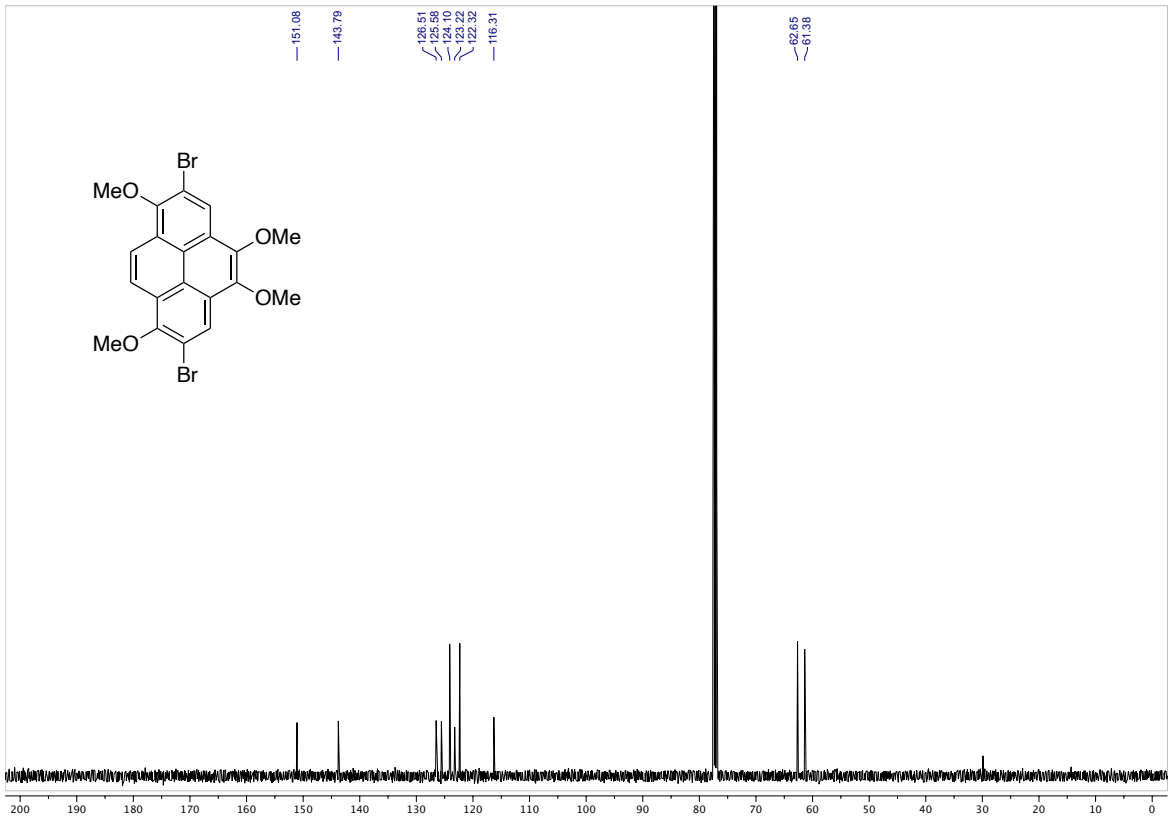
151.08
143.79
126.51
125.58
124.10
123.22
122.32
116.31
62.65
61.38
Br
MeO
OMe
OMe
MeO
Br

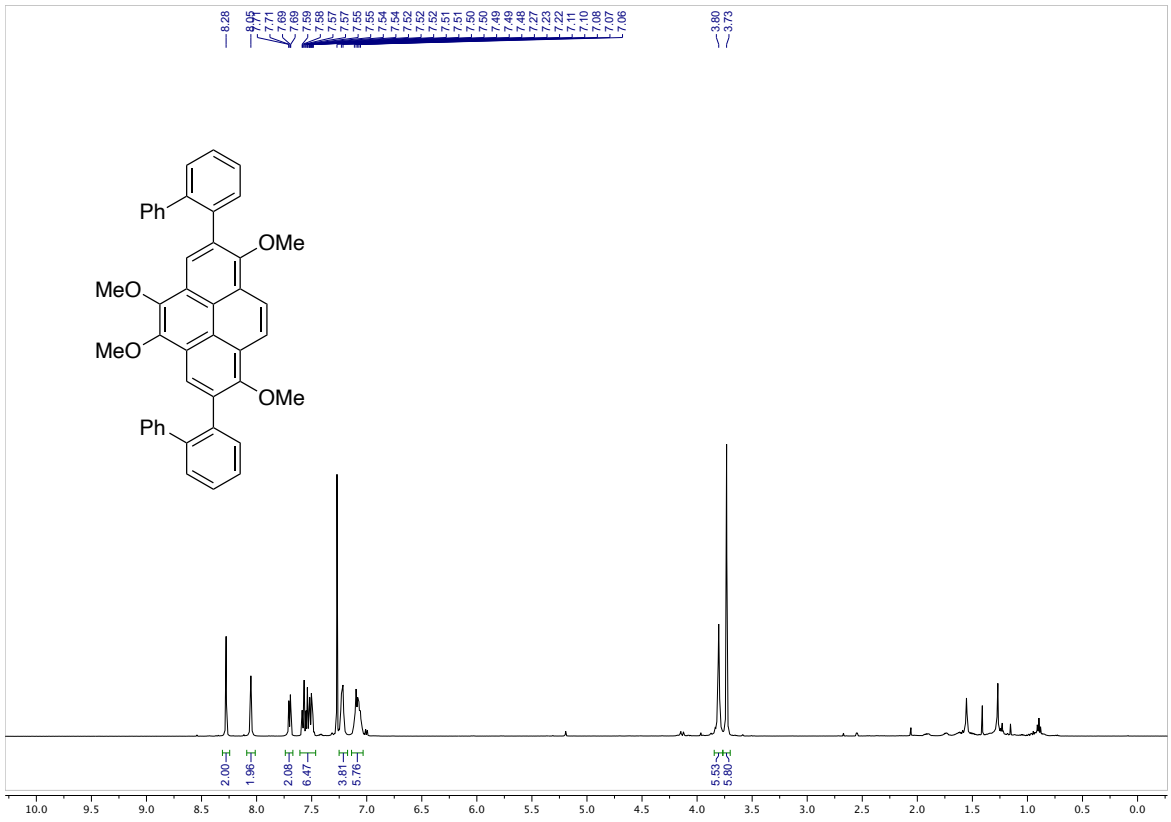
8.28
7.71
7.69
7.59
7.58
7.57
7.57
7.55
7.54
7.52
7.52
7.51
7.51
7.50
7.50
7.49
7.48
7.27
7.23
7.22
7.11
7.10
7.08
7.07
7.06
3.80
3.73
Ph
OMe
MeO
MeO
OMe
Ph
2.00
1.96
2.08
6.47
3.81
5.76
5.53
5.80

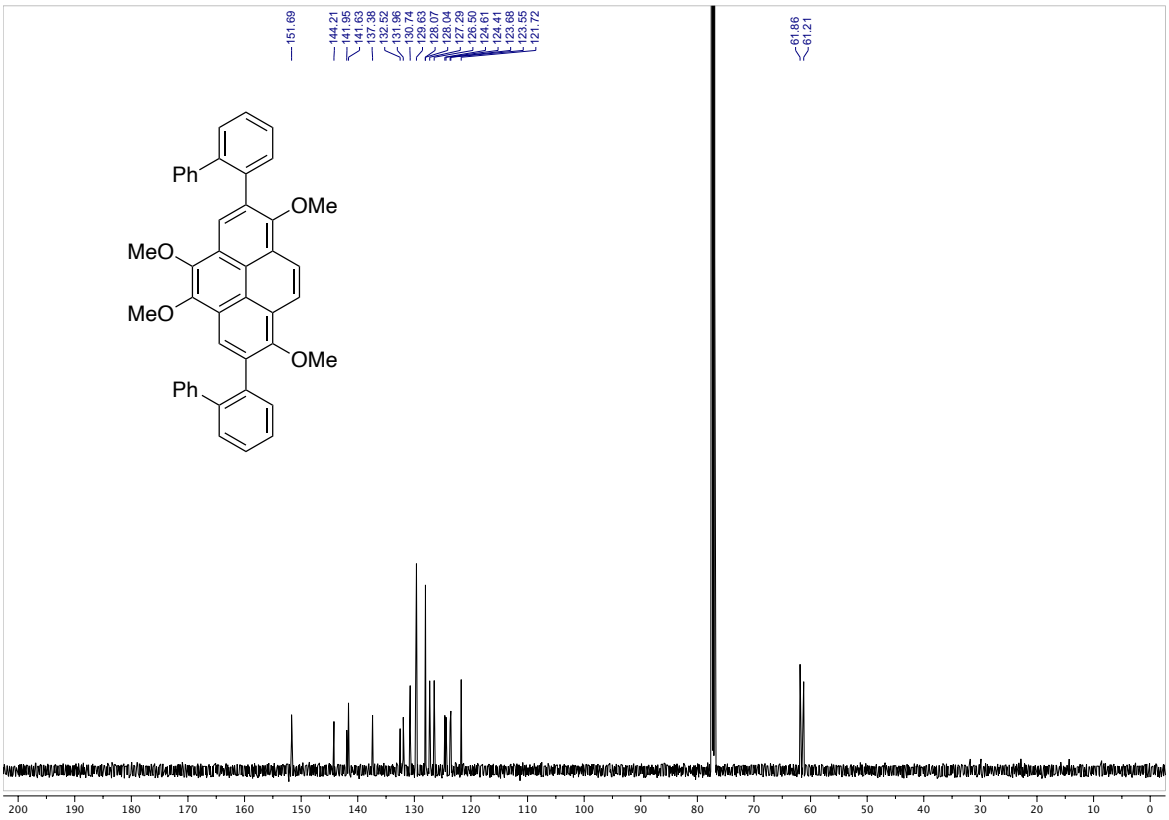
151.69
144.21
141.95
141.63
137.38
132.52
131.96
130.74
128.63
128.07
128.04
127.29
126.50
124.61
124.41
123.68
123.55
121.72
61.86
61.21
Ph
OMe
MeO
MeO
OMe
Ph

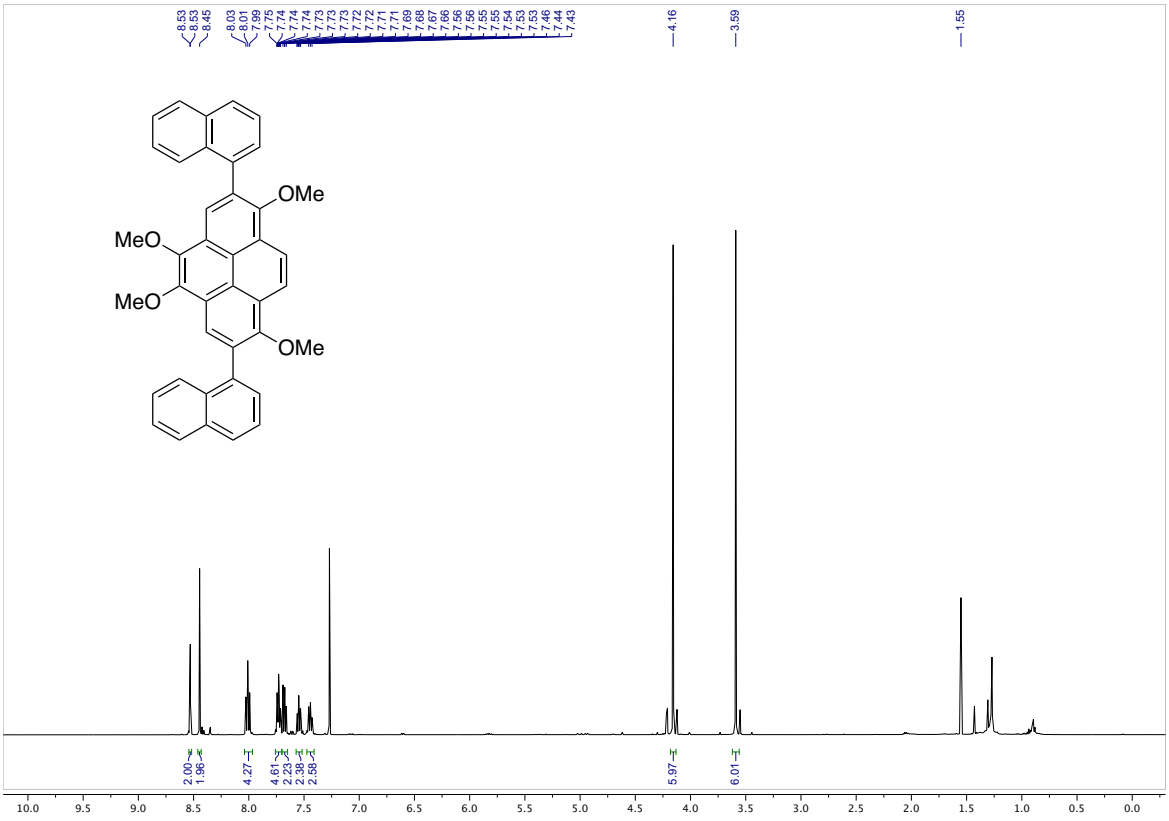
8.53
8.53
8.45
8.03
8.01
7.99
7.75
7.74
7.74
7.74
7.73
7.73
7.73
7.72
7.72
7.71
7.71
7.69
7.69
7.67
7.66
7.56
7.56
7.55
7.55
7.54
7.53
7.53
7.46
7.44
7.43
4.16
3.59
1.55
OMe
MeO
MeO
OMe
2.00
1.96
4.27
4.61
2.23
2.38
2.58
5.97
6.01

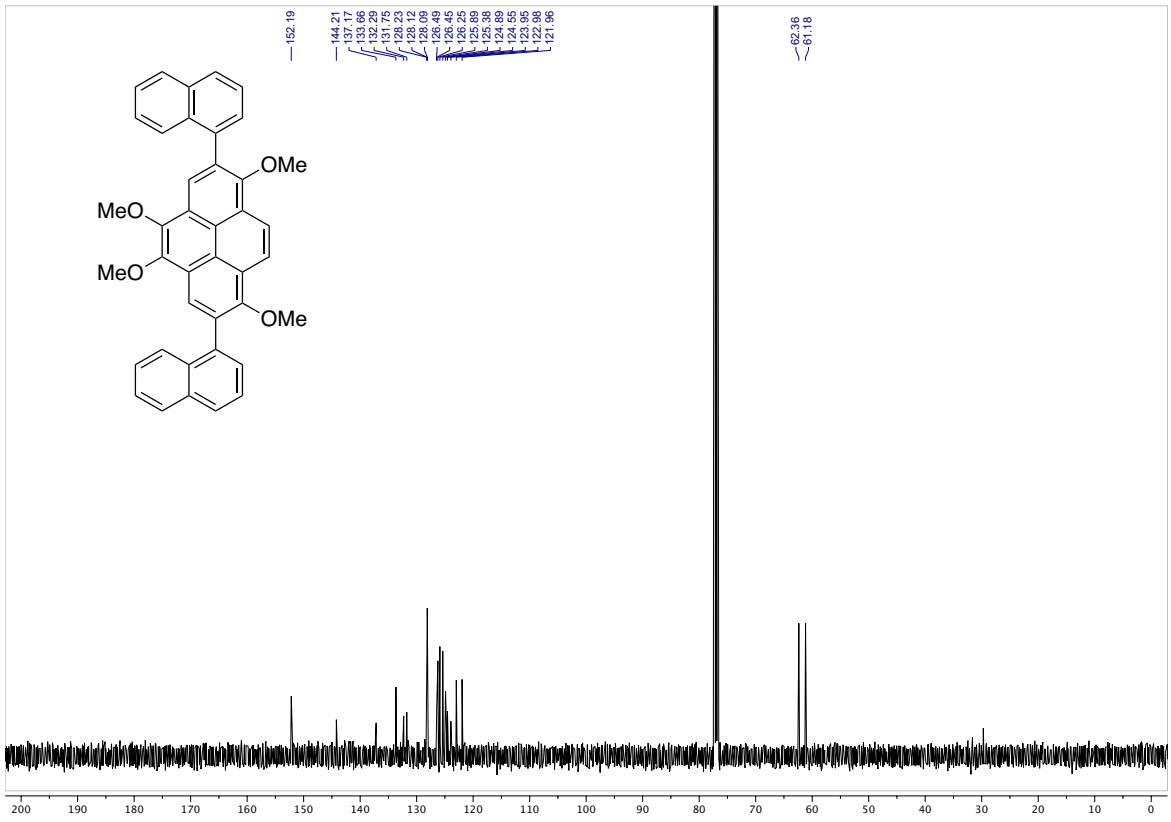
152.19
144.21
137.17
133.66
132.29
131.75
128.23
128.12
128.09
126.49
126.45
126.25
125.89
125.38
124.89
124.55
123.95
122.98
121.96
62.36
61.18
OMe
MeO
MeO
OMe
200
190
180
170
160
150
140
130
120
110
100
90
80
70
60
50
40
30
20
10
0

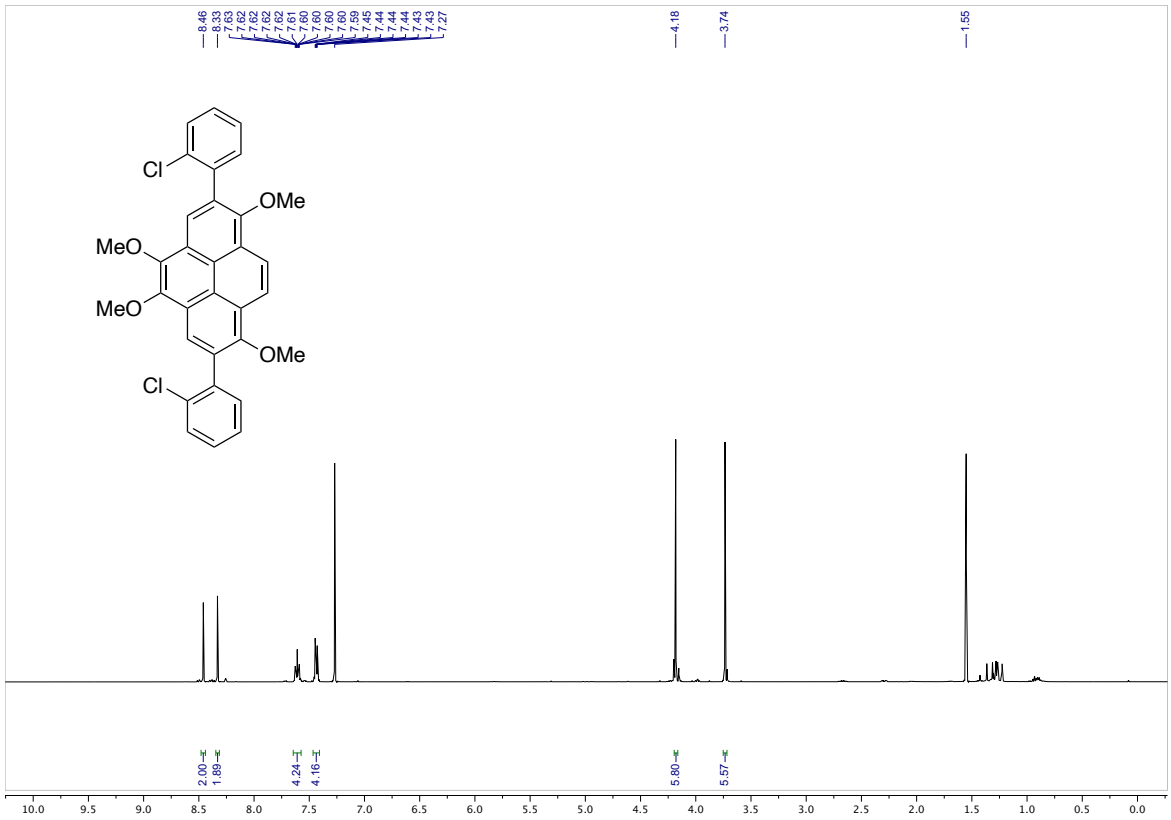
8.46
8.33
7.63
7.62
7.62
7.62
7.62
7.61
7.60
7.60
7.60
7.60
7.59
7.45
7.44
7.44
7.44
7.43
7.43
7.27
4.18
3.74
1.55
Cl
OMe
MeO
MeO
OMe
Cl
2.00
1.89
4.24
4.16
5.80
5.57
10.0
9.5
9.0
8.5
8.0
7.5
7.0
6.5
6.0
5.5
5.0
4.5
4.0
3.5
3.0
2.5
2.0
1.5
1.0
0.5
0.0

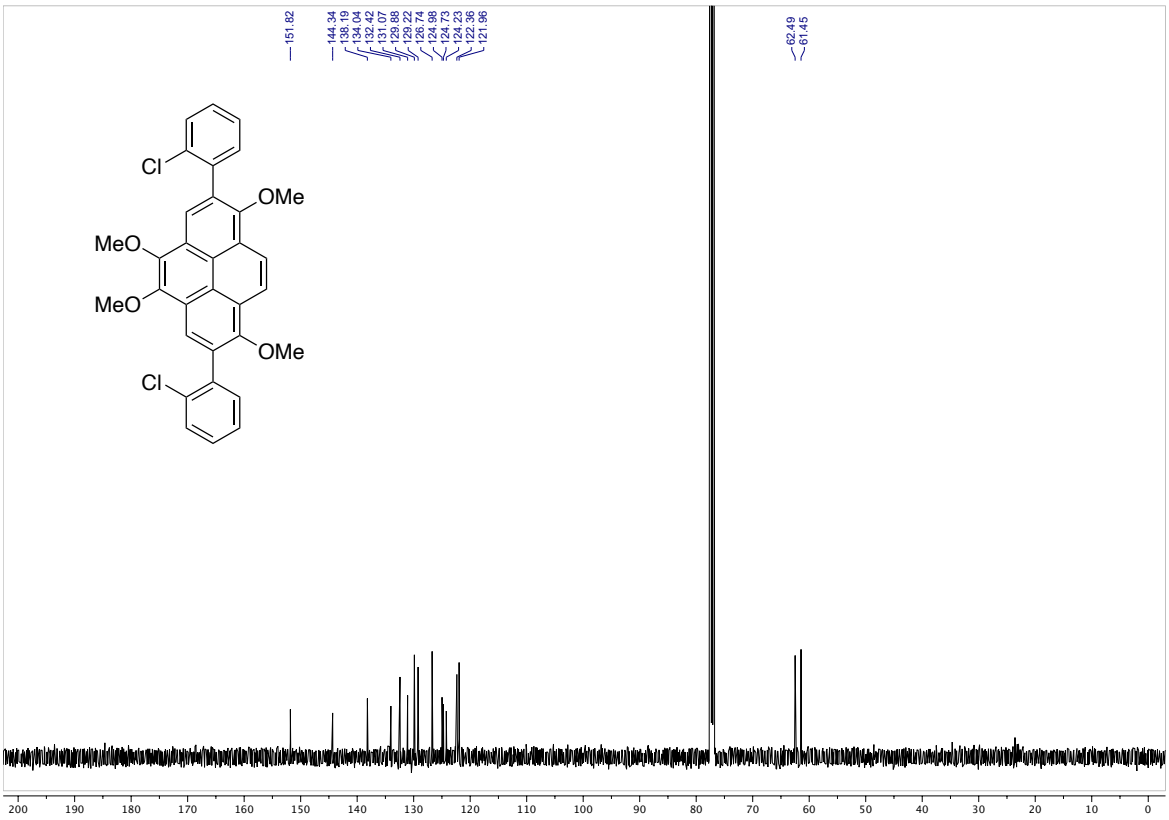
151.82
144.34
138.19
134.04
132.42
131.07
129.88
129.22
128.74
124.98
124.73
124.23
122.36
121.96
62.49
61.45
Cl
OMe
MeO
MeO
OMe
Cl
200
190
180
170
160
150
140
130
120
110
100
90
80
70
60
50
40
30
20
10
0

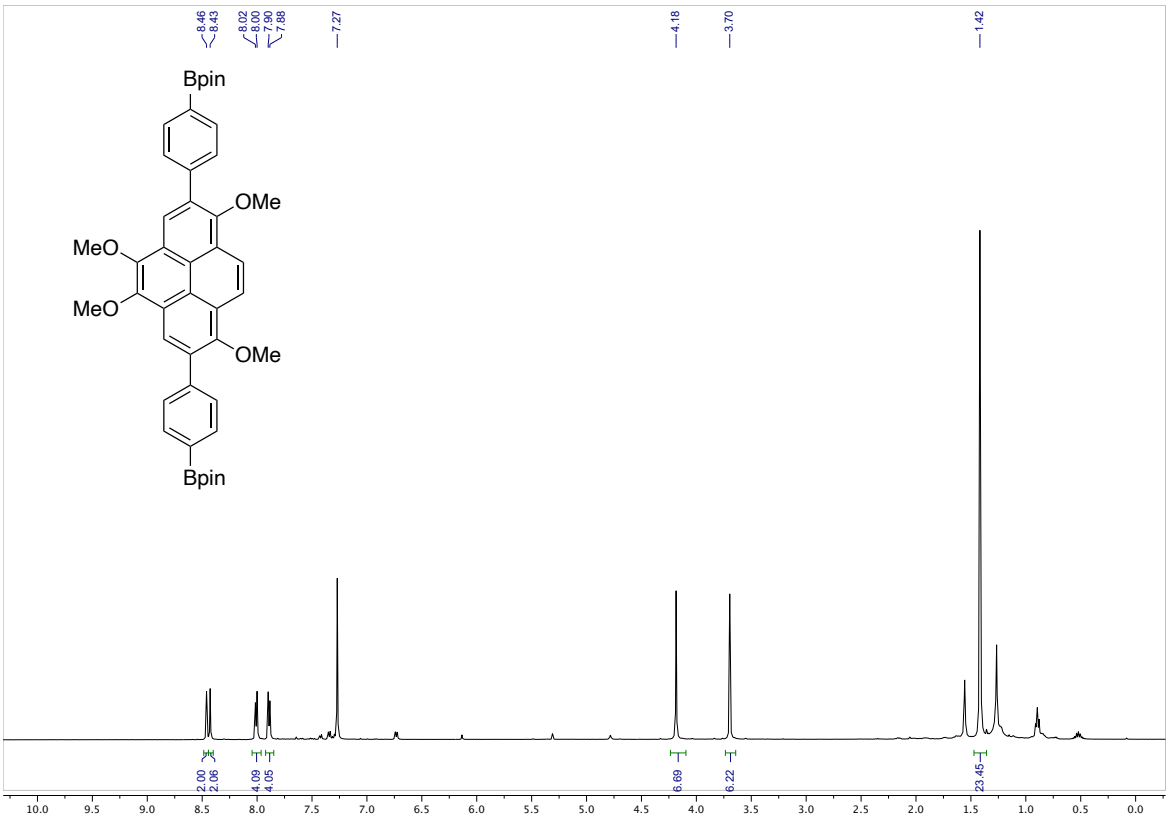
8.46
8.43
8.02
8.00
7.90
7.88
7.27
4.18
3.70
1.42
Bpin
OMe
MeO
MeO
OMe
Bpin
2.00
2.06
4.09
4.05
6.69
6.22
23.45
10.0
9.5
9.0
8.5
8.0
7.5
7.0
6.5
6.0
5.5
5.0
4.5
4.0
3.5
3.0
2.5
2.0
1.5
1.0
0.5
0.0

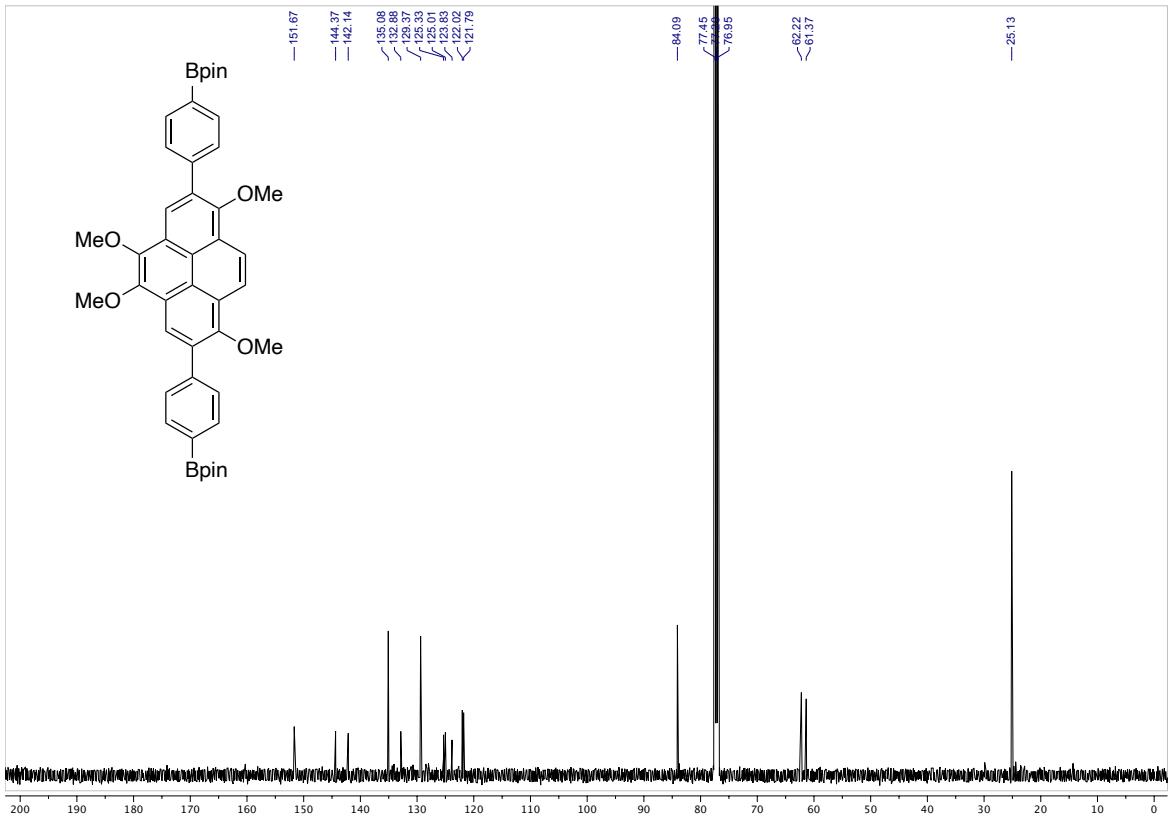
151.67
144.37
142.14
135.08
132.88
129.37
125.33
125.01
123.83
122.02
121.79
84.09
77.45
76.95
62.22
61.37
25.13
Bpin
OMe
MeO
MeO
OMe
Bpin

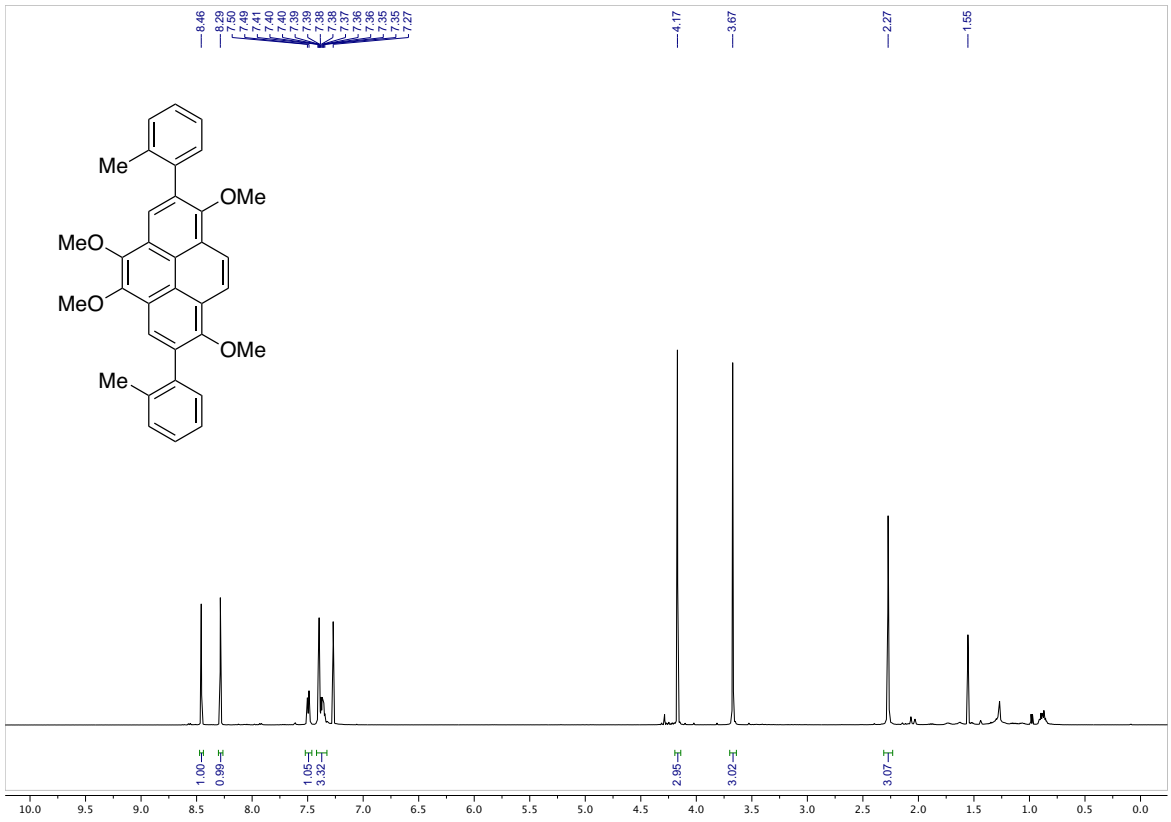
8.46
8.29
7.50
7.49
7.41
7.40
7.40
7.39
7.39
7.38
7.38
7.37
7.36
7.36
7.35
7.35
7.27
4.17
3.67
2.27
1.55
Me
OMe
MeO
MeO
OMe
Me
1.00
0.99
1.05
3.32
2.95
3.02
3.07

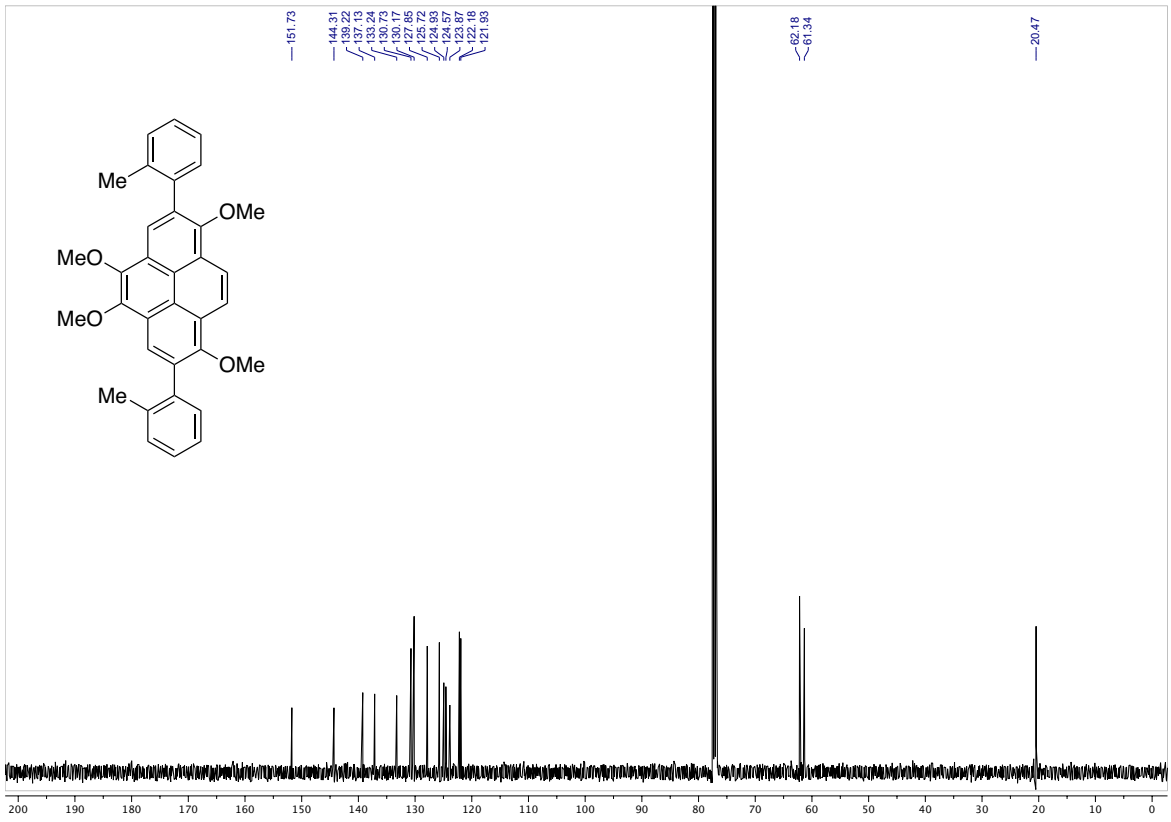
151.73
144.31
139.22
137.13
133.24
130.73
130.17
127.85
125.72
124.93
124.57
123.87
122.18
121.93
62.18
61.34
20.47
Me
OMe
MeO
MeO
OMe
Me
200
190
180
170
160
150
140
130
120
110
100
90
80
70
60
50
40
30
20
10
0

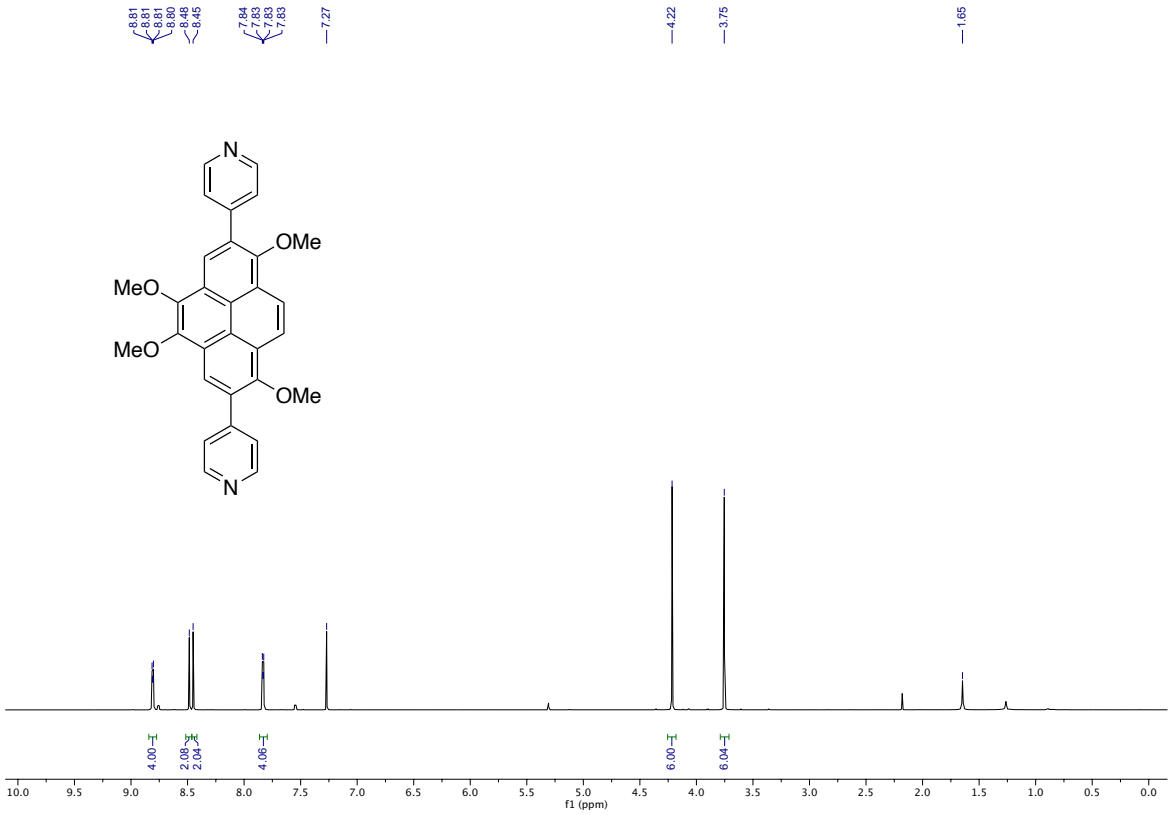
8.81
8.81
8.81
8.80
8.48
8.45
7.84
7.83
7.83
7.83
7.27
4.22
3.75
1.65
N
OMe
MeO
MeO
OMe
N
4.00
2.08
2.04
4.06
6.00
6.04
10.0
9.5
9.0
8.5
8.0
7.5
7.0
6.5
6.0
5.5
5.0
4.5
4.0
3.5
3.0
2.5
2.0
1.5
1.0
0.5
0.0
f1 (ppm)

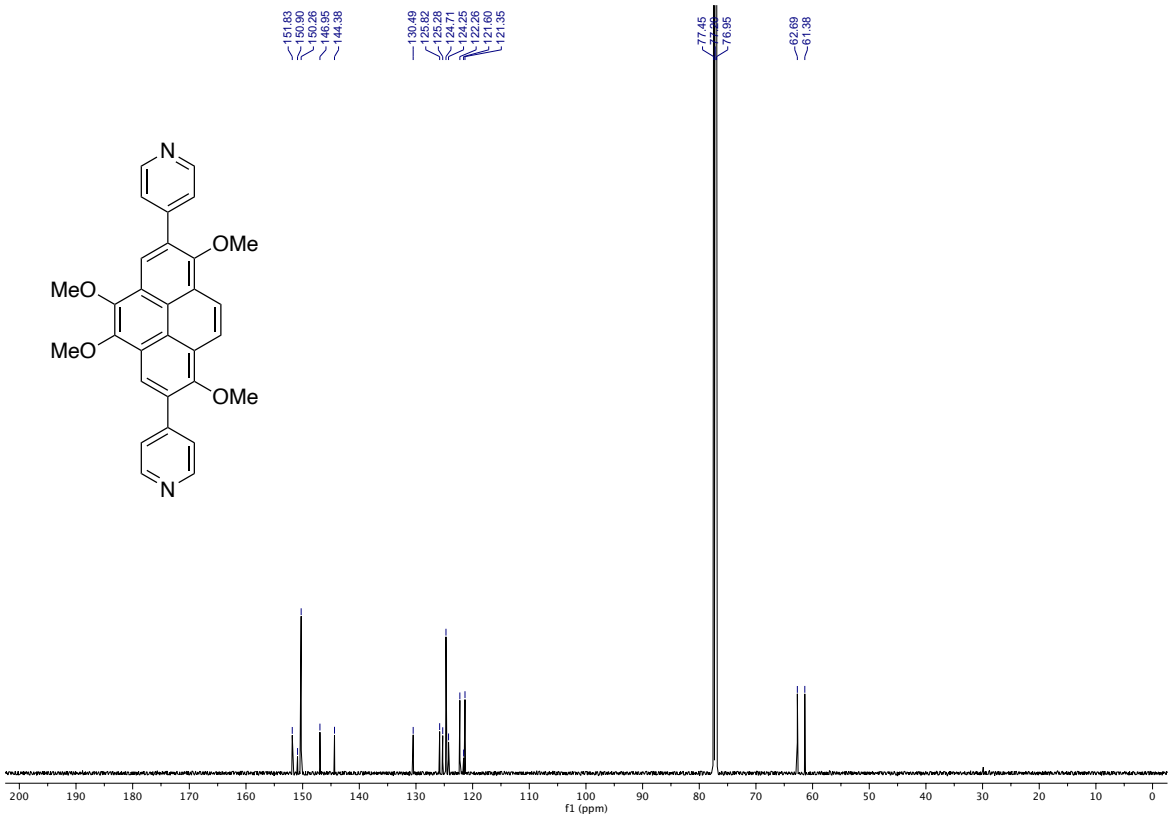
151.83
150.90
150.26
146.65
144.38
130.49
125.82
125.28
124.71
124.25
122.26
121.60
121.35
77.45
77.20
76.95
62.69
61.38
N
OMe
MeO
MeO
OMe
N
200
190
180
170
160
150
140
130
120
110
100
90
80
70
60
50
40
30
20
10
0
f1 (ppm)

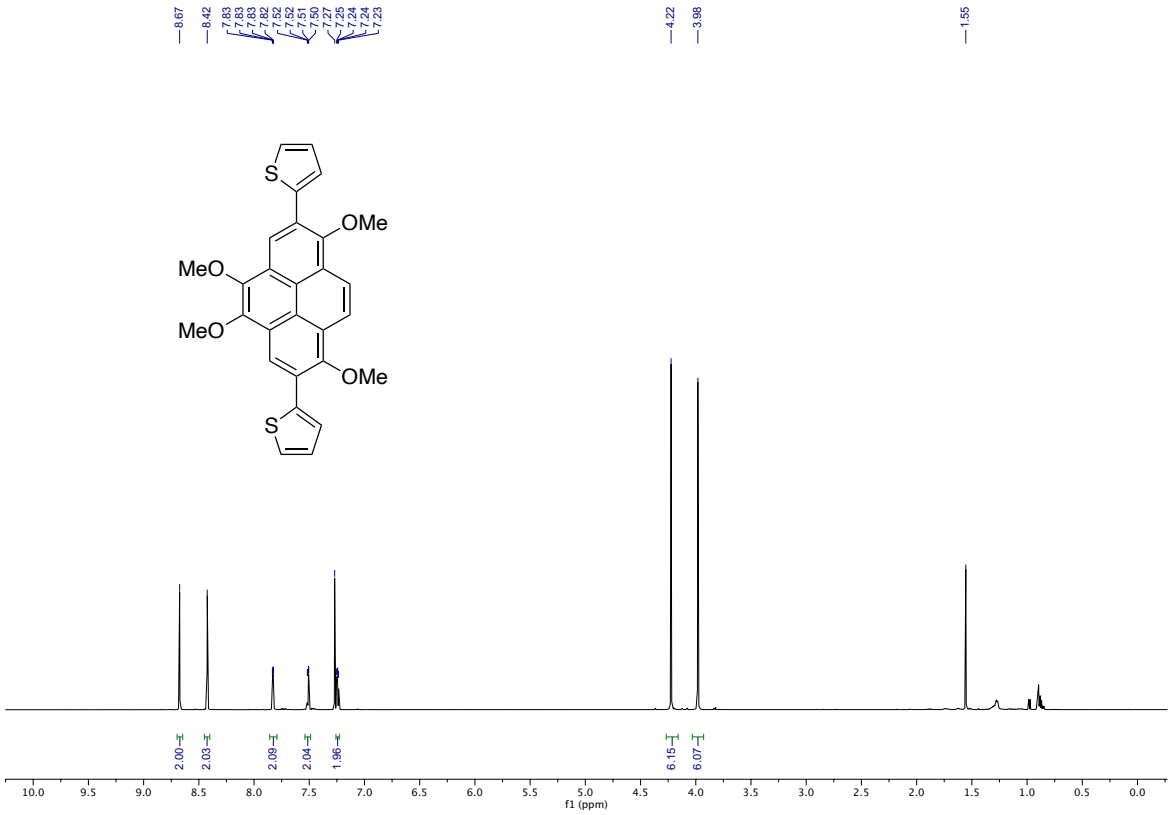
8.67
8.42
7.83
7.83
7.83
7.82
7.52
7.52
7.51
7.50
7.27
7.25
7.24
7.24
7.23
4.22
3.98
1.55
S
OMe
MeO
MeO
OMe
S
2.00
2.03
2.09
2.04
1.96
6.15
6.07
10.0
9.5
9.0
8.5
8.0
7.5
7.0
6.5
6.0
5.5
5.0
4.5
4.0
3.5
3.0
2.5
2.0
1.5
1.0
0.5
0.0
f1 (ppm)

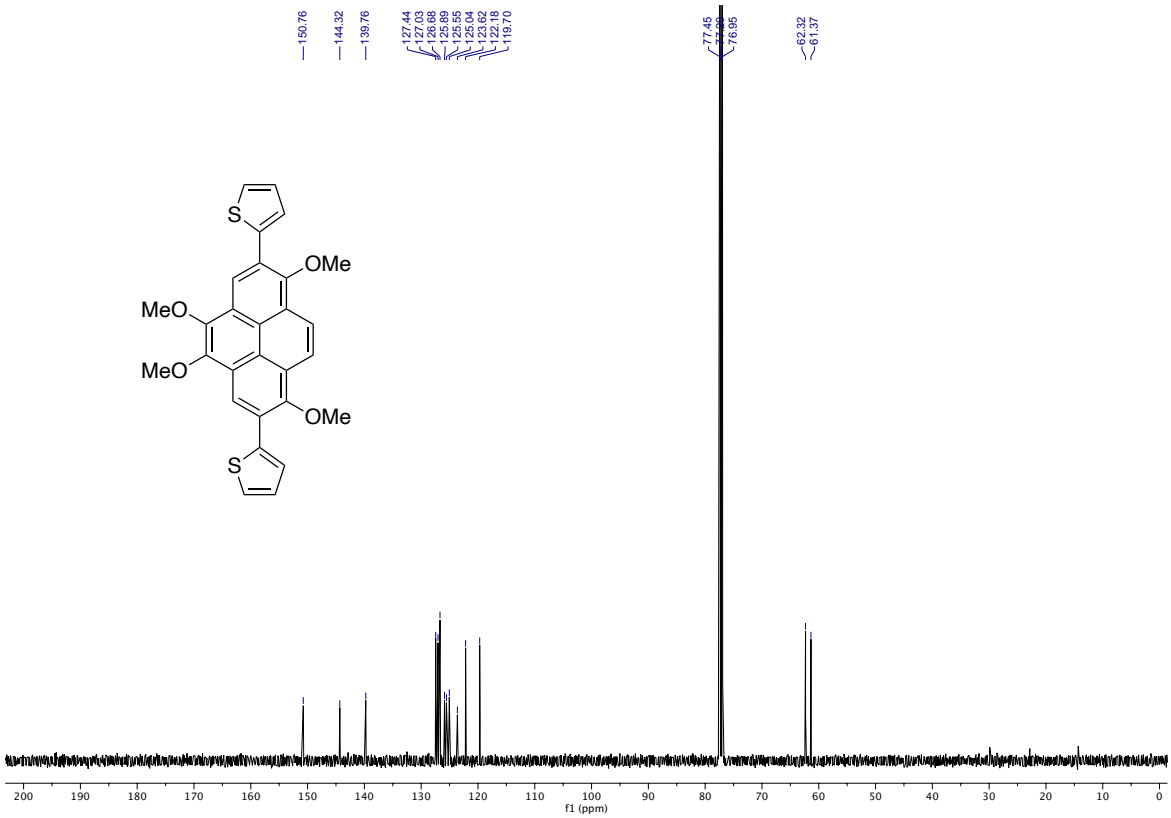
150.76
144.32
139.76
127.44
127.03
126.68
125.89
125.55
125.04
123.62
122.18
119.70
77.45
77.00
76.95
62.32
61.37
S
OMe
MeO
MeO
OMe
S
200
190
180
170
160
150
140
130
120
110
100
90
80
70
60
50
40
30
20
10
0
f1 (ppm)

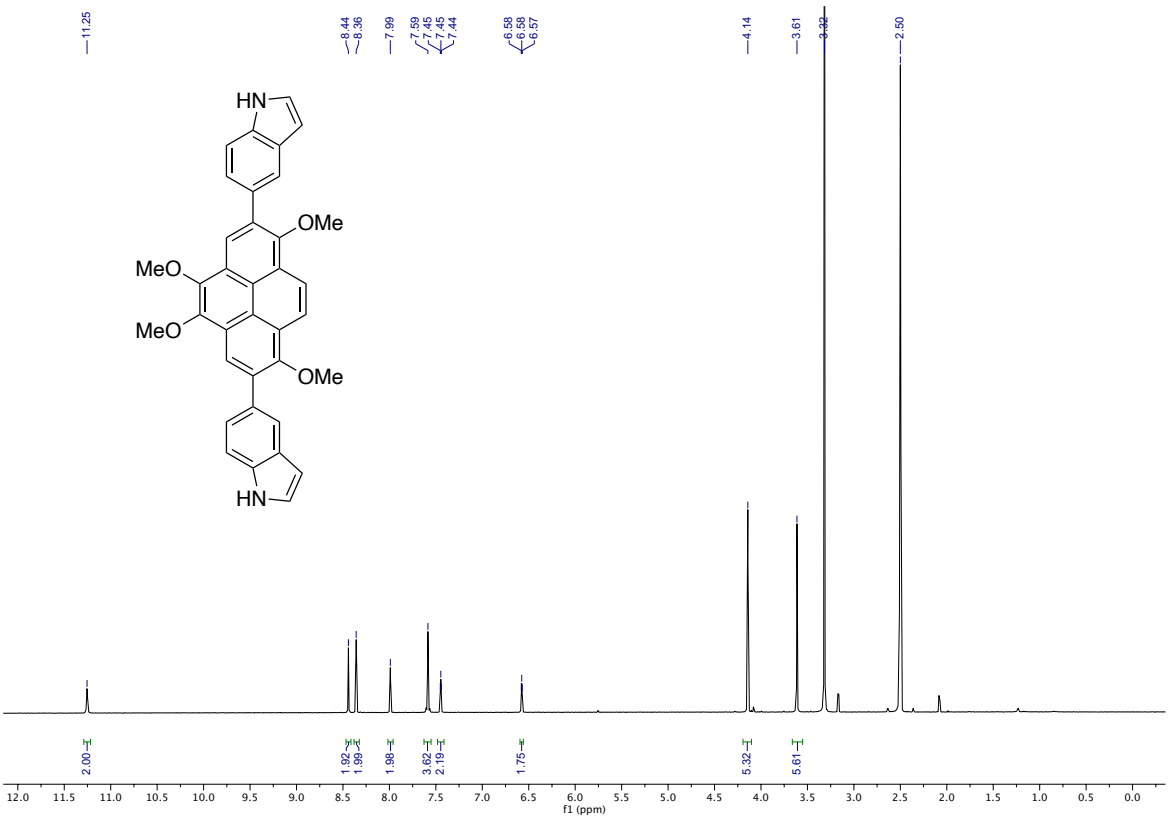
11.25
8.44
8.36
7.99
7.59
7.45
7.45
7.44
6.58
6.58
6.57
4.14
3.61
3.32
2.50
HN
OMe
MeO
MeO
OMe
HN
2.00
1.92
1.99
1.98
3.62
2.19
1.75
5.32
5.61
f1 (ppm)

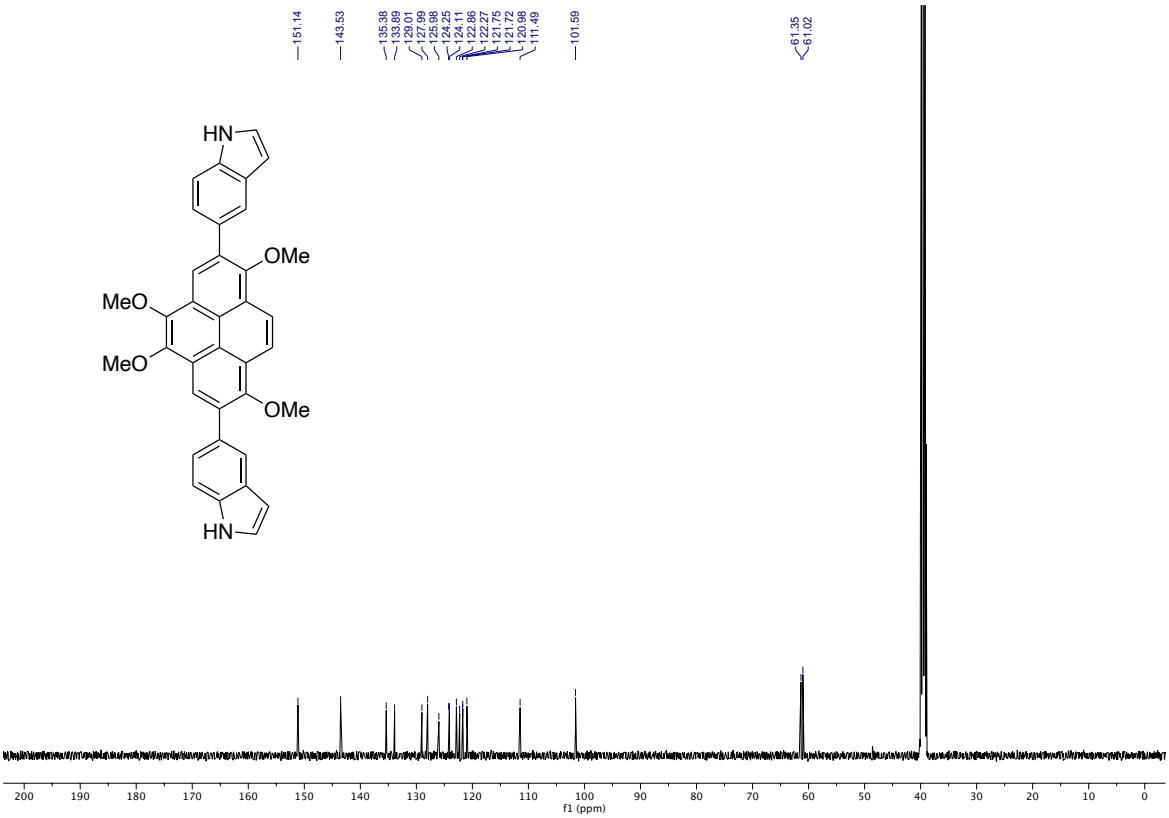
151.14
143.53
135.38
133.89
129.01
127.88
125.88
124.25
124.11
122.86
122.27
121.75
121.72
120.98
111.49
101.59
61.35
61.02
HN
OMe
MeO
MeO
OMe
HN
f1 (ppm)

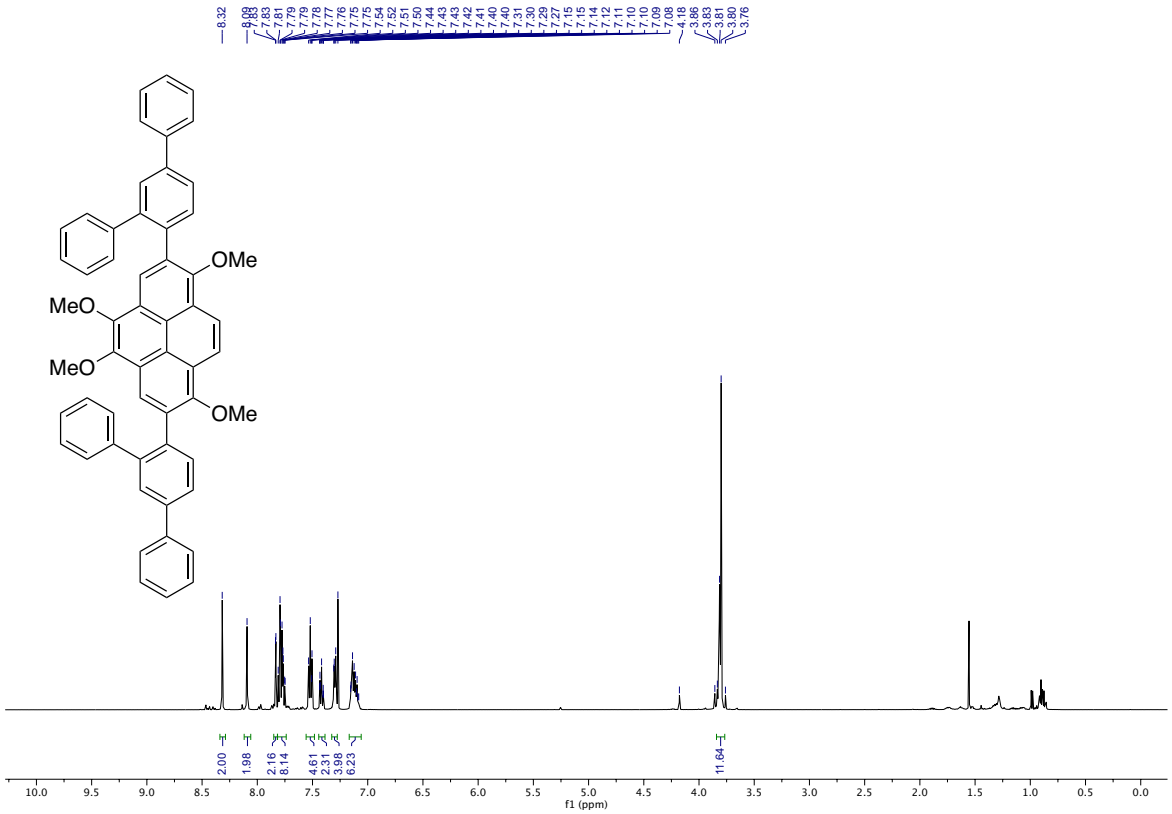
8.32
7.83
7.81
7.79
7.78
7.77
7.76
7.75
7.54
7.52
7.51
7.50
7.44
7.43
7.42
7.41
7.40
7.31
7.30
7.29
7.27
7.15
7.14
7.12
7.11
7.10
7.09
7.08
4.18
3.86
3.83
3.81
3.80
3.76
OMe
MeO
MeO
OMe
2.00
1.98
2.16
8.14
4.61
2.31
3.98
6.23
11.64
f1 (ppm)

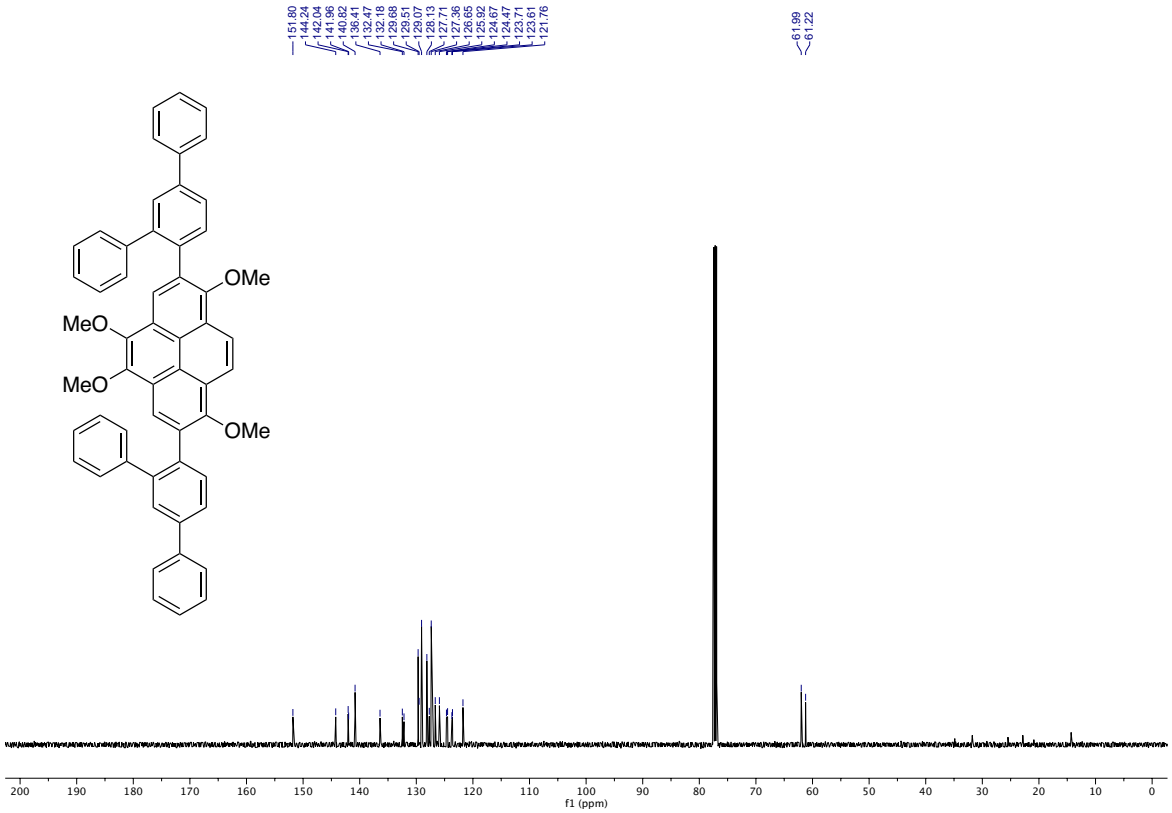
151.80
144.24
142.04
141.96
140.82
138.41
132.47
132.18
129.68
129.51
129.07
128.13
127.71
127.36
126.65
125.92
124.67
124.47
123.71
123.61
121.76
61.99
61.22
OMe
MeO
MeO
OMe
f1 (ppm)

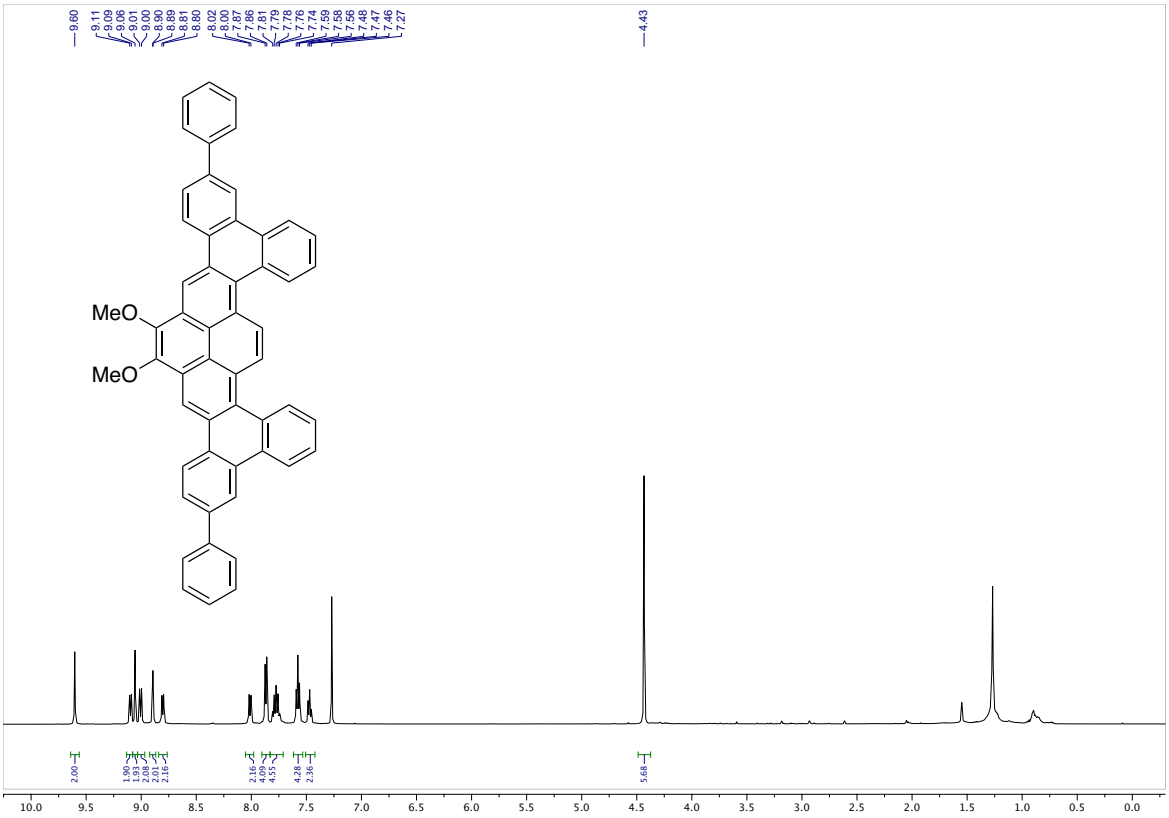
9.60
9.11
9.09
9.06
9.01
9.00
8.90
8.89
8.81
8.80
8.02
8.00
7.87
7.86
7.81
7.79
7.78
7.76
7.74
7.59
7.58
7.56
7.48
7.47
7.46
7.27
4.43
MeO
MeO
2.00
1.90
1.93
2.08
2.01
2.16
2.16
4.09
4.55
4.28
2.36
5.68
10.0
9.5
9.0
8.5
8.0
7.5
7.0
6.5
6.0
5.5
5.0
4.5
4.0
3.5
3.0
2.5
2.0
1.5
1.0
0.5
0.0

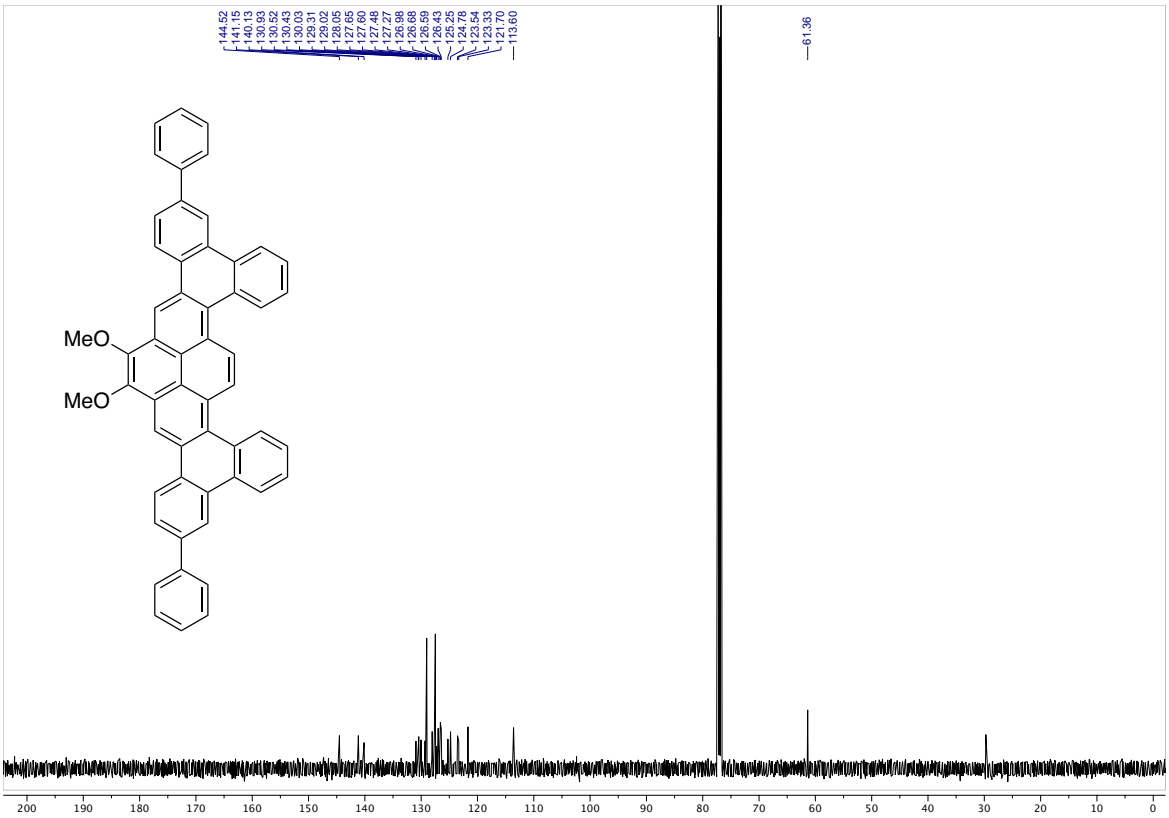
144.52
141.15
140.13
130.93
130.52
130.43
130.03
129.31
129.02
128.85
127.65
127.60
127.48
127.27
126.98
126.68
126.59
126.43
125.25
124.78
123.54
123.33
121.70
113.60
61.36
MeO
MeO
200
190
180
170
160
150
140
130
120
110
100
90
80
70
60
50
40
30
20
10
0

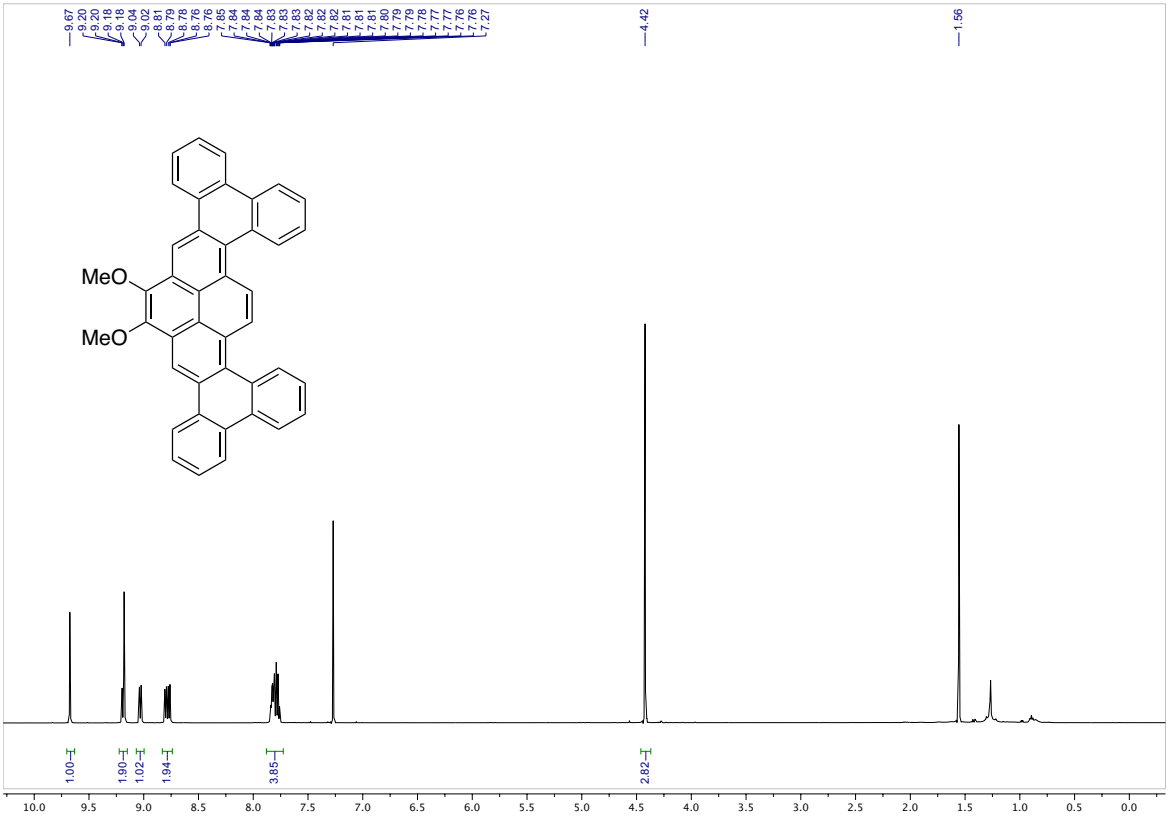
9.67
9.20
9.20
9.18
9.18
9.04
9.02
8.81
8.79
8.78
8.76
8.76
7.85
7.84
7.84
7.84
7.83
7.83
7.82
7.82
7.81
7.81
7.81
7.80
7.79
7.79
7.78
7.77
7.77
7.76
7.76
7.27
4.42
1.56
MeO
MeO
1.00
1.90
1.02
1.94
3.85
2.82
10.0
9.5
9.0
8.5
8.0
7.5
7.0
6.5
6.0
5.5
5.0
4.5
4.0
3.5
3.0
2.5
2.0
1.5
1.0
0.5
0.0

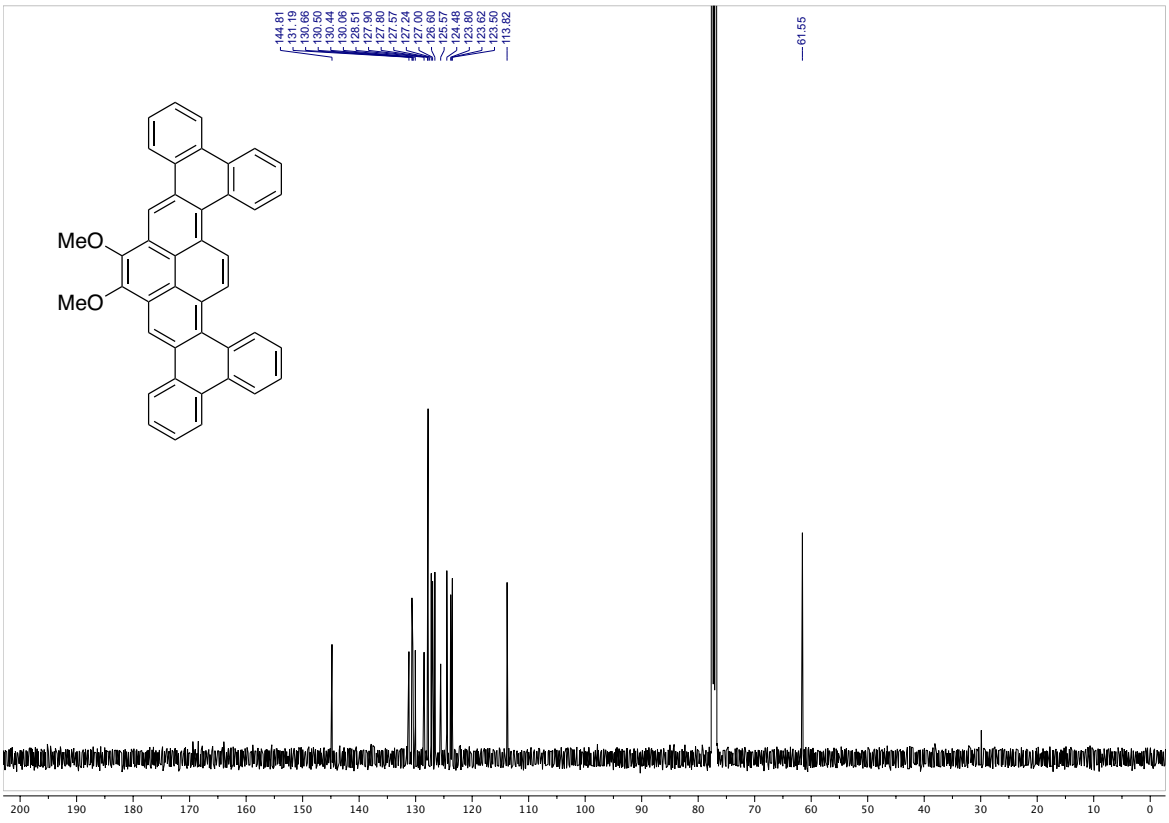
144.81
131.19
130.66
130.50
130.44
130.06
128.51
127.90
127.80
127.57
127.24
127.00
126.60
125.57
124.48
123.80
123.62
123.50
113.82
61.55
MeO
MeO
200
190
180
170
160
150
140
130
120
110
100
90
80
70
60
50
40
30
20
10
0

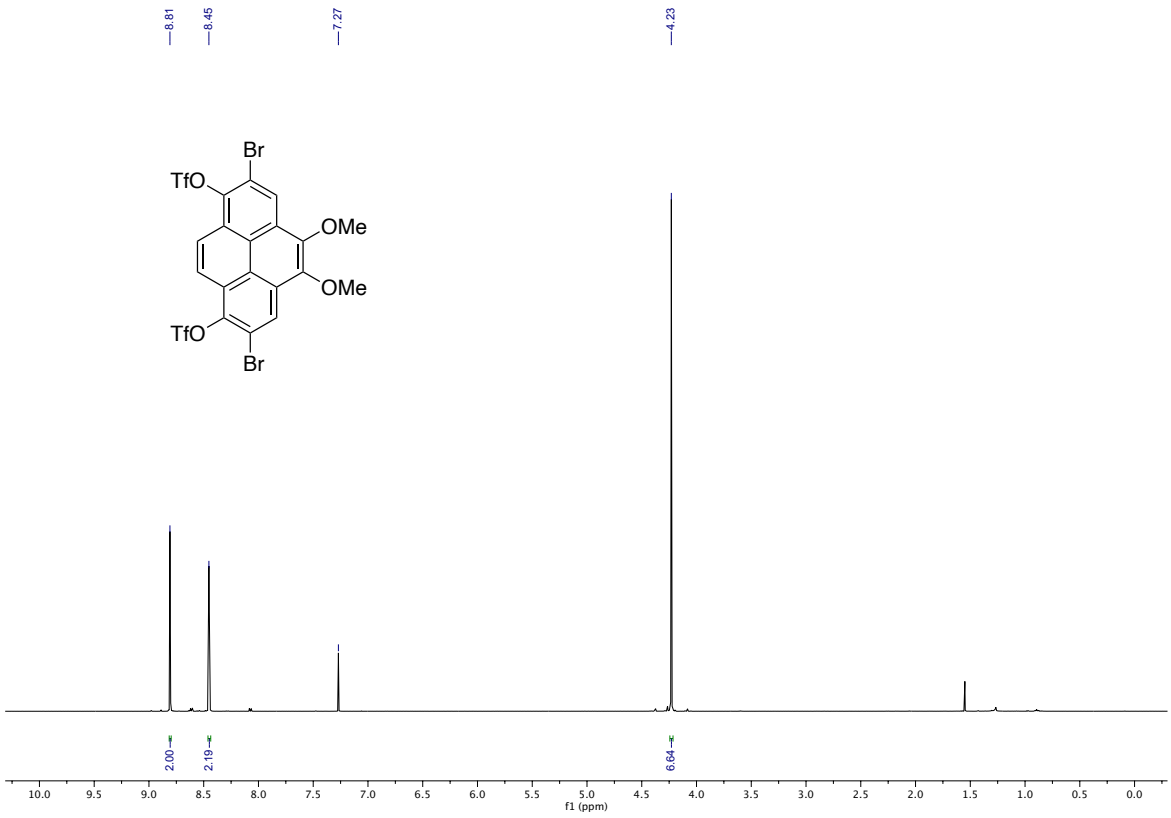
8.81
8.45
7.27
4.23
Br
TfO
OMe
OMe
TfO
Br
2.00
2.19
6.64
f1 (ppm)

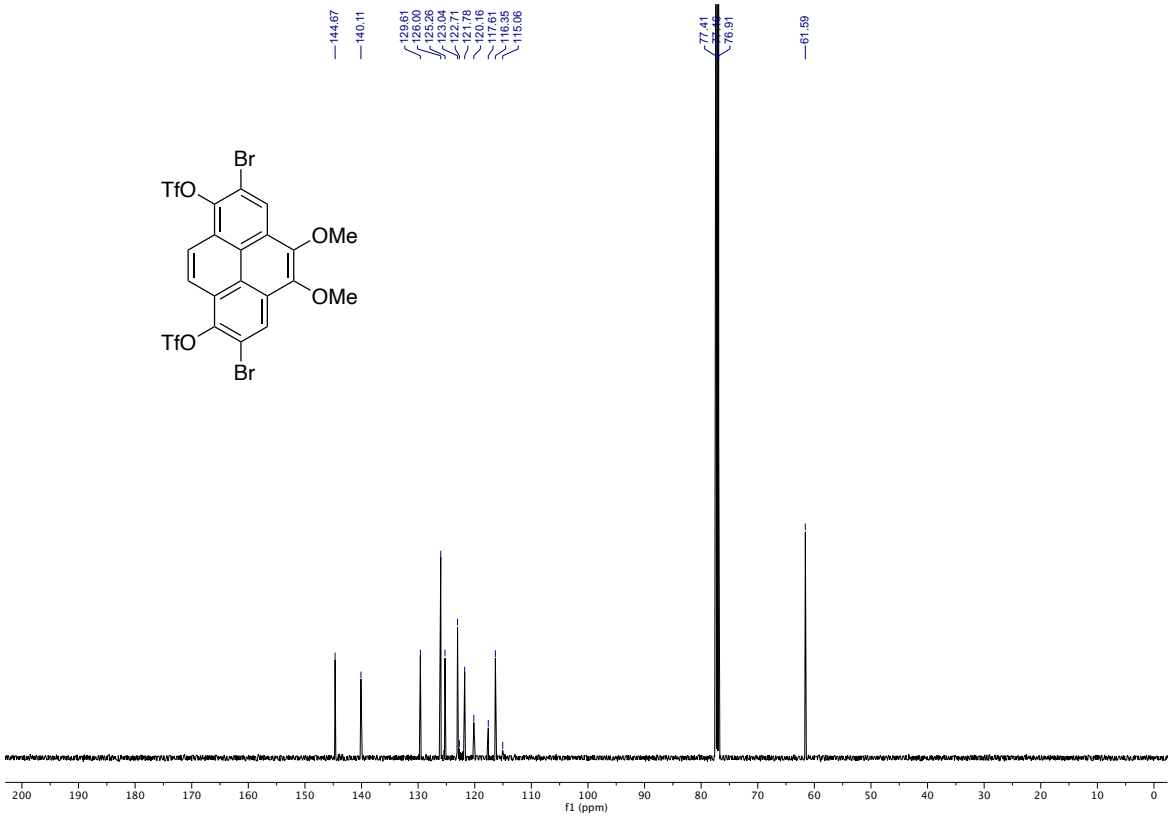
144.67
140.11
129.61
126.00
125.26
123.04
122.71
121.78
120.16
117.61
116.35
115.06
77.41
76.91
61.59
Br
TfO
OMe
OMe
TfO
Br
f1 (ppm)

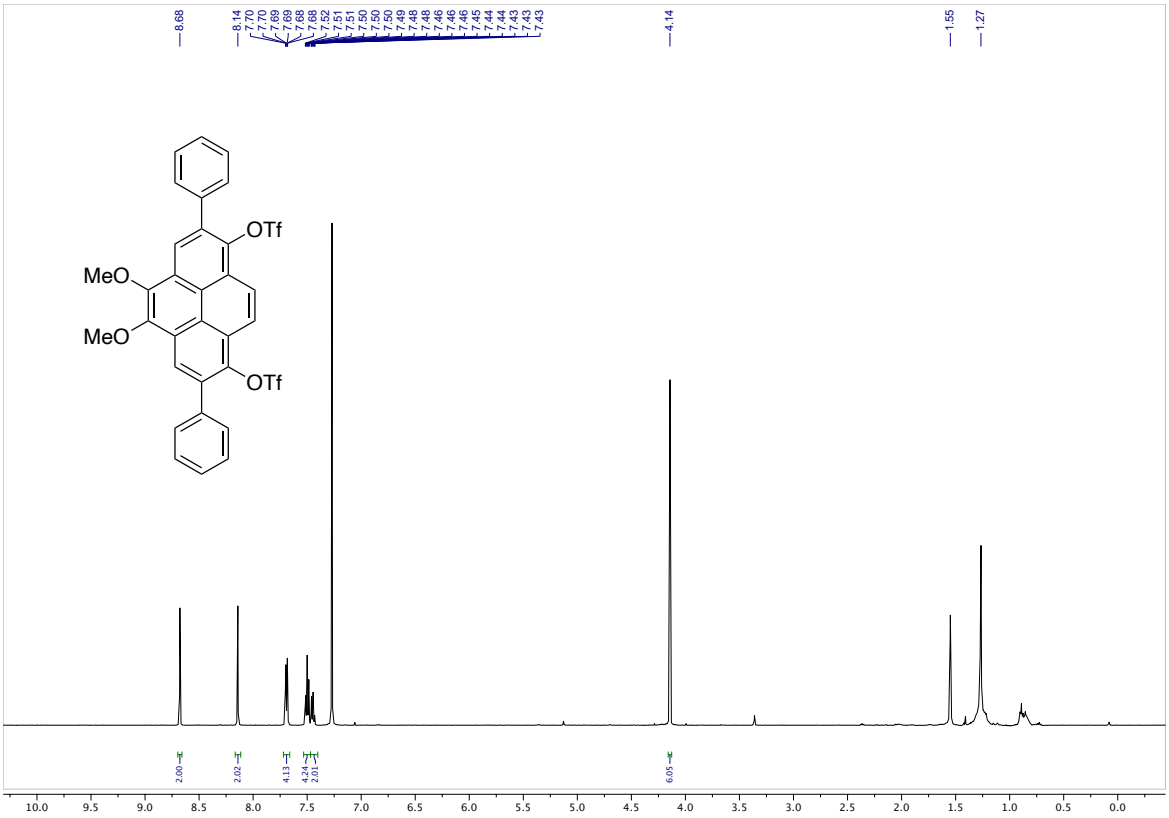
8.68
8.14
7.70
7.70
7.69
7.69
7.68
7.68
7.52
7.51
7.51
7.50
7.50
7.50
7.49
7.48
7.48
7.46
7.46
7.46
7.45
7.44
7.44
7.43
7.43
7.43
4.14
1.55
1.27
OTf
MeO
MeO
OTf
2.00
2.02
4.13
4.24
2.01
6.05
10.0
9.5
9.0
8.5
8.0
7.5
7.0
6.5
6.0
5.5
5.0
4.5
4.0
3.5
3.0
2.5
2.0
1.5
1.0
0.5
0.0

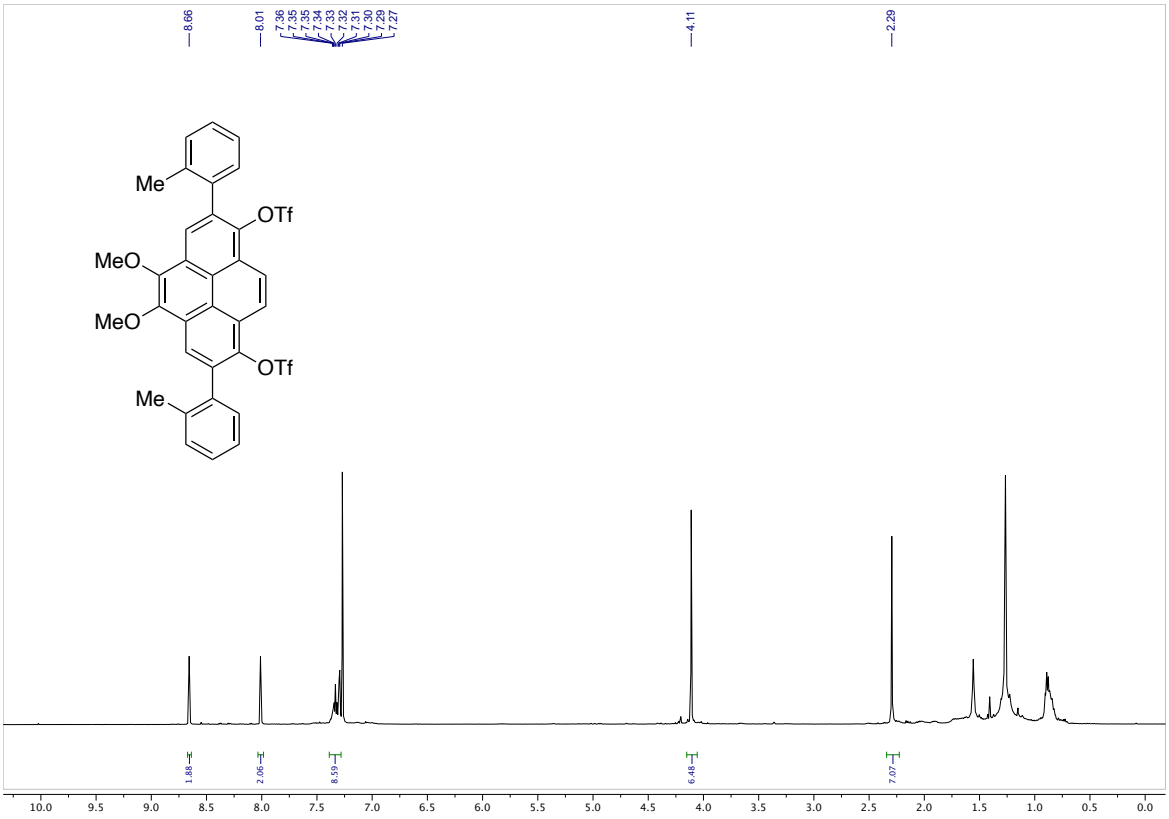
8.66
8.01
7.36
7.35
7.35
7.34
7.33
7.32
7.31
7.30
7.29
7.27
4.11
2.29
Me
OTf
MeO
MeO
OTf
Me
1.88
2.06
8.59
6.48
7.07
10.0
9.5
9.0
8.5
8.0
7.5
7.0
6.5
6.0
5.5
5.0
4.5
4.0
3.5
3.0
2.5
2.0
1.5
1.0
0.5
0.0

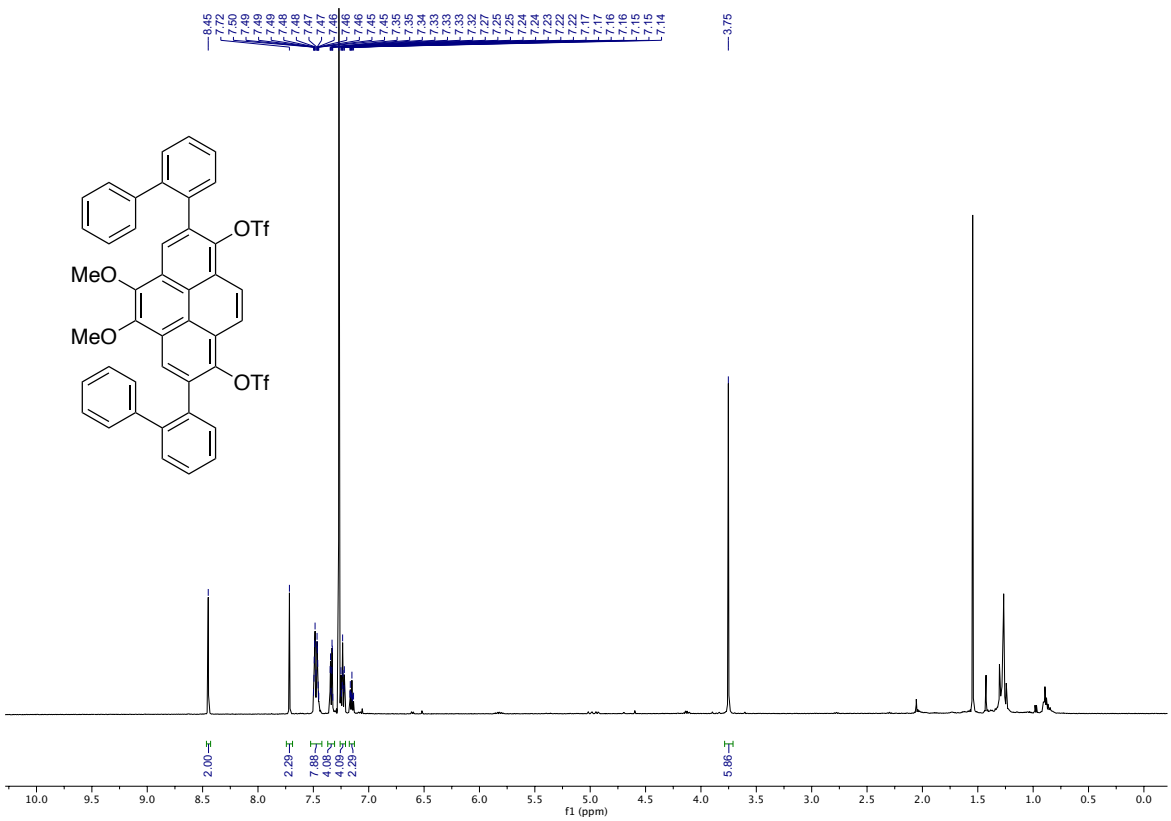
OTf
MeO
MeO
OTf
f1 (ppm)

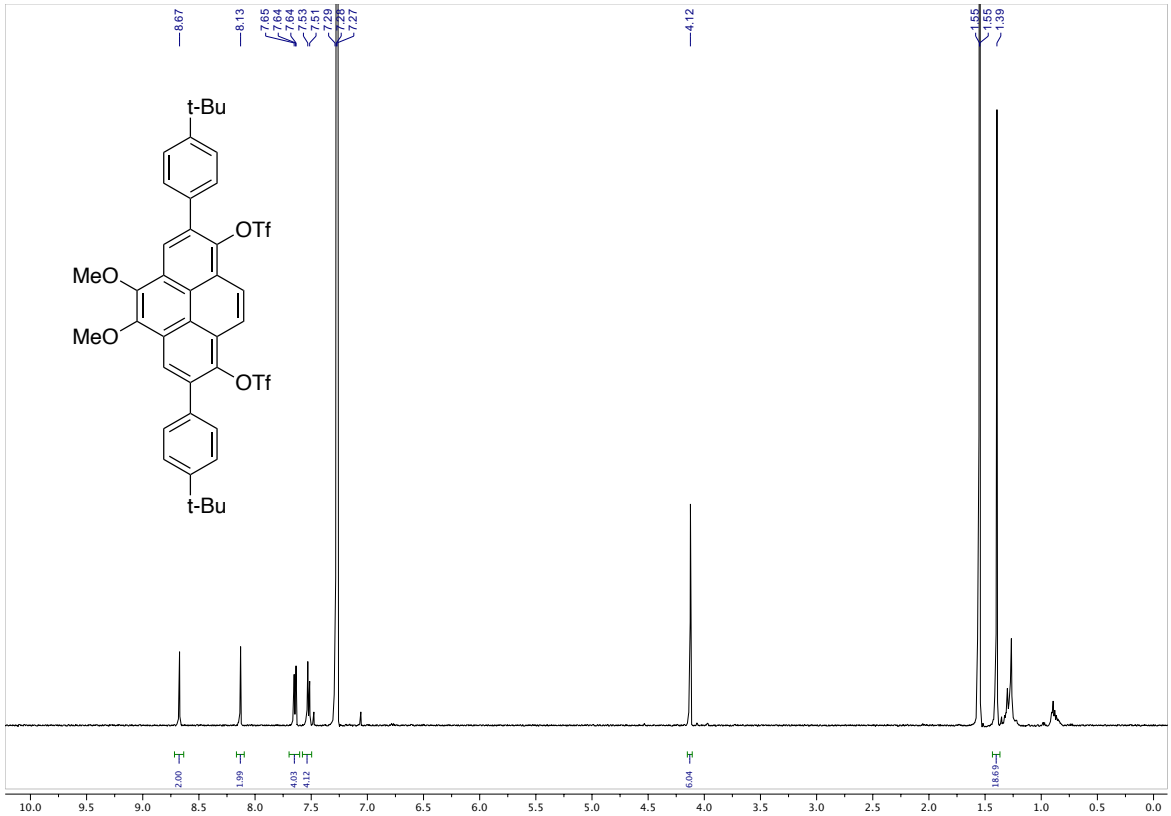
t-Bu
OTf
MeO
MeO
OTf
t-Bu

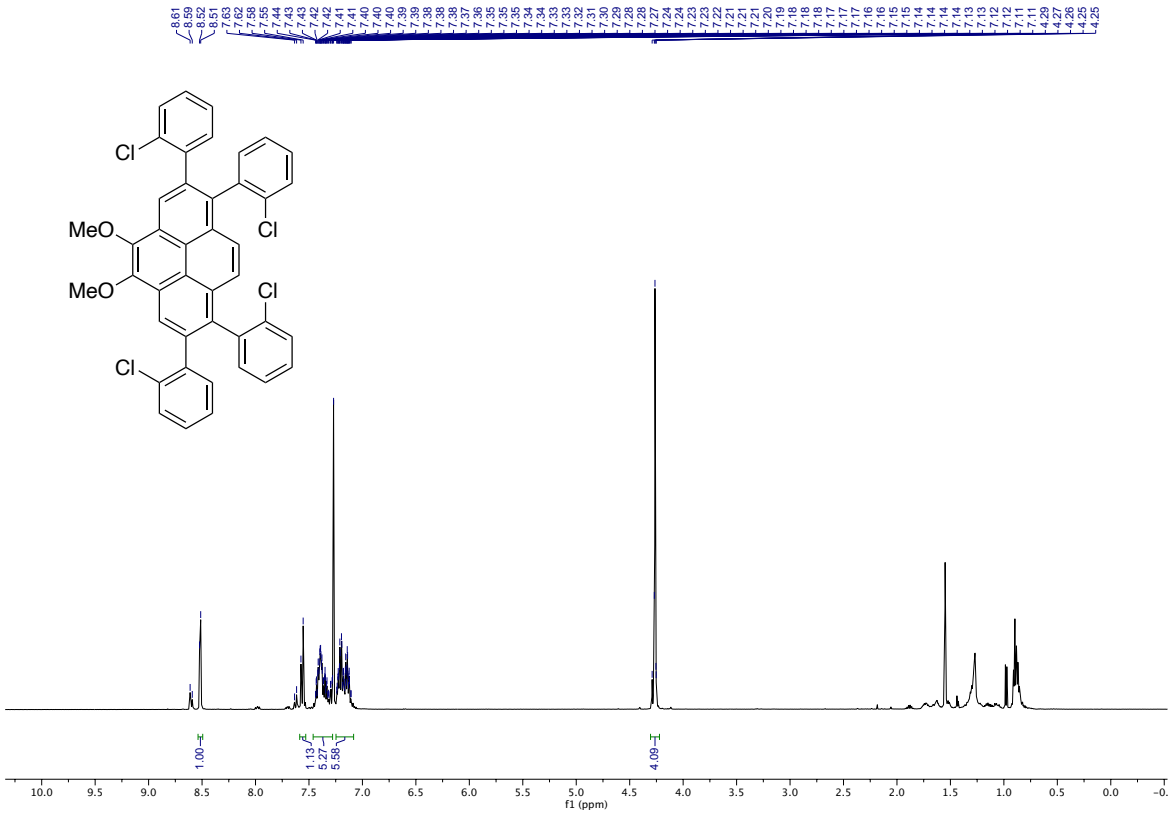
8.61
8.59
8.52
8.51
7.63
7.62
7.58
7.55
7.44
7.43
7.43
7.42
7.42
7.41
7.41
7.40
7.40
7.40
7.39
7.39
7.38
7.38
7.38
7.37
7.36
7.35
7.35
7.35
7.34
7.34
7.33
7.33
7.32
7.31
7.30
7.29
7.28
7.28
7.27
7.24
7.24
7.23
7.23
7.22
7.21
7.21
7.21
7.20
7.19
7.18
7.18
7.17
7.17
7.17
7.16
7.16
7.15
7.15
7.14
7.14
7.14
7.13
7.13
7.12
7.12
7.11
7.11
4.29
4.27
4.26
4.25
4.25
Cl
Cl
MeO
MeO
Cl
Cl
1.00
1.13
5.27
5.58
4.09
10.0
9.5
9.0
8.5
8.0
7.5
7.0
6.5
6.0
5.5
5.0
4.5
4.0
3.5
3.0
2.5
2.0
1.5
1.0
0.5
0.0
f1 (ppm)

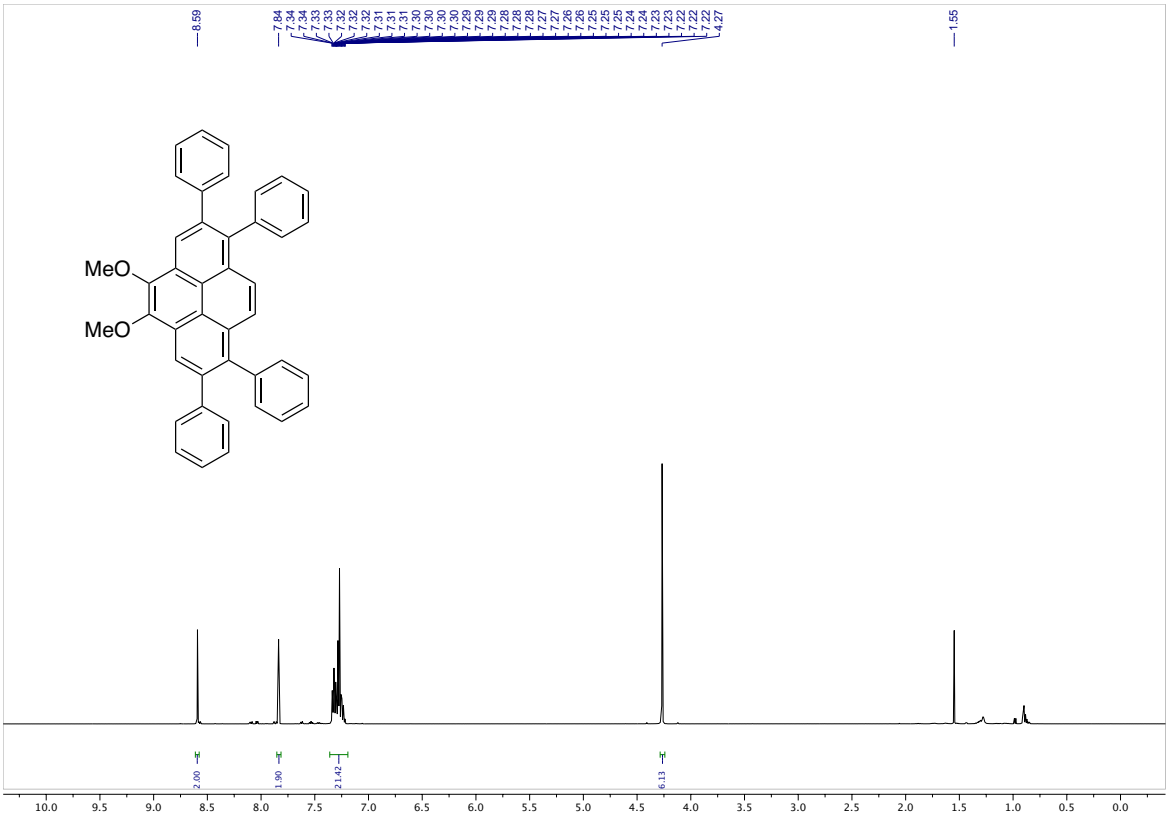
8.59
7.84
7.34
7.34
7.33
7.33
7.32
7.32
7.32
7.31
7.31
7.31
7.30
7.30
7.30
7.30
7.29
7.29
7.29
7.29
7.28
7.28
7.28
7.27
7.27
7.26
7.26
7.25
7.25
7.25
7.24
7.24
7.23
7.23
7.22
7.22
7.22
4.27
1.55
MeO
MeO
2.00
1.90
21.42
6.13
10.0
9.5
9.0
8.5
8.0
7.5
7.0
6.5
6.0
5.5
5.0
4.5
4.0
3.5
3.0
2.5
2.0
1.5
1.0
0.5
0.0

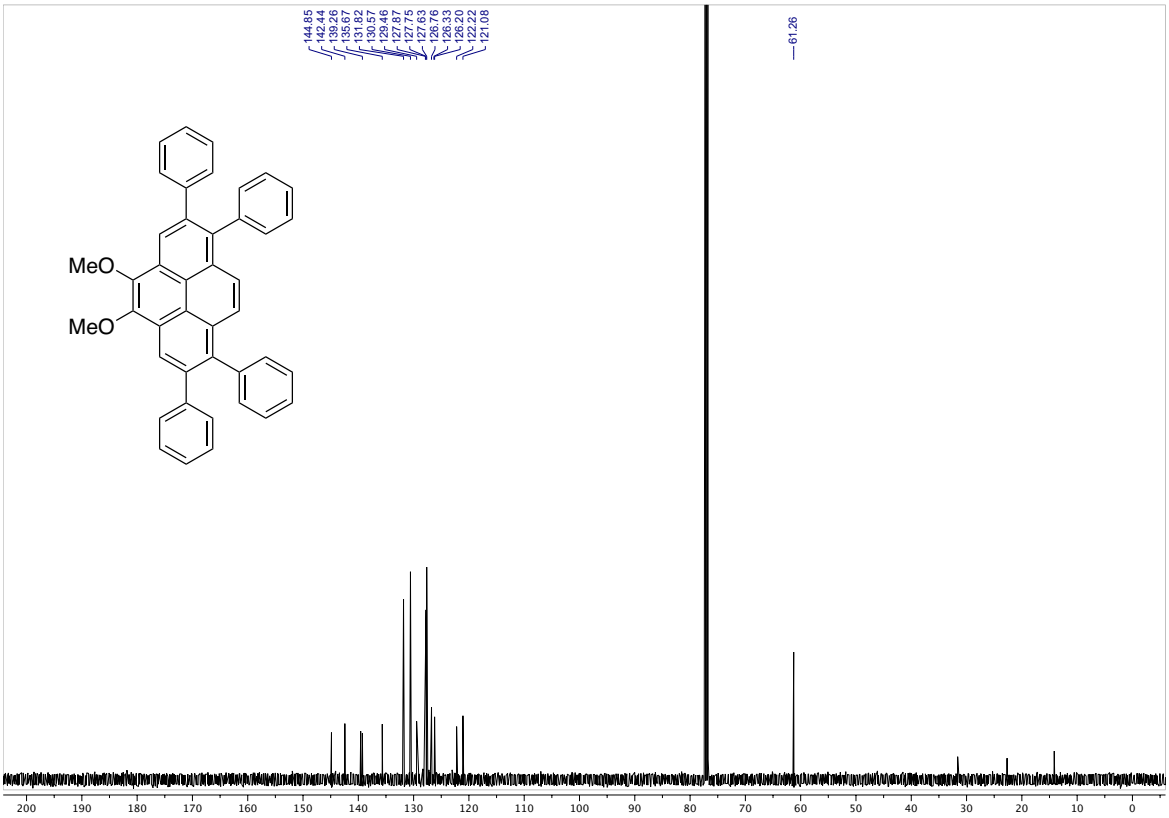
144.85
142.44
139.26
135.67
131.82
130.57
129.46
127.87
127.75
127.63
127.16
126.33
126.20
122.22
121.08
61.26
MeO
MeO
200
190
180
170
160
150
140
130
120
110
100
90
80
70
60
50
40
30
20
10
0

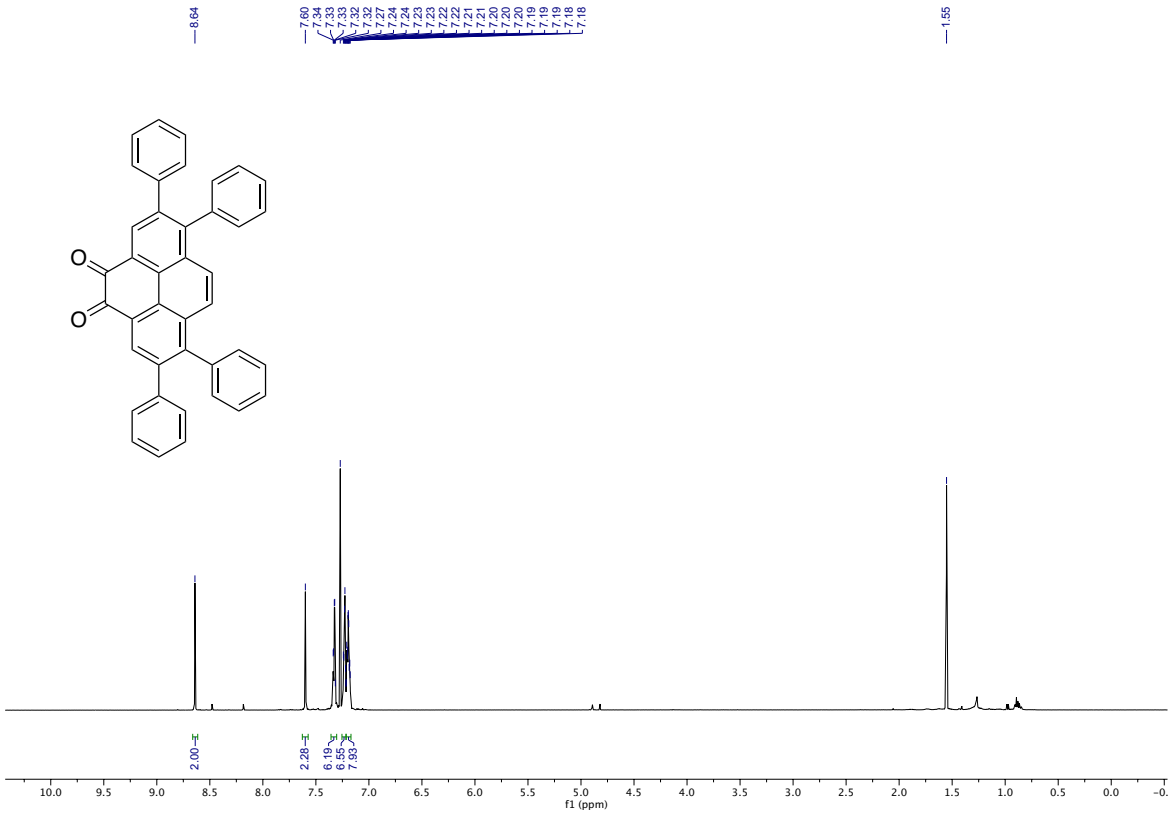
8.64
7.60
7.34
7.33
7.33
7.32
7.32
7.27
7.24
7.24
7.23
7.23
7.22
7.22
7.21
7.21
7.20
7.20
7.20
7.19
7.19
7.19
7.18
7.18
1.55
O
O
2.00
2.28
6.19
6.55
7.93
f1 (ppm)

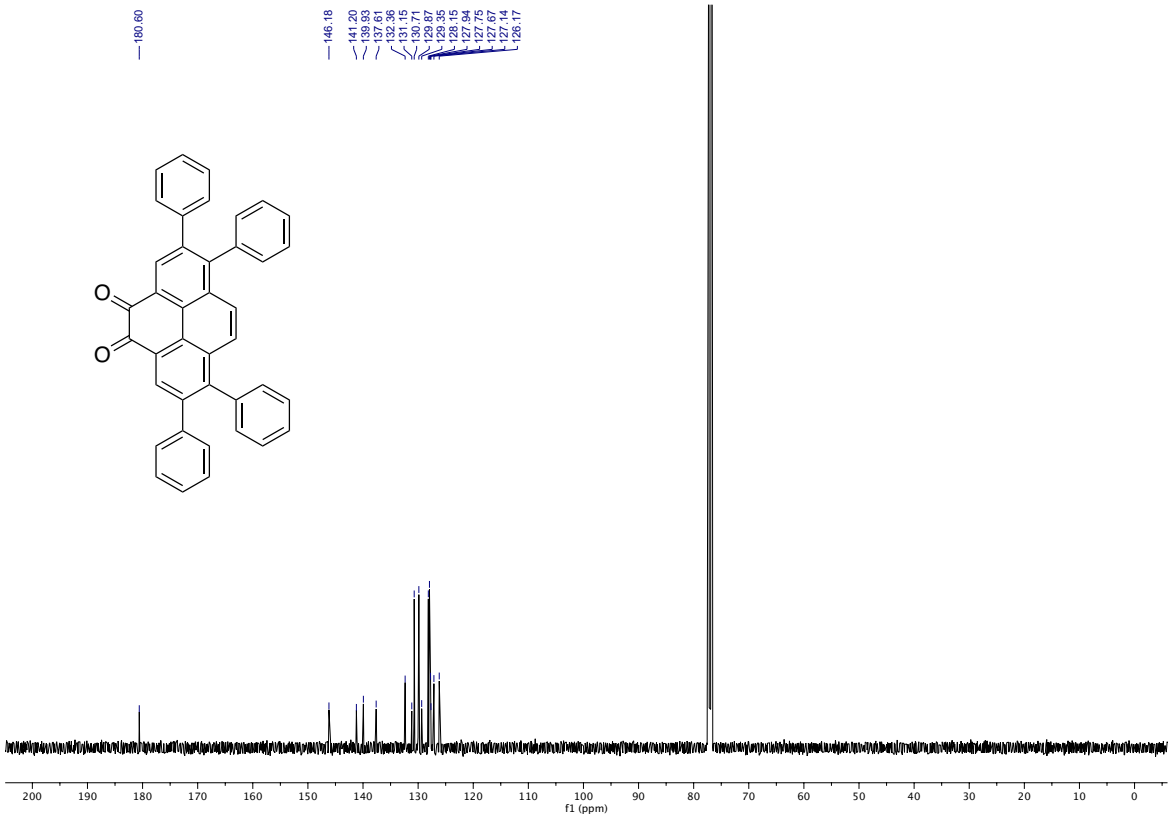
180.60
146.18
141.20
139.53
137.61
132.36
131.15
130.71
129.87
129.35
128.15
127.94
127.75
127.67
127.14
126.17
O
O
f1 (ppm)

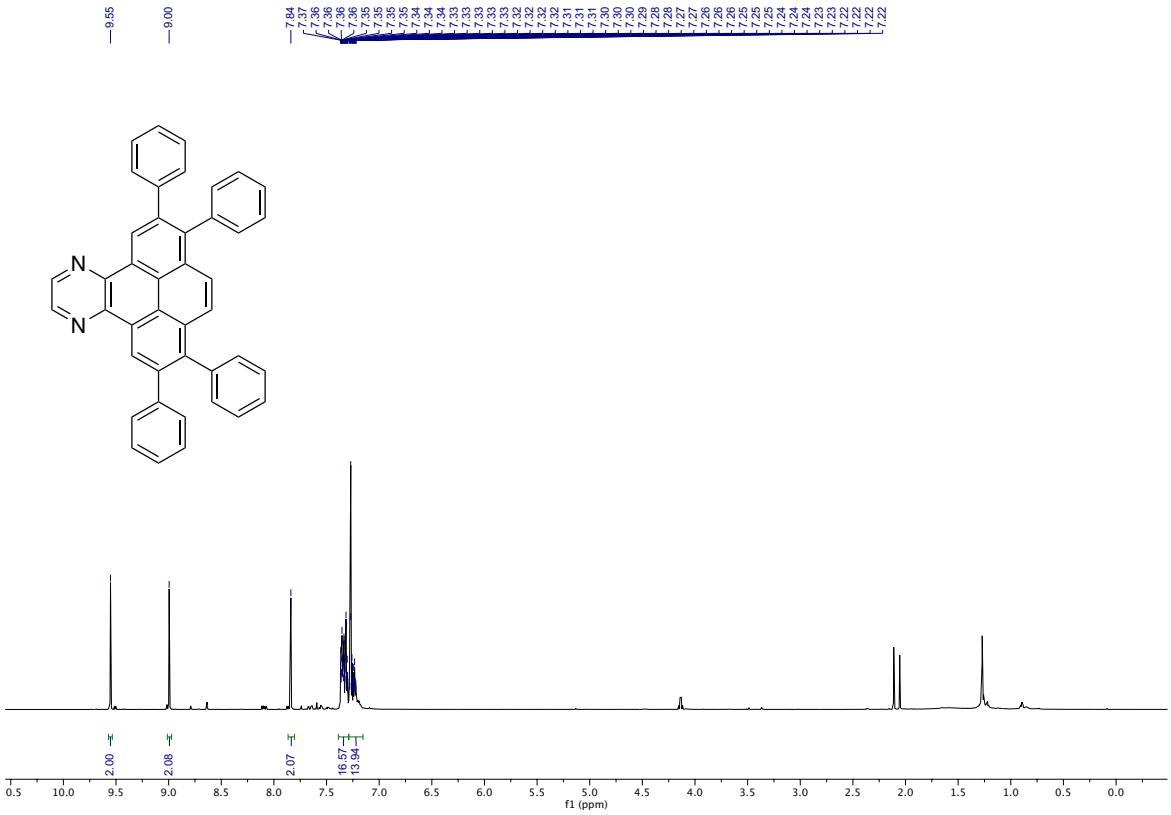
9.55
9.00
7.84
7.37
7.36
7.36
7.36
7.35
7.35
7.35
7.35
7.34
7.34
7.34
7.33
7.33
7.33
7.33
7.33
7.32
7.32
7.32
7.31
7.31
7.31
7.30
7.30
7.30
7.29
7.28
7.28
7.27
7.27
7.26
7.26
7.25
7.25
7.25
7.24
7.24
7.24
7.23
7.22
7.22
7.22
7.22
N
N
2.00
2.08
2.07
16.57
13.94
0.5
10.0
9.5
9.0
8.5
8.0
7.5
7.0
6.5
6.0
5.5
5.0
4.5
4.0
3.5
3.0
2.5
2.0
1.5
1.0
0.5
0.0
f1 (ppm)

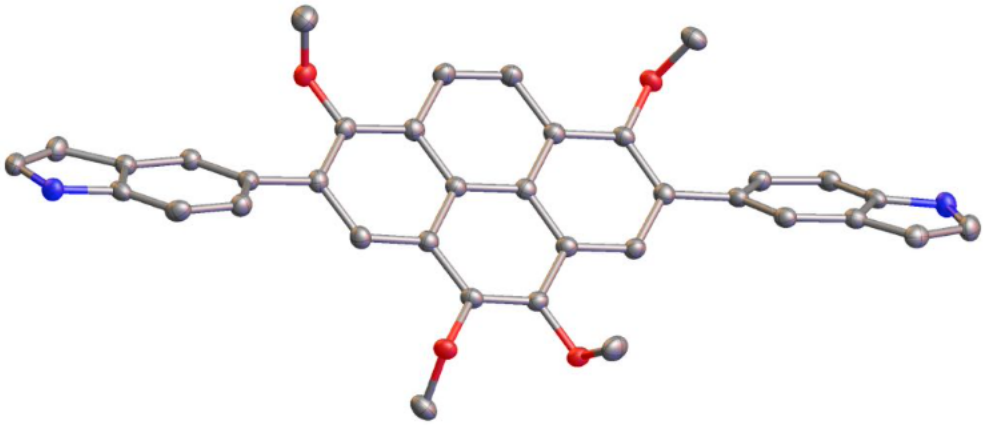

Table 1: Sample and crystal data for MernerMW102121

Identification code	MernerMW102121
Chemical formula	$C_{36}H_{28}N_2O_4$
Formula weight	552.60 g/mol
Temperature	100(2) K
Wavelength	1.54178 Å
Crystal size	0.040 x 0.065 x 0.220 mm
Crystal habit	colorless needle
Crystal system	monoclinic
Space group	P 1 21/c 1
Unit cell dimensions	a = 13.5040(3) Å α = 90°
	b = 12.3433(3) Å β = 112.7840(10)°
	c = 17.3885(4) Å γ = 90°
Volume	2672.23(11) $Å^3$
Z	4
Density (calculated)	1.374 g/cm^3
Absorption coefficient	0.721 mm^{-1}
F(000)	1160

Table 2: Data collection and structure refinement for MernerMW102121

Diffractometer	Bruker D8 VENTURE κ-geometry diffractometer
Radiation source	Incoatec IμS DIAMOND microfocus sealed tube (Cu Kα, λ = 1.54178 Å)
Theta range for data collection	3.55 to 74.53°
Index ranges	-16<=h<=16, -15<=k<=15, -21<=l<=21

Reflections collected	70484	
Independent reflections	5467 [R(int) = 0.0275]	
Coverage of independent reflections	99.9%	
Absorption correction	Multi-Scan	
Max. and min. transmission	0.9720 and 0.8570	
Structure solution technique	direct methods	
Structure solution program	SHELXT 2018/2 (Sheldrick, 2018)	
Refinement method	Full-matrix least-squares on F^2	
Refinement program	SHELXL-2018/3 (Sheldrick, 2018)	
Function minimized	$\Sigma\, w(F_o^2 - F_c^2)^2$	
Data / restraints / parameters	5467 / 0 / 389	
Goodness-of-fit on F^2	1.043	
Final R indices	5256 data; I>2σ(I)	R1 = 0.0486, wR2 = 0.1268
	all data	R1 = 0.0498, wR2 = 0.1278
Weighting scheme	$w=1/[\sigma^2(F_o^2)+(0.0600P)^2+2.4352P]$ where $P=(F_o^2+2F_c^2)/3$	
Largest diff. peak and hole	0.695 and -0.278 eÅ^{-3}	
R.M.S. deviation from mean	0.053 eÅ^{-3}	

Table 3: Atomic coordinates and equivalent isotropic atomic displacement parameters (Å^2) for MernerMW102121

U(eq) is defined as one third of the trace of the orthogonalized U_{ij} tensor.

	x/a	y/b	z/c	U(eq)
O1	0.82748(8)	0.78080(9)	0.68098(7)	0.0214(2)
O2	0.37097(8)	0.97275(9)	0.64544(7)	0.0209(2)

	x/a	y/b	z/c	U(eq)
O3	0.22302(8)	0.80548(9)	0.60993(7)	0.0215(2)
O4	0.46524(9)	0.35274(9)	0.62839(7)	0.0249(3)
N1	0.95682(11)	0.26870(11)	0.69886(9)	0.0233(3)
N2	0.98833(11)	0.17077(11)	0.53126(9)	0.0224(3)
C1	0.88649(14)	0.33252(14)	0.63715(11)	0.0262(3)
C2	0.79088(13)	0.28171(13)	0.60129(10)	0.0231(3)
C3	0.79969(12)	0.17986(13)	0.64303(10)	0.0201(3)
C4	0.90599(12)	0.17410(13)	0.70454(10)	0.0206(3)
C5	0.94163(12)	0.08829(13)	0.75933(10)	0.0218(3)
C6	0.87115(12)	0.00368(13)	0.75203(10)	0.0209(3)
C7	0.76592(12)	0.00411(13)	0.68937(10)	0.0198(3)
C8	0.73036(12)	0.09276(13)	0.63640(10)	0.0202(3)
C9	0.69221(12)	0.91073(13)	0.67890(9)	0.0194(3)
C10	0.72357(12)	0.80354(13)	0.67396(9)	0.0190(3)
C11	0.65292(12)	0.71596(13)	0.66272(9)	0.0194(3)
C12	0.54551(12)	0.73744(13)	0.65322(9)	0.0184(3)
C13	0.51223(12)	0.84609(13)	0.65596(9)	0.0190(3)
C14	0.58643(12)	0.93010(13)	0.67036(10)	0.0199(3)
C15	0.40169(12)	0.86669(12)	0.64248(9)	0.0190(3)
C16	0.33024(12)	0.78454(13)	0.62737(9)	0.0190(3)
C17	0.36249(12)	0.67329(12)	0.62675(9)	0.0190(3)
C18	0.47106(12)	0.65105(12)	0.63972(9)	0.0185(3)
C19	0.50397(12)	0.54195(13)	0.63812(10)	0.0202(3)
C20	0.61363(13)	0.52237(13)	0.64913(10)	0.0224(3)
C21	0.68401(12)	0.60508(13)	0.65964(10)	0.0221(3)
C22	0.42859(13)	0.45799(13)	0.62414(10)	0.0207(3)
C23	0.32000(12)	0.47932(13)	0.60809(10)	0.0197(3)
C24	0.28994(12)	0.58788(13)	0.61153(10)	0.0201(3)
C25	0.23418(12)	0.39543(13)	0.58558(10)	0.0199(3)
C26	0.13252(13)	0.42265(13)	0.52311(10)	0.0221(3)
C27	0.04499(12)	0.35380(13)	0.50069(10)	0.0233(3)
C28	0.05879(12)	0.25518(13)	0.54117(10)	0.0207(3)
C29	0.15924(12)	0.22415(13)	0.60313(10)	0.0203(3)
C30	0.24726(12)	0.29549(13)	0.62472(10)	0.0200(3)
C31	0.14370(14)	0.11763(13)	0.62992(11)	0.0256(3)
C32	0.04152(14)	0.08899(13)	0.58616(11)	0.0262(4)
C33	0.84557(13)	0.80515(15)	0.60648(11)	0.0263(4)
C34	0.33377(15)	0.02387(14)	0.56526(11)	0.0289(4)
C35	0.20237(14)	0.82391(15)	0.68343(11)	0.0288(4)

	x/a	y/b	z/c	U(eq)
C36	0.45727(15)	0.31029(15)	0.55036(12)	0.0322(4)

Table 4: Bond lengths (Å) for MernerMW102121

O1-C10	1.3894(18)	O1-C33	1.440(2)
O2-C15	1.3802(18)	O2-C34	1.432(2)
O3-C16	1.3839(17)	O3-C35	1.428(2)
O4-C22	1.3820(19)	O4-C36	1.419(2)
N1-C1	1.373(2)	N1-C4	1.377(2)
N2-C28	1.376(2)	N2-C32	1.384(2)
C1-C2	1.351(2)	C2-C3	1.433(2)
C3-C8	1.401(2)	C3-C4	1.421(2)
C4-C5	1.381(2)	C5-C6	1.385(2)
C6-C7	1.417(2)	C7-C8	1.391(2)
C7-C9	1.487(2)	C9-C14	1.398(2)
C9-C10	1.402(2)	C10-C11	1.405(2)
C11-C12	1.420(2)	C11-C21	1.439(2)
C12-C13	1.421(2)	C12-C18	1.421(2)
C13-C14	1.396(2)	C13-C15	1.441(2)
C15-C16	1.354(2)	C16-C17	1.442(2)
C17-C24	1.393(2)	C17-C18	1.421(2)
C18-C19	1.422(2)	C19-C22	1.406(2)
C19-C20	1.438(2)	C20-C21	1.358(2)
C22-C23	1.407(2)	C23-C24	1.408(2)
C23-C25	1.489(2)	C25-C30	1.387(2)
C25-C26	1.422(2)	C26-C27	1.384(2)
C27-C28	1.382(2)	C28-C29	1.420(2)
C29-C30	1.408(2)	C29-C31	1.437(2)

Table 5: Bond angles (°) for MernerMW102121

C10-O1-C33	113.34(12)	C15-O2-C34	112.26(12)
C16-O3-C35	112.58(12)	C22-O4-C36	113.76(13)
C1-N1-C4	109.22(14)	C28-N2-C32	108.48(13)
C2-C1-N1	110.04(15)	C1-C2-C3	107.24(14)
C8-C3-C4	118.13(14)	C8-C3-C2	135.22(15)
C4-C3-C2	106.65(14)	N1-C4-C5	130.51(14)
N1-C4-C3	106.84(14)	C5-C4-C3	122.57(14)

C4-C5-C6	118.14(14)	C5-C6-C7	121.09(15)
C8-C7-C6	119.91(14)	C8-C7-C9	119.06(14)
C6-C7-C9	121.04(14)	C7-C8-C3	120.08(14)
C14-C9-C10	118.37(14)	C14-C9-C7	119.23(14)
C10-C9-C7	122.35(14)	O1-C10-C9	120.27(14)
O1-C10-C11	117.73(13)	C9-C10-C11	122.00(14)
C10-C11-C12	118.73(14)	C10-C11-C21	123.03(14)
C12-C11-C21	118.23(14)	C11-C12-C13	119.64(14)
C11-C12-C18	120.30(14)	C13-C12-C18	120.06(14)
C14-C13-C12	119.53(14)	C14-C13-C15	121.64(14)
C12-C13-C15	118.83(14)	C13-C14-C9	121.67(14)
C16-C15-O2	121.05(13)	C16-C15-C13	121.00(14)
O2-C15-C13	117.95(13)	C15-C16-O3	120.62(14)
C15-C16-C17	121.35(14)	O3-C16-C17	118.02(13)
C24-C17-C18	119.36(14)	C24-C17-C16	122.00(14)
C18-C17-C16	118.61(14)	C17-C18-C12	120.10(14)
C17-C18-C19	119.40(14)	C12-C18-C19	120.49(14)
C22-C19-C18	119.38(14)	C22-C19-C20	122.57(14)
C18-C19-C20	118.04(14)	C21-C20-C19	121.50(15)
C20-C21-C11	121.40(14)	O4-C22-C19	117.59(14)
O4-C22-C23	120.70(14)	C19-C22-C23	121.69(14)
C22-C23-C24	117.71(14)	C22-C23-C25	124.56(14)
C24-C23-C25	117.72(14)	C17-C24-C23	122.36(14)
C30-C25-C26	119.13(14)	C30-C25-C23	123.46(14)
C26-C25-C23	117.35(14)	C27-C26-C25	122.47(15)
C28-C27-C26	117.74(14)	N2-C28-C27	130.75(15)
N2-C28-C29	107.56(14)	C27-C28-C29	121.66(14)
C30-C29-C28	119.55(14)	C30-C29-C31	134.40(15)
C28-C29-C31	106.04(14)	C25-C30-C29	119.43(14)
C32-C31-C29	107.75(15)	C31-C32-N2	110.16(15)

Table 6: Torsion angles (°) for MernerMW102121

C4-N1-C1-C2	-0.8(2)	N1-C1-C2-C3	0.78(19)
C1-C2-C3-C8	178.93(17)	C1-C2-C3-C4	-0.51(18)
C1-N1-C4-C5	-176.42(17)	C1-N1-C4-C3	0.41(18)
C8-C3-C4-N1	-179.49(13)	C2-C3-C4-N1	0.06(17)
C8-C3-C4-C5	-2.4(2)	C2-C3-C4-C5	177.20(14)
N1-C4-C5-C6	178.12(15)	C3-C4-C5-C6	1.7(2)
C4-C5-C6-C7	0.9(2)	C5-C6-C7-C8	-2.9(2)
C5-C6-C7-C9	176.91(14)	C6-C7-C8-C3	2.3(2)

C9-C7-C8-C3	-177.60(14)	C4-C3-C8-C7	0.3(2)
C2-C3-C8-C7	-179.10(17)	C8-C7-C9-C14	-47.2(2)
C6-C7-C9-C14	132.96(16)	C8-C7-C9-C10	130.26(16)
C6-C7-C9-C10	-49.6(2)	C33-O1-C10-C9	-76.80(18)
C33-O1-C10-C11	103.80(16)	C14-C9-C10-O1	179.13(13)
C7-C9-C10-O1	1.7(2)	C14-C9-C10-C11	-1.5(2)
C7-C9-C10-C11	-178.95(14)	O1-C10-C11-C12	-178.39(13)
C9-C10-C11-C12	2.2(2)	O1-C10-C11-C21	1.1(2)
C9-C10-C11-C21	-178.33(15)	C10-C11-C12-C13	-0.5(2)
C21-C11-C12-C13	179.99(14)	C10-C11-C12-C18	178.49(14)
C21-C11-C12-C18	-1.0(2)	C11-C12-C13-C14	-1.8(2)
C18-C12-C13-C14	179.15(14)	C11-C12-C13-C15	177.25(14)
C18-C12-C13-C15	-1.8(2)	C12-C13-C14-C9	2.6(2)
C15-C13-C14-C9	-176.44(14)	C10-C9-C14-C13	-1.0(2)
C7-C9-C14-C13	176.56(14)	C34-O2-C15-C16	-89.34(17)
C34-O2-C15-C13	90.65(16)	C14-C13-C15-C16	179.02(14)
C12-C13-C15-C16	0.0(2)	C14-C13-C15-O2	-1.0(2)
C12-C13-C15-O2	179.97(13)	O2-C15-C16-O3	3.6(2)
C13-C15-C16-O3	-176.40(13)	O2-C15-C16-C17	-178.06(13)
C13-C15-C16-C17	1.9(2)	C35-O3-C16-C15	-81.53(18)
C35-O3-C16-C17	100.06(16)	C15-C16-C17-C24	179.82(15)
O3-C16-C17-C24	-1.8(2)	C15-C16-C17-C18	-2.0(2)
O3-C16-C17-C18	176.37(13)	C24-C17-C18-C12	178.40(14)
C16-C17-C18-C12	0.2(2)	C24-C17-C18-C19	-0.9(2)
C16-C17-C18-C19	-179.10(14)	C11-C12-C18-C17	-177.35(14)
C13-C12-C18-C17	1.7(2)	C11-C12-C18-C19	1.9(2)
C13-C12-C18-C19	-179.05(14)	C17-C18-C19-C22	-0.3(2)
C12-C18-C19-C22	-179.61(14)	C17-C18-C19-C20	178.28(14)
C12-C18-C19-C20	-1.0(2)	C22-C19-C20-C21	177.65(15)
C18-C19-C20-C21	-0.9(2)	C19-C20-C21-C11	1.9(2)
C10-C11-C21-C20	179.63(15)	C12-C11-C21-C20	-0.9(2)
C36-O4-C22-C19	-92.30(17)	C36-O4-C22-C23	89.00(18)
C18-C19-C22-O4	-175.92(13)	C20-C19-C22-O4	5.6(2)
C18-C19-C22-C23	2.8(2)	C20-C19-C22-C23	-175.76(15)
O4-C22-C23-C24	174.78(14)	C19-C22-C23-C24	-3.9(2)
O4-C22-C23-C25	-6.9(2)	C19-C22-C23-C25	174.48(14)
C18-C17-C24-C23	-0.3(2)	C16-C17-C24-C23	177.86(14)
C22-C23-C24-C17	2.6(2)	C25-C23-C24-C17	-175.85(14)
C22-C23-C25-C30	43.1(2)	C24-C23-C25-C30	-138.51(16)
C22-C23-C25-C26	-139.79(16)	C24-C23-C25-C26	38.6(2)

C30-C25-C26-C27	1.2(2)	C23-C25-C26-C27	-176.01(15)
C25-C26-C27-C28	-0.2(2)	C32-N2-C28-C27	179.16(17)
C32-N2-C28-C29	0.96(17)	C26-C27-C28-N2	-178.63(16)
C26-C27-C28-C29	-0.6(2)	N2-C28-C29-C30	178.87(14)
C27-C28-C29-C30	0.5(2)	N2-C28-C29-C31	-0.76(17)
C27-C28-C29-C31	-179.16(15)	C26-C25-C30-C29	-1.3(2)
C23-C25-C30-C29	175.68(14)	C28-C29-C30-C25	0.6(2)
C31-C29-C30-C25	-179.94(17)	C30-C29-C31-C32	-179.28(17)
C28-C29-C31-C32	0.28(18)	C29-C31-C32-N2	0.32(19)
C28-N2-C32-C31	-0.81(19)		

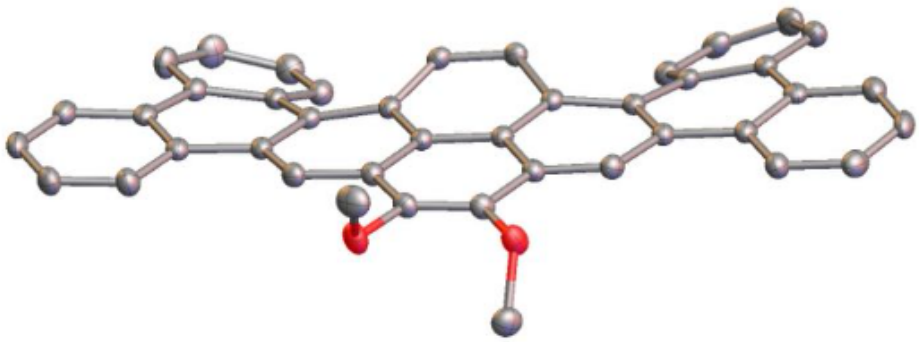

Table 7: Sample and crystal data for MernerMW120721

Identification code	MernerMW120721	
Chemical formula	$C_{42}H_{26}O_2$	
Formula weight	562.63 g/mol	
Temperature	100(2) K	
Wavelength	1.54178 Å	
Crystal size	0.050 x 0.050 x 0.275 mm	
Crystal habit	pale yellow needle	
Crystal system	orthorhombic	
Space group	P 21 21 21	
Unit cell dimensions	a = 7.0390(3) Å	α = 90°
	b = 17.2366(7) Å	β = 90°
	c = 44.1459(18) Å	γ = 90°
Volume	5356.2(4) $Å^3$	
Z	8	
Density (calculated)	1.395 g/cm^3	
Absorption coefficient	0.657 mm^{-1}	
F(000)	2352	

Table 8: Data collection and structure refinement for MernerMW120721

Diffractometer	Bruker D8 VENTURE κ-geometry diffractometer	
Radiation source	Incoatec IμS DIAMOND microfocus sealed tube (Cu Kα, λ = 1.54178 Å)	
Theta range for data collection	2.00 to 74.54°	
Index ranges	-6<=h<=8, -21<=k<=19, -54<=l<=54	
Reflections collected	54645	
Independent reflections	10905 [R(int) = 0.0315]	
Coverage of independent reflections	99.7%	
Absorption correction	Multi-Scan	
Max. and min. transmission	0.9680 and 0.8400	
Structure solution technique	direct methods	
Structure solution program	SHELXT 2018/2 (Sheldrick, 2018)	
Refinement method	Full-matrix least-squares on F^2	
Refinement program	SHELXL-2018/3 (Sheldrick, 2018)	
Function minimized	$\Sigma w(F_o^2 - F_c^2)^2$	
Data / restraints / parameters	10905 / 0 / 797	
Goodness-of-fit on F^2	1.050	
Δ/σ_{max}	0.001	
Final R indices	10822 data; I>2σ(I)	R1 = 0.0303, wR2 = 0.0809
	all data	R1 = 0.0306, wR2 = 0.0811
Weighting scheme	$w=1/[\sigma^2(F_o^2)+(0.0412P)^2+1.4259P]$ where $P=(F_o^2+2F_c^2)/3$	

Absolute structure parameter	-0.10(4)
Largest diff. peak and hole	0.228 and -0.169 eÅ^{-3}
R.M.S. deviation from mean	0.037 eÅ^{-3}

Table 9: Atomic coordinates and equivalent isotropic atomic displacement parameters (Å^2) for MernerMW120721

U(eq) is defined as one third of the trace of the orthogonalized U_{ij} tensor.

	x/a	y/b	z/c	U(eq)
O1	0.04510(17)	0.25591(7)	0.75135(3)	0.0206(3)
O2	0.69813(18)	0.21474(7)	0.72288(3)	0.0213(3)
C1	0.9588(3)	0.30288(10)	0.73004(4)	0.0180(3)
C2	0.7921(3)	0.28266(10)	0.71665(4)	0.0179(3)
C3	0.7015(3)	0.33398(10)	0.69539(4)	0.0167(3)
C4	0.7874(2)	0.40653(10)	0.68836(4)	0.0156(3)
C5	0.9650(2)	0.42704(10)	0.70204(4)	0.0150(3)
C6	0.0527(2)	0.37459(10)	0.72263(4)	0.0164(3)
C7	0.2233(2)	0.39486(10)	0.73624(4)	0.0178(3)
C8	0.3169(2)	0.46472(10)	0.72942(4)	0.0165(3)
C9	0.2373(2)	0.51623(10)	0.70798(4)	0.0154(3)
C10	0.0521(2)	0.49958(10)	0.69598(4)	0.0155(3)
C11	0.3431(2)	0.58618(10)	0.69992(4)	0.0165(3)
C12	0.4877(2)	0.61360(10)	0.71955(4)	0.0175(3)
C13	0.5582(3)	0.56336(11)	0.74389(4)	0.0194(3)
C14	0.4885(2)	0.48691(10)	0.74617(4)	0.0174(3)
C15	0.5770(3)	0.43508(11)	0.76651(4)	0.0216(4)
C16	0.7188(3)	0.45996(12)	0.78572(4)	0.0266(4)
C17	0.7777(3)	0.53699(13)	0.78512(5)	0.0311(4)
C18	0.7015(3)	0.58758(12)	0.76410(4)	0.0268(4)
C19	0.5709(3)	0.68648(11)	0.71354(4)	0.0207(4)
C20	0.5257(3)	0.72820(11)	0.68781(4)	0.0223(4)
C21	0.4011(3)	0.69657(11)	0.66651(4)	0.0203(4)
C22	0.3128(2)	0.62661(10)	0.67240(4)	0.0175(3)
C23	0.9361(2)	0.55498(10)	0.68047(4)	0.0160(3)
C24	0.7681(2)	0.53530(10)	0.66728(4)	0.0161(3)
C25	0.6965(2)	0.45739(10)	0.66791(4)	0.0153(3)
C26	0.5327(2)	0.43196(10)	0.65137(4)	0.0159(3)
C27	0.4431(3)	0.36201(10)	0.66023(4)	0.0167(3)

	x/a	y/b	z/c	U(eq)
C28	0.5295(3)	0.31442(10)	0.68212(4)	0.0176(3)
C29	0.2583(3)	0.34015(10)	0.64714(4)	0.0172(3)
C30	0.1694(2)	0.38996(10)	0.62619(4)	0.0180(3)
C31	0.2704(3)	0.45832(10)	0.61486(4)	0.0179(3)
C32	0.4565(3)	0.47484(10)	0.62554(4)	0.0173(3)
C33	0.5646(3)	0.53012(10)	0.60942(4)	0.0195(3)
C34	0.4876(3)	0.57403(11)	0.58630(4)	0.0235(4)
C35	0.2994(3)	0.56258(11)	0.57794(4)	0.0254(4)
C36	0.1942(3)	0.50486(11)	0.59162(4)	0.0234(4)
C37	0.9885(3)	0.36928(11)	0.61480(4)	0.0217(4)
C38	0.9019(3)	0.30084(12)	0.62285(4)	0.0234(4)
C39	0.9917(3)	0.25100(11)	0.64333(4)	0.0227(4)
C40	0.1656(3)	0.27075(11)	0.65539(4)	0.0204(4)
C41	0.9474(3)	0.25627(12)	0.77983(4)	0.0266(4)
C42	0.8081(3)	0.14510(10)	0.72005(4)	0.0248(4)
O3	0.0627(2)	0.43228(8)	0.53045(3)	0.0258(3)
O4	0.7084(2)	0.36734(8)	0.51612(3)	0.0250(3)
C43	0.9745(3)	0.44696(11)	0.50314(4)	0.0206(4)
C44	0.0671(3)	0.50077(10)	0.48294(4)	0.0194(3)
C45	0.9817(3)	0.51776(10)	0.45454(4)	0.0179(3)
C46	0.8059(3)	0.48167(10)	0.44639(4)	0.0177(3)
C47	0.7139(3)	0.43093(10)	0.46734(4)	0.0188(3)
C48	0.8025(3)	0.41600(10)	0.49626(4)	0.0206(4)
C49	0.2398(3)	0.53482(11)	0.49034(4)	0.0204(4)
C50	0.3264(3)	0.59055(10)	0.47158(4)	0.0189(3)
C51	0.2385(3)	0.61183(10)	0.44411(4)	0.0183(3)
C52	0.0735(2)	0.56960(10)	0.43434(4)	0.0176(3)
C53	0.5112(3)	0.62464(10)	0.47986(4)	0.0201(3)
C54	0.6055(3)	0.67446(10)	0.45934(4)	0.0206(4)
C55	0.7864(3)	0.70314(11)	0.46709(4)	0.0230(4)
C56	0.8702(3)	0.68566(11)	0.49447(5)	0.0249(4)
C57	0.7755(3)	0.63868(12)	0.51503(4)	0.0264(4)
C58	0.5987(3)	0.60817(12)	0.50767(4)	0.0250(4)
C59	0.5067(3)	0.70114(10)	0.43218(4)	0.0206(4)
C60	0.3175(3)	0.67596(10)	0.42648(4)	0.0198(4)
C61	0.2104(3)	0.71763(11)	0.40492(4)	0.0220(4)
C62	0.2907(3)	0.77446(11)	0.38700(5)	0.0269(4)
C63	0.4820(3)	0.79225(12)	0.39020(5)	0.0310(4)
C64	0.5865(3)	0.75706(12)	0.41272(5)	0.0275(4)

	x/a	y/b	z/c	U(eq)
C65	0.0044(3)	0.56971(10)	0.40385(4)	0.0188(3)
C66	0.8392(3)	0.53412(10)	0.39602(4)	0.0194(3)
C67	0.7217(3)	0.49551(10)	0.41769(4)	0.0177(3)
C68	0.5364(3)	0.46537(10)	0.41119(4)	0.0181(3)
C69	0.4537(3)	0.41169(10)	0.43144(4)	0.0188(3)
C70	0.5448(3)	0.39556(10)	0.45918(4)	0.0201(3)
C71	0.2739(3)	0.37312(10)	0.42362(4)	0.0199(3)
C72	0.1914(3)	0.38487(10)	0.39473(4)	0.0202(4)
C73	0.2724(3)	0.44337(11)	0.37455(4)	0.0210(4)
C74	0.4294(3)	0.48863(11)	0.38417(4)	0.0195(4)
C75	0.4673(3)	0.55883(11)	0.36856(4)	0.0217(4)
C76	0.3732(3)	0.57754(12)	0.34209(4)	0.0258(4)
C77	0.2378(3)	0.52735(13)	0.33024(4)	0.0285(4)
C78	0.1849(3)	0.46252(12)	0.34664(4)	0.0258(4)
C79	0.0224(3)	0.34533(11)	0.38769(4)	0.0246(4)
C80	0.9325(3)	0.29769(11)	0.40844(5)	0.0257(4)
C81	0.0119(3)	0.28761(11)	0.43699(5)	0.0263(4)
C82	0.1818(3)	0.32356(11)	0.44418(4)	0.0231(4)
C83	0.1207(4)	0.35325(13)	0.53489(5)	0.0343(5)
C84	0.6418(3)	0.40608(12)	0.54302(5)	0.0290(4)

Table 10: Bond lengths (Å) for MernerMW120721

O1-C1	1.382(2)	O1-C41	1.433(2)
O2-C2	1.373(2)	O2-C42	1.434(2)
C1-C2	1.359(3)	C1-C6	1.439(2)
C2-C3	1.439(2)	C3-C28	1.386(3)
C3-C4	1.423(2)	C4-C25	1.412(2)
C4-C5	1.433(2)	C5-C10	1.418(2)
C5-C6	1.423(2)	C6-C7	1.388(2)
C7-C8	1.405(2)	C8-C9	1.414(2)
C8-C14	1.467(2)	C9-C10	1.436(2)
C9-C11	1.461(2)	C10-C23	1.431(2)
C11-C22	1.417(2)	C11-C12	1.418(2)
C12-C19	1.411(3)	C12-C13	1.467(2)
C13-C14	1.410(3)	C13-C18	1.410(3)
C14-C15	1.412(2)	C15-C16	1.378(3)
C16-C17	1.391(3)	C17-C18	1.382(3)
C19-C20	1.381(3)	C20-C21	1.397(3)

C21-C22	1.381(3)	C23-C24	1.361(3)
C24-C25	1.435(2)	C25-C26	1.433(2)
C26-C27	1.416(2)	C26-C32	1.461(2)
C27-C28	1.406(2)	C27-C29	1.472(2)
C29-C30	1.409(3)	C29-C40	1.410(3)
C30-C37	1.415(2)	C30-C31	1.464(3)
C31-C36	1.408(3)	C31-C32	1.421(2)
C32-C33	1.412(3)	C33-C34	1.382(3)
C34-C35	1.389(3)	C35-C36	1.380(3)
C37-C38	1.374(3)	C38-C39	1.398(3)
C39-C40	1.378(3)	O3-C43	1.379(2)
O3-C83	1.436(3)	O4-C48	1.383(2)
O4-C84	1.441(2)	C43-C48	1.358(3)
C43-C44	1.442(3)	C44-C49	1.389(3)
C44-C45	1.421(2)	C45-C52	1.418(2)
C45-C46	1.431(2)	C46-C67	1.419(2)
C46-C47	1.428(2)	C47-C70	1.385(3)
C47-C48	1.444(2)	C49-C50	1.407(3)
C50-C51	1.410(2)	C50-C53	1.473(2)
C51-C52	1.437(3)	C51-C60	1.462(3)
C52-C65	1.431(2)	C53-C58	1.402(3)
C53-C54	1.414(3)	C54-C55	1.408(3)
C54-C59	1.461(3)	C55-C56	1.379(3)
C56-C57	1.387(3)	C57-C58	1.390(3)
C59-C64	1.408(3)	C59-C60	1.423(3)
C60-C61	1.411(3)	C61-C62	1.380(3)
C62-C63	1.388(3)	C63-C64	1.377(3)
C65-C66	1.360(3)	C66-C67	1.429(2)
C67-C68	1.433(2)	C68-C69	1.412(2)
C68-C74	1.467(2)	C69-C70	1.410(2)
C69-C71	1.471(2)	C71-C82	1.405(3)
C71-C72	1.416(3)	C72-C79	1.406(3)
C72-C73	1.461(3)	C73-C78	1.417(3)
C73-C74	1.418(3)	C74-C75	1.418(3)
C75-C76	1.381(3)	C76-C77	1.390(3)
C77-C78	1.383(3)	C79-C80	1.384(3)
C80-C81	1.390(3)	C81-C82	1.384(3)

Table 11: Bond angles (°) for MernerMW120721

C1-O1-C41	112.57(13)	C2-O2-C42	115.88(14)
C2-C1-O1	121.69(16)	C2-C1-C6	121.18(16)
O1-C1-C6	117.13(15)	C1-C2-O2	123.20(16)
C1-C2-C3	120.57(16)	O2-C2-C3	116.21(15)
C28-C3-C4	119.51(16)	C28-C3-C2	120.87(16)
C4-C3-C2	119.61(15)	C25-C4-C3	119.50(16)
C25-C4-C5	120.79(15)	C3-C4-C5	119.71(15)
C10-C5-C6	119.56(15)	C10-C5-C4	121.01(15)
C6-C5-C4	119.41(15)	C7-C6-C5	119.47(16)
C7-C6-C1	121.01(16)	C5-C6-C1	119.45(16)
C6-C7-C8	121.91(16)	C7-C8-C9	119.73(16)
C7-C8-C14	120.08(15)	C9-C8-C14	120.02(16)
C8-C9-C10	118.77(15)	C8-C9-C11	118.63(16)
C10-C9-C11	122.54(15)	C5-C10-C23	115.60(15)
C5-C10-C9	119.94(15)	C23-C10-C9	124.13(16)
C22-C11-C12	117.90(16)	C22-C11-C9	122.55(16)
C12-C11-C9	119.50(15)	C19-C12-C11	118.68(16)
C19-C12-C13	121.53(16)	C11-C12-C13	119.59(16)
C14-C13-C18	118.72(17)	C14-C13-C12	119.11(15)
C18-C13-C12	122.06(17)	C13-C14-C15	118.90(16)
C13-C14-C8	119.62(15)	C15-C14-C8	121.28(16)
C16-C15-C14	120.94(18)	C15-C16-C17	120.09(18)
C18-C17-C16	119.96(18)	C17-C18-C13	121.05(18)
C20-C19-C12	121.50(17)	C19-C20-C21	119.66(17)
C22-C21-C20	119.78(17)	C21-C22-C11	121.55(16)
C24-C23-C10	122.29(16)	C23-C24-C25	122.02(16)
C4-C25-C26	120.02(15)	C4-C25-C24	115.75(15)
C26-C25-C24	123.99(15)	C27-C26-C25	118.56(15)
C27-C26-C32	118.87(15)	C25-C26-C32	122.56(15)
C28-C27-C26	119.60(16)	C28-C27-C29	120.19(16)
C26-C27-C29	120.20(16)	C3-C28-C27	121.75(16)
C30-C29-C40	118.75(16)	C30-C29-C27	119.63(16)
C40-C29-C27	121.62(16)	C29-C30-C37	118.66(17)
C29-C30-C31	119.94(16)	C37-C30-C31	121.22(16)
C36-C31-C32	118.58(17)	C36-C31-C30	121.49(16)
C32-C31-C30	119.70(16)	C33-C32-C31	117.71(16)
C33-C32-C26	122.48(16)	C31-C32-C26	119.73(16)
C34-C33-C32	122.04(17)	C33-C34-C35	119.52(18)
C36-C35-C34	119.86(18)	C35-C36-C31	121.70(18)

C38-C37-C30	121.56(17)	C37-C38-C39	119.63(17)
C40-C39-C38	119.97(17)	C39-C40-C29	121.39(17)
C43-O3-C83	114.92(15)	C48-O4-C84	113.41(14)
C48-C43-O3	121.66(16)	C48-C43-C44	121.15(16)
O3-C43-C44	117.07(16)	C49-C44-C45	119.37(17)
C49-C44-C43	121.46(16)	C45-C44-C43	119.14(16)
C52-C45-C44	119.47(16)	C52-C45-C46	120.65(15)
C44-C45-C46	119.87(16)	C67-C46-C47	119.47(16)
C67-C46-C45	120.84(16)	C47-C46-C45	119.69(15)
C70-C47-C46	119.39(16)	C70-C47-C48	121.50(16)
C46-C47-C48	119.08(16)	C43-C48-O4	121.59(16)
C43-C48-C47	120.87(16)	O4-C48-C47	117.51(16)
C44-C49-C50	121.97(16)	C49-C50-C51	119.57(16)
C49-C50-C53	120.58(16)	C51-C50-C53	119.81(16)
C50-C51-C52	118.77(16)	C50-C51-C60	119.19(16)
C52-C51-C60	122.03(16)	C45-C52-C65	115.93(15)
C45-C52-C51	119.90(16)	C65-C52-C51	123.82(16)
C58-C53-C54	118.52(17)	C58-C53-C50	121.62(17)
C54-C53-C50	119.86(16)	C55-C54-C53	118.84(18)
C55-C54-C59	121.31(17)	C53-C54-C59	119.57(17)
C56-C55-C54	121.55(18)	C55-C56-C57	119.72(18)
C56-C57-C58	119.90(18)	C57-C58-C53	121.43(19)
C64-C59-C60	118.30(17)	C64-C59-C54	121.76(17)
C60-C59-C54	119.68(16)	C61-C60-C59	117.67(17)
C61-C60-C51	122.74(17)	C59-C60-C51	119.49(17)
C62-C61-C60	121.92(18)	C61-C62-C63	119.74(19)
C64-C63-C62	119.61(18)	C63-C64-C59	121.93(18)
C66-C65-C52	121.96(16)	C65-C66-C67	122.34(16)
C46-C67-C66	115.74(16)	C46-C67-C68	119.87(16)
C66-C67-C68	124.17(16)	C69-C68-C67	119.08(16)
C69-C68-C74	118.83(16)	C67-C68-C74	122.09(16)
C70-C69-C68	119.45(16)	C70-C69-C71	120.39(16)
C68-C69-C71	120.16(16)	C47-C70-C69	121.99(16)
C82-C71-C72	118.68(17)	C82-C71-C69	121.35(16)
C72-C71-C69	119.97(16)	C79-C72-C71	118.47(17)
C79-C72-C73	121.99(17)	C71-C72-C73	119.21(16)
C78-C73-C74	118.13(17)	C78-C73-C72	121.43(17)
C74-C73-C72	120.07(16)	C73-C74-C75	118.08(17)
C73-C74-C68	119.57(16)	C75-C74-C68	122.13(17)
C76-C75-C74	121.35(18)	C75-C76-C77	120.13(19)

C78-C77-C76	119.39(17)	C77-C78-C73	121.79(18)
C80-C79-C72	121.91(18)	C79-C80-C81	119.37(18)
C82-C81-C80	119.99(18)	C81-C82-C71	121.52(18)

Table 12: Torsion angles (°) for MernerMW120721

C41-O1-C1-C2	-72.7(2)	C41-O1-C1-C6	107.06(18)
O1-C1-C2-O2	-0.6(3)	C6-C1-C2-O2	179.62(15)
O1-C1-C2-C3	177.60(15)	C6-C1-C2-C3	-2.2(3)
C42-O2-C2-C1	-53.1(2)	C42-O2-C2-C3	128.68(16)
C1-C2-C3-C28	-178.67(16)	O2-C2-C3-C28	-0.4(2)
C1-C2-C3-C4	0.0(2)	O2-C2-C3-C4	178.31(14)
C28-C3-C4-C25	-0.2(2)	C2-C3-C4-C25	-178.86(15)
C28-C3-C4-C5	179.92(15)	C2-C3-C4-C5	1.2(2)
C25-C4-C5-C10	1.4(2)	C3-C4-C5-C10	-178.64(15)
C25-C4-C5-C6	179.81(15)	C3-C4-C5-C6	-0.3(2)
C10-C5-C6-C7	-0.7(2)	C4-C5-C6-C7	-179.07(15)
C10-C5-C6-C1	176.54(15)	C4-C5-C6-C1	-1.8(2)
C2-C1-C6-C7	-179.69(16)	O1-C1-C6-C7	0.5(2)
C2-C1-C6-C5	3.1(3)	O1-C1-C6-C5	-176.67(14)
C5-C6-C7-C8	-2.6(2)	C1-C6-C7-C8	-179.73(16)
C6-C7-C8-C9	-0.4(3)	C6-C7-C8-C14	174.86(15)
C7-C8-C9-C10	6.4(2)	C14-C8-C9-C10	-168.84(14)
C7-C8-C9-C11	-176.30(15)	C14-C8-C9-C11	8.4(2)
C6-C5-C10-C23	-166.95(15)	C4-C5-C10-C23	11.4(2)
C6-C5-C10-C9	6.7(2)	C4-C5-C10-C9	-174.89(15)
C8-C9-C10-C5	-9.6(2)	C11-C9-C10-C5	173.24(15)
C8-C9-C10-C23	163.53(16)	C11-C9-C10-C23	-13.6(3)
C8-C9-C11-C22	157.79(16)	C10-C9-C11-C22	-25.0(2)
C8-C9-C11-C12	-19.5(2)	C10-C9-C11-C12	157.69(15)
C22-C11-C12-C19	10.9(2)	C9-C11-C12-C19	-171.68(15)
C22-C11-C12-C13	-163.97(16)	C9-C11-C12-C13	13.4(2)
C19-C12-C13-C14	-171.00(16)	C11-C12-C13-C14	3.7(2)
C19-C12-C13-C18	5.3(3)	C11-C12-C13-C18	-179.92(18)
C18-C13-C14-C15	-6.1(3)	C12-C13-C14-C15	170.31(16)
C18-C13-C14-C8	168.78(17)	C12-C13-C14-C8	-14.8(2)
C7-C8-C14-C13	-166.59(16)	C9-C8-C14-C13	8.7(2)
C7-C8-C14-C15	8.2(2)	C9-C8-C14-C15	-176.55(16)
C13-C14-C15-C16	5.4(3)	C8-C14-C15-C16	-169.46(17)

C14-C15-C16-C17	-0.5(3)	C15-C16-C17-C18	-3.6(3)
C16-C17-C18-C13	2.7(3)	C14-C13-C18-C17	2.2(3)
C12-C13-C18-C17	-174.15(19)	C11-C12-C19-C20	-5.3(3)
C13-C12-C19-C20	169.46(17)	C12-C19-C20-C21	-2.7(3)
C19-C20-C21-C22	4.9(3)	C20-C21-C22-C11	1.0(3)
C12-C11-C22-C21	-9.0(2)	C9-C11-C22-C21	173.70(16)
C5-C10-C23-C24	-12.1(2)	C9-C10-C23-C24	174.52(15)
C10-C23-C24-C25	-0.4(3)	C3-C4-C25-C26	-8.2(2)
C5-C4-C25-C26	171.67(15)	C3-C4-C25-C24	166.40(15)
C5-C4-C25-C24	-13.7(2)	C23-C24-C25-C4	13.4(2)
C23-C24-C25-C26	-172.24(16)	C4-C25-C26-C27	12.4(2)
C24-C25-C26-C27	-161.78(16)	C4-C25-C26-C32	-166.78(15)
C24-C25-C26-C32	19.0(3)	C25-C26-C27-C28	-8.2(2)
C32-C26-C27-C28	170.98(15)	C25-C26-C27-C29	170.32(15)
C32-C26-C27-C29	-10.5(2)	C4-C3-C28-C27	4.4(2)
C2-C3-C28-C27	-176.93(16)	C26-C27-C28-C3	-0.1(2)
C29-C27-C28-C3	-178.64(15)	C28-C27-C29-C30	177.30(15)
C26-C27-C29-C30	-1.2(2)	C28-C27-C29-C40	-1.7(2)
C26-C27-C29-C40	179.75(16)	C40-C29-C30-C37	1.5(2)
C27-C29-C30-C37	-177.55(15)	C40-C29-C30-C31	-173.78(15)
C27-C29-C30-C31	7.2(2)	C29-C30-C31-C36	173.31(16)
C37-C30-C31-C36	-1.8(3)	C29-C30-C31-C32	-1.2(2)
C37-C30-C31-C32	-176.36(15)	C36-C31-C32-C33	-8.5(2)
C30-C31-C32-C33	166.13(16)	C36-C31-C32-C26	174.68(16)
C30-C31-C32-C26	-10.6(2)	C27-C26-C32-C33	-160.15(16)
C25-C26-C32-C33	19.0(3)	C27-C26-C32-C31	16.5(2)
C25-C26-C32-C31	-164.36(15)	C31-C32-C33-C34	7.7(2)
C26-C32-C33-C34	-175.66(16)	C32-C33-C34-C35	-1.7(3)
C33-C34-C35-C36	-3.4(3)	C34-C35-C36-C31	2.3(3)
C32-C31-C36-C35	3.8(3)	C30-C31-C36-C35	-170.75(17)
C29-C30-C37-C38	-2.4(3)	C31-C30-C37-C38	172.80(17)
C30-C37-C38-C39	1.6(3)	C37-C38-C39-C40	0.2(3)
C38-C39-C40-C29	-1.1(3)	C30-C29-C40-C39	0.2(3)
C27-C29-C40-C39	179.25(16)	C83-O3-C43-C48	66.3(2)
C83-O3-C43-C44	-117.61(19)	C48-C43-C44-C49	177.63(17)
O3-C43-C44-C49	1.6(3)	C48-C43-C44-C45	-3.9(3)
O3-C43-C44-C45	180.00(16)	C49-C44-C45-C52	-0.5(3)
C43-C44-C45-C52	-178.94(16)	C49-C44-C45-C46	178.60(16)
C43-C44-C45-C46	0.1(2)	C52-C45-C46-C67	1.4(2)
C44-C45-C46-C67	-177.62(16)	C52-C45-C46-C47	-178.68(16)

C44-C45-C46-C47	2.3(2)	C67-C46-C47-C70	0.6(2)
C45-C46-C47-C70	-179.34(16)	C67-C46-C47-C48	178.81(16)
C45-C46-C47-C48	-1.1(2)	O3-C43-C48-O4	-0.9(3)
C44-C43-C48-O4	-176.80(16)	O3-C43-C48-C47	-178.91(16)
C44-C43-C48-C47	5.2(3)	C84-O4-C48-C43	68.6(2)
C84-O4-C48-C47	-113.33(18)	C70-C47-C48-C43	175.53(17)
C46-C47-C48-C43	-2.7(3)	C70-C47-C48-O4	-2.5(3)
C46-C47-C48-O4	179.25(15)	C45-C44-C49-C50	5.1(3)
C43-C44-C49-C50	-176.48(17)	C44-C49-C50-C51	-1.3(3)
C44-C49-C50-C53	-179.03(16)	C49-C50-C51-C52	-7.0(3)
C53-C50-C51-C52	170.79(15)	C49-C50-C51-C60	173.02(16)
C53-C50-C51-C60	-9.2(2)	C44-C45-C52-C65	165.71(16)
C46-C45-C52-C65	-13.3(2)	C44-C45-C52-C51	-7.8(2)
C46-C45-C52-C51	173.17(16)	C50-C51-C52-C45	11.5(2)
C60-C51-C52-C45	-168.52(16)	C50-C51-C52-C65	-161.46(16)
C60-C51-C52-C65	18.5(3)	C49-C50-C53-C58	-5.6(3)
C51-C50-C53-C58	176.62(17)	C49-C50-C53-C54	173.51(17)
C51-C50-C53-C54	-4.3(2)	C58-C53-C54-C55	2.4(3)
C50-C53-C54-C55	-176.74(16)	C58-C53-C54-C59	-171.53(17)
C50-C53-C54-C59	9.3(2)	C53-C54-C55-C56	-2.0(3)
C59-C54-C55-C56	171.83(17)	C54-C55-C56-C57	0.1(3)
C55-C56-C57-C58	1.4(3)	C56-C57-C58-C53	-0.9(3)
C54-C53-C58-C57	-1.0(3)	C50-C53-C58-C57	178.13(17)
C55-C54-C59-C64	-0.6(3)	C53-C54-C59-C64	173.20(17)
C55-C54-C59-C60	-174.59(16)	C53-C54-C59-C60	-0.8(2)
C64-C59-C60-C61	-10.4(2)	C54-C59-C60-C61	163.77(16)
C64-C59-C60-C51	173.12(17)	C54-C59-C60-C51	-12.7(2)
C50-C51-C60-C61	-158.54(17)	C52-C51-C60-C61	21.5(3)
C50-C51-C60-C59	17.7(2)	C52-C51-C60-C59	-162.26(16)
C59-C60-C61-C62	8.2(3)	C51-C60-C61-C62	-175.46(18)
C60-C61-C62-C63	-0.6(3)	C61-C62-C63-C64	-4.7(3)
C62-C63-C64-C59	2.2(3)	C60-C59-C64-C63	5.5(3)
C54-C59-C64-C63	-168.52(19)	C45-C52-C65-C66	12.2(2)
C51-C52-C65-C66	-174.55(17)	C52-C65-C66-C67	1.2(3)
C47-C46-C67-C66	-168.14(16)	C45-C46-C67-C66	11.8(2)
C47-C46-C67-C68	6.6(2)	C45-C46-C67-C68	-173.48(15)
C65-C66-C67-C46	-13.2(3)	C65-C66-C67-C68	172.24(16)
C46-C67-C68-C69	-10.5(2)	C66-C67-C68-C69	163.82(17)
C46-C67-C68-C74	169.40(16)	C66-C67-C68-C74	-16.3(3)
C67-C68-C69-C70	7.1(2)	C74-C68-C69-C70	-172.74(16)

C67-C68-C69-C71	-172.99(15)	C74-C68-C69-C71	7.1(2)
C46-C47-C70-C69	-4.0(3)	C48-C47-C70-C69	177.83(17)
C68-C69-C70-C47	0.1(3)	C71-C69-C70-C47	-179.81(16)
C70-C69-C71-C82	4.3(3)	C68-C69-C71-C82	-175.58(17)
C70-C69-C71-C72	-174.91(16)	C68-C69-C71-C72	5.2(2)
C82-C71-C72-C79	-1.0(3)	C69-C71-C72-C79	178.17(16)
C82-C71-C72-C73	172.52(17)	C69-C71-C72-C73	-8.3(2)
C79-C72-C73-C78	-0.7(3)	C71-C72-C73-C78	-173.99(17)
C79-C72-C73-C74	172.12(17)	C71-C72-C73-C74	-1.2(3)
C78-C73-C74-C75	11.8(3)	C72-C73-C74-C75	-161.20(16)
C78-C73-C74-C68	-173.34(16)	C72-C73-C74-C68	13.6(3)
C69-C68-C74-C73	-16.6(2)	C67-C68-C74-C73	163.54(16)
C69-C68-C74-C75	158.05(17)	C67-C68-C74-C75	-21.8(3)
C73-C74-C75-C76	-9.4(3)	C68-C74-C75-C76	175.93(17)
C74-C75-C76-C77	0.2(3)	C75-C76-C77-C78	6.3(3)
C76-C77-C78-C73	-3.5(3)	C74-C73-C78-C77	-5.7(3)
C72-C73-C78-C77	167.23(18)	C71-C72-C79-C80	2.1(3)
C73-C72-C79-C80	-171.29(17)	C72-C79-C80-C81	-0.8(3)
C79-C80-C81-C82	-1.6(3)	C80-C81-C82-C71	2.6(3)
C72-C71-C82-C81	-1.3(3)	C69-C71-C82-C81	179.53(17)